

Cardiff University  
School of Engineering

INVESTIGATION  
INTO  $\text{CF}_3\text{I}$ - $\text{CO}_2$  GAS  
MIXTURES FOR  
INSULATION OF  
GAS-INSULATED  
DISTRIBUTION  
EQUIPMENT

A Thesis submitted for the degree of Doctor of Philosophy

Phillip Widger  
June 2014

## Acknowledgements

I would like to thank my supervisors, Professor. A. Haddad and Dr. H. Griffiths for their guidance, advice and support throughout the course of this work. Without your extensive knowledge and experience this research would not have been possible.

I would also like to express my gratitude to the IET Power Networks Research Academy (PNRA) for the scholarship that allowed for this research to be conducted and the contributors to the award: National Grid, Scottish and Sothern Energy, UK Power Networks and Western Power Distribution.

Thank you to UK Power Networks for providing me with a mentor, Veronique Martre, without whose expertise and guidance I would not have attended many training courses and visits provided for by UK Power Networks.

Thank you to Schneider Electric, especially Mike Adams, without whose support and supply of much of the switchgear in this project, the work would not have been possible.

Thank you to Western Power Distribution for providing me with switchgear with which to complete this research.

Thank you to the Advanced High Voltage Engineering Research Centre at Cardiff University for the valuable discussion and friendship.

A special thanks to my parents Valerie and Martyn Widger, for their selfless commitment to my education and for continuing to teach me the sky's the limit, without whom I would not be the person I am today.

A huge thank you to Fiona Lugg for the endless support and encouragement, my best friend throughout all the trials of PhD life, I would never have finished this course without you.

Lastly, a big thank you to all the members of academic and administrative staff at the School of Engineering at Cardiff University and to everyone who has directly or indirectly contributed to this work.

## Summary

This thesis reviews the use of sulphur hexafluoride ( $\text{SF}_6$ ) as an insulating medium in the electrical power industry and quantifies the potential global warming effects associated with its continued use. A mixture of Trifluoroiodomethane ( $\text{CF}_3\text{I}$ ) and carbon dioxide ( $\text{CO}_2$ ) is suggested as a potential alternative to  $\text{SF}_6$ , and its insulation properties are examined. Pressure mixture ratios of 10%:90%, 20%:80% and 30%:70%  $\text{CF}_3\text{I}$ - $\text{CO}_2$  are used in the laboratory test programme.

A test rig has been developed to safely fill and recover gas mixtures of  $\text{CF}_3\text{I}$ - $\text{CO}_2$  in switchgear. Practical medium voltage (MV) switch disconnectors and ring main units are used to test the insulation properties of  $\text{CF}_3\text{I}$ - $\text{CO}_2$  gas mixtures and compared with  $\text{SF}_6$  using standard lightning impulses (1.2/50  $\mu\text{s}$ ). The experimental mixture ratios are used to identify how the insulation strength varies depending on the content of  $\text{CF}_3\text{I}$  used. The switchgear is filled to its normal and minimum operating pressure to observe the reduction in insulation performance of the gas mixtures when the pressure is reduced. The insulation strength is measured using the 50% breakdown voltages ( $U_{50}$ ) and withstand strengths of each gas mixture in accordance with international standards.

The effective ionisation coefficients of various  $\text{CF}_3\text{I}$ - $\text{CO}_2$  gas mixtures are calculated. This process identified the estimated critical reduced electric field strengths of several  $\text{CF}_3\text{I}$ - $\text{CO}_2$  gas mixtures. Furthermore, electric field simulations utilised the effective ionisation coefficient functions and the contact geometry of a switch disconnector to predict the likelihood of a flashover occurring for various  $\text{CF}_3\text{I}$ - $\text{CO}_2$  gas mixtures.

This investigation shows that  $\text{CF}_3\text{I}$ - $\text{CO}_2$  can successfully be used to insulate practical MV switchgear but is dependent on equipment design and operating pressure. It has previously been indicated that by-products of  $\text{CF}_3\text{I}$  make it unsuitable to interrupt high current. Therefore, it is suggested in this study that  $\text{CF}_3\text{I}$ - $\text{CO}_2$  gas mixtures can be adopted to insulate equipment such as vacuum circuit breakers.

## Table of Contents

Declaration / Statements .....	i
Acknowledgements.....	ii
Summary .....	iii
Table of Contents .....	iv
List of Figures .....	viii
List of Tables.....	xii
List of Abbreviations.....	xiv
<b>CHAPTER 1 INTRODUCTION .....</b>	<b>1</b>
1.1 Background .....	1
1.2 Thesis objectives .....	6
1.3 Contributions to new research.....	6
1.4 Thesis contents.....	7
<b>CHAPTER 2. LITERATURE REVIEW OF SF<sub>6</sub>, CF<sub>3</sub>I AND CF<sub>3</sub>I GAS MIXTURES.....</b>	<b>9</b>
2.1 Introduction .....	9
2.1.1 Gaseous properties of SF <sub>6</sub> .....	10
2.1.2 Problems with the continued use of SF <sub>6</sub> .....	10
2.1.3 Ideal qualities of a new gas insulation medium .....	11
2.2 Environmental characteristics of SF <sub>6</sub> , CF <sub>3</sub> I and CF <sub>3</sub> I gas mixtures .....	12
2.2.1 Atmospheric lifetime .....	12
2.2.2 Ozone-depletion potential (ODP) .....	13
2.2.3 Global warming potential (GWP).....	14
2.3 Electronegative gases.....	15
2.3.1 SF <sub>6</sub> bonds .....	16
2.3.2 CF <sub>3</sub> I bonds .....	18
2.3.3 Comparative dielectric strengths of SF <sub>6</sub> and other gases.....	19
2.4 SF <sub>6</sub> , CF <sub>3</sub> I and CF <sub>3</sub> I gas mixture electron interaction properties .....	21
2.4.1 Electron drift velocity .....	21
2.4.2 Effective ionization coefficients.....	22
2.4.3 Limiting field strength.....	24
2.5 Breakdown mechanisms .....	24
2.5.1 Corona stabilised breakdown .....	25
2.5.2 Leader breakdown .....	26
2.5.3 Practical breakdown levels in GIS .....	27
2.6 Review of experimental tests.....	27
2.6.1 Partial discharge inception voltage .....	27
2.6.2 Gas insulation for short rise time surges (lightning impulse) or fast transients or slowly applied switching surges.....	28

2.6.3 Breakdown voltage characteristics of SF <sub>6</sub> , CF <sub>3</sub> I and CF <sub>3</sub> I gas mixtures .....	29
2.6.4 Breakdown characteristics on the dielectric surface.....	30
2.6.5 Electrode configuration .....	31
2.6.6 Field utilization factor .....	34
2.6.7 Short line fault (SLF) and breaker terminal fault (BTF) interruption capability of CF <sub>3</sub> I and SF <sub>6</sub> .....	35
2.7 Phase change gas-liquid data .....	37
2.8 By-products and gas decomposition of CF <sub>3</sub> I .....	39
2.8.1 Measurement of fluorine by-products .....	40
2.8.2 Measurement of iodine by-products.....	41
2.8.3 Damage of iodine by-products to equipment and insulation properties of CF <sub>3</sub> I ....	43
2.8.4 Methods of reducing / eliminating fluorine and iodine by-products .....	44
2.9 Discussion and conclusion.....	48
<b>CHAPTER 3. SF<sub>6</sub> POWER PLANT AND GAS LEAKAGE .....</b>	<b>51</b>
3.1 Introduction .....	51
3.2 Historical review of SF <sub>6</sub> equipment.....	51
3.3 Typical distribution network which utilises SF <sub>6</sub> equipment .....	55
3.4 UK substation layouts.....	56
3.5 MV distribution equipment design .....	58
3.6 Worldwide / UK use of SF <sub>6</sub> and its effects.....	60
3.7 Conclusion .....	69
<b>CHAPTER 4 DEVELOPMENT OF LABORATORY EXPERIMENTAL RIGS AND TEST METHODOLOGY .</b>	<b>71</b>
4.1 Introduction .....	71
4.2 SF <sub>6</sub> switchgear for exploring applications of CF <sub>3</sub> I and CF <sub>3</sub> I-CO <sub>2</sub> mixtures .....	72
4.2.1 SF <sub>6</sub> applications for exploring applications of CF <sub>3</sub> I and CF <sub>3</sub> I-CO <sub>2</sub> mixtures .....	73
4.2.2 Schneider electric switch disconnectors specifications.....	74
4.2.3 Fluokit – ISR switch disconnector connections and operation diagrams .....	77
4.2.4 Ringmaster switch disconnector connections and operation diagrams .....	79
4.2.5 Switch disconnectors testing arrangement .....	81
4.3 Practical aspects of setup and operation of gas recovery and handling equipment .....	82
4.3.1 CF <sub>3</sub> I-CO <sub>2</sub> ideal gas mixture calculations .....	82
4.3.1.1 Ideal gas mixture calculations .....	82
4.3.1.2 Gas required for experimental testing .....	87
4.3.2 Gas handling equipment specifications.....	88
4.4 Lightning impulse generator test setup .....	90
4.4.1 Haefely lightning impulse generator test setup .....	90
4.4.2 British and IEC standards for switchgear .....	91
4.4.2.1 Basic lightning impulse U <sub>50</sub> gas insulation test.....	91
4.4.2.2 Basic lightning impulse withstand test.....	92

4.5 Preliminary tests .....	93
4.5.1 Standard lightning impulse test peak voltage value.....	94
4.5.2 Lightning impulse test oscilloscope waveforms and their interpretations .....	95
4.5.3 Closed switch phase-phase gas insulation comparison results.....	97
4.5.3.1 Closed switch phase-phase gas insulation Fluokit M24+ results .....	98
4.5.3.2 Closed switch phase-phase gas insulation Ringmaster SE6 results.....	101
4.6 Conclusion .....	105
<b>CHAPTER 5 COMPARATIVE LIGHTNING IMPULSE WITHSTAND PERFORMANCE OF SF<sub>6</sub> AND CF<sub>3</sub>I-CO<sub>2</sub> GAS FILLED SWITCH DISCONNECTORS .....</b>	<b>107</b>
5.1 Introduction .....	107
5.2 Open switch phase-earth gas insulation (U <sub>50</sub> ) comparison results.....	108
5.2.1 Breakdown voltage (U <sub>50</sub> ) on the open switch phase-earth gas insulation of the Fluokit M24+ .....	109
5.2.2 Open switch phase-earth gas insulation (U <sub>50</sub> ) Ringmaster SE6 results .....	117
5.3 Open switch phase-earth gas withstand test results .....	122
5.3.1 Open switch phase-earth gas withstand Fluokit M24+ test results .....	123
5.3.2 Open switch phase-earth gas withstand Ringmaster SE6 test results .....	124
5.4 Fluokit and Ringmaster insulation and withstand tests .....	125
5.5 Conclusion .....	128
<b>CHAPTER 6 RINGMASTER SWITCH DISCONNECTOR ELECTRIC FIELD SIMULATIONS AND EFFECTIVE IONIZATION COEFFICIENTS.....</b>	<b>129</b>
6.1 Introduction .....	129
6.2 Ringmaster switch disconnecter electric field simulations.....	130
6.3 Effective ionisation coefficients .....	135
6.4 Evaluation of flashover occurrences .....	143
6.4.1 Ringmaster Comsol simulation - air – 0 bar (g) .....	146
6.4.2 Ringmaster Comsol simulation - SF <sub>6</sub> - 0 bar (g) .....	150
6.4.3 Ringmaster net electron production region simulations.....	151
6.4.4 Ringmaster discharge probability simulations .....	152
6.5 Proposed options for Ringmaster contact design optimisation for CF <sub>3</sub> I-CO <sub>2</sub> gas mixtures .....	158
6.6 Conclusion .....	160
<b>CHAPTER 7 A PROPOSAL FOR CF<sub>3</sub>I INSULATED VACUUM SWITCHGEAR.....</b>	<b>162</b>
7.1 Introduction .....	162
7.2 Ring main unit chosen for testing .....	163
7.3 SCRMU(M) gas connections .....	165
7.4 SCRMU(M) gas mixture calculations .....	166
7.5 Lucy SCRMU(M) standard lightning impulse withstand tests and connections .....	167
7.6 Lucy SCRMU standard lightning impulse withstand test results .....	170
7.7 Conclusion .....	171
<b>CHAPTER 8. CONCLUSION .....</b>	<b>172</b>

8.1 Conclusion .....	172
8.2 CF <sub>3</sub> I / CF <sub>3</sub> I-CO <sub>2</sub> in power plant design.....	177
8.3 Power industry adoption rate .....	178
8.4 Future work.....	178
References.....	i
<b>Appendix A.....</b>	<b>vii</b>
A1. Primary substations .....	vii
A2. Urban distribution system switching arrangements and secondary substations.....	viii
A3. MV distribution equipment design .....	ix
A4. HV gas insulated switchgear (GIS).....	x
A5. Gas insulated lines (GIL).....	xi
<b>Appendix B.....</b>	<b>xiii</b>
B1. Gas connections and adapters.....	xiii
B2. Evacuation of the gas compartment with Dilo equipment.....	xv
B3. Filling the gas compartment with gas with overpressure with Dilo equipment.....	xvi
B4. Recovery and storage of the gas compartment with Dilo equipment.....	xvii
B5. Main connection diagram for gas filling and recovery.....	xix
B6. Gas connection for filling CF <sub>3</sub> I-CO <sub>2</sub> pressure-pressure mixture storage cylinders.....	xx
<b>Appendix C.....</b>	<b>xxi</b>
<b>Appendix D.....</b>	<b>xxiv</b>

## List of Figures

Figure 2.1: Electronegativity of elements .....	16
Figure 2.2: SF <sub>6</sub> octahedral molecular shape and its bonded electrons .....	17
Figure 2.3: CF <sub>3</sub> I tetrahedral molecular shape and its bonded electrons .....	19
Figure 2.4: Electron drift velocity in CF <sub>3</sub> I as a function of E/N .....	22
Figure 2.5: Electron drift velocities (V <sub>e</sub> ) in a) CF <sub>3</sub> I-N <sub>2</sub> mixtures b) CF <sub>3</sub> I-CO <sub>2</sub> mixtures as a function of E/N at different CF <sub>3</sub> I gas mixture ratios k .....	22
Figure 2.6: Effective ionization coefficient ( $\alpha - \eta$ )/N of CF <sub>3</sub> I as a function of E/N .....	23
Figure 2.7: Density-normalised effective ionization coefficients ( $\alpha - \eta$ )/N .....	23
Figure 2.8: The limiting fields (E/N) <sub>lim</sub> as a function of CF <sub>3</sub> I or SF <sub>6</sub> gas content k .....	24
Figure 2.9: AC corona onset and breakdown characteristics for a positive point 40 mm rod-plane gap in SF <sub>6</sub> .....	25
Figure 2.10: Schematic of leader development .....	26
Figure 2.11: AC PDIV and sparkover voltage (BDV) in CF <sub>3</sub> I and SF <sub>6</sub> , needle (0.5 mm)- to-plane electrode configuration, gap length is 10 mm .....	28
Figure 2.12: Positive breakdown voltage characteristics in CF <sub>3</sub> I-CO <sub>2</sub> at 0.1 MPa (abs) .....	29
Figure 2.13: Negative breakdown voltage characteristics in CF <sub>3</sub> I-CO <sub>2</sub> at 0.1 MPa (abs) .....	30
Figure 2.14 Relation between the number of flashover and time lag to flashover .....	31
Figure 2.15: Schematic diagram of electrodes .....	32
Figure 2.16: Breakdown properties of 30%:70% CF <sub>3</sub> I-CO <sub>2</sub> for various electrodes at 1 bar .....	33
Figure 2.17: Breakdown properties of 30%:70% CF <sub>3</sub> I-CO <sub>2</sub> for various gas pressures for a rod-plane electrode configuration .....	33
Figure 2.18: V-t characteristics of CF <sub>3</sub> I at 0.1 MPa, gap 10mm (positive polarity) .....	34
Figure 2.19: V-t characteristics of SF <sub>6</sub> at 0.1 MPa, gap 10mm (positive polarity) .....	35
Figure 2.20: Minimum sparkover voltage vs field utilization factor .....	35
Figure 2.21: Transition of SLF interruption performance to CF <sub>3</sub> I ratio of CF <sub>3</sub> I mixture gas .....	36
Figure 2.22: Transition of BTF interruption performance to CF <sub>3</sub> I ratio of CF <sub>3</sub> I mixture gas .....	37
Figure 2.23: Saturation vapour pressure curve in CF <sub>3</sub> I and SF <sub>6</sub> .....	37
Figure 2.24: Gaseous by-products as a function of cumulative charge q <sub>c</sub> .....	40
Figure 2.25: Density of fluorine when a) current is interrupted frequently b) current is interrupted one time only .....	41
Figure 2.26: Density of iodine when a) current is interrupted frequently b) current is interrupted one time only .....	42
Figure 2.27: The saturation vapour curve of the iodine molecule .....	43
Figure 2.28: Gaseous by-products of SF <sub>6</sub> a) without absorbent b) with molecular sieve .....	45
Figure 2.29: Density of iodine shortly after interruption when absorbent is placed .....	47
Figure 2.30: Density of iodine after absorption of about 5 mins .....	47
Figure 3.1: Types of breaking devices used according to voltage values .....	52
Figure 3.2: Development of the MV circuit breaker market in Europe .....	53
Figure 3.3: Influence of inter-electrode gap on dielectric strength .....	54
Figure 3.4: Typical distribution levels .....	55
Figure 3.5: SF <sub>6</sub> distribution equipment on a typical distribution network .....	55
Figure 3.6: Typical urban distribution system with potential replacement CF <sub>3</sub> I-CO <sub>2</sub> switches and circuit breakers .....	57
Figure 3.7: Three position rotary puffer contact design .....	59
Figure 3.8: Estimated total amount of SF <sub>6</sub> employed in UKPN MV network .....	64

Figure 3.9: Estimated 25 year leakage of UK Power Networks MV SF <sub>6</sub> distribution equipment. ....	64
Figure 3.10: Reported SF <sub>6</sub> emissions for April 2012 – March 2013 .....	65
Figure 3.11: Estimated total amount of SF <sub>6</sub> employed worldwide in MV distribution networks. ....	66
Figure 3.12: Estimated 25 year leakage of SF <sub>6</sub> worldwide MV distribution equipment.	66
Figure 3.13: Estimated total amount of SF <sub>6</sub> employed worldwide in HV distribution networks. ....	67
Figure 3.14: Estimated 25 year leakage of SF <sub>6</sub> worldwide HV distribution equipment.	68
Figure 3.15: Estimated total of SF <sub>6</sub> employed worldwide in distribution networks.....	68
Figure 3.16: Estimated 25 year leakage of SF <sub>6</sub> worldwide distribution equipment. ....	69
Figure 4.1: Schneider Electric medium voltage switchgear selection guide .....	74
Figure 4.2: a) and b) Fluokit M24+ switch disconnecter c) switch diagram .....	78
Figure 4.3: Side of Fluokit switch disconnecter unit with cable connections and gas filling point .....	79
Figure 4.4: Operation and connections of the Ringmaster switch disconnecter.....	80
Figure 4.5: Ringmaster switch disconnecter earthing connections and gas filling point. ....	80
Figure 4.6: Ringmaster SE6 and Fluokit M24+ switch disconnectors used for testing..	81
Figure 4.7: Lightning impulse generator connection to switch disconnectors.....	82
Figure 4.8: Dilo mini series complete with vacuum pump, filter, compressor and vacuum compressor for vacuuming, gassing and de-gassing switchgear .....	90
Figure 4.9: Lightning impulse generator test setup.....	91
Figure 4.10: Diagram of connection of a three-pole switching device .....	92
Figure 4.11: Connection diagram for main components of lightning impulse test setup	93
Figure 4.12: Standard 125 kV lightning impulse Fluokit M24+ (F1), Main switch Phase 3, 100% SF <sub>6</sub> , 0.45 bar G. ....	94
Figure 4.13: Applied lightning impulse (LI) voltage (orange) and current measurement (green) – no breakdown.....	95
Figure 4.14: Applied LI – air breakdown / equipment failure .....	96
Figure 4.15: Applied LI – gas breakdown .....	96
Figure 4.16: Applied LI – short time to breakdown.....	96
Figure 4.17: Applied LI – long time to breakdown .....	96
Figure 4.18: Phase to Phase lightning impulse insulation strength test connections. ....	97
Figure 4.19: Fluokit M24+ switch disconnecter lightning impulse (LI) applied to Phase 1 on a closed switch Phase-Phase gas insulation strength tests .....	99
Figure 4.20: Fluokit M24+ switch disconnecter lightning impulse (LI) closed switch Phase-Phase gas insulation strength tests when LI is applied to Phase 2.....	99
Figure 4.21: Fluokit M24+ switch disconnecter lightning impulse (LI) closed switch Phase-Phase gas insulation strength tests when LI is applied to Phase 3.....	100
Figure 4.22: Fluokit M24+ switch disconnecter lightning impulse (LI) arc path length in a closed switch Phase-Phase gas insulation strength tests when LI is applied to Phase 1 or 2 (Left) or Phase 3 (Right). ....	100
Figure 4.23: Fluokit side view with phase-phase dielectric barrier .....	101
Figure 4.24: Ringmaster SE6 switch disconnecter lightning impulse (LI) closed switch Phase-Phase gas insulation strength tests when LI is applied to Phase 1.....	102
Figure 4.25: Ringmaster SE6 switch disconnecter lightning impulse (LI) closed switch Phase-Phase gas insulation strength tests when LI is applied to Phase 3.....	103
Figure 4.26: Ringmaster SE6 switch disconnecter lightning impulse (LI) closed switch Phase-Phase gas insulation strength tests when LI is applied to Phase 2.....	103

Figure 4.27: Ringmaster SE6 switch disconnecter lightning impulse (LI) arc path length in a closed switch Phase-Phase gas insulation strength tests when LI is applied to Phase 1 or 3 (right) and Phase 2 (left). .....	103
Figure 4.28: Ringmaster side view with phase-phase dielectric barrier .....	104
Figure 5.1: Single Phase open switch Phase-Earth LI insulation strength test connections. ....	108
Figure 5.2: Fluokit M24+ switch disconnecter lightning impulse ( $U_{50}$ ) open switch Phase-Earth gas insulation results at 0.45 bar G and 0 bar G for all phases. ....	111
Figure 5.3: Percentage of gas and equipment breakdowns during Fluokit lightning impulse ( $U_{50}$ ) open switch Phase-Earth gas insulation tests at 0.45 bar G. ....	112
Figure 5.4: Percentage of gas and equipment breakdowns during Fluokit lightning impulse ( $U_{50}$ ) open switch Phase-Earth gas insulation tests at 0 bar G. ....	113
Figure 5.5: Fluokit Air breakdown between the top main switch busbar contact and the earthed metal casing above the phase connection or the closest earthed phase. ....	115
Figure 5.6: Fluokit Air gap length between the phase top main switch busbar contacts and the earthed metal casing or the nearest phase connection. ....	116
Figure 5.7: Fluokit Phase 1 epoxy resin breakdown / metal gas filling point adapter to earthed metal casing breakdown. ....	117
Figure 5.8: Fluokit Phase 2 epoxy resin failure possible caused by residual charge on the inside of the epoxy resin gas chamber.....	117
Figure 5.9: Ringmaster SE6 switch disconnecter lightning impulse ( $U_{50}$ ) open switch Phase-Earth gas insulation results at 0.35 bar G and 0 bar G for all phases. ....	119
Figure 5.10: Percentage of gas and equipment breakdowns during Ringmaster lightning impulse open switch Phase-Earth gas insulation tests at 0.35 bar G.....	121
Figure 5.11: Percentage of gas and equipment breakdowns during Ringmaster lightning impulse open switch Phase-Earth gas insulation tests at 0 bar G.....	122
Figure 5.12: Percentage gas failure per phase during a 95 kV lightning impulse withstand test in the Ringmaster SE6 switch disconnecter. ....	125
Figure 5.13: Average percentage gas failure per phase during a 95 kV lightning impulse withstand test in the Ringmaster SE6 switch disconnecter. ....	125
Figure 5.14: Fluokit M24+ switch disconnecter LI open switch Phase-Earth gas insulation results, at 0.45 bar G and 0 bar G, as an average for all phases. ....	126
Figure 5.15: Ringmaster SE6 switch disconnecter LI open switch Phase-Earth gas insulation results, at 0.45 bar G and 0 bar G, as an average for all phases. ....	127
Figure 6.1: Schneider Electric Ringmaster SE6 switch disconnecter schematics .....	130
Figure 6.2: Ringmaster SE6 switch disconnecter schematics overlayed on the unit....	131
Figure 6.3: Materials used to manufacture the Ringmaster switch disconnecter .....	131
Figure 6.4: Ringmaster full contact simulation model.....	132
Figure 6.5: Electrostatic model elements – a) 95 kV applied terminal, b) floating potential and c) grounding point. ....	132
Figure 6.6: Ringmaster Comsol model mesh. ....	133
Figure 6.7: Computed equipotentials for the Ringmaster. ....	133
Figure 6.8: a) 2d Ringmaster slice model, b) applied electrostatic conditions – 95 kV electric potential and c) grounded terminal. ....	134
Figure 6.9: 2d Ringmaster Comsol model mesh size.....	134
Figure 6.10: Computed 2d Ringmaster equipotentials and electric field lines. ....	135
Figure 6.11: Ringmaster SE6 switch disconnecter high electrical stress points.....	135
Figure 6.12: Effective ionisation coefficients in air and $SF_6$ .....	136
Figure 6.13: Electron collision cross section data used for BOLSIG+ calculations. ....	137
Figure 6.14: 30%:70% $CF_3I$ - $CO_2$ Townsend coefficients. ....	139
Figure 6.15: 30%:70% $CF_3I$ - $CO_2$ ionization rate, attachment rate and effective ionisation. ....	141

Figure 6.16: Effective ionisation for Air, CO <sub>2</sub> , CF <sub>3</sub> I, SF <sub>6</sub> , 10%:90% CF <sub>3</sub> I-CO <sub>2</sub> , 20%:80% CF <sub>3</sub> I-CO <sub>2</sub> and 30%:70% CF <sub>3</sub> I-CO <sub>2</sub> . .....	142
Figure 6.17: Ringmaster charged particle tracing simulation inlet (left) and wall (right) boundary conditions. ....	146
Figure 6.18: Electric field lines between high voltage contact (95 kV) and grounded contact and bounded region where the electric field is > 26 kV/cm bar for air. ....	147
Figure 6.19: Electric field lines between high voltage contact (75 kV) and grounded contact and bounded region where the electric field is > 26 kV/cm bar for air. ....	147
Figure 6.20: Region which has a positive net electron production (ionisation coefficient > 0) close to the positive contact (95 kV) for air at atmospheric pressure. ....	148
Figure 6.21: Region which has a positive net electron production (ionisation coefficient > 0) close to the positive contact (75 kV) for air at atmospheric pressure. ....	148
Figure 6.22: Field lines for discharges starting from the positive contact (95 kV) Air 0 bar (g). ....	149
Figure 6.23: Field lines for discharges starting from the positive contact (75 kV) Air 0 bar (g). ....	150
Figure 6.24: Electric field lines between high voltage contact (95 kV) and grounded contact and bounded region where the electric field is > 88 kV/cm bar for SF <sub>6</sub> . ....	151
Figure 6.25: Region which has a positive net electron production (electric field > critical reduced electric field strength) close to the positive contact with an applied voltage of 95 kV at 0 bar (g). ....	153
Figure 6.26: Region which has a positive net electron production (electric field > critical reduced electric field strength) close to the positive contact with an applied voltage of 95 kV at 0.35 bar (g). ....	154
Figure 6.27: Expansion rate of the region which has a positive net electron production for Air, SF <sub>6</sub> , CF <sub>3</sub> I, 30:70% CF <sub>3</sub> I-CO <sub>2</sub> , 20:80% CF <sub>3</sub> I-CO <sub>2</sub> ..... and 10:90% CF <sub>3</sub> I-CO <sub>2</sub> at 0 bar (g). ....	155
Figure 6.28: Field lines for discharges starting from the positive contact with an applied voltage of 95 kV at 0 bar (g). ....	156
Figure 6.29: Field lines for discharges starting from the positive contact with an applied voltage of 95 kV at 0.35 bar (g). ....	157
Figure 6.30: Electric field plot of Ringmaster contacts with sharp points. ....	158
Figure 6.31: Electric field plot of Ringmaster contacts with rounded edges. ....	159
Figure 7.1: A Lucy SCRMU(M) .....	164
Figure 7.2: An internal view of a Lucy switchgear sabre VRN6a RMU .....	164
Figure 7.3: Filling of the SCRMU(M) gas chamber. ....	166
Figure 7.4: Connections and operational components of the SCRMU(M). ....	168
Figure 7.5: RMU positive lightning impulse gas insulation test position for ring switch. .....	169
Figure 7.6: RMU positive lightning impulse gas insulation test position for circuit breaker. ....	170
Figure A1: Typical distribution primary substation layout: single busbar switching arrangement .....	vii
Figure A2: Rollarc R400 – 400D arc rotation contactor .....	x
Figure A3: Self blast puffer circuit breaker .....	x
Figure A4: ABB SF <sub>6</sub> gas insulated switchgear (GIS) line bay .....	xi
Figure A5: Siemens gas insulated lines .....	xii
Figure B1: a) Dilo soldering union with O-ring PN64 b) VK/A-02/8 T coupling groove part DN8 with O-ring c) 3-393-R001 gas refilling device d) Z247R21 Tee piece 0- 60 bar pressure gauge e) 4 x 10 L steel gas storage cylinder .....	xiii
Figure B2: Connections used for vacuuming, gassing and de-gassing the switch disconnectors. ....	xiv

Figure B3: Evacuation of the switch disconnectors with Dilo equipment.....	xv
Figure B4: Filling the switch disconnectors with gas with overpressure with Dilo equipment .....	xvi
Figure B5: Recovery and storage of the gas compartment with Dilo equipment .....	xviii
Figure B6: Dilo equipment connections to Fluokit and Ringmaster.....	xix
Figure B7: Filling of CF <sub>3</sub> I-CO <sub>2</sub> storage cylinders via gas mixture chamber. ....	xx
Figure B8: Complete gas connections for the Ringmaster and Fluokit switch disconnectors. ....	xx
Figure C1: Example of a 95 kV withstand (Class 1) test – Ringmaster (R2) – Phase 1 (L1) – 30:70% CF <sub>3</sub> I-CO <sub>2</sub> – 0 bar (g). ....	xxii
Figure C2: Example of U <sub>50</sub> (Class 2) tests – Ringmaster (R2) – Phase 2 (L2) and Phase 3 (L3) – 30:70% CF <sub>3</sub> I-CO <sub>2</sub> – 0 bar (g). ....	xxiii
Figure D1: A gas chamber surrounding one phase of the Ringmaster Comsol model and its schematics.....	xxiv
Figure D2: Materials used for the simulation model included: copper, steel and plastic (left to right). ....	xxiv

## List of Tables

Table 2.1: Global warming potential for SF <sub>6</sub> and CF <sub>3</sub> I.....	15
Table 2.2: Relative DC uniform-field breakdown strengths .....	20
Table 2.3: Boiling point of different gases.....	38
Table 3.1: Various switching devices, their functions and their applications.....	58
Table 3.2: Estimated MV SF <sub>6</sub> RMUs employed by UK Power Networks .....	61
Table 3.3: Estimated MV SF <sub>6</sub> RMUs employed worldwide.....	61
Table 3.4: Estimated MV SF <sub>6</sub> CBs employed by UK Power Networks .....	61
Table 3.5: Estimated MV SF <sub>6</sub> Ringmaster CBs employed by UK Power Networks.....	61
Table 3.6: Estimated SF <sub>6</sub> MV CBs employed worldwide.....	62
Table 3.7: Estimated MV SF <sub>6</sub> switches employed by UK Power Networks .....	62
Table 3.8: Estimated MV Ringmaster type SF <sub>6</sub> switches employed on UK Power Networks distribution network.....	62
Table 3.9: Estimated MV SF <sub>6</sub> switches employed worldwide.....	63
Table 3.10: Estimated MV SF <sub>6</sub> RMUs, CBs & switches employed on UK Power Networks distribution network.....	63
Table 3.11: Estimated MV SF <sub>6</sub> RMUs, CBs & switches employed worldwide.....	63
Table 3.12: Estimated HV SF <sub>6</sub> GIS employed worldwide.....	67
Table 3.13: Estimated HV SF <sub>6</sub> open type CBs employed worldwide .....	67
Table 3.14: Estimated HV SF <sub>6</sub> GIL employed worldwide .....	67
Table 4.1: Manufacturers rated insulation capabilities, tolerances and specifications of switch disconnectors.....	76
Table 4.2: CF <sub>3</sub> I and its decomposition products .....	83
Table 4.3: Calculated pressure-pressure gas mixture ratios.....	86
Table 4.4: Calculated quantity of gases required to fill the Fluokit and Ringmaster switch disconnectors.....	86
Table 4.5: Total gas needed to fill Ringmaster and Fluokit with added overpressure....	87
Table 4.6: Cost of gases from Apollo Scientific .....	88

Table 4.7: Fluokit M24+ switch disconnector lightning impulse (LI) closed switch Phase-Phase gas insulation strength tests. ....	98
Table 4.8: Ringmaster SE6 switch disconnector lightning impulse (LI) closed switch Phase-Phase gas insulation strength tests. ....	102
Table 5.1: Fluokit M24+ switch disconnector lightning impulse ( $U_{50}$ ) open switch Phase-Earth gas insulation results at the rated filling pressure of 0.45 bar G. ....	109
Table 5.2: Fluokit M24+ switch disconnector lightning impulse ( $U_{50}$ ) open switch Phase-Earth gas insulation results at the minimum operating pressure of 0 bar G. .	110
Table 5.3: Fluokit M24+ switch disconnector number of gas failures during lightning impulse open switch Phase-Earth gas insulation tests at 0.45 bar G. ....	111
Table 5.4: Fluokit M24+ switch disconnector number of gas failures during lightning impulse open switch Phase-Earth gas insulation tests at 0 bar G. ....	112
Table 5.5: Ringmaster SE6 switch disconnector lightning impulse ( $U_{50}$ ) open switch Phase-Earth gas insulation results at 0.35 bar G. ....	118
Table 5.6: Ringmaster SE6 switch disconnector lightning impulse ( $U_{50}$ ) open switch Phase-Earth gas insulation results at 0 bar G. ....	119
Table 5.7: Ringmaster SE6 switch disconnector number of gas failures during lightning impulse open switch Phase-Earth gas insulation tests at 0.35 bar G. ....	120
Table 5.8: Ringmaster SE6 switch disconnector number of gas failures during lightning impulse open switch Phase-Earth gas insulation tests at 0 bar G. ....	120
Table 5.9: Fluokit M24+ rated lightning impulse withstand test results. ....	123
Table 5.10: Ringmaster SE6 rated lightning impulse withstand test results. ....	124
Table 6.1: Relative permittivity ( $\epsilon$ ) of each material modelled from COMSOL. ....	132
Table 6.2: Transport coefficients. ....	138
Table 6.3: An example of Townsend coefficients / N ( $m^2$ ) calculated using BOLSIG+ for the gas mixture 30% $CF_3I$ – 70% $CO_2$ . ....	138
Table 6.4: Calculated electric field (V/m), ionization rate / N ( $m^2$ ), attachment rate / N ( $m^2$ ) and effective ionization (/m). ....	140
Table 6.5: Calculated electric field (kV/cm) and effective ionization (/cm). ....	140
Table 6.6: Effective ionization functions and critical field strengths for $SF_6$ , $CF_3I$ and $CF_3I$ - $CO_2$ gas mixtures. ....	145
Table 6.7: Critical reduced electric field strength and critical number of all gas mixtures .....	145
Table 7.1: Manufacturers specifications of the SCRMU(M) RMU. ....	165
Table 7.2: 30%:70% $CF_3I$ - $CO_2$ RMU 75 kV positive lightning impulse withstand voltage tests. ....	170
Table 7.3: 30%:70% $CF_3I$ - $CO_2$ RMU average 75 kV positive lightning impulse withstand voltage tests. ....	171

## List of Abbreviations

CF<sub>3</sub>I - Trifluoriodomethane  
CO<sub>2</sub> – Carbon dioxide  
SF<sub>6</sub> – Sulphur hexafluoride  
N<sub>2</sub> – Nitrogen  
F – Fluorine  
I - Iodine  
GIS – Gas insulated switchgear  
GIL – Gas insulated line  
RMU – Ring main unit  
GCB – Gas circuit breaker  
CB – Circuit breaker  
LV – Low voltage (220 V – 1 kV)  
MV – Medium voltage (1 kV – 52 kV)  
HV – High voltage (52 kV – 300 kV)  
EHV – Extra high voltage (300 kV – 800 kV)  
GWP – Global warming potential  
ODP – Ozone depleting potential  
IR – Infrared  
pptv – Parts per trillion per volume  
EN – Electronegativity  
EA – Electron affinity  
 $\alpha$  – Ionization coefficient  
 $\eta$  – Electron attachment rate  
(E/N)<sub>lim</sub> – Limiting field strength  
(E/p)<sub>crit</sub> – Critical reduced electric field strength  
 $\alpha_{\text{eff}}(E)$  - Effective ionisation function  
PD – Partial discharge  
PDIV – Partial discharge inception voltage  
BDV – Breakdown voltage  
BIL – Basic impulse level  
LI – Lighting impulse  
U<sub>50</sub> – Voltage at which there is a 50% probability of a breakdown occurring  
U<sub>p</sub> – Rated lightning impulse withstand voltage  
MPa – MegaPascal (unit of pressure)  
Td – Townsend (unit)  
abs – Absolute pressure  
bar G or bar (g) – bar gauge (unit of pressure)  
GC-MS – Gas chromatography and mass spectroscopy detector  
NOP – Normally open point  
EHC – Extra high current  
BS – British standard  
MW – Molecular weight

# CHAPTER 1

## INTRODUCTION

---

### 1.1 Background

SF<sub>6</sub> is utilised throughout the world in distribution and transmission networks as an insulating medium in a large range of gas insulated switchgear (GIS) for switching, earth switching, circuit breaking and general circuit protection. Common GIS equipment used on the distribution networks include: Ring Main Units (RMUs), switches, switch disconnectors, circuit breakers and contactors all using SF<sub>6</sub> to either insulate the equipment or to quench an arc when a circuit is broken or switched. SF<sub>6</sub> is also the insulating medium of choice in gas insulated lines (GIL) where the gas is used to insulate high voltage lines.

At the beginning of the 1980s, the main insulating medium for medium voltage (MV) [1] circuit breakers was oil or air. At that time, vacuum and SF<sub>6</sub> insulation was only used in

a small proportion of circuit breakers. However, over time the dominating insulating media for circuit breakers on the MV network has become SF<sub>6</sub> and vacuum [2]. There are numerous reasons for this change including the technical development to accommodate a higher voltage range and refinement of this equipment to occupy a small space [3]. Oil has a poor maintenance and fire hazard record [4], whilst the other media, SF<sub>6</sub> in particular, require less maintenance and are comparatively safer to operate [5] [6]. Another reason for large scale deployment of vacuum and SF<sub>6</sub> technology is based on substation design and the fact that substations can be far smaller than when air or oil is used as the insulating medium [2]. The gap needed between electrodes is relatively small in SF<sub>6</sub> and vacuum devices when compared to other technologies and can be used to break higher voltages, which has led to the development of smaller equipment [5]. This in turn results in a reduction in the space needed for substations which lowers their cost substantially, especially within urban environments. The use of vacuum technology as an interrupting dielectric is commonly used up to around 36 kV [2] but has been developed up to 132 kV [7]. At present, the development of vacuum technology as a circuit breaking medium for higher voltages is constrained whereas SF<sub>6</sub> has proven that it can be utilised in equipment up to and including 800 kV [2]. This has led to the almost exclusive use of SF<sub>6</sub> in HV (52 – 300 kV) [1] and EHV (300 to 800 kV) networks as there is currently no other alternative gas insulating medium that has the same interruption performance and insulation performance of SF<sub>6</sub>.

The reasons for SF<sub>6</sub> becoming a widely used and a popular dielectric medium can be assigned to the properties of the gas:

- It is a chemically inert gas [8]
- It has a low boiling point [9]
- It is thermally stable at temperatures less than 500°C [3]
- It has excellent arc extinction properties (strongly electronegative) [3]

- It is non-toxic [3]
- It is non-flammable [10]
- It is non-explosive [4]
- It has a breakdown voltage nearly three times that of air at atmospheric pressure [11]
- It has a very quick recovery rate after arc extinction [3]
- It is benign with regard to stratospheric ozone depletion with an ozone depletion potential (ODP) roughly equal to zero [9].

The properties of SF<sub>6</sub> have led to equipment being developed that can have:

- Smaller dimensions due to small gaps between electrodes due to the high breakdown voltage of SF<sub>6</sub> [3]
- Smaller substations due to smaller switchgear dimensions [12]
- A high performance level of insulation and circuit breaking [2]
- A high safety record due to its non-toxic, non-flammable and non-explosive nature [6]
- A low equipment and insulating medium (SF<sub>6</sub>) cost compared to other insulating media [13] due to the high volume of production and rising demand from switchgear manufacturers [2]
- Low maintenance needs (SF<sub>6</sub> vessels need not be opened for 25 – 50 years depending on manufacturer's specifications) [4].

With all these advantages a lower cost of equipment can be passed on to the distribution network operator.

The main drawbacks of the continued utilisation of SF<sub>6</sub> as an insulation medium can be found in its environmental hazards with the following being the main points of concern:

- The Global Warming Potential (GWP) of SF<sub>6</sub> is about 23,900 times that of CO<sub>2</sub> [14] as it is an efficient infrared (IR) absorber [8]

- Its chemical inertness means it cannot be readily removed from the earth's atmosphere [8]. SF<sub>6</sub> has an atmospheric lifetime around 3,200 years (est.) [9]
- If SF<sub>6</sub> is used in current interruption, the fluorine by-product density can be shown to increase exponentially, however, this can be managed with absorbents [10].

So far, the proposed solutions for replacing SF<sub>6</sub> as the main insulating medium in MV, HV and EHV networks are very few. The use of alternative vacuum technology has been suggested. However, with regards to the present research, there has been no development that could lead to the full replacement of SF<sub>6</sub> at the moment. So far, the only practical solution that has been developed is to use mixtures of SF<sub>6</sub> with another gas, so that less SF<sub>6</sub> is used in total. However, this does lead to reduced effectiveness, when compared to pure SF<sub>6</sub>, of the gas mixture ability to quench an arc and insulate equipment. So far, the use of SF<sub>6</sub>-CF<sub>4</sub> [15], SF<sub>6</sub>-Air, SF<sub>6</sub>-CO<sub>2</sub> and SF<sub>6</sub>-N<sub>2</sub> gas mixtures [16], to lower the amount of SF<sub>6</sub> needed, have been developed with SF<sub>6</sub>-N<sub>2</sub> being the gas combination that has been adopted into GIS and GIL manufacture [10] [17]. Mixture ratios of 20%:80% SF<sub>6</sub>-N<sub>2</sub> are common for GIL purposes [18]. Although the mixture of SF<sub>6</sub>-N<sub>2</sub> does reduce the breakdown strength of pure SF<sub>6</sub> the addition of nitrogen does not give a dramatic drop in performance. The mixture of SF<sub>6</sub>-N<sub>2</sub> does have the added advantage of allowing the use of SF<sub>6</sub> at lower temperatures as it reduces the boiling point of the gas [10]. Such mixtures are used for insulation purposes and not for arc interruption.

The problem that is, therefore, explored throughout this thesis is to find an alternative to SF<sub>6</sub> that may one day be used to replace its use in the distribution network altogether. This alternative, to become a viable option and utilised throughout the power industry, must have most if not all the advantages of SF<sub>6</sub> yet overcome its global environmental issues. All this must be achieved whilst no vast increase to the cost is added to the manufacturing process of distribution equipment.

One of the promising candidate alternatives to SF<sub>6</sub> is CF<sub>3</sub>I (Trifluoro-iodo-methane or Trifluoromethyl Iodine or Halon 13001) because of its promising breakdown strength in uniform electric fields and its environmental impact [19]. As no other viable alternative to SF<sub>6</sub> presently exists, this project examines the insulation strength of CF<sub>3</sub>I gas mixtures to determine whether they can be considered as a replacement for SF<sub>6</sub>.

The approach in this project is to test different mixtures of CF<sub>3</sub>I-CO<sub>2</sub> experimentally to compare their dielectric strength against that of pure SF<sub>6</sub>, CO<sub>2</sub> and air. The experimental tests were carried out on typical MV distribution switchgear units. Distribution switchgear has ‘complex’ contact geometries which will present interesting insulation challenges from the highly non-uniform electric fields created between contacts. This will help determine whether CF<sub>3</sub>I-CO<sub>2</sub> is a viable option for replacement of SF<sub>6</sub> in MV equipment and also explore application at HV and EHV level. However, in HV and EHV equipment the breakdown strength required is increased and higher gas pressures are normally used [3]. Such higher pressure may require a lower boiling point than pure CF<sub>3</sub>I can provide [10], and therefore, it is possible that a CF<sub>3</sub>I-CO<sub>2</sub> mixture will provide a low boiling point whilst maintaining CF<sub>3</sub>I’s inherent dielectric capabilities. This investigation will primarily focus on the application and insulation strength of CF<sub>3</sub>I-CO<sub>2</sub> gas mixtures. This will initially test the selected switchgear although it is known that CF<sub>3</sub>I does not have proven significant current interruption capabilities. During arcing CF<sub>3</sub>I produces iodine as a by-product, which attaches itself to contacts, reducing its performance in subsequent current interruptions [19]. It might be possible that future designs for equipment using CF<sub>3</sub>I can be engineered so that:

- Uniform electric fields are utilised between contacts to increase the breakdown voltage [19],
- Absorbents are exploited to control iodine generated when CF<sub>3</sub>I is subjected to current interruption events [9].

## 1.2 Thesis objectives

The objectives of this PhD were to:

- Survey present day SF<sub>6</sub> equipment that is used on the distribution network and procure switchgear units that could be used for experimental direct comparison of CF<sub>3</sub>I and CF<sub>3</sub>I-CO<sub>2</sub> gas mixtures with similar equipment filled with SF<sub>6</sub>.
- Set up test rigs around the acquired switchgear and carry out insulation capability tests such as lightning impulse to compare the performance of SF<sub>6</sub>, CO<sub>2</sub>, air and CF<sub>3</sub>I-CO<sub>2</sub> gas mixtures.
- Examine the internal design of the switchgear units to evaluate the breakdown performance of various CF<sub>3</sub>I-CO<sub>2</sub> gas mixtures, with particular focus upon the geometric electric field created by the internal contact design.
- Simulate the electric field created by the internal switchgear contact design, in COMSOL software, and determine possible contact geometry improvements that are particularly relevant to its use with more uniform electric fields.
- Compare the insulation strength test results of SF<sub>6</sub>, CO<sub>2</sub>, air and CF<sub>3</sub>I-CO<sub>2</sub> mixtures and determine whether CF<sub>3</sub>I or a CF<sub>3</sub>I-CO<sub>2</sub> gas mixtures, may be able to replace SF<sub>6</sub>. Opinions will be formed based on the switchgear tested and provide insights for the future use of CF<sub>3</sub>I-CO<sub>2</sub> with other MV and HV equipment for which SF<sub>6</sub> is used as an insulation medium.

## 1.3 Contributions to new research

The main contributions of this work are:

- Supplying a review of present day SF<sub>6</sub> switchgear and an extensive appraisal of the properties of CF<sub>3</sub>I and CF<sub>3</sub>I gas mixtures.

- Developing and implementing a novel test rig that can be used to test CF<sub>3</sub>I-CO<sub>2</sub> as an alternative insulation medium in practical medium voltage (MV) distribution equipment.
- Experimental investigation of CF<sub>3</sub>I insulation applications on practical MV switches.
- Experimental demonstration of the insulation properties of CF<sub>3</sub>I gas mixtures compared with SF<sub>6</sub> properties.
- Developing a simulation approach in COMSOL that can determine whether a specific mixture of CF<sub>3</sub>I-CO<sub>2</sub> gas can insulate gas insulated equipment. This uses calculated effective ionisation coefficients of various CF<sub>3</sub>I-CO<sub>2</sub> gas mixtures.
- Proposal for vacuum switchgear to use CF<sub>3</sub>I gas mixtures as a replacement insulation to SF<sub>6</sub> gas.

#### 1.4 Thesis contents

The contents of this thesis includes:

**Chapter 2:** A literature review of the present published research on CF<sub>3</sub>I and CF<sub>3</sub>I-CO<sub>2</sub> gas mixtures as alternatives to SF<sub>6</sub>. This includes the qualities that make SF<sub>6</sub> such a good insulating medium and its environmental problems. Features of CF<sub>3</sub>I are also included to examine its potential strengths and weaknesses when used as an insulating medium.

**Chapter 3:** A review of the SF<sub>6</sub> equipment that is used worldwide and on the UK distribution system and an evaluation on the effects this might have on the environment.

**Chapter 4:** A description of the laboratory equipment and testing techniques that were developed and used throughout the practical experimentation carried out in this thesis. Preliminary tests required for establishing reliable and repeatable testing on the equipment and gas mixture filling of the switchgear is also described in this chapter.

**Chapter 5:** A comparative explanation of the results obtained from lightning impulse breakdown tests of SF<sub>6</sub> and CF<sub>3</sub>I-CO<sub>2</sub> gas filled switch disconnectors. These results include the 50% breakdown voltage (U<sub>50</sub>) and the withstand strength of the distribution equipment as typically carried out by manufacturers based on BS60060-1.

**Chapter 6:** The use of the programme BOLSIG+ to calculate the effective ionisation coefficients of CF<sub>3</sub>I-CO<sub>2</sub> gas mixtures, from which likely insulating capabilities can be predicted. The results of simulations carried out using the programme COMSOL. The results are evaluated and compared against the practical results obtained in Chapter 5.

**Chapter 7:** This chapter sets out a proposal for CF<sub>3</sub>I insulated vacuum switchgear and whether it could be a viable alternative to SF<sub>6</sub> in the future.

**Chapter 8:** A conclusion of the research that has been carried out in this thesis and further studies that could be conducted in the future.

## CHAPTER 2.

# LITERATURE REVIEW OF SF<sub>6</sub>, CF<sub>3</sub>I AND CF<sub>3</sub>I GAS MIXTURES

---

### 2.1 Introduction

This chapter examines the published literature with regards to characterising various gases when utilised as an insulation medium. It also explores the various advantages and disadvantages of each gas when used for this purpose.

In this chapter, SF<sub>6</sub> is characterised and the inherent qualities which make it a widely used insulating medium today are examined. The present day use of SF<sub>6</sub> is then explored and the effects that this could have in the UK and worldwide are examined.

The next areas of interest in this chapter are the various gas alternatives to SF<sub>6</sub> that have been suggested along with alternative technologies and their limitations. The reasons why these are not used today instead of SF<sub>6</sub> are also described.

Another aspect of this chapter gives a critical appraisal of the published literature that characterises  $\text{CF}_3\text{I}$  and various gas mixtures of  $\text{CF}_3\text{I}$ . This examines research that has been conducted with  $\text{CF}_3\text{I}$  and its viability to become an alternative to  $\text{SF}_6$  in the future.

The principles of gaseous breakdown are examined in this chapter along with the mechanisms for this to take place. The reasons for contact geometry are explored and the effects they can have on the electric field and the insulating potential of various gases is examined.

### **2.1.1 Gaseous properties of $\text{SF}_6$**

Throughout the development and evaluation stages of  $\text{SF}_6$ , it has been ascertained that it has a high dielectric strength as well as a useful interruption performance, hence its current use in GIS (gas insulated switchgear) applications [10].

$\text{SF}_6$  is strongly electronegative with a high dielectric strength and a breakdown voltage nearly three times higher than that of air at atmospheric pressure [20]. Mixtures of  $\text{SF}_6$  with fluorocarbon gases, rare gases and atmospheric gases have been tried; of these the  $\text{SF}_6\text{-N}_2$  mixture has been found industrially useful for some high voltage applications including GIL [20]. Other fluorocarbons have a higher dielectric strength than  $\text{SF}_6$  but, for example,  $\text{C-C}_4\text{F}_8$  has a GWP of 11,200 and a residence time in the atmosphere of 3,200 years making it an unviable substitute gas [20].

### **2.1.2 Problems with the continued use of $\text{SF}_6$**

$\text{SF}_6$  is an efficient infrared (IR) absorber and, due to its chemical inertness, it is not readily removed from the earth's atmosphere making  $\text{SF}_6$  the potent greenhouse gas known today [20]. On the other hand,  $\text{SF}_6$  is benign with regard to stratospheric ozone depletion, since it is chemically inert [20].

In 1970, the first measurements of the purely anthropogenic (human produced) greenhouse gas SF<sub>6</sub> were 0.03 pptv (1 ppt = 1 part in 10<sup>-12</sup> per volume of atmospheric air) but this had increased, by two orders of a global mean value, to 2.8 pptv in 1992 [20]. It was clear that the atmospheric concentration of SF<sub>6</sub> was increasing and could reach 65 pptv by the year 2100 depending on the assumptions of release rates [20].

A completely new substitute equivalent to SF<sub>6</sub> gas has not yet been proposed whilst a mixture of SF<sub>6</sub>-N<sub>2</sub> gas is considered to be a moderate and probable solution if not a complete one [21]. SF<sub>6</sub> also produces highly toxic and corrosive compounds (e.g. S<sub>2</sub>F<sub>10</sub> and SOF<sub>2</sub>) when it is subject to electrical discharges [20].

SF<sub>6</sub> is a highly regulated gas that cannot be released into the atmosphere during the life-cycle of a piece of switchgear, although BS62271-1 suggests a yearly leakage rate of 0.1% is acceptable [1]. SF<sub>6</sub> is removed and dealt with at separate disposal units [3]; this increases the cost of using SF<sub>6</sub> substantially whilst having to adhere to strict regulations put in place under the Kyoto agreement [22]. The Kyoto agreement suggests that all countries involved accept and perceive the releasing of SF<sub>6</sub> to be a major problem. It is also important to have an accurate measurement on the amount of fluorine that is produced during each discharge cycle of a switchgear component [9] as this can be harmful to equipment. If absorbents are used to decrease the fluorine content this can increase the complexity of the switchgear device.

### **2.1.3 Ideal qualities of a new gas insulation medium**

It is possible to list the ideal qualities for GIS, however, some trade-off may be needed depending on the alternative insulating medium that is finally decided upon.

A new insulating medium should:

- Be a gas at normal operating temperatures i.e. have a low boiling point

- Be thermally stable at temperatures less than 500 °C
- Have excellent arc extinction properties
- Be non-flammable
- Be non-explosive
- Have a breakdown voltage similar to SF<sub>6</sub> i.e. much higher than air
- Have a low global warming potential (GWP) near zero and not absorb IR
- Have a stratospheric ozone depletion potential (ODP) near zero and be chemically inert
- Be readily decomposed in the earth's atmosphere and therefore have a short lived atmospheric lifetime (if it is released)
- Have a very low environmental impact
- Have use at high pressures
- Be non-toxic and safe for human use
- Have few harmful gas decomposition by-products and recombine readily

These qualities will be further examined in this chapter and concluded upon to evaluate the potential usefulness of a new gas insulating medium.

## **2.2 Environmental characteristics of SF<sub>6</sub>, CF<sub>3</sub>I and CF<sub>3</sub>I gas mixtures**

This section investigates the environmental effects of the various gas mixtures considered and evaluates the case for and against each gas and gas mixture with regards to the potential that each has to damage our environment.

### **2.2.1 Atmospheric lifetime**

The atmospheric lifetime is a concept based upon the simple one-box model. The lifetime (t) of species (X) in the box is defined as the average time that a molecule of X remains

in the box, that is, the ratio of the mass  $m$  (kg) of X in the box to the removal rate  $F_{out} + L + D$  (kg s<sup>-1</sup>); so that: [23]

$$t = \frac{m}{F_{out} + L + D} \quad (\text{Yr}) \quad (2.1)$$

Where:  $m$  = mass (kg),  $F_{out}$  = flow of substance X out of the box (kg/yr)

$L$  = chemical loss of substance X (kg/yr),  $D$  = deposition of substance X (kg/yr) [23]

The atmospheric lifetime of CF<sub>3</sub>I is very short in the order of hours / days rather than years [24]. CF<sub>3</sub>I has an estimated lifetime of 0.005 years or less than 1.8 days [9] [25] because it is rapidly degraded by solar radiation.

### 2.2.2 Ozone-depletion potential (ODP)

Ozone is naturally present in the atmosphere, it is mostly concentrated in the stratospheric region around 10-16 km to 50 km in altitude. In the stratosphere, ozone absorbs harmful ultraviolet radiation generated by the sun [26].

The concentration of other gases, particularly halogen source gases, in the stratosphere are being increased due to human activities. Gases that can reduce the amount of ozone in the stratospheric region are called “ozone-depleting substances” (ODS). Halogen gases can be converted to reactive gases containing chlorine and bromine that react with ozone and reduce it. Halogen gases contain fluorine (F) and iodine (I) atoms [26].

The ozone depleting potential (ODP) is a relative index that highlights the potential of a compound to destroy ozone over its lifetime in the atmosphere compared to the effects of CFC-11. In this index, the ODP of CFC-11 is set as 1. The ODP of a compound is the ratio of the impact of the chemical on the ozone compared to the impact of a similar mass of CFC-11 [27].

$$ODP_i = \frac{\text{Global } \Delta O_3 \text{ due to substance } i}{\text{Global } \Delta O_3 \text{ due to CFC-11}} \quad (2.2)$$

The ozone depleting potential of SF<sub>6</sub> is approximately zero because it is chemically inert and does not readily react with other gases found in the stratosphere. Therefore, it is not readily converted to a reactive gas that would react with and deplete ozone [9] [28].

The ODP of CF<sub>3</sub>I is very small and estimates range from 0.006 [25] to 0.008 [28] (dependent on where the emissions take place). This is because iodine can react with ozone, however, the gases that contain iodine have a very short atmospheric lifetime. Most of the iodine gases are destroyed in the troposphere (lower region of the atmosphere) and, therefore, do not reach the area where the highest concentrations of ozone reside. Gases that contain fluorine undergo conversion in the stratosphere and release fluorine atoms. However, these fluorine gases are left in a chemical form that does not cause ozone depletion [26].

### 2.2.3 Global warming potential (GWP)

To define the impact that certain emissions contribute to global warming, the simplified and purely physical GWP index is used. It has been designed in this manner so that it does not take into account uncertain regionally resolved climate change data (temperature, precipitation, winds, etc) and problematic baseline emission scenarios. The GWP index is based on 1 kg of some compound (*i*) relative to that of 1 kg of the reference gas CO<sub>2</sub>, developed by the IPCC (1990) [14] [29]. The GWP index is also adopted for use in the Kyoto Protocol. The GWP of component gas *i* is defined by:

$$GWP_i \equiv \frac{\int_0^{TH} RF_i(t) dt}{\int_0^{TH} RF_r(t) dt} = \frac{\int_0^{TH} a_i \cdot [C_i(t)] dt}{\int_0^{TH} a_r \cdot [C_r(t)] dt} \quad [14] \quad (2.3)$$

Where:

TH = time horizon, RF<sub>i</sub> = global mean radiative forcing (RF) of component gas *i*

a<sub>i</sub> = RF per unit mass increase in atmospheric abundance of component gas *i* (radiative efficiency)

[C<sub>i</sub> (t)] = time-dependent abundance of gas *i*

$a_r$  = RF per unit mass increase in atmospheric abundance of the reference gas  $\text{CO}_2$   
(radiative efficiency)

$[C_r(t)]$  = time-dependent abundance of the reference gas  $\text{CO}_2$

The numerator and denominator are called the absolute global warming potential (AGWP) of component gas ( $i$ ) and the reference gas ( $\text{CO}_2$ ) respectively.

The GWP of  $\text{SF}_6$  and  $\text{CF}_3\text{I}$  relative to  $\text{CO}_2$  are shown in Table 2.1.

Table 2.1: Global warming potential for  $\text{SF}_6$  and  $\text{CF}_3\text{I}$  [14] [9].

				Global Warming Potential for Given Time Horizon			
Common Name	Chemical Formula	Lifetime (Years)	Radiative Efficiency ( $\text{W m}^{-2} \text{ppb}^{-1}$ )	SAR (100- yr)	20 Yrs	100 Yrs	500 Yrs
Carbon Dioxide	$\text{CO}_2$	-	$1.4 \times 10^{-5}$	1	1	1	1
Sulphur Hexafluoride	$\text{SF}_6$	3200	0.52	23900	16300	22800	32600
Trifluoroiodo methane	$\text{CF}_3\text{I}$	0.005	-	-	1.2 - 5	< 5	< 5

SAR = Second assessment report by the IPCC (1995)

## 2.3 Electronegative gases

An electron pair is subject to a tug-of-war between the two atoms that share it. The covalent bond it forms acquires some ionic character if one atom has a greater pulling power than the other atom, because then the electron pair is more likely to be found closer to one atom than to the other. The electron-pulling power of an atom when it is part of a bond is called electronegativity (EN) [30].

The simplest analogy is to think of electronegativity as the ability of an atom to compete for electrons, as such, it is related to the ionization energy (I) ( $\text{kJ mol}^{-1}$ ) and electron affinity (EA) ( $\text{kJ mol}^{-1}$ ) of the element. If the ionization energy is high, then electrons are given up reluctantly. If the electron affinity is high, then no more energy is needed to attach electrons to an atom. Elements with high values of both these properties are

reluctant to lose their electrons and tend to gain them; hence, they are classified as highly electronegative. Conversely, if the ionization energy and the electron affinity are both low, then it takes very little energy for the element to give up its electrons and its tendency to gain other electrons is low; hence the electronegativity is low [30].

Figure 2.1 shows the variation of electronegativity for the main-group of elements of the periodic table based on the scale devised by Linus Pauling (1901-1994). Because ionization energies and electron affinities are highest at the top right of the periodic table (close to fluorine), it is not surprising to find that nitrogen, oxygen, bromine, chlorine, and fluorine are the elements with the highest electronegativities. Whenever these elements are present in compounds, we can expect their atoms to pull strongly on electrons shared with their neighbours. Electrons will still be shared with the less electronegative atom, but the sharing is unequal, and the electron cloud will be denser on the atom of the more electronegative element [30].

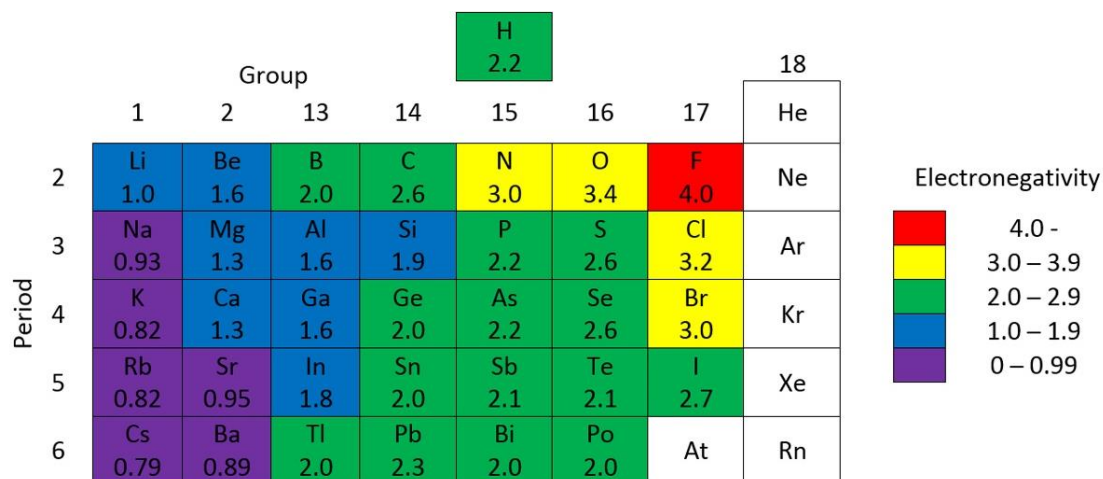


Figure 2.1: Electronegativity of elements [31].

### 2.3.1 SF<sub>6</sub> bonds

A sulphur hexafluoride molecule, SF<sub>6</sub>, has six atoms of fluorine attached to the central sulphur atom and no free electrons to form extra bonds on that atom. According to the valence-shell electron-pair repulsion (VSEPR) model, the fluorine atoms are farthest apart when four lie in a square around the equator and the remaining two above and below

the plane of the square (Fig 2.2). By referring to Lewis' structure, we see that the molecule should be classified as octahedral. All its bond angles are either  $90^\circ$  or  $180^\circ$  [31] [30].

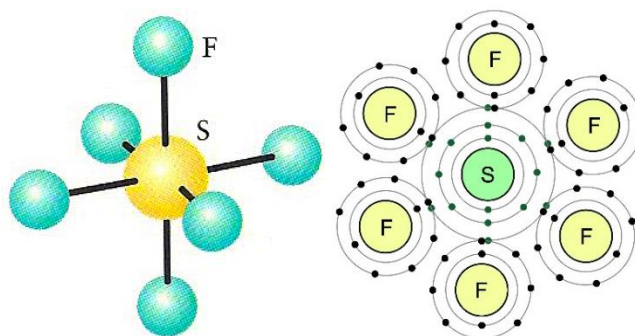


Figure 2.2:  $\text{SF}_6$  octahedral molecular shape and its bonded electrons [31].

Sulphur atoms have a relatively low ionization energy at  $1000 \text{ kJ mol}^{-1}$ , meaning that electrons can be given up, but a high electron affinity of  $+200 \text{ kJ mol}^{-1}$  means this is less likely because it is more favourable to attach electrons. Sulphur is, therefore, classified as a relatively high electronegative atom that is more likely to gain electrons than lose them as shown by its electronegativity value of 2.6 [31].

Fluorine atoms have an even higher ionization energy than sulphur at  $1680 \text{ kJ mol}^{-1}$  and have one of the strongest electron affinities at  $+328 \text{ kJ mol}^{-1}$ . The combination of fluorine's high ionization energy and strong electron affinity means that it is one of the most electronegative atoms known at 4.0 meaning that it is even more likely to gain electrons than lose them compared with sulphur [31].

As the electronegativities of sulphur and fluorine are 2.6 and 4.0 respectively there is a difference of 1.4, as this is not a large difference this means that a covalent bond is the best description of the bond formed between fluorine and sulphur. This bond will have some ionic tendencies. As the electronegativities are different, the fluorine atom, with the highest electronegativity, will have the stronger pull on the shared electron pair between each of the six fluorine and sulphur bonds [31].

In  $\text{SF}_6$ , the bonds between fluorine and sulphur produce a polar covalent bond because the fluorine atom has a higher electronegativity than the sulphur meaning it gains a greater share of the bonding electron pair. The greater share of electrons means that the fluorine atoms gain a partial negative charge whilst the sulphur gains an equal but opposite positive charge. As the  $\text{SF}_6$  molecule is built in an octahedral shape, it means that every polar covalent bond that is formed between sulphur and fluorine has an opposing partial charge polar covalent bond with the fluorine atom directly opposite. Therefore, all the partial charges built up around the sulphur atom produce a nonpolar molecule in  $\text{SF}_6$  because the dipoles of each of the individual bonds cancel one another [30].

The resulting  $\text{SF}_6$  molecule is, therefore, conditioned so that it is highly electronegative but forms a very strong structure that is difficult to break and re-combines readily.

### 2.3.2 $\text{CF}_3\text{I}$ bonds

A trifluoriodomethane molecule,  $\text{CF}_3\text{I}$ , has three fluorine atoms and one iodine atom attached to a central carbon atom. By referring to Lewis's structure, we see that the molecule should be classified as tetrahedral [31].

Carbon has a relatively low ionization energy at  $1090 \text{ kJ mol}^{-1}$  and an average electron affinity of  $+122 \text{ kJ mol}^{-1}$  meaning that is classified as a relatively high electronegative atom that is more likely to gain electrons than lose them as shown by its electronegativity of 2.6 [31].

Iodine has a relatively low ionization energy of  $1008 \text{ kJ mol}^{-1}$  and a high electron affinity of  $+295 \text{ kJ mol}^{-1}$  meaning that it is a slightly more electronegative atom than carbon at 2.7 and, therefore, even more likely to gain electrons than lose them [31].

Fluorine is one of the most electronegative atoms at 4.0 and is very likely to gain electrons rather than lose them.

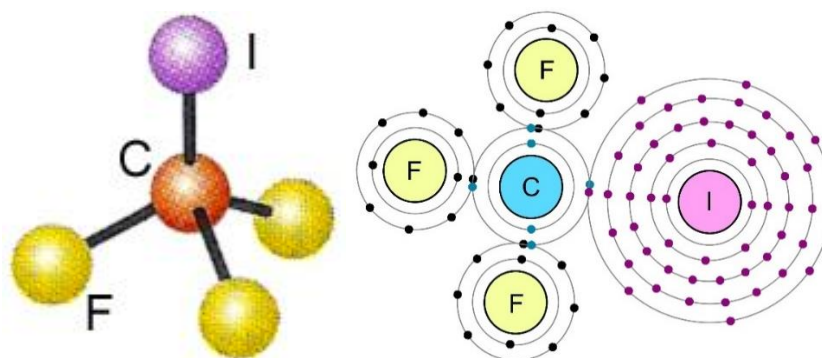


Figure 2.3: CF<sub>3</sub>I tetrahedral molecular shape and its bonded electrons [31].

Tetrahedral molecules with the same atom at each corner, such as tetrachloromethane (carbon tetrachloride), CCl<sub>4</sub>, are nonpolar because the dipoles of the four covalent bonds cancel in three dimensions. However, if one or two atoms are replaced by different atoms, as in trifluoroiodomethane, CF<sub>3</sub>I, then the bond dipoles do not cancel and the molecule is polar (denoted as an AX<sub>3</sub>E molecule) [31].

The resulting CF<sub>3</sub>I molecule is highly electronegative but more likely to cause by-products because of the weaker polar bond between carbon and iodine.

### 2.3.3 Comparative dielectric strengths of SF<sub>6</sub> and other gases

The insulation strength of SF<sub>6</sub> is due to electron attachment [11]. In this process: “a free electron moving in the applied field, which collides with a neutral molecule, may be attached to form a negative ion” [11]:



The negative ions which are formed by attachment are heavy and slowly moving and unable to accumulate the energy required to cause ionisation. This process effectively removes electrons and prevents the formation of ‘avalanches’ of electrons which might have otherwise led to breakdown [11].

This process competes with collision ionisation, by which “an electron with sufficient energy can remove an electron from a neutral molecule to create an additional free electron” [11]:



Ionisation is a cumulative process. If an electric field is high enough, successful collisions can produce ever increasing numbers of free electrons. Free electrons can result in electrical breakdown of a gas [11].

Some gases have a dielectric strength significantly greater than that of SF<sub>6</sub>; as shown on Table 2.2.

Table 2.2: Relative DC uniform-field breakdown strengths [11] [32].

<b>Gas</b>	<b>V<sub>s</sub> relative to SF<sub>6</sub></b>	<b>V<sub>s</sub> (E/N)<sub>lim</sub></b>	<b>Electron attaching</b>
C-C <sub>6</sub> F <sub>12</sub>	≈ 2.4	≈ 8.66E-15	strongly attaching
C <sub>4</sub> F <sub>6</sub>	≈ 2.3	≈ 8.30E-15	strongly attaching
C-C <sub>4</sub> F <sub>6</sub>	≈ 1.7	≈ 6.14E-15	strongly attaching
C-C <sub>4</sub> F <sub>8</sub>	1.3	4.69E-15	strongly attaching
CF <sub>3</sub> I	1.21	4.37E-15	strongly attaching
SF <sub>6</sub>	1	3.61E-15	strongly attaching
C <sub>2</sub> F <sub>8</sub>	0.9	3.25E-15	strongly attaching
N <sub>2</sub> O	0.44	1.59E-15	moderately attaching
CO	0.4	1.44E-15	moderately attaching
N <sub>2</sub>	0.36	1.3E-15	weakly attaching
CO <sub>2</sub>	0.3	1.08E-15	weakly attaching
Air	0.3	1.08E-15	weakly attaching
H <sub>2</sub>	0.18	6.5E-16	non attaching

However, the gases shown with a higher dielectric strength than SF<sub>6</sub> present problems of one kind or another, including toxicity, limited operating pressure range or production of solid carbon during arcing [11]. SF<sub>6</sub> is, therefore, the only dielectric that is accepted as suitable for GIS applications, although some gases have been considered for use in mixtures with SF<sub>6</sub>, such as N<sub>2</sub> [32].

## 2.4 SF<sub>6</sub>, CF<sub>3</sub>I and CF<sub>3</sub>I gas mixture electron interaction properties

For any gas to have reasonable insulation strength, it must have the ability to reduce the number of free electrons. The following section reviews the various research investigations that have been undertaken with CF<sub>3</sub>I and CF<sub>3</sub>I gas mixtures to explore its interaction with free electrons.

### 2.4.1 Electron drift velocity

In Figures 2.4 and 2.5, the electron drift velocity ( $v_e$ ) is shown for pure CF<sub>3</sub>I as well as mixtures of CF<sub>3</sub>I-N<sub>2</sub> and CF<sub>3</sub>I-CO<sub>2</sub>. It is beneficial for an insulation medium to have a small electron drift velocity as this shows the gases ability to slow electrons moving in the direction of the applied electric field between open contacts in switchgear. For all gas mixtures, it was noted that the value of  $v_e$  increases linearly with the ratio of the reduced electric field ( $E/N$ ). The reduced electric field ( $E/N$ ) is the ratio of the electric field  $E$  (V/cm) to the gas density  $N$  (mols/cm<sup>3</sup>). The unit of measurement for the reduced electric field is the Townsend (Td), which has a numerical value of  $10^{-17}$  Vcm<sup>2</sup> [33]. Deng Yun-Kun and Xiao Deng-Ming [34] calculated from Boltzmann's equation analysis that for gas mixtures of either CO<sub>2</sub> or N<sub>2</sub> when the mixture contains 70% CF<sub>3</sub>I or more, the trend was close to that of pure SF<sub>6</sub>. It was found that mixtures of CO<sub>2</sub> have a slightly lower electron drift velocity than mixtures with N<sub>2</sub>. The electron drift velocity for pure CF<sub>3</sub>I was lower than that of pure SF<sub>6</sub> [35].

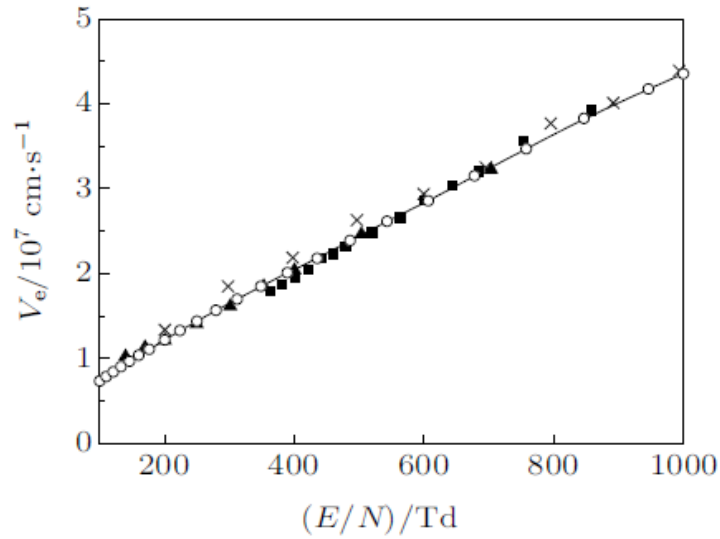


Figure 2.4: Electron drift velocity in  $\text{CF}_3\text{I}$  as a function of  $E/N$  [34],  
 ■ [35], × [36], ▲ [37], ○ [34].

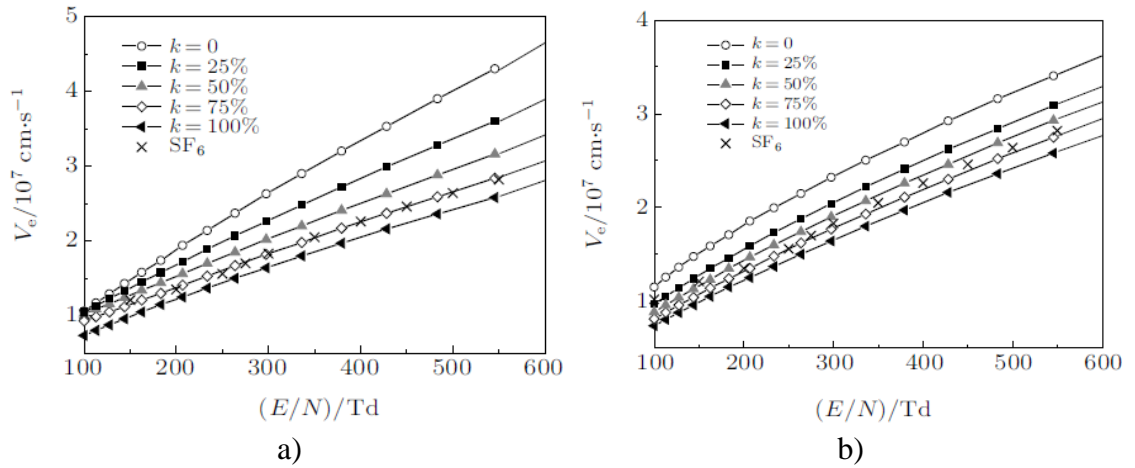


Figure 2.5: Electron drift velocities ( $V_e$ ) in a)  $\text{CF}_3\text{I-N}_2$  mixtures b)  $\text{CF}_3\text{I-CO}_2$  mixtures  
 as a function of  $E/N$  at different  $\text{CF}_3\text{I}$  gas mixture ratios  $k$  [34].

#### 2.4.2 Effective ionization coefficients

The effective ionization coefficient is the ionisation rate  $\alpha$  (alpha) minus the electron attachment rate ( $\eta$  eta) of the gas mixture being calculated, shown in Figure 2.6 for pure  $\text{CF}_3\text{I}$  as a function of the reduced electric field ( $E/N$ ). The limiting field strength  $(E/N)_{\text{lim}}$  of  $\text{CF}_3\text{I}$  is approximately 431 Td [34]. The limiting field strength or critical reduced field strength is the point at which ionization equals attachment i.e.  $\alpha - \eta = 0$ .

$(E/N)_{\text{lim}}$  of  $\text{SF}_6$  has been established to be 361 Td, this means that the insulation strength of  $\text{CF}_3\text{I}$  is approximately 1.19 times that of  $\text{SF}_6$  [34]. From the effective ionisation coefficients, shown in Figure 2.7, it is expected that the limiting field strength of a gas mixture of 75%  $\text{CF}_3\text{I}$  and 25%  $\text{CO}_2$  or  $\text{N}_2$  will have a similar insulation strength to  $\text{SF}_6$ . However, it still remains unclear as to the precise limiting field strength of gas mixtures of 20% or 30%  $\text{CF}_3\text{I}$  with  $\text{CO}_2$  or  $\text{N}_2$ . Effective ionisation coefficients are examined further in Chapter 6.

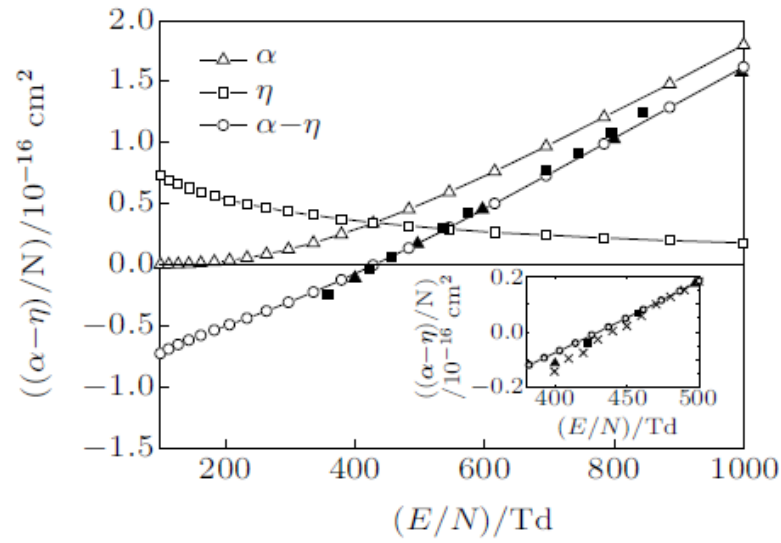


Figure 2.6: Effective ionization coefficient  $(\alpha - \eta)/N$  of  $\text{CF}_3\text{I}$  as a function of  $E/N$ ,  
 [35],  [36],  [37],  [34].

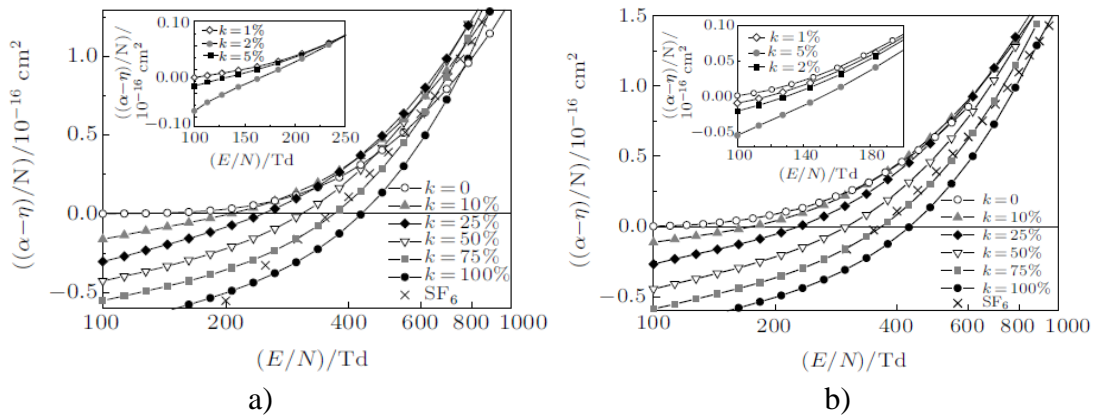


Figure 2.7: Density-normalised effective ionization coefficients  $(\alpha - \eta)/N$  of a)  $\text{CF}_3\text{I}$  and  $\text{N}_2$  mixtures b)  $\text{CF}_3\text{I}$  and  $\text{CO}_2$  mixtures as a function of  $E/N$  at different  $\text{CF}_3\text{I}$  gas mixture ratio  $k$  [34].

### 2.4.3 Limiting field strength

The limiting field strength  $(E/N)_{\text{lim}}$  has been estimated using the effective ionisation coefficients described previously. Figure 2.8 shows that  $\text{CF}_3\text{I}-\text{N}_2$  mixtures may have a slightly higher limiting field strength than  $\text{CF}_3\text{I}-\text{CO}_2$  gas mixtures but, above a 50% concentration of  $\text{CF}_3\text{I}$ , there was very little difference. It was also shown that mixtures of  $\text{CF}_3\text{I}-\text{CO}_2$  and  $\text{CF}_3\text{I}-\text{N}_2$  have a higher limiting field strength than pure  $\text{SF}_6$  when the mixture contains more than 70%  $\text{CF}_3\text{I}$  [34].

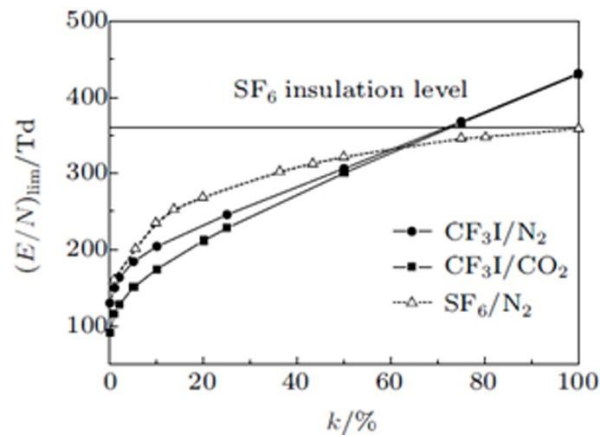


Figure 2.8: The limiting fields  $(E/N)_{\text{lim}}$  as a function of  $\text{CF}_3\text{I}$  or  $\text{SF}_6$  gas content  $k$  [34].

### 2.5 Breakdown mechanisms

There are two distinct types of breakdown, depending on the rate at which the voltage is applied to a contact gap. When voltage stress is applied relatively slowly, as with alternating voltage or long rise time switching surges, corona space charge plays an important part in controlling the field distribution by the corona stabilisation process. With shorter rise time surges i.e. lightning impulse or fast transients, breakdown occurs directly by a stepped leader mechanism [11]. For short rise time surges, the breakdown voltage is lower when the high field electrode is positive [11]. Therefore, more focus will be given to breakdown under positive point conditions. For positive point conditions, electrons trigger leader breakdown readily from the detachment of negative ions in the vicinity of the point. However, for negative point conditions, electrons are produced by field emission [11].

### 2.5.1 Corona stabilised breakdown

In Figure 2.9, the AC breakdown voltage characteristics for various point-plane gaps in  $\text{SF}_6$  is shown at various pressures. These curves are typical of all non-uniform field gaps with slowly varying voltage applied. In Figure 2.9 there is a region where breakdown voltage is much higher than the (streamer corona) onset voltage and a critical pressure at which the first streamer leads directly to breakdown [11]. The peak in the mid-pressure range is due to the effects of space charge injected by streamer activity around the point. For a positive point: “the electrons generated by the corona are quickly removed at the point while the positive ions diffuse relatively slowly into the low field region” [11]. The space charge effect shields the point and stabilises the field at a level close to the onset value. As the voltage is increased, the space charge density (and the shielding effect) intensifies, this means that a voltage considerably above onset is needed to cause breakdown. As pressure is increased, the corona region becomes smaller and is concentrated around sharp areas such as the tip of the point and stabilisation becomes less effective and so the breakdown voltage is reduced [11].

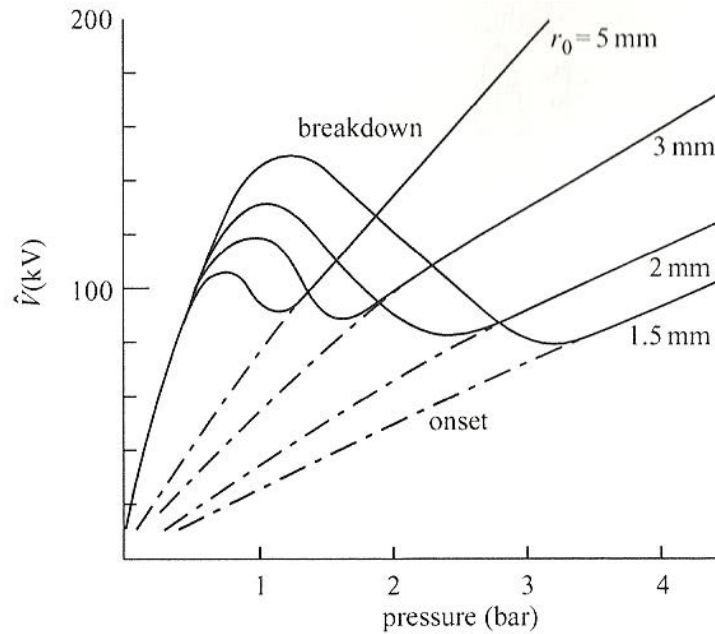


Figure 2.9: AC corona onset and breakdown characteristics for a positive point 40 mm rod-plane gap in  $\text{SF}_6$  [38].  $r_0$  is the radius of the rod contact.

### 2.5.2 Leader breakdown

If a fast-fronted surge is applied to a contact, the initial streamers can be very intense if the voltage rapidly passes through the theoretical streamer onset level [11]. These streamers may lead to the “formation of a highly ionised channel before there is time for space charge stabilisation of the field at the tip of the contact” [11]. Another factor that may play an important role is the statistical appearance of initiatory electrons. For a discharge to be initiated, a negative-ion needs to be found in the very small critical volume (where ionisation ( $\alpha$ ) > attachment ( $\eta$ )). For a fast-fronted wave, the field could be well above the minimum onset level when inception occurs, this means that the streamer corona is more vigorous than is the case for AC or DC stress. If the streamer corona is large enough, a stepped leader discharge may be initiated [11].

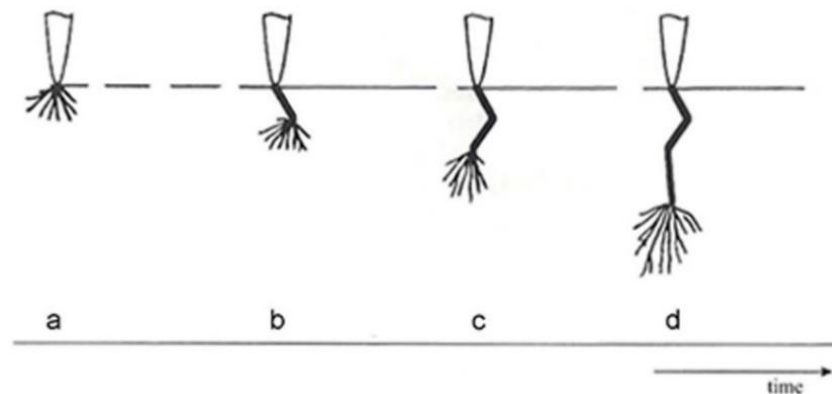


Figure 2.10: Schematic of leader development [11].

Following the initial corona, charge separation generates streamer filaments which build-up their conductivity (Figure 2.10 a). One of these streamer filaments can be transformed into a highly conducting channel step which acts as an extension of the point electrode and new corona immediately occurs at its tip (b). The length of extension of the second corona determines the second channel step (c). These steps propagate into the gas gap, typically of a few mm, until the streamer activity is too weak for further channel steps to form [11]. If the voltage is high enough, then the leader channel can cross the gas gap and breakdown occurs. The breakdown formative time lag can be greater than 1  $\mu$ s [11].

### 2.5.3 Practical breakdown levels in GIS

Usually, the design of HV GIS are configured so that the stresses exerted, under ideal conditions, are less than 50 percent of the critical electric field strength ( $E_{crit}$ ) [11]. This means that streamer inception will not occur even at the full rated impulse level [11]. However, it is important to note that, in practice, small scratches, free floating particles or other defects that affect the inner electrodes surface may result in streamer formation at reduced voltage. Such defects would probably be detected only under impulse-voltage test conditions at levels close to the lightning impulse withstand strength of the switchgear [11].

## 2.6 Review of experimental tests

This section reviews the experimental tests that have previously been undertaken with  $CF_3I$  or  $CF_3I$  gas mixtures used as an alternative insulation medium to  $SF_6$ . The principle of gaseous insulation is based on the dielectric strength of the gas that is between two electrodes and its ability to prevent a breakdown occurring between them. A breakdown signifies the collapse of the dielectric strength of the gas that is between two electrodes which in practice is shown as the collapse of the voltage that has been sustained between two electrodes before breakdown occurred.

### 2.6.1 Partial discharge inception voltage

The partial discharge inception voltage (PDIV) for  $CF_3I$  has been analysed using a needle-plane electrode system of radius tip 0.5mm and a gas gap of 10mm as shown in Figure 2.11.

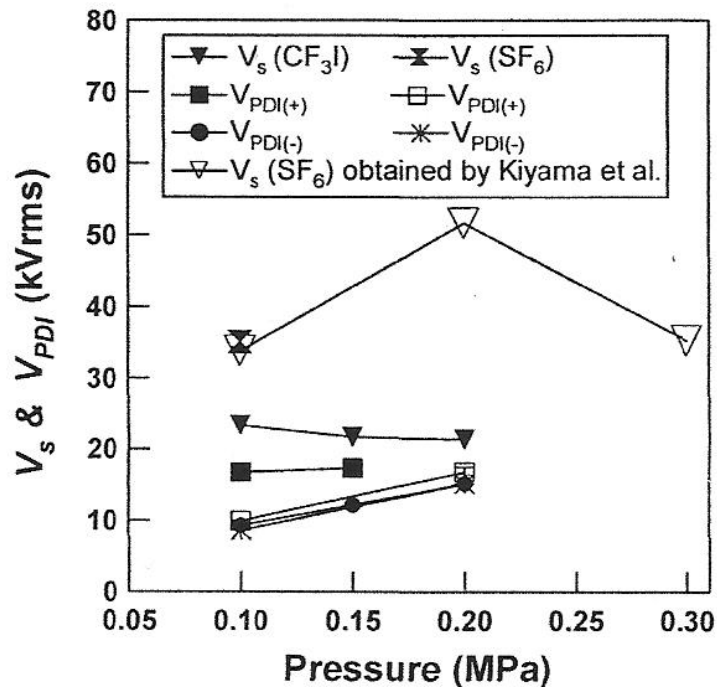


Figure 2.11: AC PDIV and sparkover voltage (BDV) in CF<sub>3</sub>I and SF<sub>6</sub>, needle (0.5 mm)-to-plane electrode configuration, gap length is 10 mm [39].

The negative partial discharge inception voltage in CF<sub>3</sub>I was almost the same as that of SF<sub>6</sub> at 0.1 MPa [39]. The positive partial discharge inception voltage in CF<sub>3</sub>I was 70% and 40% higher than that of SF<sub>6</sub> at 0.1 MPa and 0.15 MPa respectively [39].

### 2.6.2 Gas insulation for short rise time surges (lightning impulse) or fast transients or slowly applied switching surges

Most power systems use alternating voltages. However, insulation against breakdown may need to be at least twice that required for operating voltage, since transient overvoltages of higher levels may occur. These may be caused by lightning strikes, near to or upon an overhead line, by switching operations in the power system, or by temporary increases in the level of the operating voltage. Lightning strikes and switching operations are the most frequent and dangerous so the insulation is designed with this in mind [33].

The lightning impulse is an approximation of the disturbance caused by a lightning strike. These impulses may be reflected from discontinuities in the transmission line, with consequent increase in voltage. For this reason, testing of high voltage apparatus is carried

out under an impulse voltage related to, but much higher than, the proposed operating voltage [33].

### 2.6.3 Breakdown voltage characteristics of SF<sub>6</sub>, CF<sub>3</sub>I and CF<sub>3</sub>I gas mixtures

In [10], the breakdown voltage characteristics and insulation performance of CF<sub>3</sub>I, CF<sub>3</sub>I-CO<sub>2</sub> and SF<sub>6</sub> using a standard lightning impulse voltage have been investigated with fifteen breakdown tests being carried out for each gas. The experimental setup for testing the 50% breakdown voltage of different gas mixtures, at 0.1 MPa (abs), used a set of spherical electrodes made of stainless steel [10].

The 50% breakdown voltage, shown in Figure 2.12, shows gas mixtures of CF<sub>3</sub>I and CO<sub>2</sub> compared with SF<sub>6</sub>, plotted as a function of the CF<sub>3</sub>I percentage. The insulation performance of CF<sub>3</sub>I (100%) was about 1.2 times better than SF<sub>6</sub>. The insulation performance of CF<sub>3</sub>I-CO<sub>2</sub> increased linearly with the proportion of CF<sub>3</sub>I. When the CF<sub>3</sub>I content was about 60%, the dielectric strength was approximately equal to that of SF<sub>6</sub> whilst the dielectric strength of CF<sub>3</sub>I-CO<sub>2</sub> (30%:70%) was about 0.75 to 0.80 times that of SF<sub>6</sub> [10].

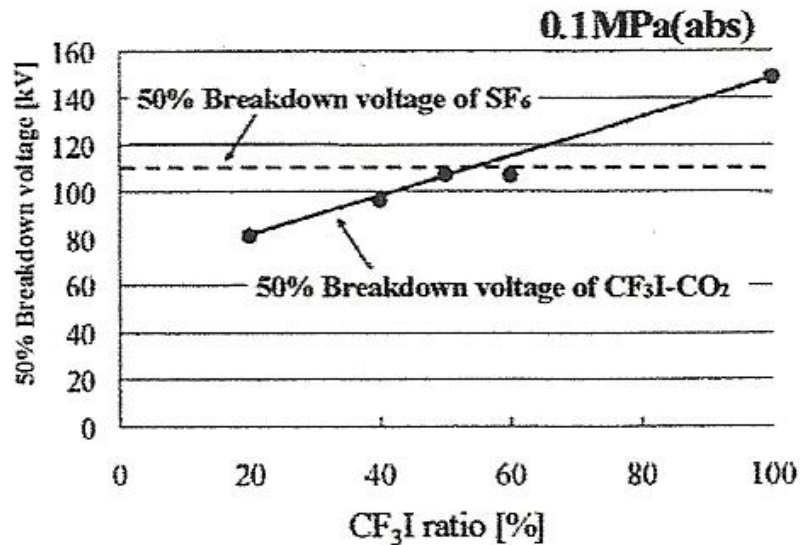


Figure 2.12: Positive breakdown voltage characteristics in CF<sub>3</sub>I-CO<sub>2</sub> at 0.1 MPa (abs), spherical-to-spherical electrode configuration (diameter 50.8 mm), gap length is 10 mm, fifteen breakdown tests for each gas mixture with a standard lightning impulse [10].

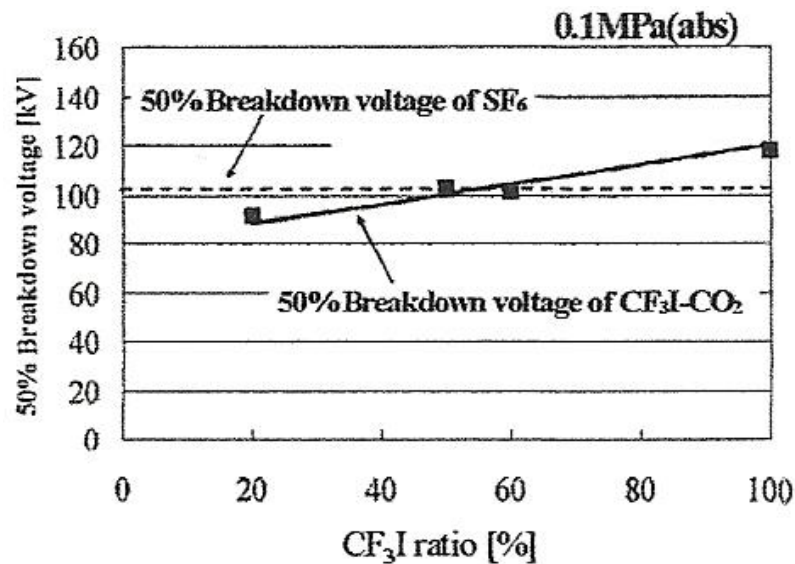


Figure 2.13: Negative breakdown voltage characteristics in CF<sub>3</sub>I-CO<sub>2</sub> at 0.1 MPa (abs), spherical-to-spherical electrode configuration (diameter 50.8 mm), gap length is 10 mm, fifteen breakdown tests for each gas mixture with a standard lightning impulse [10].

#### 2.6.4 Breakdown characteristics on the dielectric surface

In equipment that utilises an insulation gas, it is important to find out the impact of flashovers not only in the gaseous space but on solid dielectric surfaces as well [19]. T. Takeda, S. Matsuoka, A. Kumada and K. Hidaka [19] tested two different gap lengths (10mm and 20mm), with PTFE between the electrodes. Their work showed that the flashover voltage in SF<sub>6</sub> was the highest, with air being the lowest and CF<sub>3</sub>I being in between [19]. The minimum flashover voltages in SF<sub>6</sub> and air hardly changed even if the number of surface voltage discharges and occurrences were increased. In CF<sub>3</sub>I, the first surface flashover occurred on the dielectrics surface without iodine and the sparkover voltage was 1 – 1.2 times higher than SF<sub>6</sub> with a time lag to flashover longer than 1000 ns. The subsequent flashover voltage, in CF<sub>3</sub>I, was 0.6 times lower than SF<sub>6</sub> with the time lag to flashover decreased to 20-30 ns as shown in Figure 2.14 [19].

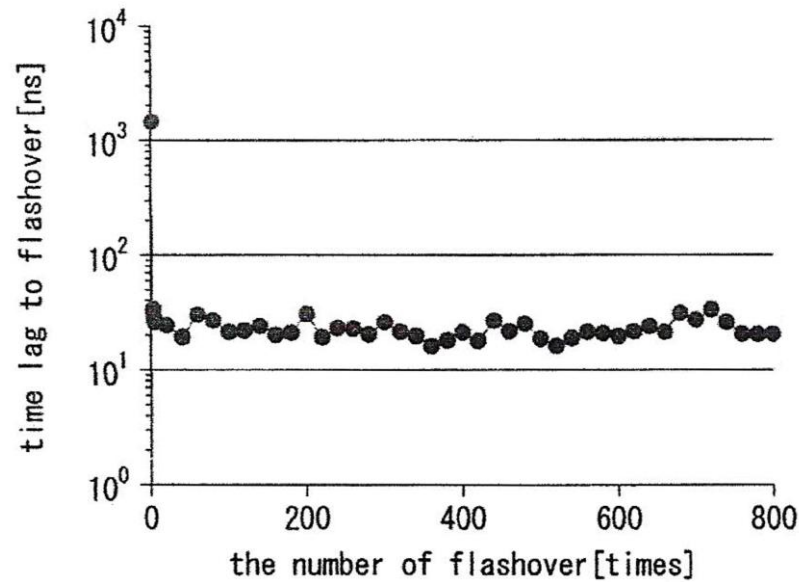


Figure 2.14 Relation between the number of flashover and time lag to flashover [19].

The minimum flashover voltage was investigated for a new sample of the insulator by the step-up method. The V-t characteristics were measured for the sample-insulator by applying a steep-front square pulse voltage for 100-200 times and measuring the minimum flashover voltage at  $t=10\mu\text{s}$ . The minimum flashover voltage for a PTFE insulator revealed that, in  $\text{CF}_3\text{I}$ , the insulator was strongly influenced by the prior discharges. Under closer examination, it was revealed that the insulators surface was stained with iodine which was suggested as the probable cause for the decrease in insulation performance [19].

### 2.6.5 Electrode configuration

Electrodes can be made of materials such as stainless steel, ferritic steel, copper, brass or aluminium. These materials do not tarnish when stored in close proximity with  $\text{CF}_3\text{I}$  or its by-products at or below  $27^\circ\text{C}$ . These materials also do not affect the chemical make-up of  $\text{CF}_3\text{I}$  [40] [41] [42].

Experiments can be conducted under three measuring conditions (Figure 2.15):

- under a uniform electric field using hemisphere-to-plane electrodes

- under a non-uniform electric field using a conical rod-to-plane electrode configuration or needle-to-plane electrode configuration
- with an insulator between two electrodes (PTFE etc) [19].

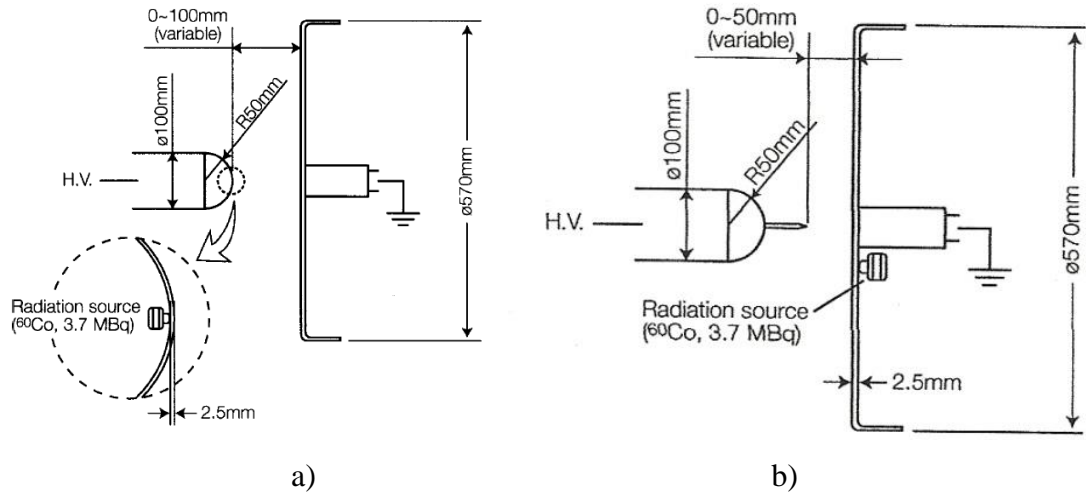


Figure 2.15: Schematic diagram of electrodes a) hemisphere-to-plane electrode [19]  
b) needle/conical rod-to-plane electrode [21].

For pure  $\text{CF}_3\text{I}$ , it has been shown that the dielectric strength of the gas is 1.2 times higher than  $\text{SF}_6$  gas in a uniform electric field (plane-plane electrode configuration) [19]. However, in a non-uniform field (rod-plane), the 50% sparkover voltage in  $\text{CF}_3\text{I}$  is equivalent to that of  $\text{SF}_6$  gas or lower. The sparkover voltage of  $\text{CF}_3\text{I}$  was found to be much more dependent on the non-uniformity of the electric field than in  $\text{SF}_6$  [21].

Figures 2.16 and 2.17 show the 50% breakdown strength ( $U_{50}$ ) of a 30%  $\text{CF}_3\text{I}$  – 70%  $\text{CO}_2$  gas mixture using a standard lightning impulse (1.2/50  $\mu\text{s}$ ). M. S. Kumarudin [43] used rod-plane, sphere-sphere and plane-plane electrodes to test the breakdown strength of  $\text{CF}_3\text{I}$ - $\text{CO}_2$  gas mixtures under various electric fields. The rod-plane electrode had a 0.5mm radius (rod) and a 90mm diameter for the plane. The sphere-sphere electrodes had a radius of 25mm and the plane-plane electrodes had a diameter of 90mm. The gap length refers to the amount of gas separating each electrode.

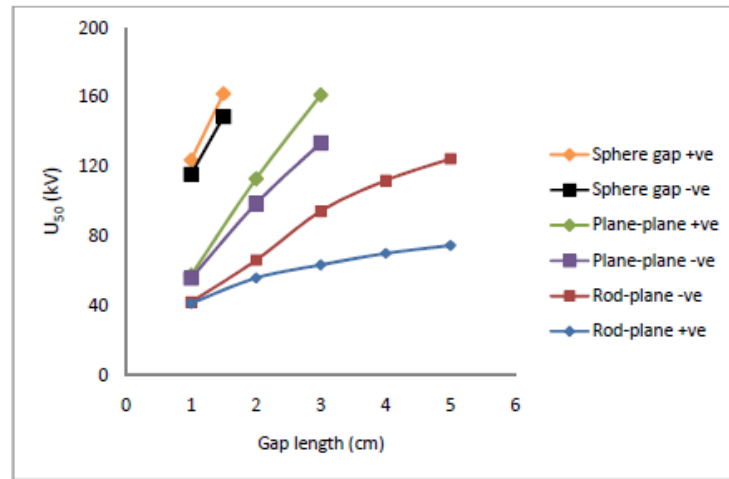


Figure 2.16: Breakdown properties of 30%:70%  $\text{CF}_3\text{I-CO}_2$  for various electrodes at 1 bar [43].

The results in Figure 2.16 show that the more uniform the field between electrodes (plane-plane) was the higher the breakdown strength of the  $\text{CF}_3\text{I-CO}_2$  gas mixture. In Figure 2.16 the field between the small plane-plane electrodes had a higher non-uniformity than the sphere-sphere electrodes, hence the results are lower than would normally be expected. If a sharp point exists between contacts in a piece of switchgear, the breakdown strength of a  $\text{CF}_3\text{I-CO}_2$  gas mixture will be lower.

The results in Figure 2.17 [43] show that for a higher pressure in the gas chamber, a higher breakdown strength of the  $\text{CF}_3\text{I-CO}_2$  gas mixture was obtained. The results also show that the breakdown strength increased as the gas gap between contacts increased.

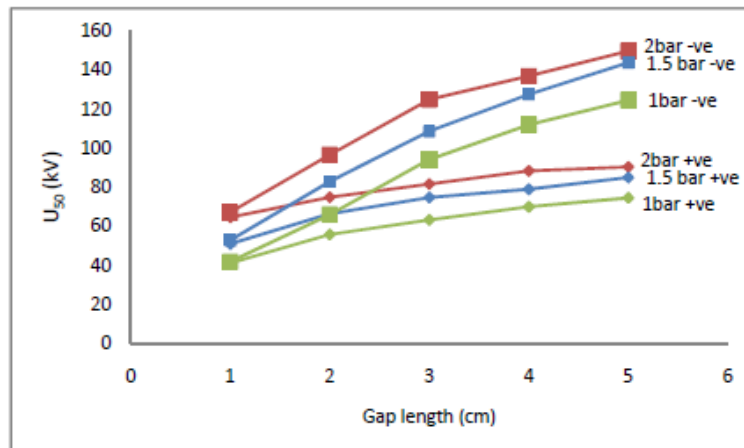


Figure 2.17: Breakdown properties of 30%:70%  $\text{CF}_3\text{I-CO}_2$  for various gas pressures for a rod-plane electrode configuration [43].

### 2.6.6 Field utilization factor

The field utilisation factor can be expressed using the following equation [19]:

$$\text{Field Utilisation Factor} = \frac{\text{Average Strength of Electric Field}}{\text{Maximum Strength of Electric Field}} \quad (2.6)$$

The field utilisation factor has been investigated using the voltage-time characteristics (V-t characteristics) of four different types of electrodes. The V-t characteristics of breakdown for CF<sub>3</sub>I and SF<sub>6</sub> revealed that [19]:

- The sparkover voltage of CF<sub>3</sub>I was lower than that of SF<sub>6</sub> in a non-uniform electric field.
- The sparkover voltage of CF<sub>3</sub>I was higher than that of SF<sub>6</sub> under a uniform electric field.
- The V-t characteristics observed in CF<sub>3</sub>I were largely dependent on the field utilization factor, unlike for SF<sub>6</sub> (Figure 2.18 and 2.19).
- When the field utilization factor was less than 0.38, the sparkover voltage of CF<sub>3</sub>I was lower than that of SF<sub>6</sub>. However, when the field utilization factor was above 0.38, the sparkover voltage of CF<sub>3</sub>I was higher than that of SF<sub>6</sub> (Figure 2.20).

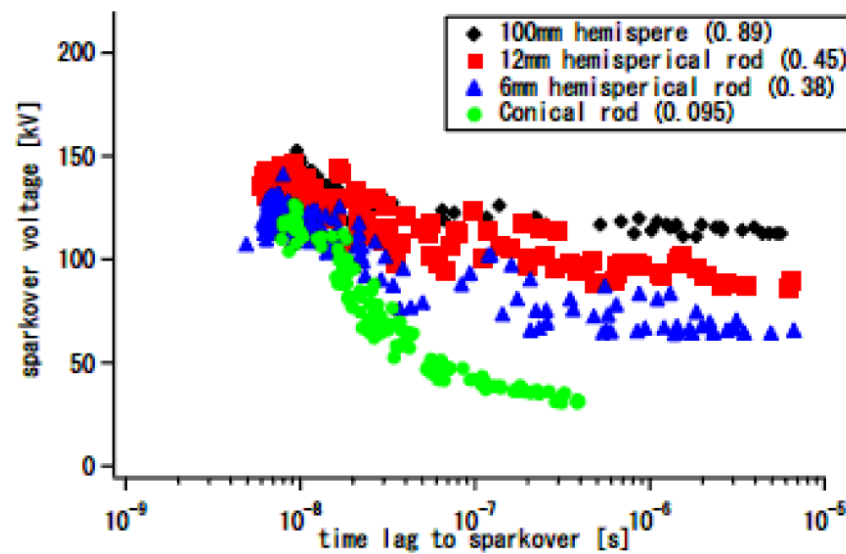


Figure 2.18: V-t characteristics of CF<sub>3</sub>I at 0.1 MPa, gap 10mm (positive polarity) [19].

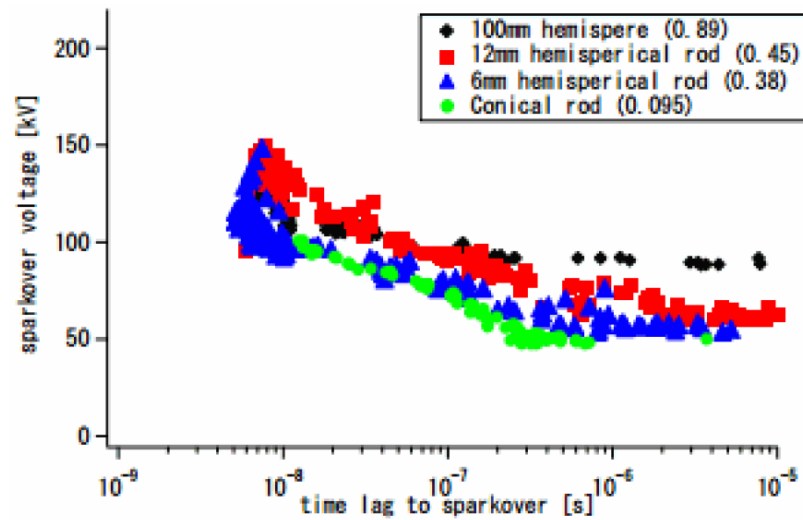


Figure 2.19: V-t characteristics of SF<sub>6</sub> at 0.1 MPa, gap 10mm (positive polarity) [19].

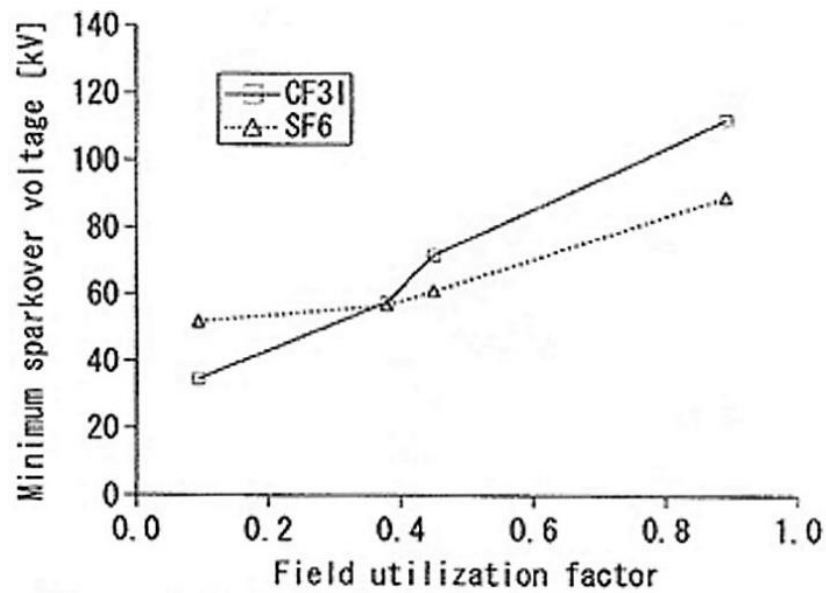


Figure 2.20: Minimum sparkover voltage vs field utilization factor [19].

### 2.6.7 Short line fault (SLF) and breaker terminal fault (BTF) interruption capability of CF<sub>3</sub>I and SF<sub>6</sub>

H. Katagiri, H. Kasuya, H. Mizoguchi and S. Yanabu [10] have shown the capabilities of CF<sub>3</sub>I, CF<sub>3</sub>I-CO<sub>2</sub> and CF<sub>3</sub>I-N<sub>2</sub> gas mixtures to interrupt a short line fault (SLF) and a breaker terminal fault (BTF). Their experiment used a model arc extinguisher chamber to push a gas flow over the moving opening contacts at 0.2 MPa (abs) [10].

Tests undertaken showed that the borderline between a successful and failed SLF interruption of CF<sub>3</sub>I was slightly below that of SF<sub>6</sub> [10], the SLF interruption performance

of  $\text{CF}_3\text{I}$  was about 0.9 times that of  $\text{SF}_6$ . It was also found that the SLF interruption performance of  $\text{CF}_3\text{I}-\text{N}_2$  (20-80%) was nearer to  $\text{N}_2$  than that of  $\text{CF}_3\text{I}$  [10]. The SLF interruption performance of 20%-80%  $\text{CF}_3\text{I}-\text{CO}_2$  was approximately 95% of pure  $\text{CF}_3\text{I}$ . The SLF interruption performance of  $\text{CF}_3\text{I}-\text{CO}_2$  (20-80%) was nearer to  $\text{CF}_3\text{I}$  than that of  $\text{CO}_2$  [10].

The SLF interruption performance of  $\text{CF}_3\text{I}-\text{N}_2$  had a linear characteristic as the proportion of  $\text{CF}_3\text{I}$  was increased, whereas the performance of the  $\text{CF}_3\text{I}-\text{CO}_2$  mixture changed non-linearly in the range encountered. The performance of a  $\text{CF}_3\text{I}-\text{CO}_2$  gas mixture was approximately the same as pure  $\text{CF}_3\text{I}$  when a concentration of 20%  $\text{CF}_3\text{I}$  or above was used [10], as shown in Figure 2.21.

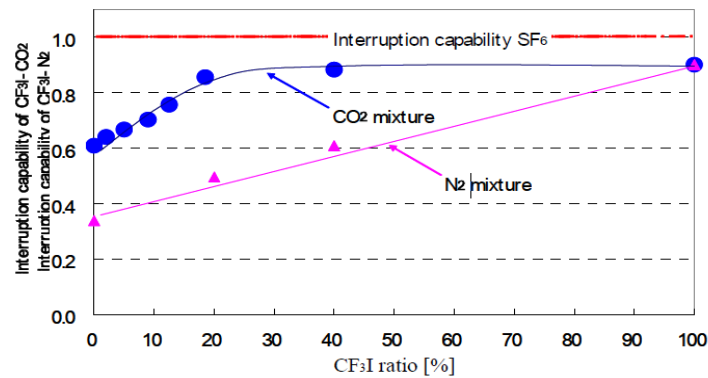


Figure 2.21: Transition of SLF interruption performance to  $\text{CF}_3\text{I}$  ratio of  $\text{CF}_3\text{I}$  mixture gas [10].

The BTF interruption capability of  $\text{CF}_3\text{I}$  was found to be 0.67 times that of  $\text{SF}_6$  and the BTF interruption capability of  $\text{CF}_3\text{I}-\text{N}_2$  changes linearly with the increase in the proportion of  $\text{CF}_3\text{I}$  [10].

The BTF performance of  $\text{CF}_3\text{I}-\text{N}_2$  (30-70%) was about 0.32 times that of  $\text{SF}_6$ , whereas the BTF interruption capability of  $\text{CF}_3\text{I}-\text{CO}_2$  mixture changes non-linearly [10]. The BTF performance of  $\text{CF}_3\text{I}-\text{CO}_2$  to pure  $\text{CF}_3\text{I}$  was approximately the same when  $\text{CF}_3\text{I}$  exceeds the proportion of 30% [10].

Comparison of  $\text{CF}_3\text{I}-\text{CO}_2$  and  $\text{CF}_3\text{I}-\text{N}_2$  BTF interruption capabilities at the same  $\text{CF}_3\text{I}$  ratio shows  $\text{CF}_3\text{I}-\text{CO}_2$  to be superior, as shown in Figure 22 [10].

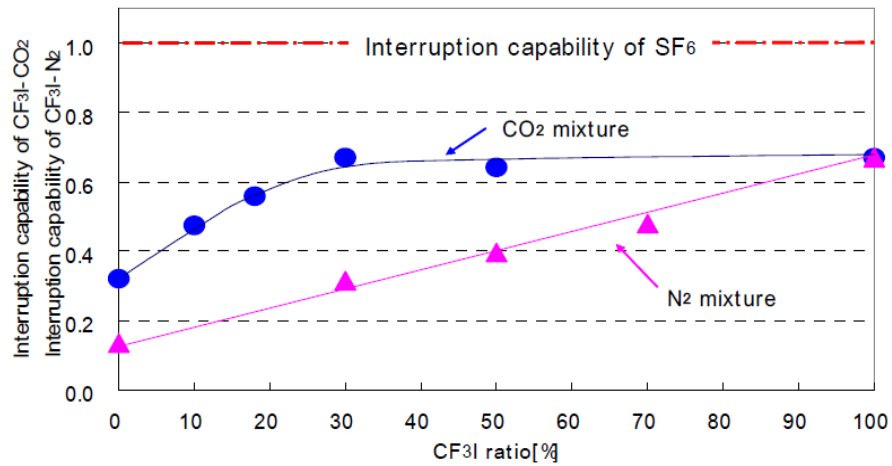


Figure 2.22: Transition of BTF interruption performance to  $\text{CF}_3\text{I}$  ratio of  $\text{CF}_3\text{I}$  mixture gas [10].

## 2.7 Phase change gas-liquid data

One of the main challenges with using  $\text{CF}_3\text{I}$  in distribution equipment is its high boiling point. At atmospheric pressure (0.1 MPa), the high boiling point of  $\text{CF}_3\text{I}$  is  $-22.5^\circ\text{C}$  and this means that  $\text{CF}_3\text{I}$  rapidly converts to a liquid state at higher pressures.  $\text{SF}_6$  has a boiling point of  $-63.9^\circ\text{C}$  at atmospheric pressure. The saturation curves for  $\text{CF}_3\text{I}$  and  $\text{SF}_6$  are shown in Figure 2.23.

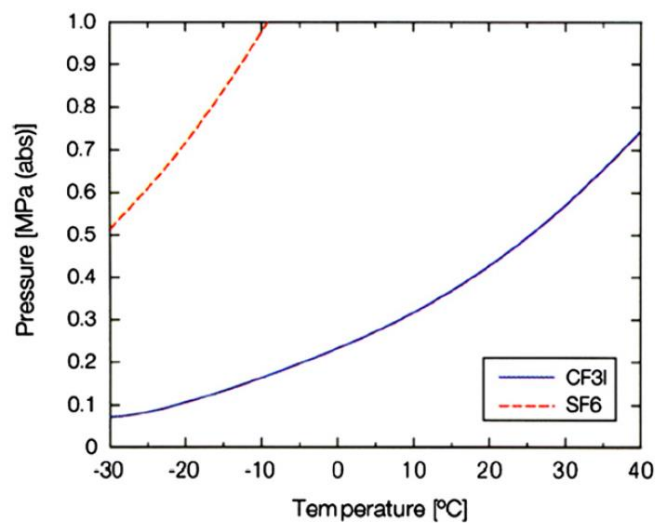


Figure 2.23: Saturation vapour pressure curve in  $\text{CF}_3\text{I}$  and  $\text{SF}_6$  [44].

Typically, SF<sub>6</sub> is used in distribution equipment from 0.1 MPa (megapascals) (abs) up to 0.5 MPa (abs) depending on the withstand voltage required by the switchgear [10]. SF<sub>6</sub> is normally filled above atmospheric pressure (0.1 MPa (abs)) so that if leakage occurs SF<sub>6</sub> is leaked outwards, this ensures that air is not brought into the gas chamber creating problems.

Typically, 0.5 MPa (abs) is used as the minimum working pressure in GCB (gas circuit breakers) applying for GIS (gas insulated switchgear) [9]. SF<sub>6</sub> at 0.5 MPa (abs) is used in GCB for GIS applications without any problems but at 0.5 MPa the boiling point of CF<sub>3</sub>I is about 25°C [10] and so impossible to use under these conditions as shown in Figure 2.23. As CF<sub>3</sub>I cannot be used at a pressure of 0.5 MPa, gas mixtures with small quantities of CF<sub>3</sub>I have been examined to ascertain whether the dielectric strength of CF<sub>3</sub>I can be kept whilst preventing liquefaction by decreasing partial pressure of the gas [45].

At atmospheric pressure, the boiling point of CF<sub>3</sub>I is -22.5 °C [25], as show in Table 2.3. However, MV switchgear can use SF<sub>6</sub> at a much lower pressure rating than 0.5 MPa (abs), therefore, avoiding the problem. For switchgear using gas a pressure of 0.2 MPa and below, pure CF<sub>3</sub>I could be used in indoor situations as its boiling point is close to -5 °C [1] (the preferred ambient air temperature for indoor GIS as stated in BS62271-1 [1]).

Table 2.3: Boiling point of different gases [10] [25] [9] [3] [46].

Pressure [MPa]	Note	Boiling point of Gas composition [°C]			
		SF <sub>6</sub>	CF <sub>3</sub> I	30% CF <sub>3</sub> I – 70% CO <sub>2</sub>	40% CF <sub>3</sub> I – 60% CO <sub>2</sub>
0.1	Atmospheric pressure	-63.9	-22.5	-	-
0.2	MV GIS applications	-50	-3	-22	-
0.5	HV GIS applications	-28	+25	-12.5	-5

As a countermeasure for the high boiling point of CF<sub>3</sub>I, a mixture with CO<sub>2</sub> can be formed. GIS for indoor use has a regulation boiling point of -5°C or less [1] which can be obtained by mixing CF<sub>3</sub>I-CO<sub>2</sub> at a ratio of 30% - 70% to obtain a boiling point of -12.5°C at 0.5 MPa [25]. GIS for outdoor use has a regulation point of -25°C or less [1] which can be obtained by a mixture of 30%:70% CF<sub>3</sub>I-CO<sub>2</sub> providing it is used under a pressure of 0.2 MPa.

According to Dalton's law, the total pressure of a mixture of ideal gases is equal to the sum of the partial pressures of the individual gases present in the mixture [30]. The partial pressure in a CF<sub>3</sub>I-CO<sub>2</sub> gas mixture can be formed and expressed as [30]:

$$P_{gas\ mixture} = P_{CF_3I} + P_{CO_2} \quad (2.7)$$

Where

$P_{gas\ mixture}$ : total pressure of the gas mixture

$P_{CF_3I}$ : partial pressure of CF<sub>3</sub>I gas

$P_{CO_2}$ : partial pressure of CO<sub>2</sub> gas

## 2.8 By-products and gas decomposition of CF<sub>3</sub>I

Although CF<sub>3</sub>I is known to undergo rapid photolysis in the presence of sunlight, the by-products of the photo-degradation process due to partial discharge (PD) need further investigation with regard to the possible occurrence of stress in electrical power apparatus [39].

M. Kamarol, Y. Nakayama, T. Hara, S. Ohtsuka and M. Hikita [39] have examined the partial discharge (PD) quantity with cumulative charge (qc) to analyse the by-products of CF<sub>3</sub>I gas suffering PD. The gas by-products formed after the PD test were analysed using a gas chromatography and mass spectroscopy detector (GC-MS) [39].

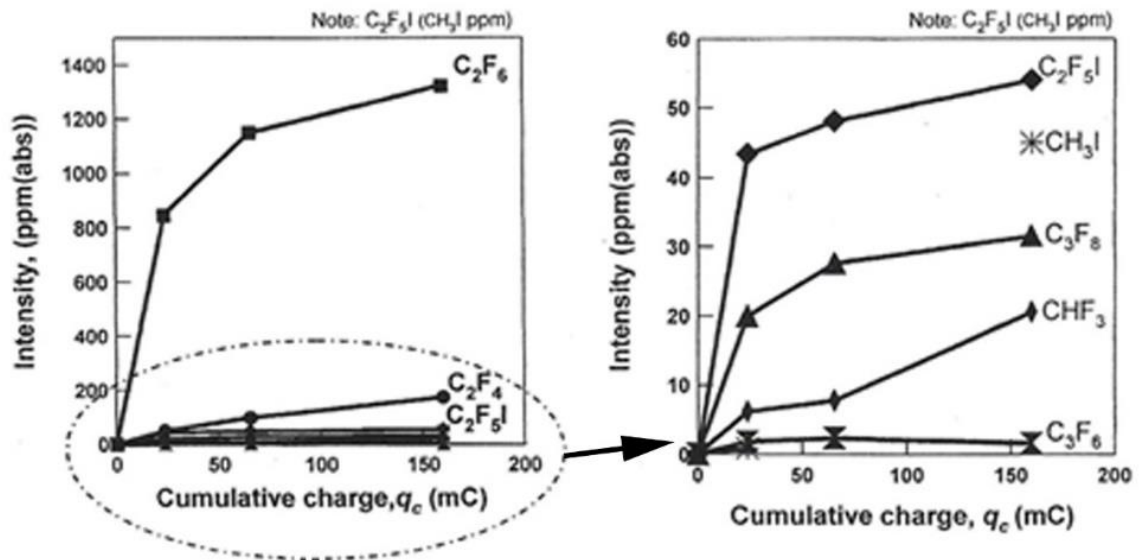


Figure 2.24: Gaseous by-products as a function of cumulative charge  $q_c$  [39].

It was found that hexafluoroethane ( $C_2F_6$ ), tetrafluoroethane ( $C_2F_4$ ), pentafluoroethyl iodide ( $C_2F_5I$ ), octafluoropropane ( $C_3F_8$ ), trifluoromethane ( $CHF_3$ ), hexafluoropropene ( $C_3F_6$ ) and methyl iodide ( $CH_3I$ ) were the gas by-products of  $CF_3I$  under partial discharge stress (Figure 2.24) [39].

The dominant gas by-products of  $CF_3I$  were  $C_2F_6$  (1300 ppm),  $C_2F_4$  (200 ppm) and  $C_2F_5I$  (55 ppm) with the other gas by-products  $C_3F_8$ ,  $CH_3I$ ,  $CHF_3$  and  $C_3F_6$  being detected at less than 50 ppm [39]. Analysis of the temporal change of the amount of decomposition products 20 hours after the partial discharge test, revealed that all by-products were present except  $CH_3I$  [39].

### 2.8.1 Measurement of fluorine by-products

In reference [10], the by-product fluorine content of  $CF_3I$  was measured, because of its harmful nature towards insulating materials and because it is toxic. This was then compared against that of the known fluorine production level in  $SF_6$ .

When  $SF_6$  was interrupted, at various current levels ( $A_{rms}$ ), the fluorine density for  $SF_6$  was shown to increase exponentially with the current. In contrast the fluorine level of

CF<sub>3</sub>I was very small throughout interruption. In 30%-70% CF<sub>3</sub>I-CO<sub>2</sub> gas mixtures, the density of fluorine was not detected at all [10].

At 400 A<sub>rms</sub>, the fluorine density generated from SF<sub>6</sub>, when the current was interrupted frequently, increased in proportion to the number of interruptions [9]. The density of fluorine from CF<sub>3</sub>I was very low even if the current was interrupted 10 times in a row (Figure 2.25 a) [9]. The density of fluorine from CF<sub>3</sub>I-CO<sub>2</sub> (30%-70%) was not detected at all [9]. When the interruption current level (A<sub>rms</sub>) was varied, for one current interruption at a time, it was found that the fluorine value from SF<sub>6</sub> increased exponentially with the current value [9]. The fluorine density from CF<sub>3</sub>I was very small even when the interruption current reached its highest value (Figure 2.25 b) [9].

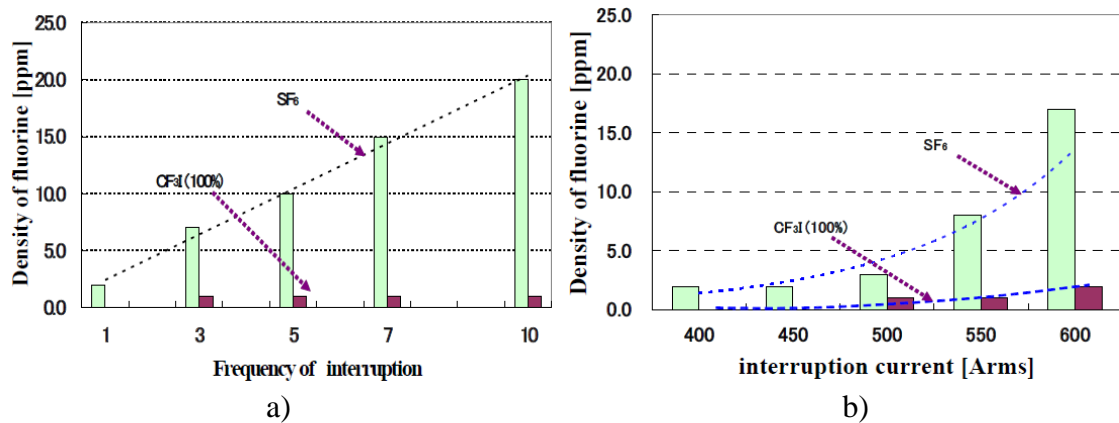


Figure 2.25: Density of fluorine when a) current is interrupted frequently b) current is interrupted one time only [9].

### 2.8.2 Measurement of iodine by-products

CF<sub>3</sub>I generates iodine when subject to a breakdown, and it is possible for the iodine to reduce its dielectric strength and voltage withstand capability because iodine particles are metallic [10].

When current was interrupted in CF<sub>3</sub>I and a mixture of CF<sub>3</sub>I-CO<sub>2</sub> (30-70%) with a variable level of current, the density of iodine from pure CF<sub>3</sub>I increased exponentially with the current, as did iodine from the CF<sub>3</sub>I-CO<sub>2</sub> mixture but at a rate 1/3 that of pure

CF<sub>3</sub>I. This was in line with the mixture ratio of CF<sub>3</sub>I [10] [25], and can be shown in Figure 2.26.

The density of C<sub>2</sub>F<sub>6</sub> increased almost linearly with the amount of flashovers, for either measurement under a uniform or a non-uniform field [47]. C<sub>2</sub>F<sub>6</sub> was generated by the chemical reaction:



Iodine (I<sub>2</sub>) was observed on the surface of the electrode after spark discharge, and its amount seemed to increase with the number of discharges [47]. As for the C<sub>2</sub>F<sub>6</sub> generated ratio, it was noted that the generated amount of C<sub>2</sub>F<sub>6</sub> depends largely on the applied voltage [47].

It can be said that partial discharges result in the production of C<sub>2</sub>F<sub>6</sub> gas and the dissociation of I<sub>2</sub> [39]. Iodine was not detected by the use of gas chromatography and a mass spectroscopy detector, probably because it was attached to the plane of the electrode in a solid state [39].

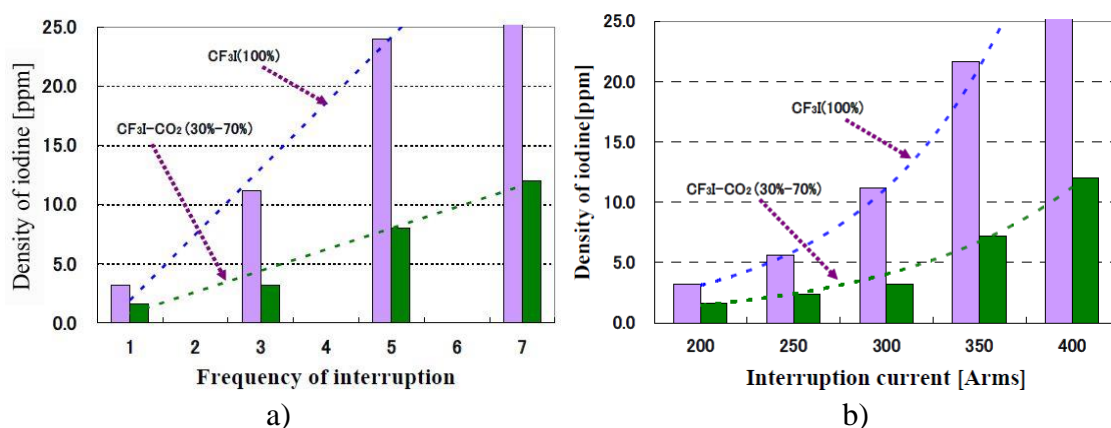


Figure 2.26: Density of iodine when a) current is interrupted frequently b) current is interrupted one time only [9].

The saturation vapour curve of iodine is shown in Figure 2.27. The molecule presents a melting point at 386.85 K (113.7 °C) and a boiling point at 457.4 K (184.3 °C) [48]. From

the saturation curve, it is possible to predict that the iodine, initially in gas form, will change into solid or liquid as the temperature of 300K is re-established. This is due to the high temperature of the arc. Therefore, the iodine molecule in solid state will be deposited on contacts and on moving parts. This deposit can lead to degradation of electrical insulation characteristic of the gas and have harmful corrosive effects on some materials. A possible solution is to trap the iodine using adsorbing techniques before the cooling of the insulating gas [9]. These are discussed in detail in section 2.8.4.

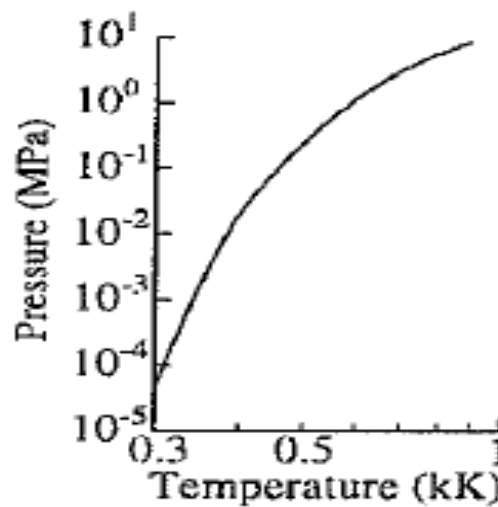


Figure 2.27: The saturation vapour curve of the iodine molecule [48].

### 2.8.3 Damage of iodine by-products to equipment and insulation properties of $\text{CF}_3\text{I}$

The influence of iodine ( $\text{I}_2$ ) adhered to a dielectric surface and the resulting insulation performance was evaluated with relation to the flashover voltage and time lag to flashover [19]. When examining the number of flashovers, from 0 to 800 times, the first flashover occurred without any  $\text{I}_2$  present on the dielectric's surface and the time lag to flashover was longer than 1000 ns. From the second flashover onwards, the flashover occurred with  $\text{I}_2$  on the dielectric's surface, and as a result, the time lag to flashover was decreased to 20-30 ns [19]. The insulation performance of the dielectric and  $\text{CF}_3\text{I}$  decreased down to 50% once a flashover occurred. The second and subsequent flashovers hardly influenced the insulation performance [19]. The decrease in insulation was accounted for by  $\text{I}_2$

adhesion on the insulator's surface as discharge formed one thick main conducting channel which developed easily between contacts. This allowed for an even greater point of  $I_2$  adhesion [19].

Other research has been carried out to evaluate the insulation property of deteriorated gas, without an insulator between the contacts, V-t characteristics were measured with the following conditions, in source [47]:

- A. V-t characteristics with 'used' electrode and 'used'  $CF_3I$
- B. V-t characteristics with 'used' electrode and fresh  $CF_3I$
- C. V-t characteristics with clear electrode and fresh  $CF_3I$

'Used electrode' and 'used  $CF_3I$ ' meant using the electrodes and  $CF_3I$  gas after they have been subjected to 1300 sparkovers in a uniform electric field. The sparkover voltage of condition A was the lowest and the sparkover voltage of condition C was the highest. Each sparkover voltage was normalized by that of condition A at each time lag, and for conditions B and C, the insulation performances deteriorated to less than 95% and 90% from condition A, respectively [47].

The largest by-product produced by  $CF_3I$  was  $C_2F_6$ , but even after 1400 sparkovers in a uniform contact gap, the density of  $C_2F_6$  was less than 150ppm ( $=0.014\%$ ). The difference of insulation performance between conditions B and C can be explained by the sublimation of  $I_2$ . When the gas was replaced, the gas chamber was evacuated for about 10 minutes with a vacuum pump and part of  $I_2$  remained in solid state on the electrodes surface unless they were replaced [47].

#### **2.8.4 Methods of reducing / eliminating fluorine and iodine by-products**

In  $SF_6$ , the main decomposition by-products, identified by GC-MS, are shown in Figure 2.28. Some of these by-products can be toxic but are easy to absorb using materials such

as activated alumina or molecular sieves [3]. The advantages of using a molecular sieve with  $\text{SF}_6$  is clearly shown in Figure 2.28, however, this process only works because most by-products of  $\text{SF}_6$  have a smaller critical diameter and are absorbed without affecting the insulation materials [49]. The same molecular sieve could not be used for a mixture of  $\text{CF}_3\text{I}-\text{CO}_2$  because  $\text{CO}_2$  has a smaller critical diameter than  $\text{CF}_3\text{I}$  and so would be absorbed into the molecular sieve, thus affecting the gas mixture ratio.

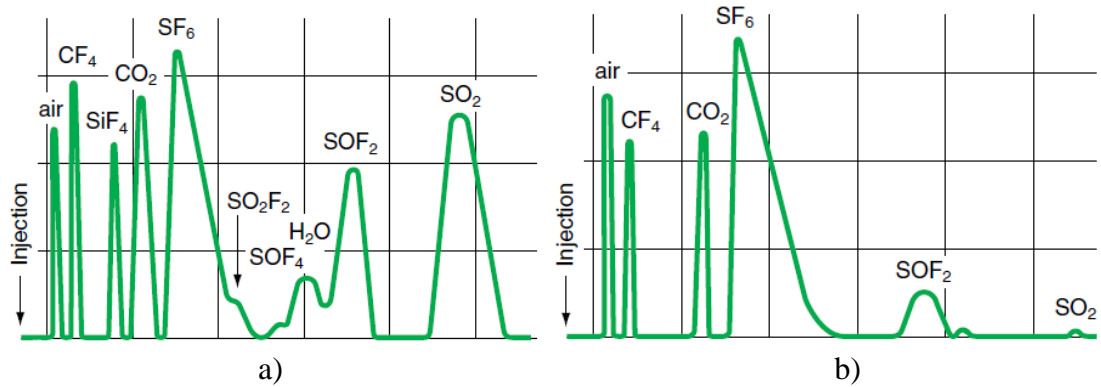


Figure 2.28: Gaseous by-products of  $\text{SF}_6$   
a) without absorbent b) with molecular sieve [3].

In early research of  $\text{CF}_3\text{I}$ , the authors [10] expected that the removal of iodine by gas flow would be necessary to improve the repeated interruption performance of  $\text{CF}_3\text{I}$  for a large current. However, it was later found that the iodine became attached to the surface of the electrodes and that gas flow would not always be effective in removing this adhesion.

H. Kasuya, H. Katagiri, Y. Kawamura, D. Saruhashi, Y. Nakamura, H. Mizoguchi and S. Yanabu [25] conducted experiments to remove all the iodine from an arc extinguisher chamber by using an absorbent. With the absorbent being placed in the way of the gas flow it was hoped that the decomposed gas would be thrown compulsorily into the absorbent and the iodine absorbed. The amount of absorbent that was needed to completely remove the iodine generated was explored. The absorbent used was  $\text{C}_2\text{X}$ , which is an activated carbon that is highly purifying [25]. This research was then

replicated to find out whether the absorbent can maintain its effect by repeatedly interrupting current [25].

A detecting tube was used to measure the iodine density, after current interruption, and filled with different amounts of absorbent (10, 30, 60 and 90g) along with the investigated mixture of 30%:70%  $\text{CF}_3\text{I}-\text{CO}_2$  [25].

By using different amounts of the absorbent i.e. 0, 10, 30, 60 and 90g, it was found that by increasing the amount of absorbent, it was possible to completely remove the iodine when 60g or over of absorbent was used [25].

The durability of the absorbent was recorded and current interruption repeated 22 times, with the iodine density measured every 3 current interruptions. The interruption occurs each time by the use of a new gas mixture and the durability of the absorbent was examined. The iodine density increased when the interruption frequency increased and it was found that the effect of the absorbent weakened gradually [25].

No iodine was detected, in 22 current interruptions, when 90g of absorbent was used. Thus, when the amount of absorbent was increased, it was found that the iodine could be completely removed with the absorptivity sustained throughout [25].

It was surmised, in reference [25], that, to be able to completely remove the iodine, an increased amount of absorbent from the experimental results would be needed in a real life practical situation.

In reference [9], the absorbent  $\text{C}_2\text{X}$  was used in a mesh with a specific surface area of 1.100-1.250  $\text{m}^2/\text{g}$  and with an aperture of 3.35-4.75 mm. When 5 grams of absorbent was placed in the chamber and the iodine density measured shortly after the interruption, with the current being varied for one interruption each time, the iodine content stayed the same

for pure  $\text{CF}_3\text{I}$  and decreased a little for  $\text{CF}_3\text{I}-\text{CO}_2$  as shown in Figure 2.29. When 5 grams of the absorbent was placed in the chamber and the iodine content was measured 5 minutes after interruption, with varying current levels, it was shown that the iodine for pure  $\text{CF}_3\text{I}$  decreased to 1/5 of the original value without the absorbent. The iodine from a 30%:70%  $\text{CF}_3\text{I}-\text{CO}_2$  mixture was less than 1/10 that of the original value without the absorbent as shown in Figure 2.30 [9].

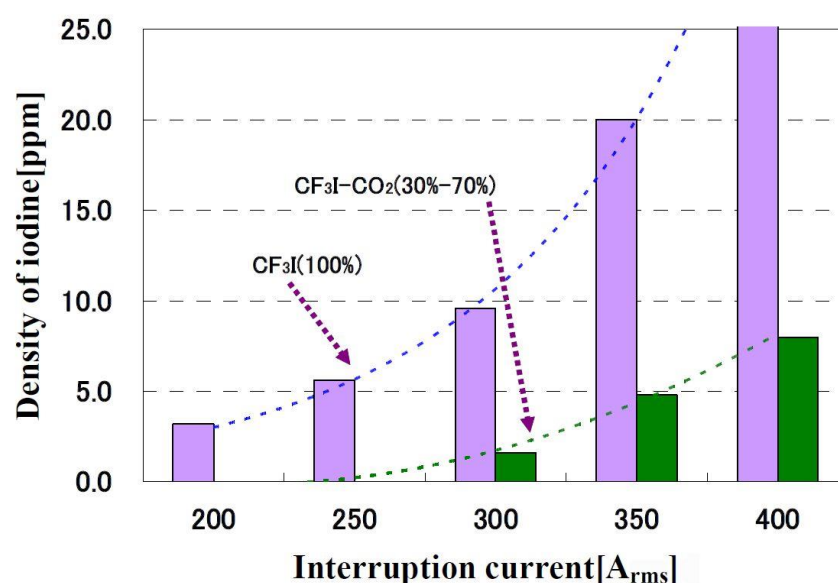


Figure 2.29: Density of iodine shortly after interruption when absorbent is placed [9].

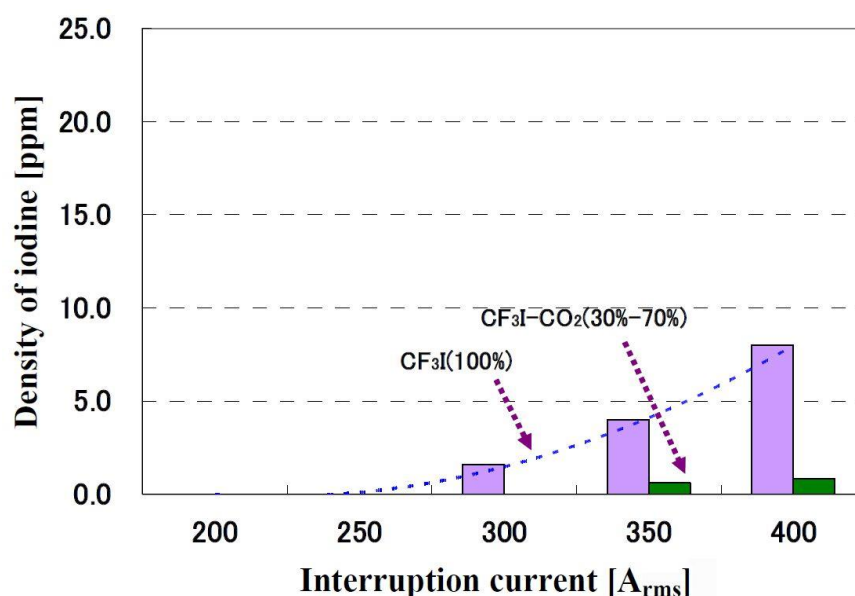


Figure 2.30: Density of iodine after absorption of about 5 mins [9].

## 2.9 Discussion and conclusion

CF<sub>3</sub>I is non-carcinogenic [10], colourless, non-flammable [10] and has a very low environmental impact [10], especially when compared to SF<sub>6</sub>. CF<sub>3</sub>I has a global warming potential (GWP) of less than 5 [9] and an ozone depleting potential (ODP) of 0.008 [28]. These factors can be attributed to CF<sub>3</sub>I having an extremely short atmospheric lifetime of less than 2 days (estimated) [24] because it is rapidly decomposed by solar light [10]. It remains unclear how much SF<sub>6</sub> equipment exists worldwide and the effect this could have on the environment, this issue is examined in Chapter 3.

CF<sub>3</sub>I is highly electronegative [11] [32] and, therefore, should be a good insulator. The effective ionization coefficient gives a limiting field strength for CF<sub>3</sub>I of 431 Td [34] which is higher than 361 Td for SF<sub>6</sub> [34] leading to CF<sub>3</sub>I having an insulation strength approximately 1.19 times that of SF<sub>6</sub> [34]. Although, the effective ionization coefficient can show that as the amount of CF<sub>3</sub>I in a gas mixture is lowered, so is the limiting field strength and insulation capability [34]. In Chapter 3, the effective ionization coefficients are calculated for 10:90%, 20:80% and 30:70% CF<sub>3</sub>I-CO<sub>2</sub> to determine their insulation strength against that of SF<sub>6</sub>.

The electric field and the field utilization factor are dependent on the electrode configuration, if the electrodes produce a uniform field (plane-plane), then the insulation strength and sparkover voltage of CF<sub>3</sub>I is higher than SF<sub>6</sub> [43]. However, the sparkover voltage and insulation strength of CF<sub>3</sub>I is lower than that of SF<sub>6</sub> under a non-uniform electric field (rod-plane) [43]. It remains unclear how the complex contact geometry found in practical switchgear will influence the uniformity of the electric field and, therefore, the insulation strength of CF<sub>3</sub>I. This issue is explored in more detail in practical experiments in Chapter 5 and in simulations in Chapter 6.

The 50% breakdown voltage has been shown to increase linearly with the amount of  $\text{CF}_3\text{I}$  in a  $\text{CF}_3\text{I}-\text{CO}_2$  gas mixture, the dielectric strength of 30%:70%  $\text{CF}_3\text{I}-\text{CO}_2$  is about 0.75 – 0.8 times that of  $\text{SF}_6$ . 60%-40%  $\text{CF}_3\text{I}-\text{CO}_2$  has a dielectric strength approximately equal to  $\text{SF}_6$ , this is dependent on electrodes [10]. Increasing the pressure of a  $\text{CF}_3\text{I}$  gas mixture further increases its insulation strength [43]. It remains unclear how the 50% breakdown voltage will vary when mixtures of 10:90%, 20:80% and 30:70%  $\text{CF}_3\text{I}-\text{CO}_2$  are tested in practical switchgear as shown in Chapter 5. It is also unknown how much influence small increments in the pressure of  $\text{CF}_3\text{I}-\text{CO}_2$  gas mixtures will affect the results of 50% breakdown voltage, this is also explored in Chapter 5.

$\text{CF}_3\text{I}$  has a high boiling point compared to  $\text{SF}_6$  making it impossible to use pure  $\text{CF}_3\text{I}$  at a pressure of 0.5 MPa (abs) or above [10]. A mixture of  $\text{CF}_3\text{I}$  and another gas may be used to decrease its boiling point [25]. In MV indoor switchgear, pure  $\text{CF}_3\text{I}$  could be used. In HV switchgear, where the pressure of the equipment is higher, a mixture of  $\text{CF}_3\text{I}$  and another gas must be used [10]. In Chapter 5 mixtures of  $\text{CF}_3\text{I}-\text{CO}_2$  are explored to determine their effects in MV switchgear, however, the results are transferrable to determine their viability in HV equipment.

When interrupting short line faults and breaker terminal faults  $\text{CF}_3\text{I}-\text{CO}_2$  and  $\text{CF}_3\text{I}-\text{N}_2$  gas mixtures do not perform as well as  $\text{SF}_6$ ,  $\text{CF}_3\text{I}-\text{CO}_2$  gas mixtures appear to have better interruption capabilities with less  $\text{CF}_3\text{I}$  than  $\text{N}_2$  [10].  $\text{CF}_3\text{I}$  generates iodine under high current interruption which can reduce dielectric strength and interruption capability of the gas as iodine particles are metallic. Research has been conducted using absorbents to decrease the amount of iodine that is produced. Without an absorbent  $\text{CF}_3\text{I}$  can only be used to interrupt a small current, such as 100A or lower, without iodine being produced in large quantities [9]. However, the fluorine level after  $\text{CF}_3\text{I}$  is utilised for current

interruption is very small throughout [28], the fluorine level increases as  $\text{SF}_6$  is used for current interruption.

From the research reviewed in this chapter, it is clear that  $\text{CF}_3\text{I}$  could be considered as an alternative insulation medium for distribution network applications. However, to maintain the high dielectric performance of  $\text{SF}_6$  in distribution equipment some problems need first be overcome before  $\text{CF}_3\text{I}$  can be used as an insulation medium in switchgear.

Further research is required to concentrate on which mixtures of  $\text{CF}_3\text{I}$  and another gas, such as  $\text{CO}_2$ , could be used to insulate equipment at all voltage levels. Gas mixtures of  $\text{CF}_3\text{I}$  and another insulating gas must consider the trade-off of the dielectric strength compared to the prevention of liquefaction by decreasing partial pressure of the gas. Experimentation must also use practical switchgear to examine the insulation capabilities of  $\text{CF}_3\text{I}$  gas mixtures on industrial equipment that has complex contact geometry. It is noted that iodine deposits may have an effect on the results obtained over a long period of time. These tests can be used to observe whether there are any issues associated with replacing  $\text{SF}_6$  in practical equipment and whether a certain  $\text{CF}_3\text{I}$  gas mixture could be a viable environmentally friendly insulator for the future.

## CHAPTER 3.

### SF<sub>6</sub> POWER PLANT AND GAS LEAKAGE

---

#### 3.1 Introduction

In this chapter, the widespread use of SF<sub>6</sub> in the distribution network is examined over the last 30 years. Various pieces of equipment that are insulated by SF<sub>6</sub> and that are common on the network today are also examined. Calculations of the amount of gas leakage that can be expected from SF<sub>6</sub> equipment, that has already been installed worldwide, and the effect this could have on the environment are given.

#### 3.2 Historical review of SF<sub>6</sub> equipment

To understand the significant role that SF<sub>6</sub> plays, within the power industry worldwide today, it is important to examine how SF<sub>6</sub> has been utilised throughout history. It is also important to understand the reasons why specific designs of SF<sub>6</sub> equipment have been implemented, specifically contact designs. From this historical and present day

knowledge a typical distribution network, with the currently employed SF<sub>6</sub> equipment, can be examined and an idea for how much SF<sub>6</sub> needs to be replaced can be gleaned.

Sulphur hexafluoride (SF<sub>6</sub>) was first introduced and widely used as an insulating medium in the power industry around the start of the 1980's and has been steadily adopted worldwide in electrical networks to insulate various types of equipment [3]. Figure 3.1 shows the difference between various insulation media and the voltage levels they are employed at in the power industry. From the graph, it is clear that SF<sub>6</sub> can be used extensively throughout all voltage levels in a power network whereas other insulating media cannot. SF<sub>6</sub> can insulate equipment up to 800 kV whereas, at present, other insulation media are not capable of such high voltage insulation, except for compressed air which can only accomplish this with very large contact gaps. SF<sub>6</sub> is also capable of high current interruption and, therefore, is sometimes used as an interruption medium to break high current but sometimes it is used to insulate equipment only.

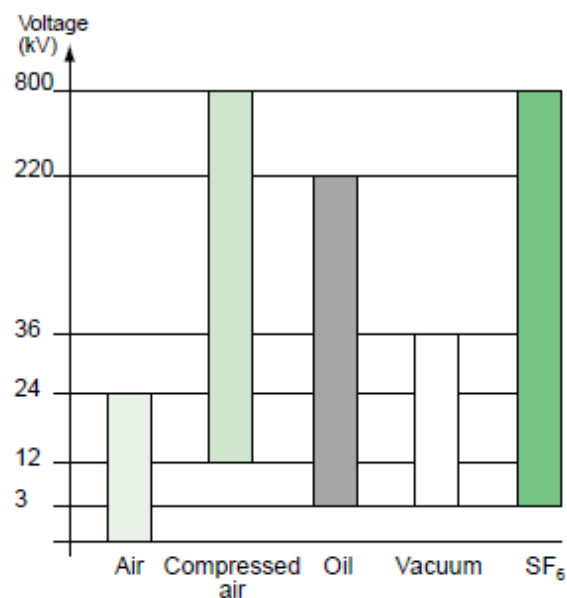


Figure 3.1: Types of breaking devices used according to voltage values [2].

Figure 3.2 indicates the development of MV circuit breakers in Europe from 1980 to 1998 and shows how the use of SF<sub>6</sub> has increased dramatically during that time. In Figure 3.2, the development of MV breakers is shown because it is the only voltage range in which

all technologies: air, oil, vacuum and SF<sub>6</sub> have been used as an insulation and current interruption medium. In Figure 3.2, SF<sub>6</sub> and vacuum have replaced oil and air as the only dielectrics used. SF<sub>6</sub> and vacuum have replaced current interruption in air because the equipment for these technologies costs less and requires less space [2]. Furthermore, SF<sub>6</sub> and vacuum have replaced current interruption in oil in MV applications because of the reliability the equipment has had over the last 30 years. More importantly, SF<sub>6</sub> equipment requires little to no maintenance [6], due to the sealed-for-lifetime nature of the equipment [2], and as a result, has a high safety record to date [4].

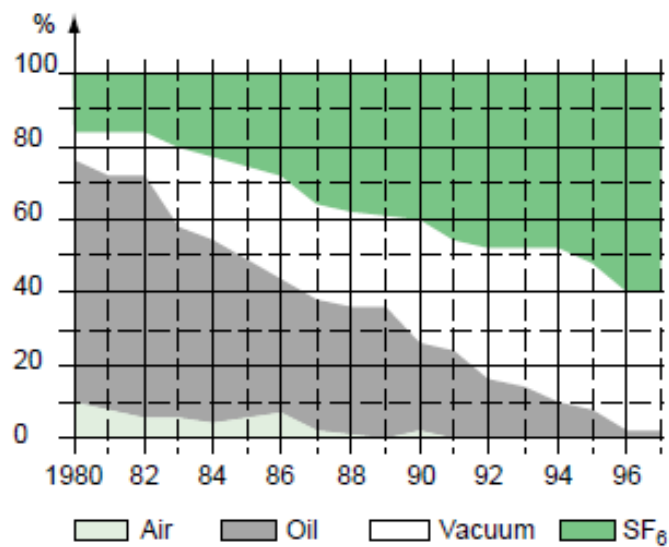


Figure 3.2: Development of the MV circuit breaker market in Europe [2].

Figure 3.3 shows breakdown voltage as a function of the inner-electrode distance and pressure of the equipment for SF<sub>6</sub>, air, vacuum and oil. It is important to note from the graph that SF<sub>6</sub> can cope with a much higher voltage than any other insulation medium so long as the pressure is high with a much smaller contact gap. This allows for much smaller equipment to be produced at HV and EHV than for any other insulation medium [50]. The insulation strength of vacuum technology is dependent on the pressure of the vacuum that can be achieved on the equipment through its seals and the vacuum pump utilised for this process [4]. The insulation strength of vacuum stabilises at a contact gap of roughly 25 mm. Therefore, vacuum cannot be used above 200 kV in the very best circumstances despite any changes that can be made to the electrode design or separation distance from

one another [2]. At 1 bar, the breakdown voltage of air does not increase anywhere near as rapidly as SF<sub>6</sub> when the inner electrode gap is increased. This means that as the voltage is increased the gap between the electrodes needs to be much larger in air equipment. Therefore, air equipment with the same breakdown strength as SF<sub>6</sub> equipment will be larger [5]. As the pressure of SF<sub>6</sub> is increased, the gap between electrodes can be further decreased for the same voltage withstand, as can be seen in Figure 3.3 when SF<sub>6</sub> has a pressure of 5 bars. This means that air equipment at 1 bar compared to SF<sub>6</sub> equipment at 5 bars will be much larger.

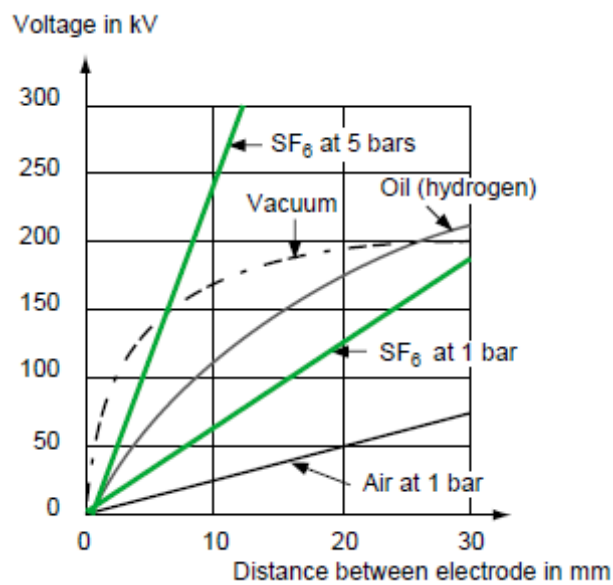


Figure 3.3: Influence of inter-electrode gap on dielectric strength [2].

In the LV distribution network, magnetically activated air breakers are predominantly used. This is because air breaking has the longest service record at this voltage, and although other insulating media could be used they are simply not necessary. For this voltage level, other insulating media would be more expensive and complex rather than the relatively cheap air technology currently used [2].

In EHV, SF<sub>6</sub> is practically the only insulating medium used because this technology is the most cost effective, and the equipment is much smaller [12]. Typically, the lowest voltage level that an SF<sub>6</sub> piece of equipment would normally be found operating at on the

network is between 1 kV and 52 kV at MV. It was, therefore, decided to focus on this voltage range to identify a potential alternative to SF<sub>6</sub>.

### 3.3 Typical distribution network which utilises SF<sub>6</sub> equipment

A typical distribution network from power generation to end user is shown in Figure 3.4 and 3.5 and depicts the various levels where SF<sub>6</sub> equipment might be found, although other insulation media are used at some of these voltage levels as well.

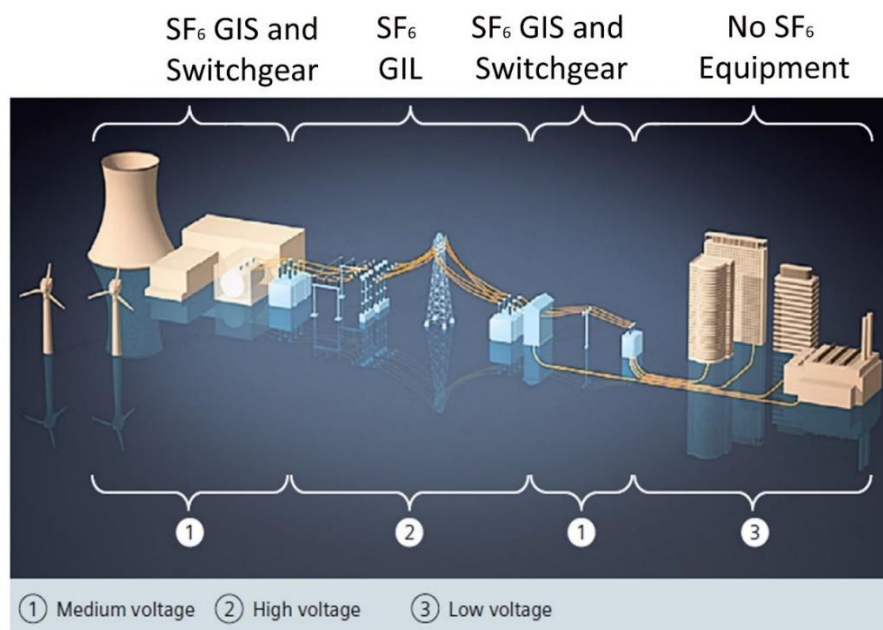


Figure 3.4: Typical distribution levels [12].

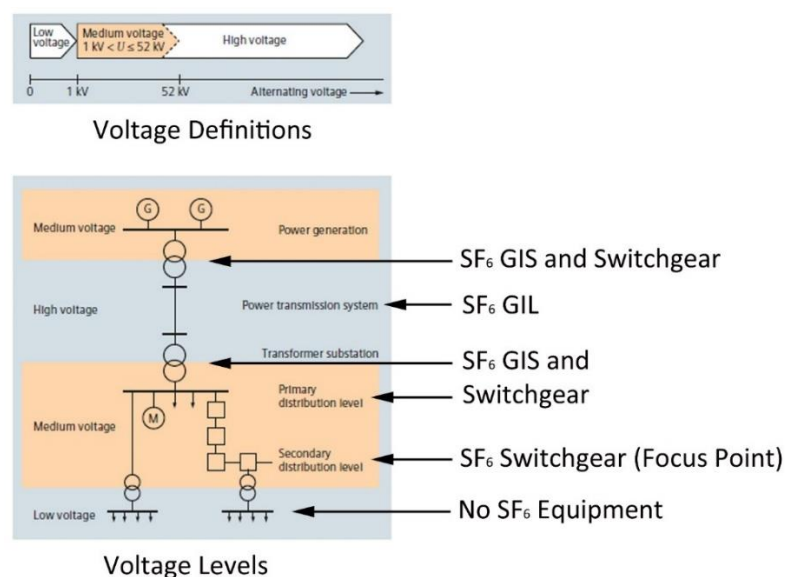


Figure 3.5: SF<sub>6</sub> distribution equipment on a typical distribution network [12].

For this project, the emphasis was to determine whether an alternative to SF<sub>6</sub> insulation in distribution equipment could be found. It was decided that to first prove the insulation capability of an alternative insulation medium, tests must be undertaken at the lowest voltage level for which SF<sub>6</sub> equipment is presently used i.e. MV. In Figure 3.5, it is shown that the lowest voltage level, for which SF<sub>6</sub> equipment is presently installed on the network, is at the secondary distribution level and, therefore, importance was placed on finding equipment that operated at this level.

### 3.4 UK substation layouts

To assess the potential of replacing SF<sub>6</sub> gas in equipment with CF<sub>3</sub>I-CO<sub>2</sub> gas mixture, it is important to understand how switchgear is utilised within the UK distribution network. It is, therefore, important to ascertain which distribution system switching arrangements and substation layouts are typical in the UK. These layouts will be particularly focused upon urban environments, as SF<sub>6</sub> equipment is most commonly employed in these situations [51] due to demand in the local area and the fact that urban substations are often restrained by size restrictions.

Figure 3.6 shows a typical urban distribution system with a primary single busbar layout substation and secondary open ring circuit substations. Along this network, there is equipment, within which the SF<sub>6</sub> insulation medium could be replaced with CF<sub>3</sub>I-CO<sub>2</sub>, as indicated on switches and other potential switchgear such as circuit breakers and ring main units.

Further information on this section can be found in Appendix A.

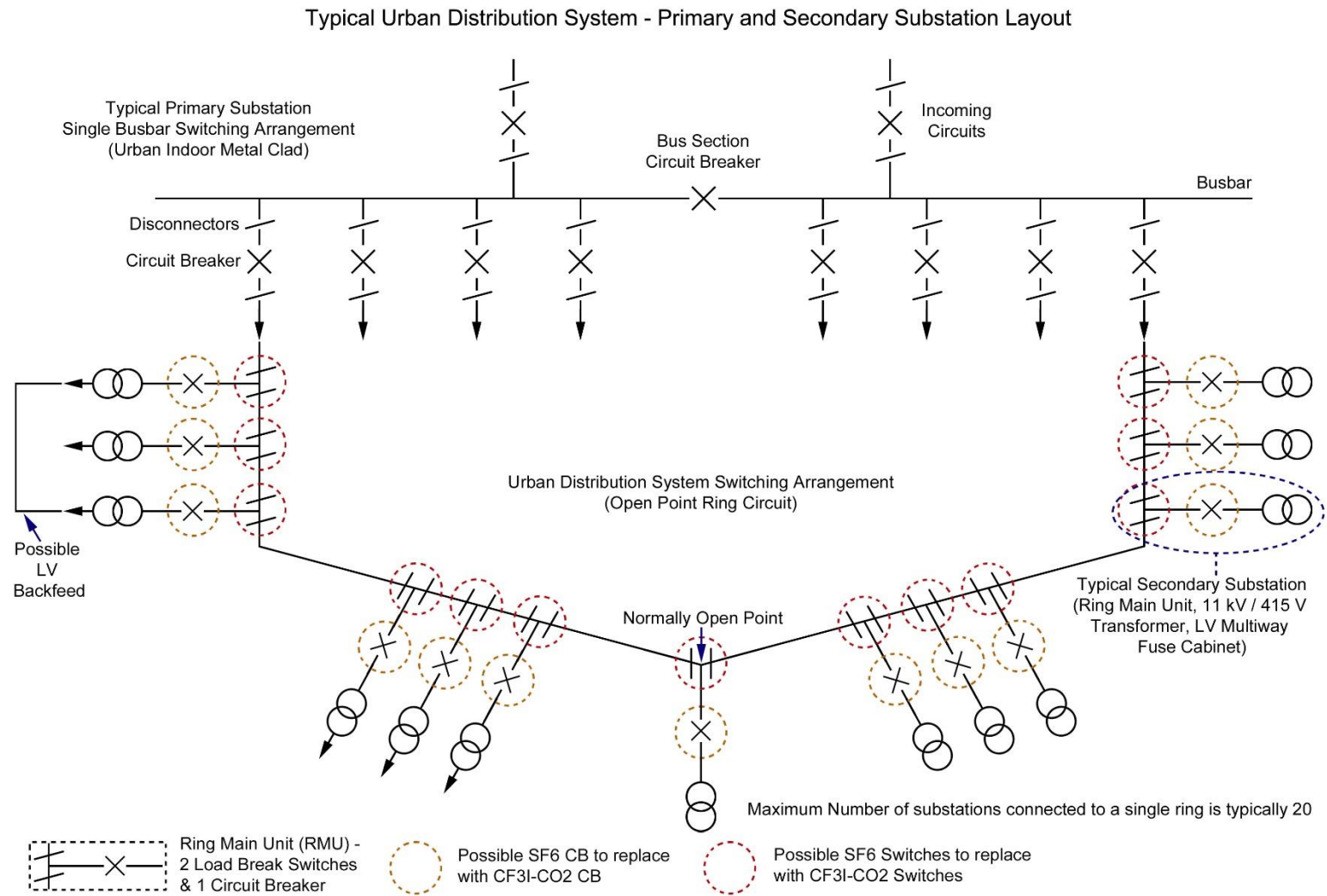


Figure 3.6: Typical urban distribution system with potential replacement  $\text{CF}_3\text{I-CO}_2$  switches and circuit breakers [51].

### 3.5 MV distribution equipment design

Table 3.1 defines some of the SF<sub>6</sub> equipment commonly used in the MV network as well as their functions and applications.

Table 3.1: Various switching devices, their functions and their applications [2].

	■ IEC definition ■ Function	Opening			Closing			Isolating
		○	●	⚡	○	●	⚡	
<b>Disconnecter</b>	<ul style="list-style-type: none"> <li>■ Mechanical connection device which in an open position guarantees satisfactory isolating distance under specific conditions.</li> <li>■ Intended to guarantee safe isolation of a circuit, it is often associated with an earthing switch.</li> </ul>	yes	no	no	yes	no	yes □	yes
<b>Earthing switch</b>	<ul style="list-style-type: none"> <li>■ Specially designed switch for connecting phase conductors to the earth.</li> <li>■ Intended for safety in case of work on the circuits, it relays the de-energized active conductors to the earth.</li> </ul>	yes	no	no	yes	no	yes □	no
<b>Switch</b>	<ul style="list-style-type: none"> <li>■ Mechanical connection device capable of establishing, sustaining and breaking currents under normal circuit conditions eventually including overload currents in service.</li> <li>■ Intended to control circuits (opening and closing), it is often intended to perform the insulating function. In public and private MV distribution networks it is frequently associated with fuses.</li> </ul>	yes	yes	no	yes	yes	yes	yes □
<b>Contactor</b>	<ul style="list-style-type: none"> <li>■ Mechanical connection device with a single rest position, controlled other than by hand, capable of establishing, sustaining and breaking currents under normal circuit conditions, including overvoltage conditions in service.</li> <li>■ Intended to function very frequently, it is mainly used for motor control.</li> </ul>	yes	yes	no	yes	yes	yes	no
<b>Circuit breaker</b>	<ul style="list-style-type: none"> <li>■ Mechanical connection device capable of establishing, sustaining and breaking currents under normal circuit conditions and under specific abnormal circuit conditions such as during a short-circuit.</li> <li>■ General purpose connection device. Apart from controlling the circuits it guarantees their protection against electrical faults. It is replacing contactors in the control of large MV motors.</li> </ul>	yes	yes	yes	yes	yes	yes	no

○ = at no load    ● = under load    ⚡ = short-circuit    □ = depending on the case

The rotary puffer contact design, shown in Figure 3.7 for switchgear, consists of a moving contact that rotates away from the incoming terminal to open the contacts. In some cases the contacts may not only rotate away from each other but also slide inwards away from

each other increasing the gap between contacts even further [52]. In a switch disconnector, and depending on the type of equipment being used, an earthing contact is provided so that the rotating arm for which the outgoing terminal is attached can be directly connected to earth, therefore, earthing the equipment in question. When the rotating arm moves away from the incoming terminal, SF<sub>6</sub> gas will be pushed into the resulting gap between contacts and insulate the outgoing terminal. The further away the open contacts are from each other will determine the amount of gas between the contacts and the resulting insulation strength, this is dependent on the amount of rotation of the moving arm. The SF<sub>6</sub> gas is also used to extinguish any arcs that may occur when the contacts are opened.

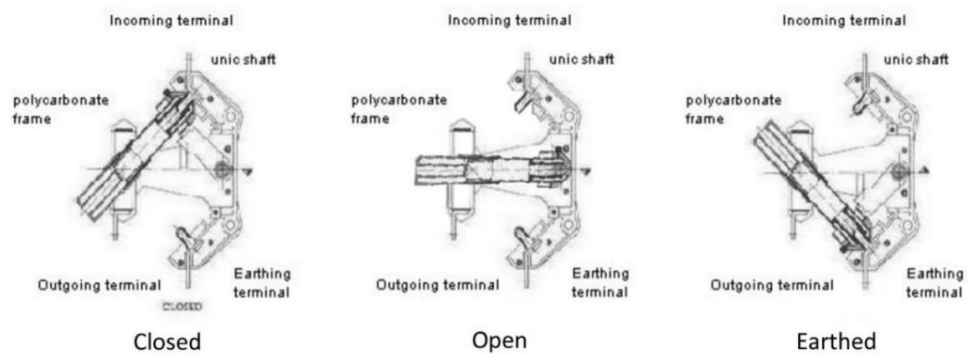


Figure 3.7: Three position rotary puffer contact design [52].

A switch disconnector in a GIS installation is used mainly to isolate different sections of busbars either for operational reasons or for safety during maintenance and refurbishment. Switch disconnectors are also used for duties, such as load transfer from one busbar to another, off-load connection and disconnection of busbars and circuit-breakers. Disconnectors are not intended to interrupt circuit currents but will be required to interrupt small capacitive currents associated with either open circuit-breakers or adjacent live circuits. When closed, the disconnector must be capable of carrying its rated load current and also a rated short-circuit current. In its open position, it must provide isolation both against the rated power frequency voltage and associated switching or lightning impulse voltages that may be superimposed thereon [50].

### 3.6 Worldwide / UK use of SF<sub>6</sub> and its effects

In the following section an estimate is given for the gas leakage from both UK and worldwide SF<sub>6</sub> equipment. A 0.1% leakage rate per year [1] is used to give these estimations, as specified by IEC 62271-1 for SF<sub>6</sub> equipment to fulfil the requirements for sealed pressure systems. It is noted that the leakage rate per year may be less or more than the value used but is often dependent on the age and degradation of the equipment. The calculations performed over the equipment's lifetime of 25 years represent a 0.1% leakage rate without gas replacement each year. These estimates do not include leakage from gas handling operations or gas chamber containment failure.

There are approximately 17,000 RMUs (Ring Main Units) in London only, owned by UK Power Networks, that are insulated by SF<sub>6</sub> or oil. There are approximately 48,892 RMUs operating on UK Power Networks' distribution network as a whole. An estimated 72% of these RMUs are SF<sub>6</sub> insulated. Therefore, there are an estimated 35,202 RMUs operating on UK Power Networks' distribution network that are filled with SF<sub>6</sub> [53].

The remaining 28% of RMUs are oil-filled. Therefore, there are approximately 13,690 RMUs operating on UK Power Networks' distribution network that are filled with oil [53].

If all the 35,202 RMUs on UK Power Networks' distribution network are filled with approximately 0.6 kg of SF<sub>6</sub>, it is estimated that 21121 kg of SF<sub>6</sub> is employed in these RMUs. The average filling weight of each RMU (0.6 kg) is based on an estimation by Schneider Electric but is dependent on the model and manufacturer of the unit [3]. Assuming a 0.1% leakage rate per year on all of these RMUs [1], there would be approximately 21 kg of SF<sub>6</sub> released into the atmosphere each year. From this number, an estimated 522 kg of SF<sub>6</sub> will be released over the 25 year lifetime [54] of the 35,202

RMUs employed on UK Power Networks' distribution network as shown in Table 3.2. An estimation of the leakage of all MV SF<sub>6</sub> RMUs employed worldwide is also given in Table 3.3.

Table 3.2: Estimated MV SF<sub>6</sub> RMUs employed by UK Power Networks [53].

Total No. of RMU's	Total No. of SF <sub>6</sub> Insulated RMU's	Total No. of Oil filled RMU's	Estimated SF <sub>6</sub> Mass per unit	Total Amount of SF <sub>6</sub> employed in all RMU's	Average Yearly leakage of SF <sub>6</sub> from all RMU's	25 Year leakage of SF <sub>6</sub> from all RMU's
48,892	35,202	13,690	0.6 kg	21,121 kg	21 kg	522 kg

Table 3.3: Estimated MV SF<sub>6</sub> RMUs employed worldwide [3].

Total No. of SF <sub>6</sub> Insulated RMU's	Estimated SF <sub>6</sub> Mass per unit	Total Amount of SF <sub>6</sub> employed in all RMU's	Average Yearly leakage of SF <sub>6</sub> from all RMU's	25 Year leakage of SF <sub>6</sub> from all RMU's
2,322,600	0.6 kg	1,393,560 kg	1,376 kg	34,424 kg

Similar leakage rate calculations can be carried out for SF<sub>6</sub> insulated CBs (circuit breakers) operating on UK Power Networks' (UKPN) distribution network and worldwide as shown in Table 3.4 and 3.6. Table 3.5 also takes into consideration the specific amount of these units that are from the Schneider Electric Ringmaster range [53]. For each SF<sub>6</sub> insulated CB, it approximated that 0.3 kg of SF<sub>6</sub> is required to fill the gas chamber [3] with an approximate 0.1% leakage rate per year [1] over a 25 year lifetime [54].

Table 3.4: Estimated MV SF<sub>6</sub> CBs employed by UK Power Networks [53].

Total No. of SF <sub>6</sub> Insulated CB's	Estimated SF <sub>6</sub> Mass per unit	Total Amount of SF <sub>6</sub> employed in all CB's	Average Yearly leakage of SF <sub>6</sub> from all CB's	25 Year leakage of SF <sub>6</sub> from all CB's
4,900	0.3 kg	1,470 kg	1.45 kg	36 kg

Table 3.5: Estimated MV SF<sub>6</sub> Ringmaster CBs employed by UK Power Networks [53].

Total No. of Ringmaster SF <sub>6</sub> Insulated CB's	Estimated SF <sub>6</sub> Mass per unit	Total Amount of SF <sub>6</sub> employed in all CB's	Average Yearly leakage of SF <sub>6</sub> from all CB's	25 Year leakage of SF <sub>6</sub> from all CB's
3,773	0.3 kg	1,132 kg	1.12 kg	28 kg

Table 3.6: Estimated SF<sub>6</sub> MV CBs employed worldwide [3].

Total No. of SF <sub>6</sub> Insulated CB's	Estimated SF <sub>6</sub> Mass per unit	Total Amount of SF <sub>6</sub> employed in all CB's	Average Yearly leakage of SF <sub>6</sub> from all CB's	25 Year leakage of SF <sub>6</sub> from all CB's
500,000	0.3 kg	150,000 kg	148 kg	3705 kg

Leakage calculations can be approximated for SF<sub>6</sub> insulated switches operating on UKPN distribution network and worldwide as shown in Table 3.7 and 3.9. Table 3.8 also takes into consideration the specific amount of these units that are from the Schneider Electric Ringmaster range [53]. If each one of the switches was similarly filled with SF<sub>6</sub> as the SE6 switch disconnecter used for testing at the start of their lifetime when originally placed on the network then each switch will contain 0.429 kg of SF<sub>6</sub> [55]. It is approximated that each switch has a 0.1% leakage rate per year [1] over a 25 year lifetime [54]. Since SF<sub>6</sub> has a GWP of about 23,900 times that of CO<sub>2</sub> [25], an approximate figure of 22 kg of SF<sub>6</sub> being released into the atmosphere from all switches is the equivalent of approximately 525,800 kg of CO<sub>2</sub> being released into the atmosphere [53]. It can be suggested from Tables 3.7 and 3.9 that the total leakage of UK Power Networks MV SF<sub>6</sub> switches (22 kg) represents approximately 0.31 % of the total worldwide leakage of switches provided they have a similar leakage rates to Ringmaster design over a 25 year period.

Table 3.7: Estimated MV SF<sub>6</sub> switches employed by UK Power Networks [53].

Total No. of SF <sub>6</sub> Insulated Switches	Estimated SF <sub>6</sub> Mass per unit	Total Amount of SF <sub>6</sub> employed in all Switches	Average Yearly leakage of SF <sub>6</sub> from all Switches	25 Year leakage of SF <sub>6</sub> from all Switches
2,100	0.429 kg	900 kg	0.89 kg	22 kg

Table 3.8: Estimated MV Ringmaster type SF<sub>6</sub> switches employed on UK Power Networks distribution network [53].

Total No. of Ringmaster SF <sub>6</sub> Insulated Switches	Estimated SF <sub>6</sub> Mass per unit	Total Amount of SF <sub>6</sub> employed in all Switches	Average Yearly leakage of SF <sub>6</sub> from all Switches	25 Year leakage of SF <sub>6</sub> from all Switches
1,533	0.429 kg	658 kg	0.65 kg	16 kg

Table 3.9: Estimated MV SF<sub>6</sub> switches employed worldwide [3].

Total No. of SF <sub>6</sub> Insulated Switches	Estimated SF <sub>6</sub> Mass per unit	Total Amount of SF <sub>6</sub> employed in all Switches	Average Yearly leakage of SF <sub>6</sub> from all Switches	25 Year leakage of SF <sub>6</sub> from all Switches
677,400	0.429 kg	290,604 kg	287 kg	7178 kg

From the above tables we can give an estimation of how much SF<sub>6</sub> is used in MV distribution equipment worldwide and by UK Power Networks in the UK. The total amount of leakage of this equipment for a 25 year lifetime [54] is also shown in Tables 3.10 and 3.11 for both worldwide present consumption and UK Power Networks present distribution network.

Table 3.10: Estimated MV SF<sub>6</sub> RMUs, CBs & switches employed on UK Power Networks distribution network [53].

Total No. of MV SF <sub>6</sub> Insulated RMU's	Total No. of MV SF <sub>6</sub> Insulated CB's	Total No. of MV SF <sub>6</sub> Insulated Switches	Total Amount of SF <sub>6</sub> employed in all MV RMU's, CB's & Switches	Average Yearly leakage of SF <sub>6</sub> from all MV RMU's, CB's & Switches	25 Year leakage of SF <sub>6</sub> from all MV RMU's, CB's & Switches
35,202	4,900	2,100	23492 kg	23 kg	580 kg

Table 3.11: Estimated MV SF<sub>6</sub> RMUs, CBs & switches employed worldwide [3].

Total No. of MV SF <sub>6</sub> Insulated RMU's	Total No. of MV SF <sub>6</sub> Insulated CB's	Total No. of MV SF <sub>6</sub> Insulated Switches	Total Amount of SF <sub>6</sub> employed in all MV RMU's, CB's & Switches	Yearly leakage of SF <sub>6</sub> from all MV RMU's, CB's & Switches	25 Year leakage of SF <sub>6</sub> from all MV RMU's, CB's & Switches
2,322,600	500,000	677,400	1,834,164 kg	1,812 kg	45,308 kg

The total estimated number of each type of switchgear is shown in Figure 3.8 for UK Power Networks MV distribution network. The majority of the units employed on the MV network are RMUs, these contain most of the SF<sub>6</sub> utilised at MV. The switches and CBs amount to a smaller proportion of the total amount of SF<sub>6</sub> utilised because there are less of these units on the UK network. The CBs and switches shown in Figure 3.8 are divided into two sections, one for the Ringmaster type units and one for all other makes utilised within UK Power Networks distribution network. It can clearly be seen from the figure that the majority of the switches and CBs are of Ringmaster design.

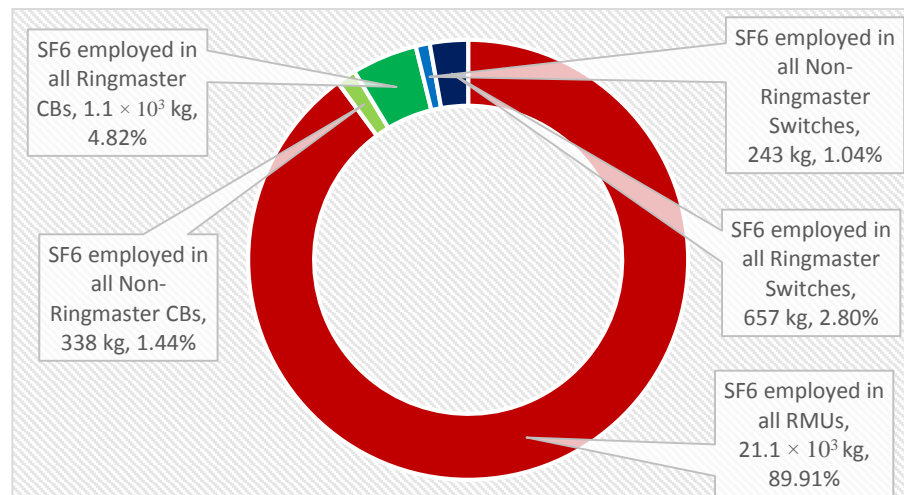


Figure 3.8: Estimated total amount of SF<sub>6</sub> employed in UKPN MV network.

The total estimated 25 year leakage of all the devices on UK Power Networks MV distribution network is shown in Figure 3.9. These results have been based on a 0.1% yearly leakage [1] of the total amount of each type of switchgear. As there are more RMUs, there is more leakage from these units. The total estimated 25 year leakage [54] for MV switchgear on UK Power Networks distribution network is 580 kg, the majority of this is from RMUs (521 kg) which is roughly 90%.

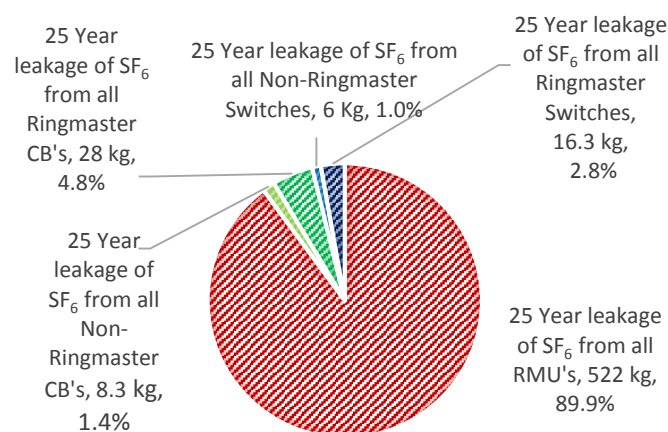


Figure 3.9: Estimated 25 year leakage of UK Power Networks MV SF<sub>6</sub> distribution equipment.

From an SF<sub>6</sub> emissions report published by UK Power Networks [56] it can be shown that the estimated average yearly leakage from all MV RMU's, CB's & switches (23 kg – Table 3.10) equates to roughly 21% of all UK Power Networks SF<sub>6</sub> leakage. The other

87.75 kg of SF<sub>6</sub> released into the atmosphere, in one year, must have been released by HV equipment or gas operations. Figure 3.10 shows that UK Power Networks released less SF<sub>6</sub> into the atmosphere than Western Power Distribution and that even more SF<sub>6</sub> was released by Scottish and Southern Energy (SSE) in the UK, therefore indicating that SSE utilise the most SF<sub>6</sub> insulated equipment [56] [57] [58].

The total estimated SF<sub>6</sub> gas used on worldwide MV distribution networks is 1,834,164.6 kg, as shown in Figure 3.11. An estimated 75% of this SF<sub>6</sub> is required to fill RMUs with approximately 1,393,560 kg of SF<sub>6</sub>. The total amount of SF<sub>6</sub> employed in UK Power Networks' MV distribution networks is 1.281% of the worldwide MV distribution networks usage.

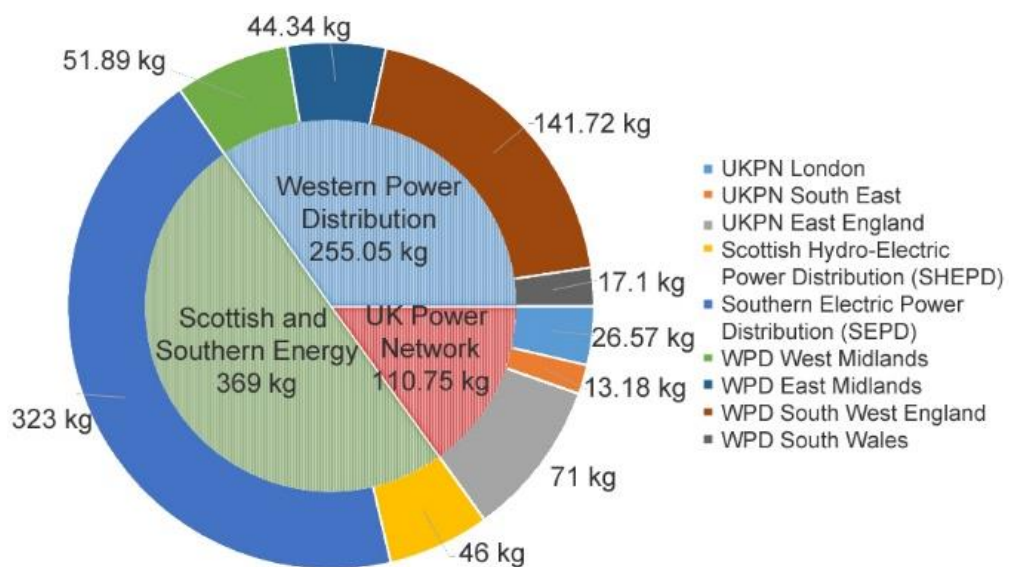


Figure 3.10: Reported SF<sub>6</sub> emissions for April 2012 – March 2013 by UK Power Networks [56], Western Power Distribution [57] and Scottish and Southern Energy [58].

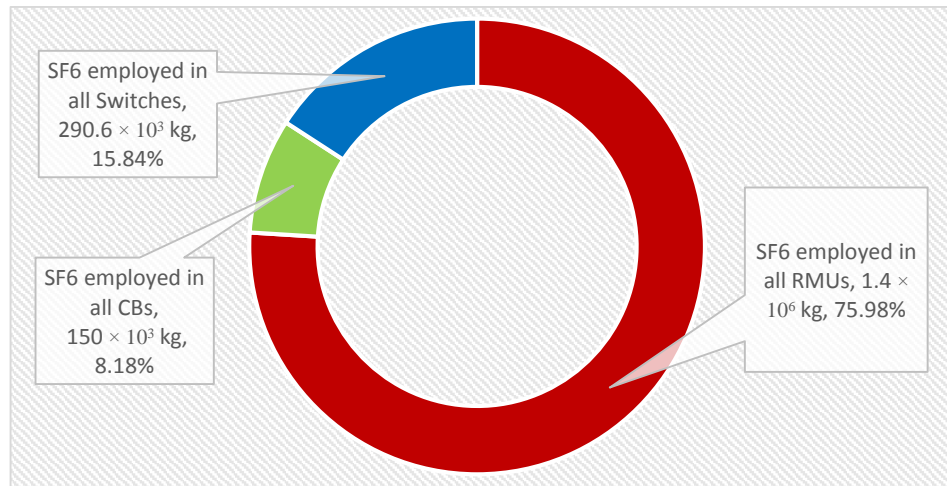


Figure 3.11: Estimated total amount of SF<sub>6</sub> employed worldwide in MV distribution networks.

The estimated 25 year leakage [54] of the total worldwide SF<sub>6</sub> MV distribution equipment is shown in Figure 3.12, this is based on a 0.1% yearly leakage [1]. RMUs can account for 75% (34,424.12 kg) of SF<sub>6</sub> being released into the atmosphere.

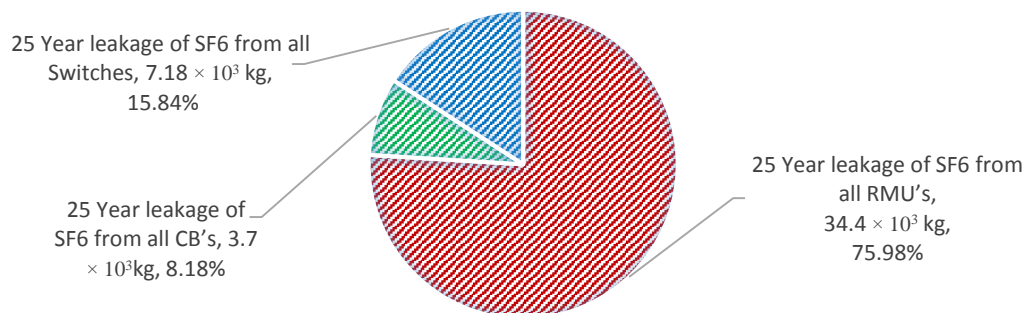


Figure 3.12: Estimated 25 year leakage of SF<sub>6</sub> worldwide MV distribution equipment.

For high voltage (HV) switchgear, an estimation for the total SF<sub>6</sub> required to fill all the HV GIS, open type CBs and GIL is shown in Tables 3.12, 3.13 and 3.14 respectively [3]. From Tables 3.12, 3.13 and 3.14 it is shown that GIS is the main use for SF<sub>6</sub> in the HV worldwide distribution networks, followed by open type CBs and then GIL. SF<sub>6</sub> leakage rates for GIS and open type CBs are expressed in terms of how much gas is used per unit whereas for GIL it is expressed by the total number of metres of gas insulated line. It is noted that GIL is often buried underground or under sea level so it is unclear whether a 0.1% leakage rate per year is still appropriate for this calculation.

Table 3.12: Estimated HV SF<sub>6</sub> GIS employed worldwide [3].

Total No. of SF <sub>6</sub> Insulated GIS	Estimated SF <sub>6</sub> Mass per unit (kg)	Total Amount of SF <sub>6</sub> employed in all GIS (kg)	Average Yearly leakage of SF <sub>6</sub> from all GIS (kg)	25 Year leakage of SF <sub>6</sub> from all GIS (kg)
20,000	500	10000000	9881	247023

Table 3.13: Estimated HV SF<sub>6</sub> open type CBs employed worldwide [3].

Total No. of SF <sub>6</sub> Insulated Open Type CBs	Estimated SF <sub>6</sub> Mass per unit (kg)	Total Amount of SF <sub>6</sub> employed in all Open Type CBs (kg)	Average Yearly leakage of SF <sub>6</sub> from all Open Type CBs (kg)	25 Year leakage of SF <sub>6</sub> from all Open Type CBs (kg)
100,000	50	5000000	4940	123511

Table 3.14: Estimated HV SF<sub>6</sub> GIL employed worldwide [3].

Total No. of SF <sub>6</sub> Insulated GIL (m)	Estimated SF <sub>6</sub> Mass per m (kg)	Total Amount of SF <sub>6</sub> employed in all GIL (kg)	Average Yearly leakage of SF <sub>6</sub> from all GIL (kg)	25 Year leakage of SF <sub>6</sub> from all GIL (kg)
30,000	30.24	907184	896	22410

An estimation for the total amount of SF<sub>6</sub> used worldwide in HV distribution networks from the Tables 3.12, 3.13 and 3.14 is shown in the Figure 3.13. It shows that roughly 63% of the worldwide consumption of SF<sub>6</sub> in HV distribution networks is used in GIS and 31% in open type CBs with only 6% being used in GIL.

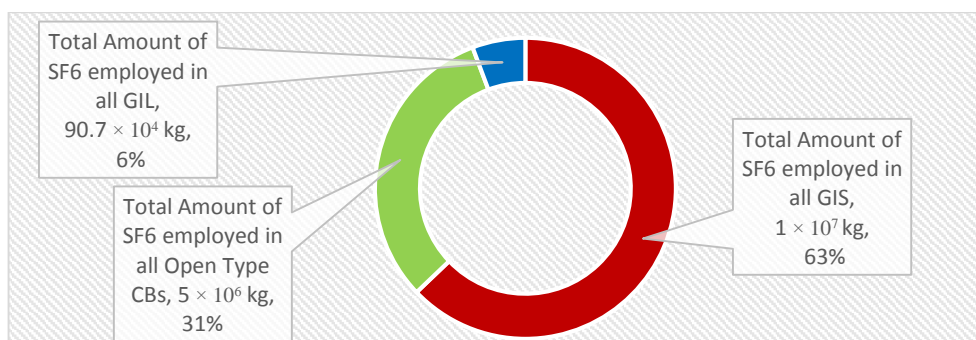


Figure 3.13: Estimated total amount of SF<sub>6</sub> employed worldwide in HV distribution networks.

An estimation of the accumulative 25 year leakage [54] of SF<sub>6</sub> equipment in HV distribution networks worldwide is shown (Figure 3.14). It is estimated that all the GIS

used worldwide would release 247023 kg of SF<sub>6</sub> into the atmosphere over a 25 year lifetime [54] and that Open type CBs would release 123511 kg into the atmosphere.

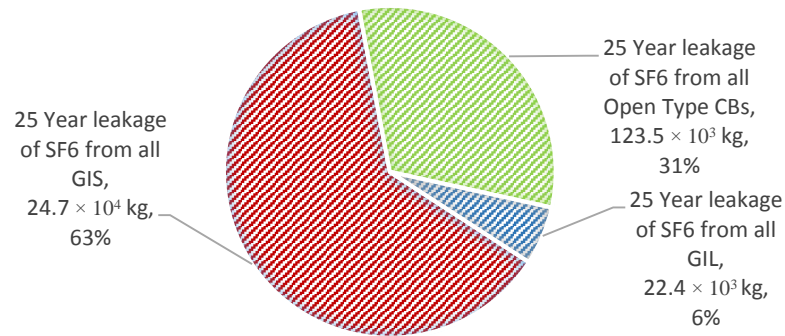


Figure 3.14: Estimated 25 year leakage of SF<sub>6</sub> worldwide HV distribution equipment.

An estimated total amount of SF<sub>6</sub> used worldwide in all distribution networks (MV and HV) is shown in Figure 3.15. The calculated results show that 89% of the world's SF<sub>6</sub> usage in distribution networks is HV equipment and that only 11% is from MV equipment. This is probably because less gas is used in MV equipment at lower pressures. Figure 3.15 also shows that the majority of SF<sub>6</sub> on distribution networks is employed in HV GIS and HV open type CBs, estimated at 84% of the total usage. This means that only 16% of SF<sub>6</sub> is used in MV distribution networks and HV GIL.

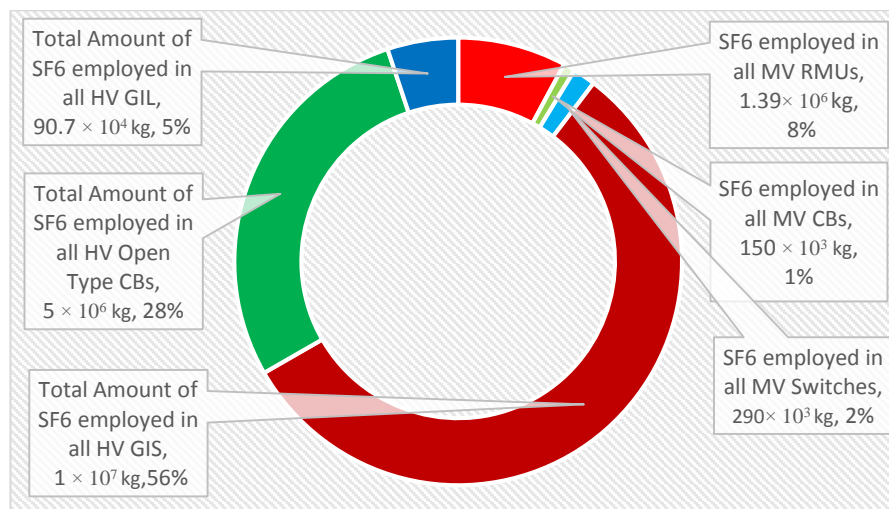


Figure 3.15: Estimated total of SF<sub>6</sub> employed worldwide in distribution networks.

From the total amount of SF<sub>6</sub> used worldwide in distribution networks, Figure 3.16 shows a 0.1% leakage [1] of all distribution equipment worldwide over its 25 year lifetime [54].

Figure 3.16 shows that HV GIS equipment worldwide over a lifetime of 25 years [54] will release 247023 kg of SF<sub>6</sub> into the atmosphere and HV open type CBs will release 123511 kg of SF<sub>6</sub> into the atmosphere. For each of these calculated results an equivalent ratio of CO<sub>2</sub> emissions is that for every 1 kg of SF<sub>6</sub> released into the atmosphere it is equivalent to 23,900 kg of CO<sub>2</sub> being released into the atmosphere.

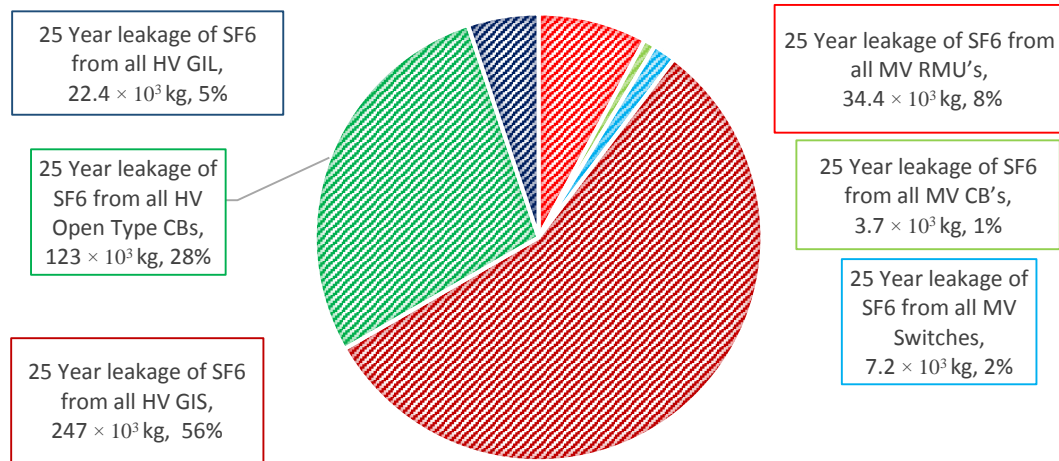


Figure 3.16: Estimated 25 year leakage of SF<sub>6</sub> worldwide distribution equipment.

It can be estimated from Figure 3.16 that the worldwide leakage from all HV and MV SF<sub>6</sub> equipment over a 25 year period is approximately 438 tons of SF<sub>6</sub>. This is the equivalent of 10468 ktons of CO<sub>2</sub>. It has been estimated that worldwide 34453427 ktons of CO<sub>2</sub> was released into the atmosphere in 2012 alone [59].

### 3.7 Conclusion

This chapter examines and identifies the equipment typically used on the distribution network, in the UK, that utilise SF<sub>6</sub> as an insulating medium. A typical distribution system layout for the UK is also explored and potential SF<sub>6</sub> equipment that could be replaced in the future identified. A wide range of equipment over all typical operating network voltages has been explored and SF<sub>6</sub> equipment designs, ratings and purposes examined. It is determined that practical experimentation for a replacement for SF<sub>6</sub> equipment

should focus on MV distribution equipment at the lowest voltage SF<sub>6</sub> is presently used on the network. This is because an alternative to SF<sub>6</sub> needs to first be able to prove its insulating capability at MV before it can be tested at HV. This will ascertain whether CF<sub>3</sub>I-CO<sub>2</sub> could be implemented and identify any problems that may arise.

This chapter further describes the potential problems that are apparent when calculating the estimated SF<sub>6</sub> leakage for equipment currently installed on the UK network, as well as worldwide. This highlights the potential problems with gas equipment leaking and the estimated amount of gas that will be released into the atmosphere during the installed equipment's lifetime on the network. These calculations do not include any extra leakage from gas handling operations and gas chamber failures that could further supplement the problem. Although SF<sub>6</sub> emissions are not as large as CO<sub>2</sub>, the long lifetime of SF<sub>6</sub> in the atmosphere makes its leakage a far reaching problem into the future.

## CHAPTER 4

# DEVELOPMENT OF LABORATORY EXPERIMENTAL RIGS AND TEST METHODOLOGY

---

### 4.1 Introduction

This chapter examines the experimental test setup developed to examine different mixtures of  $\text{CF}_3\text{I-CO}_2$  and the various pieces of equipment that were needed to make this research possible. Particular emphasis is given to the equipment that is commonly used in the industry when  $\text{SF}_6$  gas is the insulation medium being implemented.

Section 4.2 examines various pieces of  $\text{SF}_6$  switchgear and the selection process for choosing a piece of switchgear that could be utilised for testing, especially when the switchgear is filled with a gas such as a  $\text{CF}_3\text{I-CO}_2$  mixture. It is also relevant to examine whether this new mixture would cause any problems to the equipment that were specific to  $\text{CF}_3\text{I-CO}_2$  but not with  $\text{SF}_6$ .

Section 4.3 examines the gas handling equipment with particular attention being paid to the vacuuming / gassing / de-gassing of the particular switchgear chosen. The connections between the switchgear and the gas handling equipment were developed so that they were safe and secure. This section also examines the safe storage of various  $\text{CF}_3\text{I}$ - $\text{CO}_2$  gas mixtures, how much could be stored, its cost and how to achieve specific pressure-pressure ratios of  $\text{CF}_3\text{I}$ - $\text{CO}_2$  gas mixtures.

Section 4.4 examines the HV impulse generator test setup and the various British / IEC standards related to applying a lightning impulse to a piece of switchgear. Section 4.5 describes the preliminary testing required in order to establish a reliable and repeatable test condition. Lastly, section 4.6 concludes the development of an experimental rig and the testing techniques undertaken.

#### **4.2 $\text{SF}_6$ switchgear for exploring applications of $\text{CF}_3\text{I}$ and $\text{CF}_3\text{I}$ - $\text{CO}_2$ mixtures**

Worldwide today, various pieces of  $\text{SF}_6$  equipment exist including equipment that is used over a wide range of networks, current ratings, pressure ratings and voltage networks including Medium Voltage (MV), High Voltage (HV) and Extra High Voltage (EHV).

For the test setup being developed, it was important that the switchgear chosen had real relevance to equipment that is presently used on the network. It was important to focus on a piece of equipment that had not already been outdated by a different form of interruption medium. It was clear that the research should be focused on the potential of  $\text{CF}_3\text{I}$  and  $\text{CF}_3\text{I}$ - $\text{CO}_2$  gas mixtures as an alternative insulation medium inside a piece of MV  $\text{SF}_6$  equipment. There was also a need to ensure that the  $\text{SF}_6$  equipment chosen for testing would have a voltage / current rating that can be generated with the facilities available at Cardiff University.

Another issue faced was the availability of the switchgear equipment. To that end, a partnership was established with one of the main manufacturers of SF<sub>6</sub> switchgear (Schneider Electric) and the units used for testing were decided upon from the equipment that could be provided.

#### **4.2.1 SF<sub>6</sub> applications for exploring applications of CF<sub>3</sub>I and CF<sub>3</sub>I-CO<sub>2</sub> mixtures**

The MV switchgear product range for Schneider Electric is shown in Figure 4.1 [60] which was available for testing. It is important to note that there are also similar pieces of SF<sub>6</sub> equipment available which are manufactured by other companies.

In Figure 4.1, undesirable specifications for testing specific to this project have been highlighted in red such as units using only vacuum interruption technology or have a higher voltage rating i.e. 36 kV and above. Desirable features of a particular piece of switchgear have been highlighted in green. It was important that the contact design in the equipment chosen be as simple as possible but still being of the complex nature found in practical switchgear. This simplicity meant that any effects of the new insulating gas could be easier to interpret, and simulation of the contact design could also be conducted. Therefore, a load break switch was thought to be the best option for testing and simulation. Other specifications of particular interest included the switchgear current rating, which it was important to pick as low as possible, and the fact that the equipment could be operated indoors where testing was to take place.

The units chosen for testing with CF<sub>3</sub>I-CO<sub>2</sub> gas mixtures and SF<sub>6</sub> were the Fluokit and Ringmaster switch disconnectors because of their specifications and partly because of their availability. It is also important to note that the Ringmaster unit is employed in the UK MV distribution network and, therefore, very relevant for UK power companies.













Air insulated switchgear			Gas insulated switchgear									
												
Unisarc	SM6	SM6-24	SM6-36	Fluokit	HVL	HVL/cc	Ringmaster	FBX	RM6	CAS36	DV-CAS	Flusarc
IEC	IEC	IEC	IEC	IEC	ANSI	ANSI	IEC	IEC	IEC	IEC	IEC / ANSI	IEC / ANSI
<b>RATED VOLTAGE</b>												
17.5 kV	17.5 kV	17.5 kV	17.5 kV	17.5 kV	17.5 kV	17.5 kV	17.5 kV	17.5 kV	17.5 kV	17.5 kV	17.5 kV	17.5 kV
<b>MAX. RATED CURRENT</b>												
630 A	630 A & 1250 A	630 A	1250 A	630 A	630/1250 A	1200 A	1200 A	630 A	630 A	630 A	630 A	630 A
<b>MAX. RATED SHORT CIRCUIT CURRENT</b>												
20 kA	25 kA	20 kA	25 kA	25 kA	20 kA	20 to 61 kA	32 kA	40 kA	21 kA	25 kA	20 kA	25 kA
Vacuum CB	SF6/vacuum CB	SF6 CB	SF6 CB (Optional)	Open-air Switch	SF6 switch	SF6 CB	SF6 LBS	Vacuum CB	SF6 CB	SF6 LBS	Vacuum CB	Vacuum CB
Complete system of modular cubicles	Complete system of modular cubicles	Complete system of modular cubicles	Complete system of modular cubicles	Complete system of modular cubicles	Complete system of modular cubicles	Compact and modular switchgear combining all MV functional units	Compact and modular switchgear combining all MV functional units	Compact and modular switchgear combining all MV functional units	Compact and modular switchgear combining all MV functional units	Compact and modular switchgear combining all MV functional units	Wind dedicated modular switchgear combining all MV functional units used in wind farms	Compact and modular switchgear combining all MV functional units
Indoor	Indoor	Indoor	Indoor	Indoor	Indoor	Indoor and outdoor	Indoor	Indoor	Indoor	Indoor	Indoor	Indoor
IAC	IAC	IAC	IAC	IAC	IAC	IAC	IAC	IAC	IAC	IAC	IAC	IAC

Figure 4.1: Schneider Electric medium voltage switchgear selection guide specifications that are attractive for testing with  $\text{CF}_3\text{I-CO}_2$  mixtures are highlighted in green, unattractive specifications of the switchgear are highlighted in red [60] [61].

#### 4.2.2 Schneider electric switch disconnectors specifications

Normally, distribution switchgear is routinely tested (type-tested) before it is placed under working conditions within the network [1]. For distribution switchgear, the tests vary depending on the unit's intended purpose, the materials it is built from and its anticipated number of operations. This in turn determines the distribution switchgear rated insulation capabilities, specifications and tolerances throughout its lifetime [13]. There are three main types of tests used to ascertain the insulation integrity of a piece of switchgear, these are the power frequency, basic impulse and partial discharge tests [1].

For testing purposes throughout this research, switches will be used to evaluate the performance of  $\text{CF}_3\text{I}$  and  $\text{CF}_3\text{I-CO}_2$  gas mixtures against that of  $\text{SF}_6$ , which is currently used as an insulating medium in switchgear. All switchgear must be capable of:

- a) Carrying and interrupting its rated normal current safely,
- b) Closing its contacts onto a fault and carrying that fault for a rated specified time,
- c) Safely withstanding its rated power-frequency system voltage and rated lightning impulse voltage across its contacts when in the open position.

When a switch and a circuit breaker are compared, both can open and close onto the rated load current and close onto fault current but it is important to emphasize that a circuit breaker can interrupt a short-circuit fault current, whereas a switch cannot [13].

A disconnect switch is a mechanical switch that must be able to carry a defined rated normal and short-circuit current and, in the open position, it should be able to provide a defined level of insulation between its contacts, usually defined by an impulse voltage withstand level. This impulse voltage withstand level is an important discussion point when comparing the insulation capabilities of  $\text{SF}_6$  and  $\text{CF}_3\text{I}$  within a disconnect switch.

Dielectric tests of switchgear throughout this research programme will be conducted in accordance with IEC 60060-1 [62] unless otherwise specified. In compliance with BS EN 62271-1: High-Voltage switchgear and controlgear – Part 1: Common specifications [1].

According to BS EN 62271-1:

- i. The condition of the switchgear during dielectric tests shall be made on “completely assembled equipment, as in service, the outside surfaces of insulating parts shall be in clean condition” [1].
- ii. “When the distance between the poles of switchgear is not inherently fixed by the design, the distance between the poles for the test shall be the minimum value stated by the manufacturer” [1].

- iii. For switchgear using compressed gas for insulation, “dielectric tests shall be performed at minimum functional pressure (density) for insulation as specified by the manufacturer” [1].
- iv. “The temperature and pressure of the gas during the tests shall be noted and recorded in the test report” [1].

In the switchgear intended to be used throughout testing, the insulation capabilities of CF<sub>3</sub>I will be evaluated against SF<sub>6</sub> in the Fluokit ISR switch and the Ringmaster range load break switch. The manufacturer’s (Schneider Electric) specifications are shown in Table 4.1.

Table 4.1: Manufacturers rated insulation capabilities, tolerances and specifications of switch disconnectors: Fluokit (ISR switch) [63] [64] and Ringmaster (SE6-S1) [65] [55].

Abbreviation	Description	Fluokit	Ringmaster
$U_p$	Rated lightning impulse withstand voltage	125 kV	95 kV pk
$U_d$	Rated short-duration power-frequency withstand voltage	50 kV (r.m.s value)	38 kV (r.m.s value)
$U_r$	Rated voltage	24 kV	13.8 kV
$f_r$	Rated frequency	50 Hz	50/60 Hz
$I_p$	Rated peak withstand current	31,5 kA	53 kA
$I_k$	Rated short-time withstand current	12,5 kA (r.m.s)	21 kA
$t_k$	Rated duration of short-circuit	3 s	3 s
$U_s$	Rated switching impulse withstand voltage (for rated voltages 300 kV and above)	> 300 kV	> 300 kV
$I_r$	Rated normal current	400 – 630 A (r.m.s)	630 A (r.m.s)
$P_{re}$	Rated filling pressure for insulation and/or operation	0.045 MPa or 0.45 bar (g)	0.035 MPa or 0.35 bar (g)
$M$	Mechanical endurance class of disconnector	M1	M1
$E$	Electrical endurance class of earthing switch	E2	E2
$m$	Mass of Unit	125 kg	350 kg
$SF_6\ m$	Mass of SF <sub>6</sub> gas	110 g	429 g

It is important to note from the specifications that although both units fulfil the same purpose i.e. they are both switch disconnectors, they have some very different ratings and specifications. Of particular interest is the fact that the Fluokit M24+ unit has a rated lightning impulse withstand voltage of 125 kV but the Ringmaster SE6 unit only has a lightning impulse withstand voltage rating of 95 kV. It is also relevant to note that the Fluokit has a normal power frequency operating voltage rating of up to 24 kV whereas the Ringmaster is only up to 13.8 kV, although both units have a rated normal current rating of up to 630 A (r.m.s). Another important feature, especially for this research, is the filling pressure of each unit. The Fluokit switch disconnector has a filling pressure of 0.45 bar G whereas the Ringmaster has a lower filling pressure of 0.35 bar G. The amount of gas that each unit is filled with is very important for cost and leakage purposes. The Fluokit switch disconnector is filled with 110 g of SF<sub>6</sub>, at a pressure of 0.45 bar (g). The Ringmaster unit is filled with 429 g of SF<sub>6</sub> at a pressure of 0.35 bar (g). This indicates that the Ringmaster gas chamber is much larger than the Fluokit.

The contacts in both switch disconnectors produce a non-uniform field because the contacts are designed to separate quickly when the switch is operated into the open position. The contacts must also link together to form a strong union when the load switch is placed in the closed position. A difficulty with testing practical units was that the contacts do not always give exactly the same gas gap distance each time they are operated, as would be expected in a fixed contact experiment. This allows for some variation in the results but the effect could be limited by producing an average over all three phases of each unit.

#### **4.2.3 Fluokit – ISR switch disconnector connections and operation diagrams**

The Fluokit M24+ switch disconnector is shown in Figure 4.2.

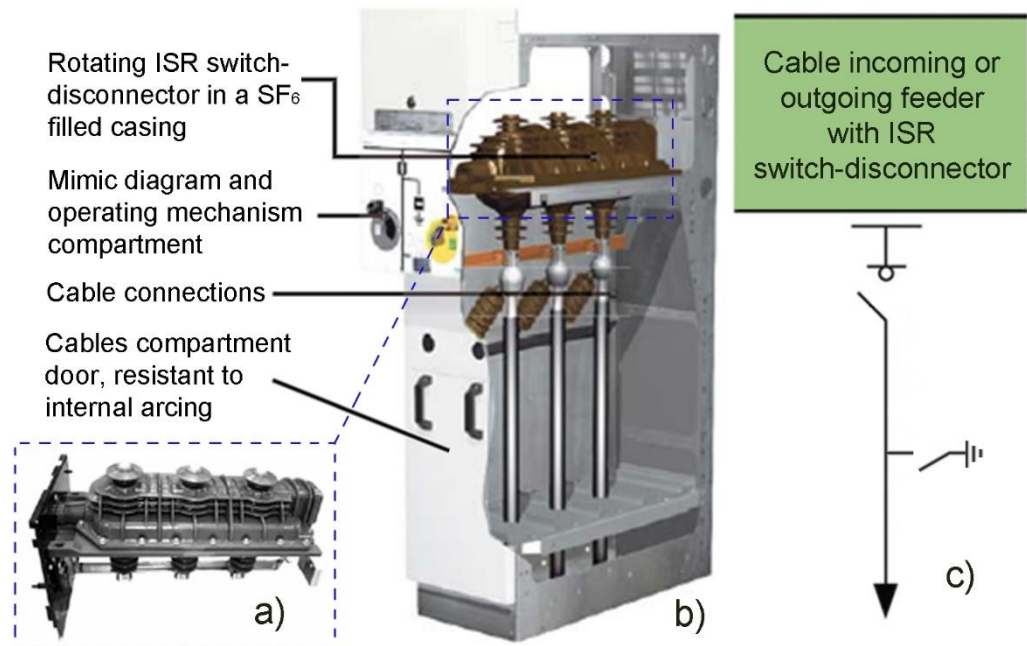


Figure 4.2: a) and b) Fluokit M24+ switch disconnector c) switch diagram [63] [66] [67].

From Figure 4.2, it is important to note the small area which is occupied by the gas chamber within, compared to the full size of the unit. This is because the space that is located beneath the gas chamber, where Figure 4.2 indicates cable connections, can also be used to house a 3 phase  $\text{SF}_6$  circuit breaker. This has been specifically designed to fit in this compact space so that the unit can house both an  $\text{SF}_6$  insulated switch disconnector and circuit breaker. Another important aspect of the design is to note the connection points, where testing equipment can be connected, which are at the top and the bottom of the gas chamber.

Fluokit M24+ switch disconnectors, in a MV substation, can be connected together. This means that a row of switch disconnectors can be employed as a switchboard, in a common busbar arrangement, but occupy as little space as possible.

Figure 4.3 shows the cable connections for the Fluokit M24+ switch disconnector which are located above the gas chamber for the busbar connections and below for the cable connections. The gas filling point of the Fluokit switch disconnector is also shown.

However, it is important to note that the Raccord valve gas connection shown has a permanent adapter connected to it for testing. The Raccord valve is only meant for lifetime filling i.e. once for 25 years and not for permanently gassing and de-gassing the units as was required for testing.

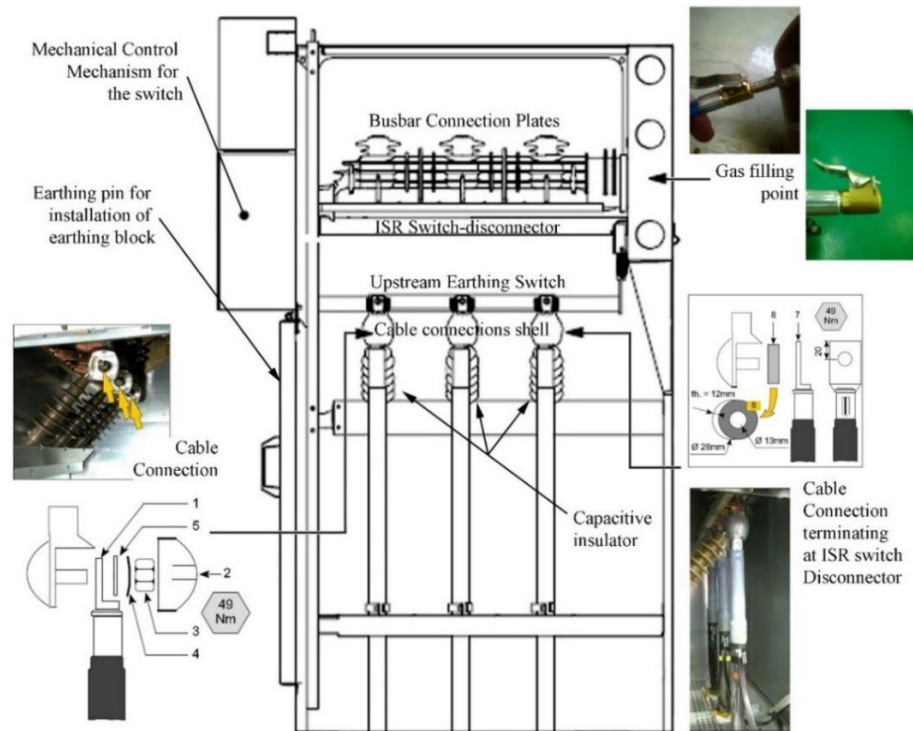


Figure 4.3: Side of Fluokit switch disconnecter unit with cable connections and gas filling point [63] [66].

#### 4.2.4 Ringmaster switch disconnecter connections and operation diagrams

The Ringmaster unit is shown in Figure 4.4 along with the operation and cable connections that can be made to the switch disconnecter. The Ringmaster unit has one operating mechanism that can choose between the operation of the load switch and the earth switch positions in contrast to the Fluokit which has two mechanisms for each position. The Ringmaster range is also fitted with a gas pressure indicator whereas the Fluokit is not.

Figure 4.5 shows the connection points through which the switch disconnecter can be earthed when the earth switch is placed in the closed position. These earthing points are connected to the main earthing point of the whole unit. The metal casing of the switch is

also connected to the main earthing point to ensure the switch has a permanent earth connection. Figure 4.5 also indicates the position where the gas filling / de-gassing point can be accessed so that the switch can be filled for testing with mixtures of  $\text{CF}_3\text{I}-\text{CO}_2$  gas. The gas indicator is shown in Figure 4.5, and indicates the optimum filling pressure of 0.35 bar G. The red line on the pressure gauge is the minimum operating pressure (for  $\text{SF}_6$ ) for the unit which is 0 bar G, below this point it is no longer safe to operate the unit.

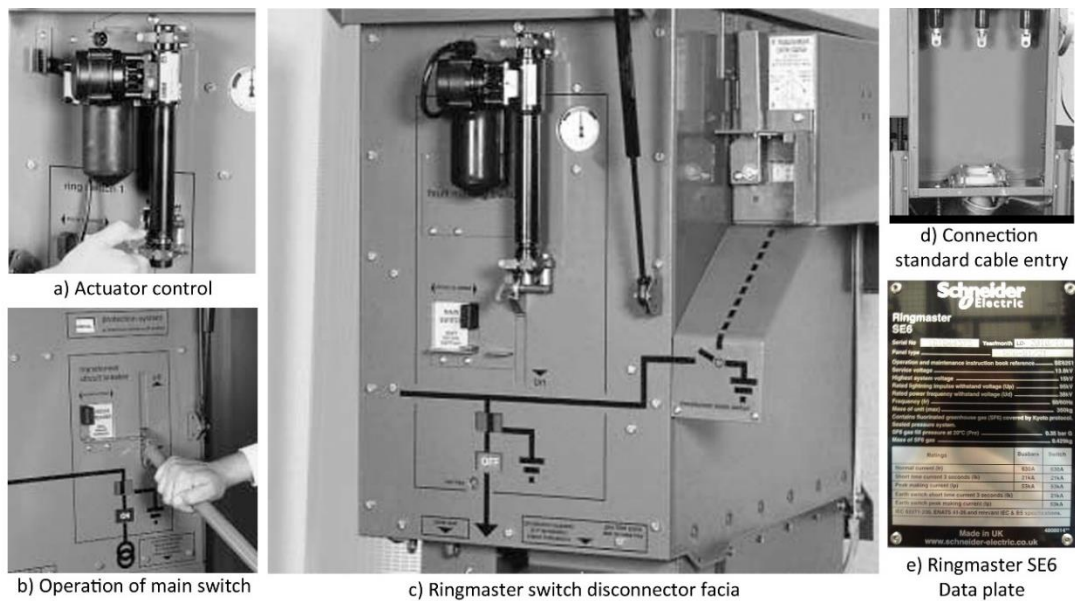


Figure 4.4: Operation and connections of the Ringmaster switch disconnector [65].

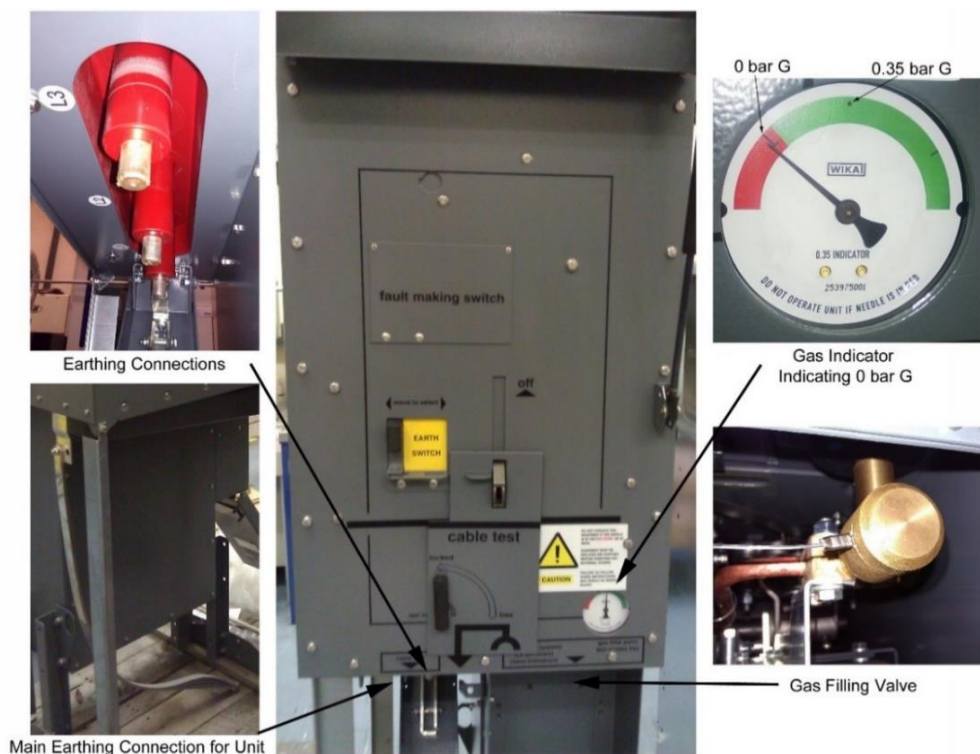


Figure 4.5: Ringmaster switch disconnector earthing connections and gas filling point.

#### 4.2.5 Switch disconnectors testing arrangement

Throughout testing four switch disconnectors, 2 x Ringmaster SE6-S1 and 2 x Fluokit ISR units, were utilised. One of each switch disconnector was permanently filled with SF<sub>6</sub> gas and the other of each type was filled with different pressure-pressure ratios of CF<sub>3</sub>I-CO<sub>2</sub> gas as shown in Figure 4.6.

The permanently filled SF<sub>6</sub> switch disconnectors remained the same as they are out of the factory i.e. filled for life. Therefore, the gas did not need removing and this solved the issue of requiring a qualification to be able to handle SF<sub>6</sub>. Releasing SF<sub>6</sub> is highly regulated by the Kyoto protocol due to its global warming potential. The lightning impulse generator, as described in section 4.4, was connected to each phase in turn to the busbar connections at the top of the switch disconnectors during testing, as shown in Figure 4.7.



- Ringmaster (R1)  
– permanently filled with SF<sub>6</sub>
- Ringmaster (R2)  
– filled with mixtures of CF<sub>3</sub>I-CO<sub>2</sub>
- Fluokit (F1)  
– permanently filled with SF<sub>6</sub>
- Fluokit (F2)  
– filled with mixtures of CF<sub>3</sub>I-CO<sub>2</sub>

Figure 4.6: Ringmaster SE6 and Fluokit M24+ switch disconnectors used for testing  
red indicates SF<sub>6</sub> gas filled devices, blue indicates CF<sub>3</sub>I-CO<sub>2</sub> gas filled devices.

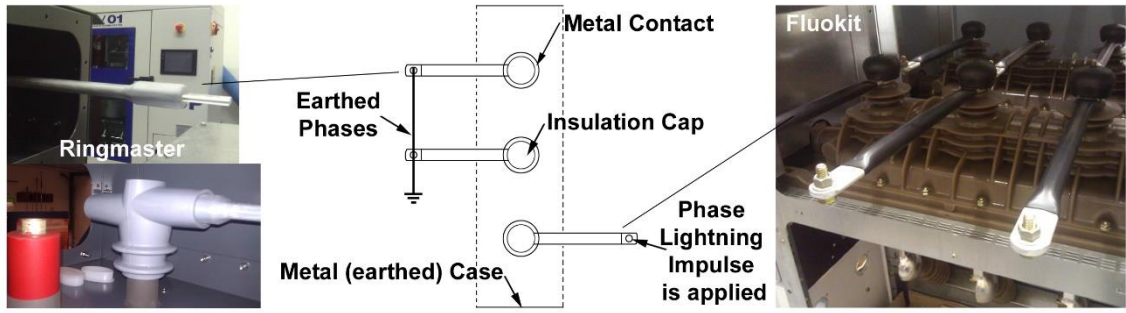


Figure 4.7: Lightning impulse generator connection to switch disconnectors.

### 4.3 Practical aspects of setup and operation of gas recovery and handling equipment

This section examines equipment used for handling SF<sub>6</sub> gas and then explores how this equipment can be utilised to handle various mixtures of CF<sub>3</sub>I-CO<sub>2</sub> gas. The various issues with this approach are then discussed and the most viable option for testing is suggested. Table 4.2 shows useful information for handling gas mixtures of CF<sub>3</sub>I and its by-products after a sparkover. The stability of the substance, toxicology description, personal protection action and possible transportation restriction are described.

#### 4.3.1 CF<sub>3</sub>I-CO<sub>2</sub> ideal gas mixture calculations

The following section examines ideal gas mixture calculations for filling the Ringmaster and Fluokit switch disconnectors with different ratios of CF<sub>3</sub>I-CO<sub>2</sub> pressure-pressure gas mixtures. The amount of gas required for testing is determined for a range of pressure-pressure mixtures of CF<sub>3</sub>I-CO<sub>2</sub>, the gas connections needed for this and an appropriate storage method for various gas mixtures.

##### 4.3.1.1 Ideal gas mixture calculations

The ideal gas law principle is as follows [30]:

$$MW = K \left( \frac{m}{P} \right) \quad (4.1)$$

Table 4.2: CF<sub>3</sub>I and its decomposition products [68] [69] [70] [71] [72] [73].

By-product	Molecular Weight	Stability	Toxicology Description	Transport information	Personal Protection	EU code	
						R	S
CF <sub>3</sub> I	195.91	Avoid strong oxidizing agents. Hazardous decomposition products	May be harmful if inhaled. Irritant.	UN No 1956 Hazard Class 2.2	Safety Goggles Gloves Impervious Clothing	Irritating to eyes, respiratory system and skin. Possible risk of irreversible effects	Do not breathe gas/fumes/vapour/spray. Avoid contact with skin and eyes. In case of contact with eyes, rinse immediately with plenty of water and seek medical advice. Wear suitable protective clothing and gloves. Wear eye/face protection. In case of accident or if you feel unwell seek medical advice immediately.
C <sub>2</sub> F <sub>6</sub>	138.01	Avoid strong oxidizing agents	May be harmful if inhaled. Suffocation if present in high concentrations	UN No 2193 Hazard class 2.2	Good ventilation Gloves Safety Goggles Impervious Clothing	Irritating to eyes, respiratory system and skin. Risk of explosion if heated under confinement. Vapours may cause drowsiness and dizziness	Keep container in well ventilated place. In case of insufficient ventilation wear suitable respiratory equipment. Use only in well-ventilated areas
CHF <sub>3</sub>	70.01	Stable Incompatible with strong oxidizing agent	May be harmful if inhaled Rapid suffocation Narcotic effect	UN No 1984 Non-flammable gas Hazard class 2.2	Good ventilation Safety Goggles Gloves Impervious Clothing	-	In case of insufficient ventilation wear suitable respiratory equipment
C <sub>3</sub> F <sub>8</sub>	188.02	Stable under normal conditions. Thermal decomposition yields toxic products which can be corrosive in the presence of moisture.	Not Established Hazard : asphyxiation Frostbite, Irritating to eyes, respiratory system and skin	UN No 2424 Hazard Class 2,2 Store in cool, dry place	Ensure adequate ventilation. Safety Goggles Gloves Impervious Clothing	Irritating to eyes, respiratory system and skin. Risk of explosion if heated under confinement. Vapours may cause drowsiness and dizziness	Keep container in well ventilated place. In case of insufficient ventilation wear suitable respiratory equipment. Use only in well-ventilated areas
C <sub>3</sub> F <sub>6</sub>	150.02	Stable, Avoid direct sunlight Avoid heat sources	Inhalation (Toxic) Irritant, frostbite	UN No 1858 Hazard class 2.2	Gloves Safety Goggles Impervious Clothing	-	-
C <sub>2</sub> F <sub>5</sub> I	245.92	Risk of explosion if heated under confinement. Incompatible with strong oxidizing agent Not compatible with aluminium	May be harmful if inhaled. Irritant to eyes, respiratory system and skin.	UN No 3163 Hazard class 2.2 Transport category 3	Good ventilation Safety glasses Impervious Clothing	Irritating to eyes, respiratory system and skin. Risk of explosion if heated under confinement. Possible risk of irreversible effects	Keep container tightly closed. Do not breathe gas/fumes/vapour/spray. Avoid contact with skin and eyes. In case of contact with eyes, rinse immediately with plenty of water and seek medical advice. Wear suitable protective clothing and gloves. In case of insufficient ventilation wear suitable respiratory equipment. Wear eye/face protection. In case of accident or if you feel unwell seek medical advice immediately

Where 
$$K = \frac{RT}{V} \quad (4.2)$$

Therefore giving: 
$$MW = \frac{RT}{V} \times \left(\frac{m}{p}\right) \quad (4.3)$$

or 
$$V = \frac{mRT}{MW \times P} \quad (4.4)$$

or 
$$m = \frac{MW \times PV}{RT} \quad (4.5)$$

Where: m = mass of gas (grams), T = temperature (Kelvin), P = pressure (bar),

MW = molecular weight (g mol<sup>-1</sup>), R = ideal gas constant, V = volume (litres).

R = 0.0821 [30], MW of SF<sub>6</sub> = 146.0554192 g mol<sup>-1</sup>,

MW of CF<sub>3</sub>I = 195.9104 g mol<sup>-1</sup>, MW of CO<sub>2</sub> = 44.01 g mol<sup>-1</sup>

Molecular Weight = sum of all the atoms in a molecule

i.e. MW of CO<sub>2</sub> = MW of carbon + (2 × MW of oxygen) [30]

For 100% SF<sub>6</sub> filled Ringmaster switch disconnecter:

m = 429 g, T = 20 °C = 293.15 K, P = 0.135 MPa = 1.35 bar (absolute).

Therefore, the volume of the switch disconnecter can be shown using Equation 4.4:

$$V = \frac{mRT}{MW \times P} = \frac{(429 \times 0.0821 \times 293.15)}{(146.0554192 \times 1.35)} = 52.36 \text{ L} \quad (4.6)$$

For 100% SF<sub>6</sub> filled Fluokit switch disconnecter:

m = 110g, T = 20 °C = 293.15 K, P = 0.145 MPa = 1.45 bar.

Therefore, the volume of the Fluokit switch disconnecter can be calculated as 12.5 L.

To fill the Fluokit switch disconnecter with 100% CF<sub>3</sub>I at 0.45 bar (g) Equation (4.5):

$$m = \frac{MW \times PV}{RT} = \frac{(195.9104 \times 1.45 \times 12.5)}{(0.0821 \times 293.15)} = 147.53751 \text{ g} \quad (4.7)$$

Therefore, 147.54 grams of CF<sub>3</sub>I is needed to fill the switch disconnecter with 100%

CF<sub>3</sub>I. To fill the Fluokit switch disconnecter with 100% CO<sub>2</sub> at 0.45 bar (g), the same calculation can be performed to learn that 33.14 grams of CO<sub>2</sub> gas is needed to fill the switch disconnecter.

For 30%-70% CF<sub>3</sub>I-CO<sub>2</sub> mixture at pressure 1.45 bar:

- 30% CF<sub>3</sub>I is at pressure  $(1.45 \times 0.3) = 0.435$  bar
- 70% CO<sub>2</sub> is at pressure  $(1.45 \times 0.7) = 1.015$  bar

Using Dalton's Law [30]:

30% CF<sub>3</sub>I + 70% CO<sub>2</sub> = Total pressure,

Therefore: 0.435 bar + 1.015 bar = 1.45 bar

For the Schneider Electric 30% CF<sub>3</sub>I filled Fluokit switch disconnecter:

$$m = \frac{MW \times PV}{RT} = \frac{(195.9104 \times 0.435 \times 12.5)}{(0.0821 \times 293.15)} = 44.26125 \text{ g} \quad (4.8)$$

Therefore, 44.26 grams of CF<sub>3</sub>I gas is needed to fill the switch disconnecter to 30% pressure with CF<sub>3</sub>I.

For the Schneider Electric 70% CO<sub>2</sub> filled Fluokit switch disconnecter:

$$m = \frac{MW \times PV}{RT} = \frac{(44.01 \times 1.015 \times 12.5)}{(0.0821 \times 293.15)} = 23.2 \text{ g} \quad (4.9)$$

Therefore, 23.2 grams of CO<sub>2</sub> gas is needed to fill the switch disconnecter to 70% pressure with CO<sub>2</sub>.

Therefore, the mixture ratio at:

$$T = 20^\circ\text{C} = 293.15 \text{ K}, P = 0.145 \text{ MPa} = 1.45 \text{ bar and } V = 12.5 \text{ L}$$

For pressure-pressure ratio: 30% - 70% (CF<sub>3</sub>I – CO<sub>2</sub>) is:

$$\text{CF}_3\text{I} : \text{CO}_2 = 44.26125 \text{ g} : 23.2 \text{ g}$$

Giving the final pressure-pressure ratio of 30% : 70% (CF<sub>3</sub>I : CO<sub>2</sub>) of:

$$1.9078125 \text{ g} : 1 \text{ g (CF}_3\text{I : CO}_2\text{)}$$

Ideal gas mixture calculations lead to the following summations with regards to the actual amount of gas that is needed for each pressure-pressure gas mixture ratio. The ratios of

various gas mixtures is shown in Table 4.3. The different molecular weights of the gases account for the fact that CF<sub>3</sub>I can be roughly estimated as 4 times as heavy as CO<sub>2</sub>, hence, the pressure-pressure mixture ratios being almost 1:1 for a 20:80% CF<sub>3</sub>I-CO<sub>2</sub> mixture.

Table 4.3: Calculated pressure-pressure gas mixture ratios.

<b>Pressure Mixture Ratio CF<sub>3</sub>I : CO<sub>2</sub> (%)</b>	<b>CF<sub>3</sub>I (g)</b>	<b>CO<sub>2</sub> (g)</b>
<b>10 : 90</b>	1	2.021
<b>20 : 80</b>	1.112	1
<b>30 : 70</b>	1.908	1
<b>40 : 60</b>	2.967	1
<b>50 : 50</b>	4.451	1
<b>70 : 30</b>	10.386	1

The gas required for testing is shown in Table 4.4 and indicates the amount of gas needed to make all of these gas mixtures for each device. It also shows the amount of gas that would be needed if the gas was not re-used or if the gas was re-used.

Table 4.4: Calculated quantity of gases required to fill the Fluokit and Ringmaster switch disconnectors.

<b>Pressure Mixture Ratio CF<sub>3</sub>I : CO<sub>2</sub> (%)</b>	<b>CF<sub>3</sub>I (g) Fluokit</b>	<b>CO<sub>2</sub> (g) Fluokit</b>	<b>CF<sub>3</sub>I (g) Ringmaster</b>	<b>CO<sub>2</sub> (g) Ringmaster</b>
<b>10 : 90</b>	14.75	29.83	57.54	116.33
<b>20 : 80</b>	29.51	26.52	115.08	103.41
<b>30 : 70</b>	44.26	23.2	172.62	90.48
<b>40 : 60</b>	59.02	19.89	230.15	77.56
<b>50 : 50</b>	73.77	16.57	287.69	64.63
<b>70 : 30</b>	103.28	9.94	402.77	38.78
<b>100 : 0</b>	147.54	0	575.38	0
<b>0 : 100</b>	0	33.14	0	129.26
<b>Total for each device</b>	<b>472.12</b>	<b>159.09</b>	<b>1841.23</b>	<b>620.45</b>
<b>Maximum Quantity Needed (if gas is re-used)</b>			<b>1841.23</b>	<b>620.45</b>
<b>Maximum Quantity Needed (if gas is not re- used)</b>			<b>2313.35</b>	<b>779.54</b>

#### 4.3.1.2 Gas required for experimental testing

Extra pressure is needed in the storage cylinders to create the overpressure which is required to fill the switch disconnectors. This includes the gas pressure which is lost due to the extra volume of the hoses and gas handling equipment whilst gassing or de-gassing takes place. To increase the pressure of all storage cylinders, the amount of CF<sub>3</sub>I and CO<sub>2</sub> needed in each gas mixture is increased to raise the total pressure in each storage cylinder by 2 bar. 2 extra bar was required to accommodate for loss of 1 bar in the cylinder to return it to atmospheric pressure and 1 bar for loss of pressure in the gas handling equipment and hoses. The total in each 10 L storage cylinder will, therefore, be 8 bar (g), and the various gas mixtures have been re-calculated as in Table 4.5. It is important to note that, for pure CO<sub>2</sub>, the amount of gas required is not changed because the gas is cheap and can be released after each test. So, there is no requirement for a storage cylinder. A quotation for the cost of the gas required for experimentation can be calculated from Table 4.6.

Table 4.5: Total gas needed to fill Ringmaster and Fluokit with added overpressure.

Pressure Mixture Ratio CF <sub>3</sub> I : CO <sub>2</sub> (%)	CF <sub>3</sub> I Ringmaster + Fluokit + Overpressure (g)	CO <sub>2</sub> Ringmaster + Fluokit + Overpressure (g)
10 : 90 (10 L)	88.01375	177.9455
20 : 80 (10 L)	176.0275	158.1738
30 : 70 (40 L)	412.5113	216.227
40 : 60 (10 L)	352.055	118.6303
50 : 50 (10 L)	440.0688	98.86167
70 : 30 (10 L)	616.0963	59.313
100 : 0 (10 L)	880.1375	0
0 : 100	0	162.4033
<b>Total</b>	<b>2964.91</b>	<b>991.5546</b>
<b>Total for 10:90, 20:80, 30:70 and 0:100</b>	<b>676.5525</b>	<b>714.7496</b>

Table 4.6: Cost of gases from Apollo Scientific (AS - UK) [74], Synquest (S - USA) [75] and Sigma Aldrich (SA - UK) [76] (2012).

	SF <sub>6</sub> (AS)	SF <sub>6</sub> (SA)	CF <sub>3</sub> I (AS)	CF <sub>3</sub> I (S)	CF <sub>3</sub> I (SA)
25 g	-	-	£ 172.00	£ 60.52	£ 153.00
100 g	-	-	£ 274.00	£ 124.22	£ 387.50
250 g	£ 185.00	£ 256.50	£ 425.00	-	-
500 g	£ 370.00 *	£ 513.00 *	£ 675.00	£ 442.72	-
1 kg	£ 740.00 *	£ 1026.00 *	£ 900.00	-	-
2 kg	£ 1480.00 *	£ 2052.00 *	£ 1400.00	-	-

\* Estimated cost based on quotation for 250 g of gas.

#### 4.3.2 Gas handling equipment specifications

The equipment decided upon for gassing and de-gassing switchgear with CF<sub>3</sub>I and CF<sub>3</sub>I-CO<sub>2</sub> gas mixtures was Dilo equipment. Dilo is a manufacturer that makes equipment specific for SF<sub>6</sub> gas usage and is regularly used to gas and de-gas switchgear by Schneider Electric. It was decided to use this equipment because of its connections which are specifically designed with O-rings incorporated into each connection so that near zero gas is released. All equipment and storage cylinders designed by Dilo have a specific rating for the maximum pressure and the amount of gas that can be held [77].

The Dilo Mini Series (Figure 4.8) is the smallest piece of equipment in the range which can handle the amount of gas to be used throughout testing. The Mini Series has been designed so that it can evacuate the air and moisture via its vacuum pump from switchgear such as the switch disconnectors chosen for testing. The Mini Series is capable of recovering and storing gas from switchgear and has a filter that can purify gas during recovery from switchgear (Figure 4.8). The Mini Series can achieve direct liquefaction of gas into an approved storage cylinder, which is very important considering the high

boiling point of  $\text{CF}_3\text{I}$  gas. The Mini Series is also pressure-regulated for safe refilling of switchgear [78].

The exact specifications of the Dilo Z579R02 Mini Series components mounted on a cylinder cart for liquid storage are shown in Figure 4.8.

It is important to note that the Dilo Mini Series was filled with  $\text{SF}_6$  gas for transport so that it could be kept at atmospheric pressure and so that no air would leak into the system causing problems when used. In order to evacuate this  $\text{SF}_6$ , another Dilo Mini Series was used to safely remove the gas with the help of a technician from Schneider Electric, trained to handle  $\text{SF}_6$ . This allowed the evacuated Mini Series to be used exclusively with  $\text{CF}_3\text{I}$ - $\text{CO}_2$  gas mixtures.

Pressure gauges and various connections were acquired to carry out gas filling of the switchgear. However, it is noted that more accurate pressure gauges are available, at a higher cost, which would increase the accuracy of the following tests. These pressure gauges have an effect on the accuracy of the gas mixtures that could be mixed. Other influences such as temperature have a slight effect on the gas being used and its pressure within the gas chamber, therefore, affecting gas mixtures.

The various connections, adapters, fixtures and fittings required to fill the Ringmaster and Fluokit switch disconnectors with mixtures of  $\text{CF}_3\text{I}$ - $\text{CO}_2$  are described in Appendix B. Appendix B also describes and outlines the vacuuming, gassing and de-gassing operations which can be achieved with the Dilo Mini Series.



- Compressor (1 m<sup>3</sup>/h, final pressure 50 bar) with filling pressure reducer (0 – 10 bar)
- Vacuum compressor (1.3 m<sup>3</sup>/h, final pressure < 10 mbar)
- Vacuum pump 10m<sup>3</sup>/h (final vacuum < 1 mbar)
- B077R11 pre-filter unit
- Pressure gauges
- Operating voltage: 220-240 V / 50/60 Hz AC
- Width: 580 mm, Depth: 1150 mm, Height: 1400 mm, Weight: 123 kg

Figure 4.8: Dilo mini series complete with vacuum pump, filter, compressor and vacuum compressor for vacuuming, gassing and de-gassing switchgear [78].

#### 4.4 Lightning impulse generator test setup

This section examines the test setup that was used to generate lightning impulses to be applied to the switch disconnectors. Various standards are set out to explain the procedures undertaken to apply lightning impulses to the switch disconnectors to test the gas mixtures withstand strength and 50% probability of breakdown occurring ( $U_{50}$ ).

##### 4.4.1 Haefely lightning impulse generator test setup

The lightning impulse generator used for testing was manufactured by Haefely and can be used in several different configurations to provide either a lightning (1.2/50) or a switching impulse which can be either positive or negative in polarity to any test object.

A capacitive impulse divider with a response time of 49 ns at a ratio of 27931 to 1 is used throughout testing (Figure 4.9). A digital storage oscilloscope (Lecroy Wave Jet 100 MHz) was used to store and examine the impulse shape.

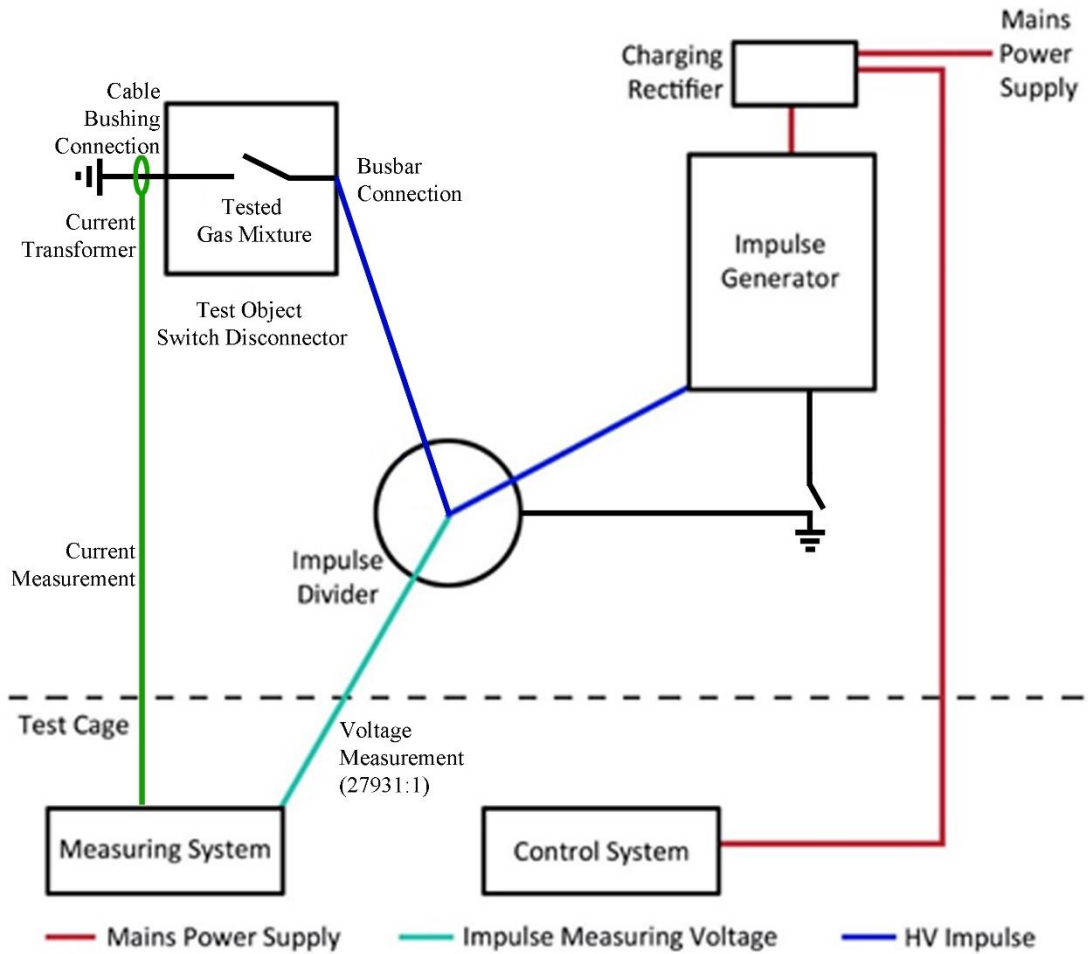


Figure 4.9: Lightning impulse generator test setup [79].

#### 4.4.2 British and IEC standards for switchgear

This section examines the British standards and IEC regulations for tests pertaining to the insulation strength and withstand capability of an insulation medium in switchgear.

##### 4.4.2.1 Basic lightning impulse $U_{50}$ gas insulation test

The 50% probability of a breakdown voltage ( $U_{50}$ ) occurring across the gas gap is determined using the ‘up-and-down’ method. There are six different test configurations in total. The test configuration is dependent to which phase the test voltage is applied (L1, L2 or L3) and whether the load switch is open or closed as shown in Figure 4.10. This ensures that the insulation across all contact gaps is examined. An example of the recording of the  $U_{50}$  breakdown test is shown in Appendix C (Figure C2).

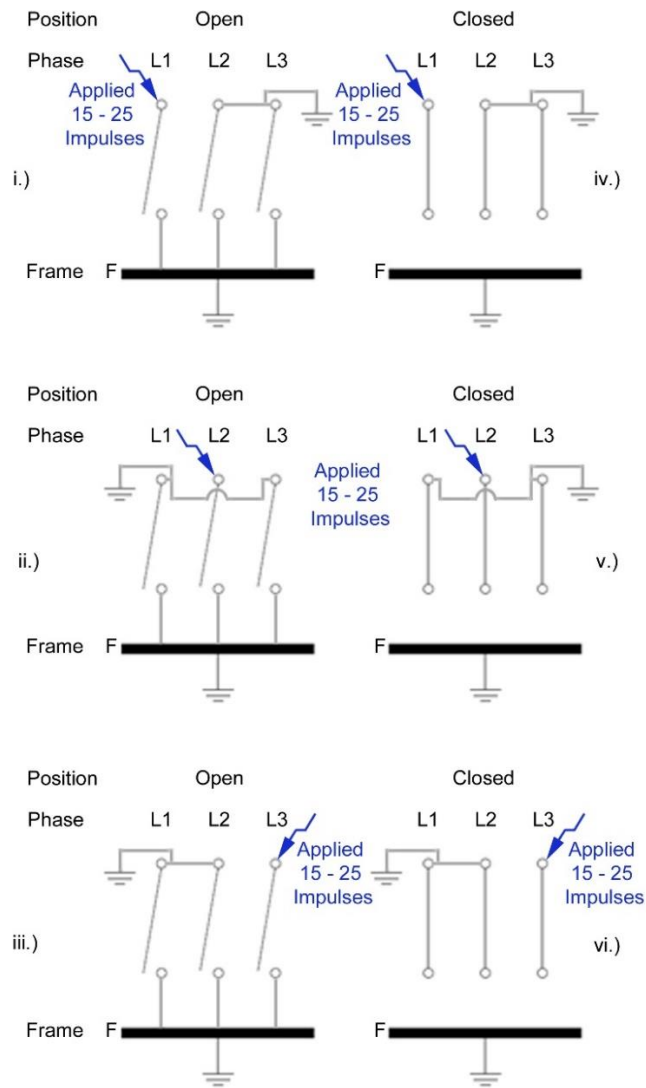


Figure 4.10: Diagram of connection of a three-pole switching device [1].

#### 4.4.2.2 Basic lightning impulse withstand test

The basic impulse level (BIL) withstand test is designed to stress the insulation of switchgear by the repeated application of a very steep fronted voltage wave and is a very searching test of the unit's insulation integrity. The shape of the impulse voltage is specified to be the standard lightning impulse (1.2/50) [13] according to BS EN 60060-1 [62]. According to BS EN 62771-1, for  $U_r \leq 245$  kV, switchgear and controlgear shall be subjected to lightning impulse voltage tests in dry conditions only.

The test procedure and an example of the recording of the basic lightning impulse withstand test is shown in Appendix C (Figure C1).

#### 4.5 Preliminary tests

This section examines the preliminary tests that were required for establishing a reliable and repeatable testing setup for the results obtained in Chapter 5. Figure 4.11 indicates the main connection points for all the main components required for testing the gas filled switch disconnectors with a standard lightning impulse. The Dilo equipment is required to fill the switch disconnectors with different mixtures of gas and is detached when actual lightning impulses are applied to the units once the gas is at the required pressure for each test. The control system is required to communicate with the impulse generator and charging rectifier to apply all safety systems fitted and allow for adjustment of peak test voltage values whilst testing is being undertaken.

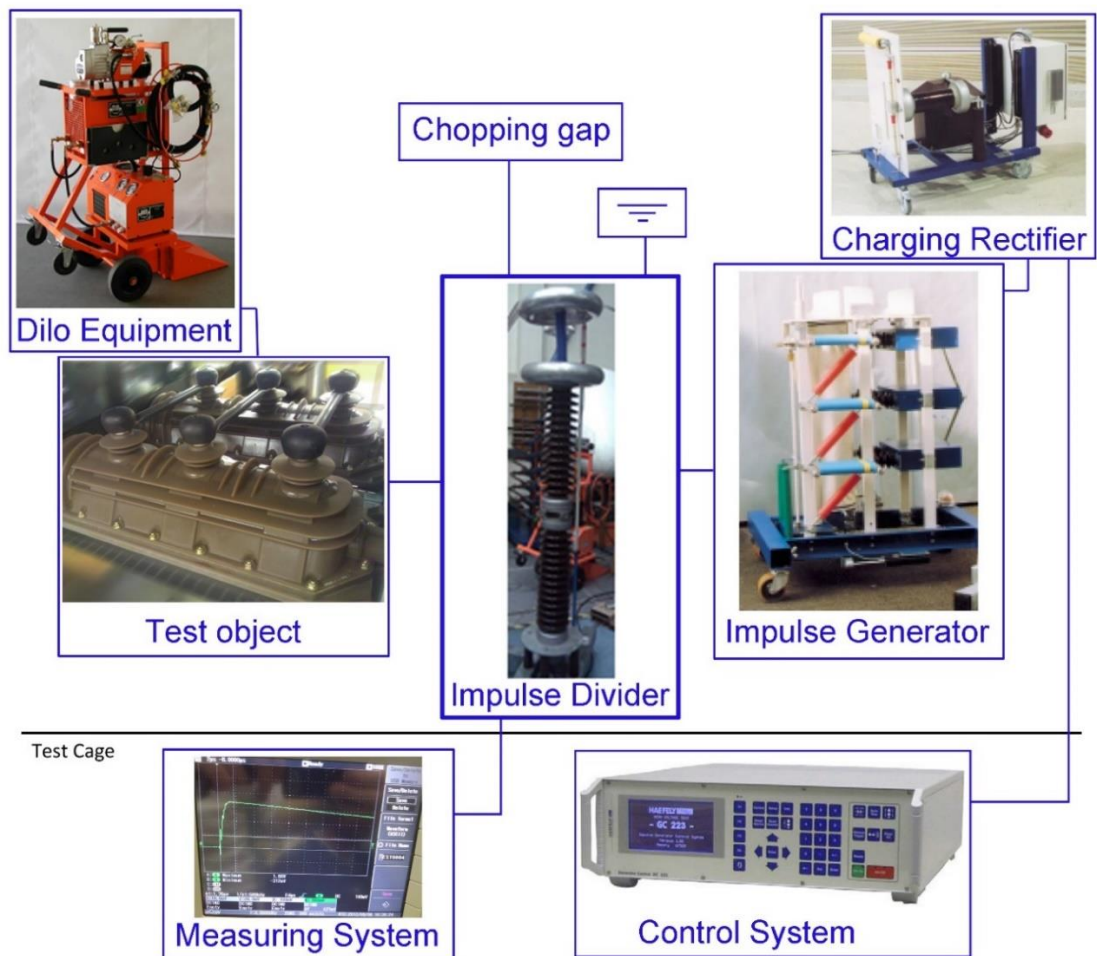


Figure 4.11: Connection diagram for main components of lightning impulse test setup.

#### 4.5.1 Standard lightning impulse test peak voltage value

The test voltage value is the peak voltage of a measured waveform which is then compared to the peak voltage that was intended to be generated from the lightning impulse generator. The measured voltage must be  $\pm 3\%$  of the intended applied voltage to fit within the parameters set out in BS60060-1 [62].

Figure 4.12 shows results for three standard 125 kV lightning impulses applied between the busbar connection for phase 3 of the Fluokit M24+ (F1) switch disconnector and ground. The switch disconnector was filled with 100% SF<sub>6</sub> at a pressure of 0.45 bar G.

As can be seen in Figure 4.12, all three measured lightning impulses are  $\pm 1.2\%$  of the intended applied peak voltage and all tests carried out were within the  $\pm 3\%$  variation allowed for the test voltage value. The generator impulse shape has a front time of 1.18  $\mu$ s and a time to half peak of 43  $\mu$ s which are within the tolerances of the standards.

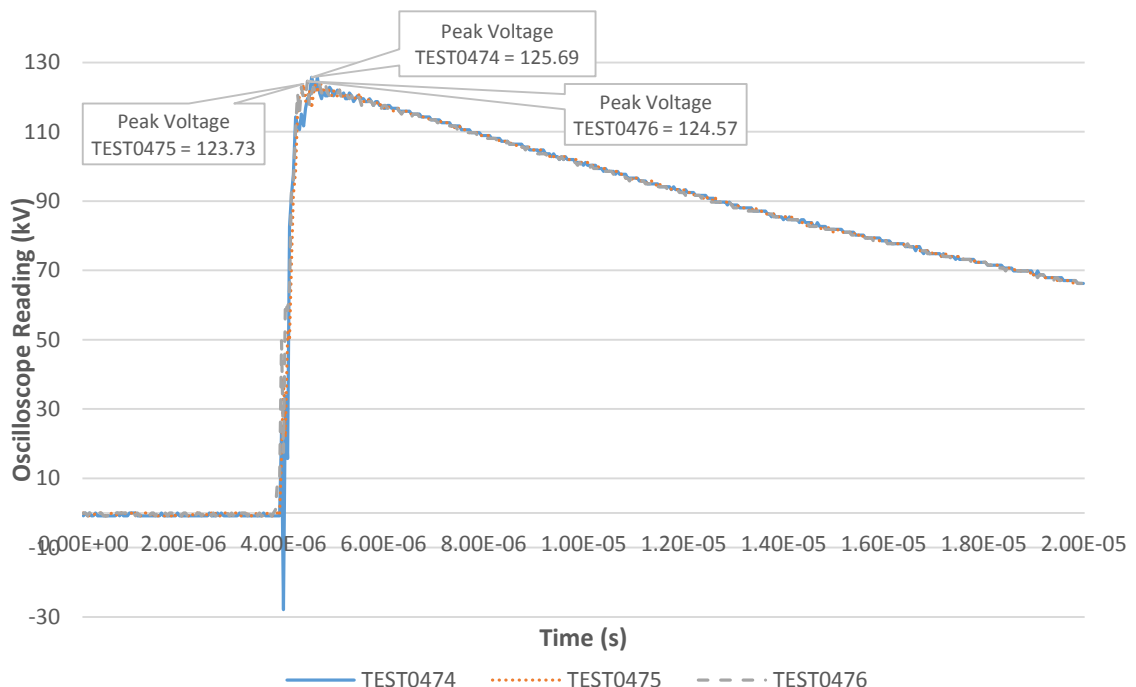


Figure 4.12: Standard 125 kV lightning impulse Fluokit M24+ (F1),  
Main switch Phase 3, 100% SF<sub>6</sub>, 0.45 bar G.

#### 4.5.2 Lightning impulse test oscilloscope waveforms and their interpretations

The following section examines various waveforms that are screen shots of the oscilloscope captures. These waveforms are then examined, for the various gas mixtures, to interpret the results being obtained.

Figure 4.13 shows a recorded typical waveform of a lightning impulse (1.2/50) that was applied to a switch disconnector. The gas mixture, which was between the contacts in the switch disconnector at the time, is shown to withstand the applied voltage of the lightning impulse. The measured peak voltage is 111.2 kV.

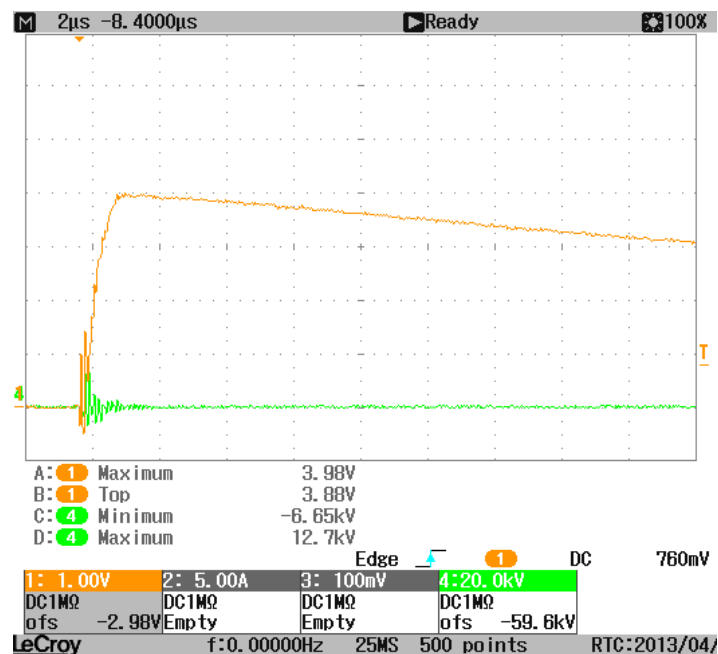


Figure 4.13: Applied lightning impulse (LI) voltage (orange) and current measurement (green) – no breakdown.

The next example (Figure 4.14) shows a standard lightning impulse that was applied to a switch disconnector when a breakdown occurred. The impulse made contact with an earthed point leading to the waveform that is shown in Figure 4.14 (Orange). However, because no increase in current is registered (shown in green) when the lightning impulse causes a breakdown, this means that the breakdown current is not earthed through the lead on which the current transformer (CT) is located but through another phase or piece of metal casing. The CT is located on the earth lead connected to the contact on the

opposite side of the switch disconnecter to which the lightning impulse is applied (Figure 4.9). The measured voltage is 112.8 kV.

Figure 4.15 shows a screen shot of a lightning impulse applied to a switch disconnecter where a breakdown occurred (orange), at this point the current transformer picks up a large increase in current (green). This indicates that the gas mixture, with which the switch disconnecter is filled, failed to withstand the applied impulse and the impulse earthed itself through the contact on the opposite side of the switch disconnecter, to which the CT was attached (Figure 4.9). For Figure 4.15, the peak measured voltage was 112 kV.

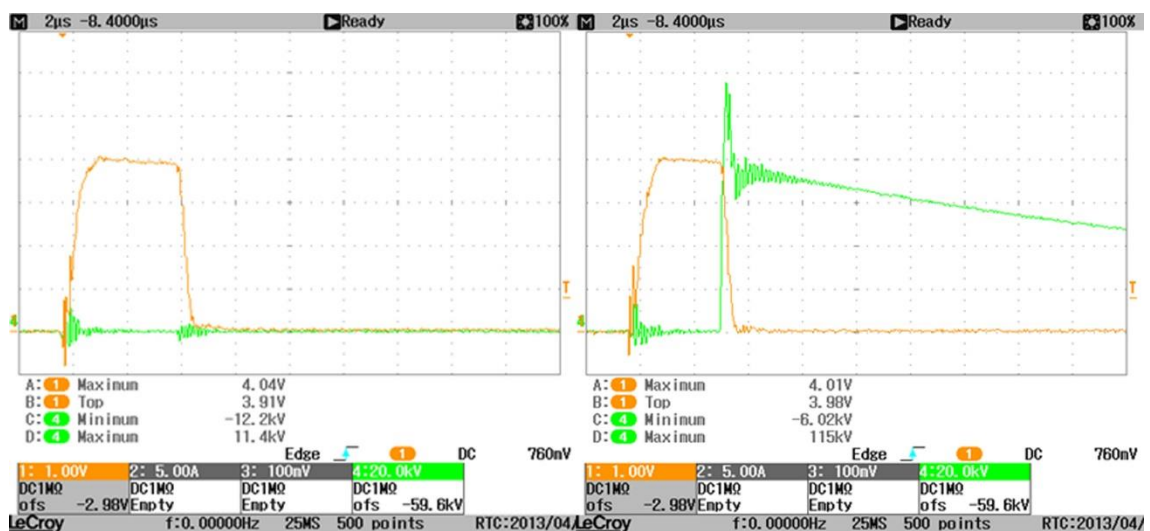


Figure 4.14: Applied LI to the Ringmaster 20%-80% CF<sub>3</sub>I-CO<sub>2</sub> switch disconnecter – Air breakdown / equipment failure

Figure 4.15: Applied LI to the Ringmaster 20%-80% CF<sub>3</sub>I-CO<sub>2</sub> switch disconnecter – gas breakdown

Figure 4.16 shows an applied lightning impulse to a gas mixture through which breakdown occurred very quickly. The breakdown appears approximately 0.5  $\mu$ s after the peak voltage had been applied to the test object. The measured voltage is 107.5 kV.

Figure 4.17 shows a flashover to the switch disconnectors earthed metal casing which appears to have done so with a relatively long time gap between the peak lightning impulse voltage being applied and when the actual breakdown occurred. The breakdown

itself occurred approximately 11  $\mu\text{s}$  after the peak lightning impulse was applied. The measured voltage is 158.4 kV.



Figure 4.16: Applied LI to the Ringmaster 20%-80% CF<sub>3</sub>I-CO<sub>2</sub> switch disconnector – short time to breakdown

Figure 4.17: Applied LI to the Fluokit 20%-80% CF<sub>3</sub>I-CO<sub>2</sub> switch disconnector – long time to breakdown

### 4.5.3 Closed switch phase-phase gas insulation comparison results

The Phase – Phase gas insulation test in the switch disconnector units is an experiment designed to test the insulation strength of the gas when the switch is in the closed position. A lightning impulse is applied to one phase and the other two phases are earthed, as shown in Figures 4.10 and 4.18.

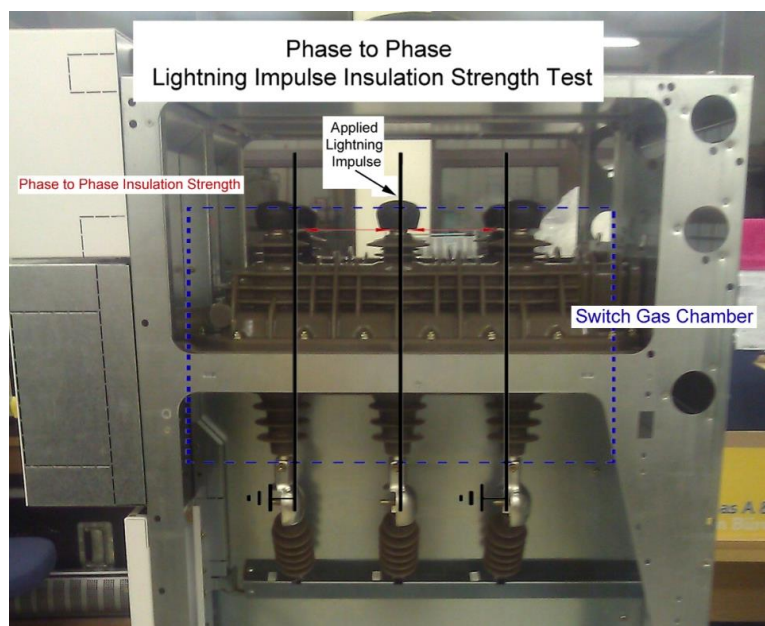
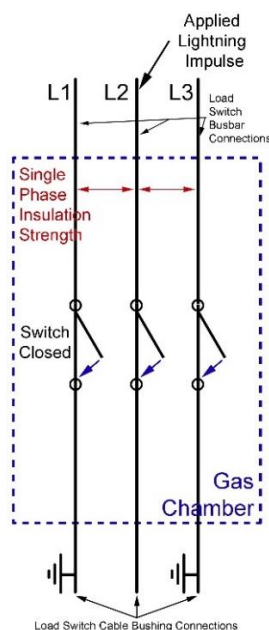


Figure 4.18: Phase to Phase lightning impulse insulation strength test connections.

This test was intended to obtain the 50% probability of a breakdown voltage ( $U_{50}$ ) occurring across phases in the gas chamber determined using the ‘up-and-down’ method.

#### 4.5.3.1 Closed switch phase-phase gas insulation Fluokit M24+ results

Phase-phase gas insulation test results for the Fluokit M24+ switch disconnector, when filled with 100%  $SF_6$  and a 20:80%  $CF_3I:CO_2$  gas mixture, are shown in Table 4.7.

Table 4.7: Fluokit M24+ switch disconnector lightning impulse (LI) closed switch Phase-Phase gas insulation strength tests.

<b>Fluokit M24+ switch disconnector lightning impulse (LI) closed switch Phase-Phase gas insulation strength tests – <math>U_{50}</math> breakdown level (<math>\pm 3\%</math>)</b>				
	<b>Phase 1</b>	<b>Phase 2</b>	<b>Phase 3</b>	<b>Switch Disconnector Average</b>
<b>100% <math>SF_6</math> Standard LI Phase-Phase Breakdown Level (0.45 bar G)</b>	<b>99</b>	<b>91</b>	<b>109</b>	<b>100 kV</b>
<b>20-80% <math>CF_3I-CO_2</math> Standard LI Phase-Phase Breakdown Level (0.45 bar G)</b>	<b>99</b>	<b>102</b>	<b>109</b>	<b>103 kV</b>

The manufacturer’s specified rated lightning impulse withstand voltage ( $U_p$ ) for the Fluokit switch disconnector is 125 kV. However, the results for all 3 phases show an average breakdown strength of 100 kV for  $SF_6$  and 103 kV for 20:80%  $CF_3I:CO_2$ . A high speed camera (DRS’s lightning RDT high speed digital camera) [80] was utilised to determine the point at which the lightning impulse breakdown was occurring. From the high speed video recordings, still images were obtained that showed that the breakdown was occurring either across phases in air on the bottom main switch cable bushing contact to the closest grounded phase or to the earthed metal casing of the switch disconnector.

Figure 4.19 shows a lightning impulse (LI) breakdown occurring from Phase 1 (right) to Phase 2 (left) through air at the lower main switch cable bushing contacts. Figure 4.20 shows a breakdown occurring from Phase 2 (right) to Phase 3 (left) through air at the

lower main switch cable bushing contacts. The sharpest point at the bottom main switch cable bushing contact is the screw to which the cable connection attaches (Figure 4.22). From this screw, the lightning impulse earths from phase 1 and 2 to the nearest phase (Figure 4.19 and 4.20), similar to the 12.5 cm path shown in Figure 4.22.

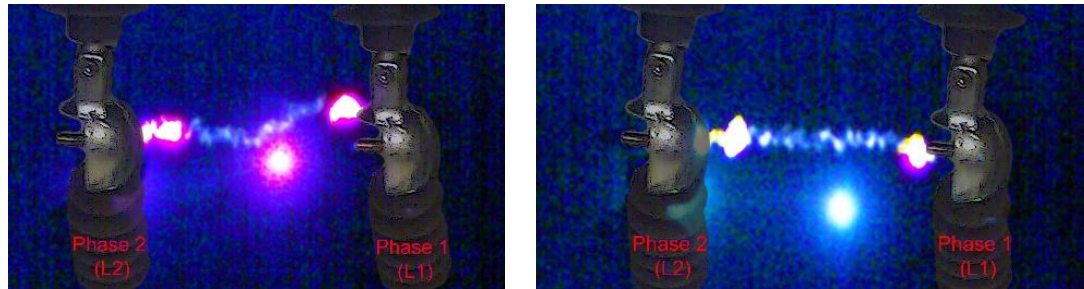


Figure 4.19: Fluokit M24+ switch disconnector lightning impulse (LI) applied to Phase 1 on a closed switch Phase-Phase gas insulation strength tests.

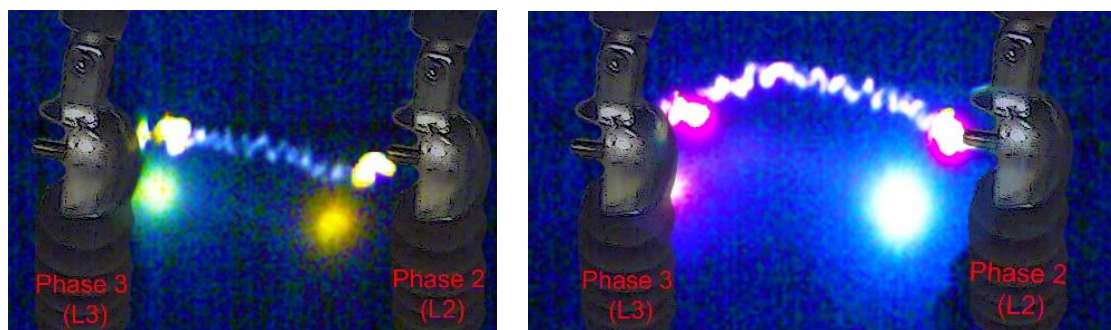


Figure 4.20: Fluokit M24+ switch disconnector lightning impulse (LI) closed switch Phase-Phase gas insulation strength tests when LI is applied to Phase 2.

Figure 4.21 shows a LI breakdown occurring from Phase 3 to the earthed metal casing of the switch through air at the lower main switch cable bushing contacts. For phase 3, without an earthing point directly in front of the cable connecting screw, the impulse earths on the metal casing (Figure 4.21) along a path similar to the 15 cm shown in Figure 4.22. As this path (15 cm) is slightly longer than between phases (12.5 cm), the breakdown results are higher for phase 3 (Table 4.7).

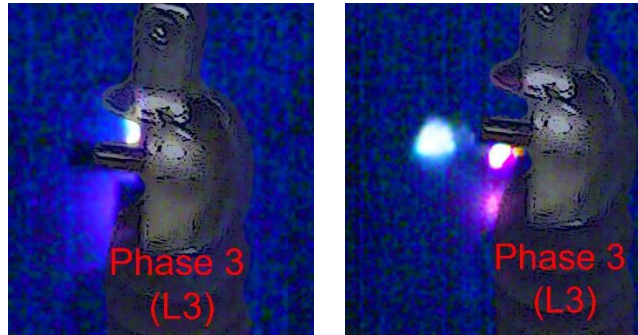


Figure 4.21: Fluokit M24+ switch disconnector lightning impulse (LI) closed switch Phase-Phase gas insulation strength tests when LI is applied to Phase 3.

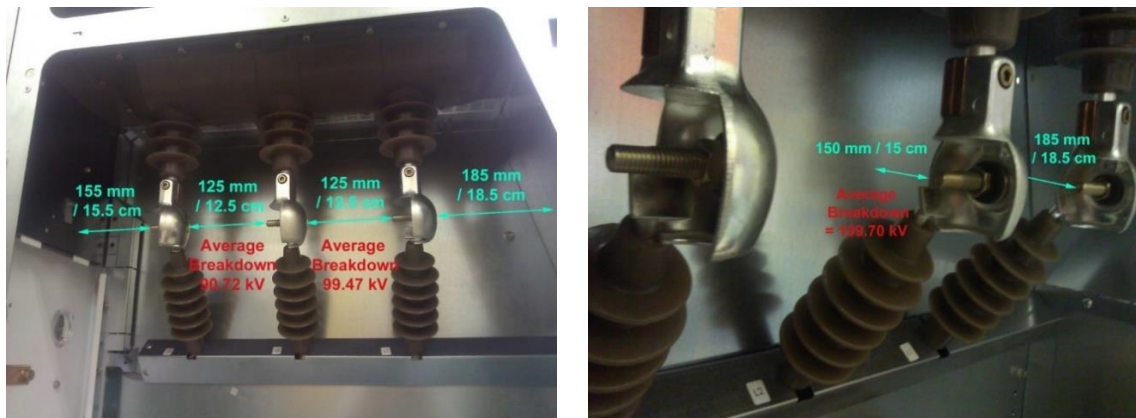


Figure 4.22: Fluokit M24+ switch disconnector lightning impulse (LI) arc path length in a closed switch Phase-Phase gas insulation strength tests when LI is applied to Phase 1 or 2 (Left) or Phase 3 (Right).

The breakdown voltage shown in Table 4.7 and the arc path shown in Figures 4.19, 4.20 and 4.21 is the same no matter which gas the switch was filled with i.e. either  $\text{SF}_6$  or any gas mixture of  $\text{CF}_3\text{I}-\text{CO}_2$ . This is because the breakdown occurs through the air on the outside of the gas chamber not through the insulating gas.

$\text{SF}_6$  has an insulation strength of 3.34 times that of air at atmospheric pressure [11], and so, the breakdown strength of the gas is likely to be significantly higher than the results obtained within the gas chamber. The Fluokit switch disconnector also has a solid dielectric barrier inside the gas chamber that is used as extra protection against phase-phase breakdown within the unit (Figure 4.23). This will increase the level at which the unit will breakdown in this manner between phases.

Given that the rated lightning impulse withstand voltage ( $U_p$ ) for the Fluokit switch disconnector is 125 kV, it was decided to discontinue this test. This was due to the fact that the insulating gases are likely to breakdown well above 125 kV. Also, it would be very difficult to get the breakdown to occur through the insulating gas rather than the air between any exposed metal point of the phase, through which the impulse is applied, and the earthed metal casing of the switch as shown in the results of Chapter 5.

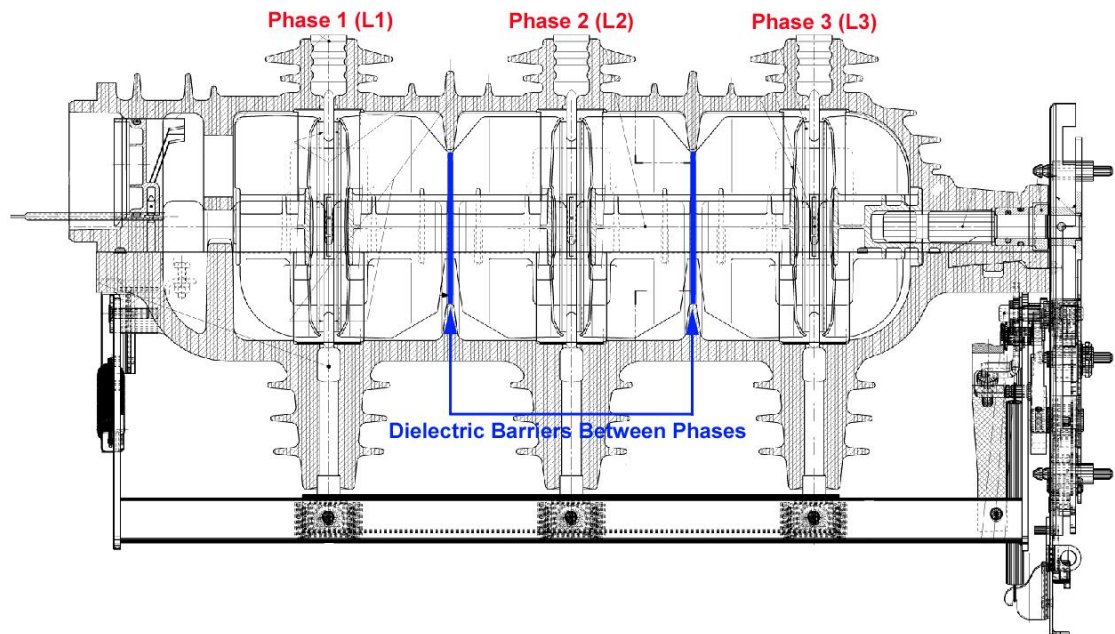


Figure 4.23: Fluokit side view with phase-phase dielectric barrier [81].

#### 4.5.3.2 Closed switch phase-phase gas insulation Ringmaster SE6 results

The results of the lightning impulse tests on the unit R1 ( $\text{SF}_6$  - 100%) and unit R2 (20:80%  $\text{CF}_3\text{I}-\text{CO}_2$ ) are shown in Table 4.8. As can be seen from Table 4.8, all test results are below the rated lightning impulse withstand voltage ( $U_p$ ) for the Ringmaster switch disconnector which is 95 kV. The results show the average breakdown occurs at 67 kV across all 3 phases for  $\text{SF}_6$  and 70 kV for 20:80%  $\text{CF}_3\text{I}:\text{CO}_2$ .

Table 4.8: Ringmaster SE6 switch disconnector lightning impulse (LI) closed switch  
Phase-Phase gas insulation strength tests.

<b>Ringmaster SE6 switch disconnector lightning impulse (LI) gas insulation strength tests – U<sub>50</sub> breakdown level (± 3%)</b>				
	<b>Phase 1</b>	<b>Phase 2</b>	<b>Phase 3</b>	<b>Switch Disconnector Average</b>
<b>100% SF<sub>6</sub> Standard LI Phase-Phase Breakdown Level (0.35 bar G)</b>	<b>67</b>	<b>65</b>	<b>69</b>	<b>67 kV</b>
<b>20-80% CF<sub>3</sub>I-CO<sub>2</sub> Standard LI Phase-Phase Breakdown Level (0.35 bar G)</b>	<b>67</b>	<b>74</b>	<b>68</b>	<b>70 kV</b>

Breakdowns were recorded with a high speed camera and from single frames, obtained from that video, it can be shown that the breakdown occurs in air from the bottom main switch cable bushing contact to the earthed metal casing of the switch disconnector.

Breakdown occurred from Phase 1 to the earthed metal casing through air at the lower main switch cable bushing contacts (Figure 4.24). Breakdown occurred from Phase 3 to the earthed metal casing through air at the lower main switch cable bushing contacts (Figure 4.25). The sharpest point on the main switch cable bushing contact is the top edge of the metal contact where there is a hole for a screw to attach to the cable. From this point, the lightning impulse earths itself in phases 1 and 3 (Figure 4.24 and 4.25) to the earthed metal casing along a path similar to the 8 cm shown in Figure 4.27.

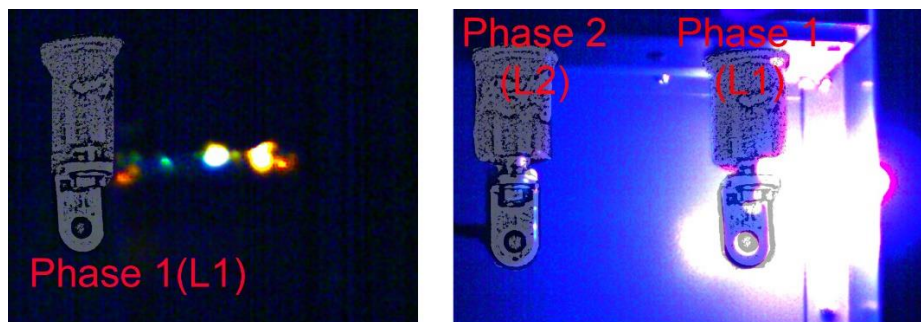


Figure 4.24: Ringmaster SE6 switch disconnector lightning impulse (LI) closed switch  
Phase-Phase gas insulation strength tests when LI is applied to Phase 1.

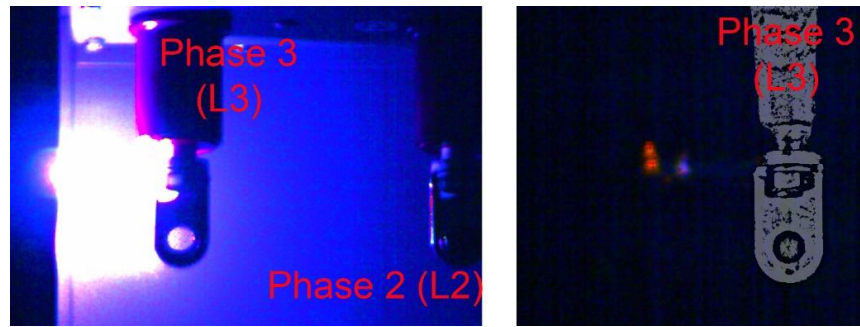


Figure 4.25: Ringmaster SE6 switch disconnector lightning impulse (LI) closed switch Phase-Phase gas insulation strength tests when LI is applied to Phase 3.

In Phase 2, breakdown occurred to the earthed metal casing through air at the lower main switch cable bushing contacts (Figure 4.26). In phase 2, there is a large earthing path to phases 1 and 3 (12.5 cm), the lightning impulses' shortest arcing path is directly behind the contact to earthed metal casing along a path similar to the 8 cm (with a screw) shown in Figure 4.27.

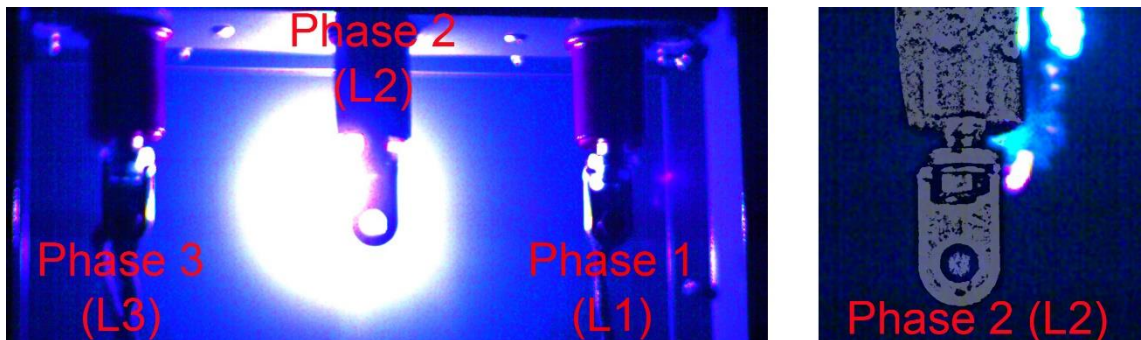


Figure 4.26: Ringmaster SE6 switch disconnector lightning impulse (LI) closed switch Phase-Phase gas insulation strength tests when LI is applied to Phase 2.

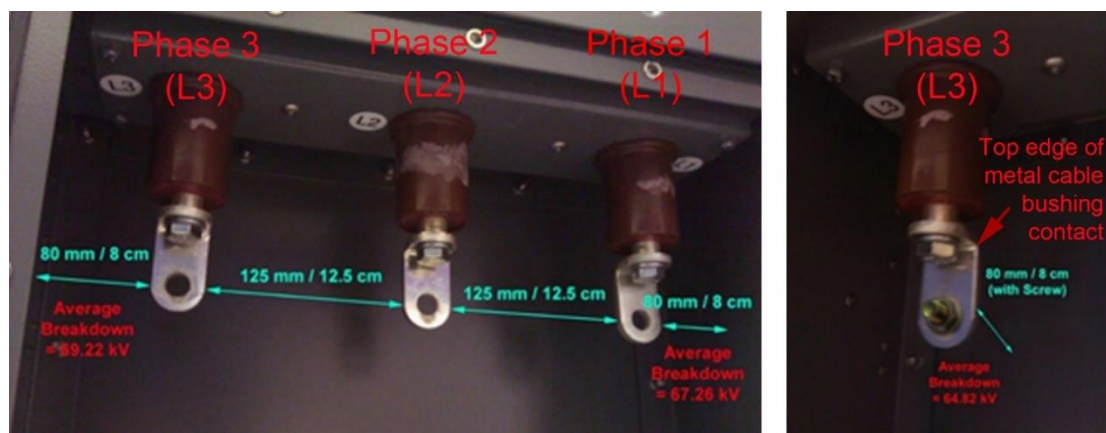


Figure 4.27: Ringmaster SE6 switch disconnector lightning impulse (LI) arc path length in a closed switch Phase-Phase gas insulation strength tests when LI is applied to Phase 1 or 3 (right) and Phase 2 (left).

The level at which the breakdown occurs on each phase and the position at which the arc path follows (Figure 4.24, 4.25 and 4.26) is the same no matter which gas is in the gas chamber of the switch.

From the results, with the Fluokit unit, it has been shown (Figures 4.19 and 4.20) that the flashover would next occur between phases in air rather than to the metal casing. This flashover would occur in air on the outside of unit before it would through the gas in the pressurised chamber because the insulation strength of air is a lot less than  $\text{SF}_6$  or the  $\text{CF}_3\text{I}-\text{CO}_2$  mixture being tested. Within the gas chamber of the Ringmaster switch disconnect, there are solid dielectric barriers (Figure 4.28), in between the phases, which increase the phase-phase breakdown level. These dielectric barriers also make it very difficult to achieve a breakdown across the phases in the gas chamber.

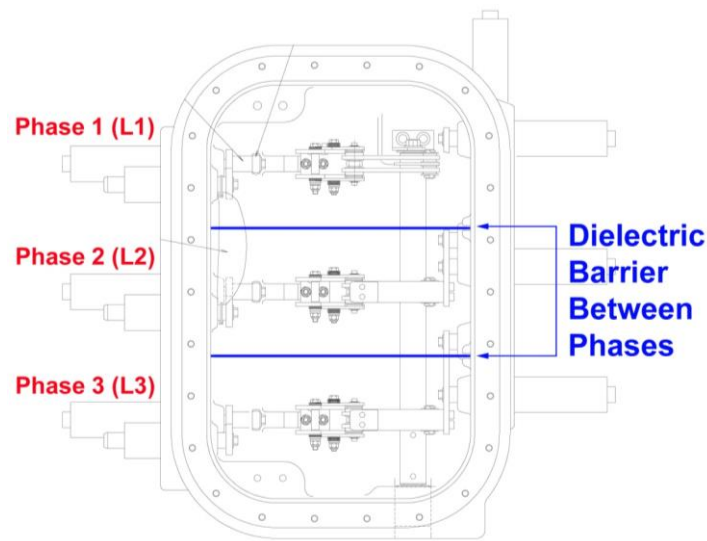


Figure 4.28: Ringmaster side view with phase-phase dielectric barrier [82].

It is clear that the phase-phase breakdown level of  $\text{SF}_6$  or 20:80%  $\text{CF}_3\text{I}-\text{CO}_2$  is far higher than the lightning impulse withstand voltage ( $U_p$ ) for the Ringmaster (95 kV). It is known that the gas gap between open contacts in the gas chamber is smaller than that between phases outside the unit in air. Therefore, there is a smaller arc path to an earthing point between the open switch contacts in the gas chamber. This meant that the weakest point of the gas insulation in the gas chamber was between the contacts of the open switch.

Therefore, it was decided to test the insulation strength of the  $\text{CF}_3\text{I-CO}_2$  gas mixture across the open contacts of the load switch rather than across phases.

From the results of the closed switch phase-phase gas insulation tests, it is clear that breakdown through air around the outside of the unit would prove a problem throughout testing. This is because the insulation strength of the gas mixtures have a much higher dielectric strength than air. It is worth noting that this round of testing was only meant as initial testing of  $\text{CF}_3\text{I-CO}_2$  gas mixtures and, up until these tests, there was no way of knowing whether  $\text{CF}_3\text{I-CO}_2$  was going to be able to insulate the equipment at all. If the switchgear had been used with heat shrinks and dielectric barriers around its bushing contacts, the withstand strength would have been increased but the same problem would still have occurred above the rated lightning impulse withstand voltage level.

#### 4.6 Conclusion

This chapter describes the selection process and acquisition of MV switchgear units and identifies the Ringmaster and the Fluokit switch disconnectors as the units chosen for experimentation with an alternative insulation medium to  $\text{SF}_6$ . Four MV switchgear units were obtained for testing, two units were permanently filled with  $\text{SF}_6$  and two units were empty to be filled with mixtures of  $\text{CF}_3\text{I-CO}_2$ .

Dilo gas handling equipment was obtained and commissioned to safely carry out operations to vacuum, gas and de-gas the switchgear throughout testing. Ideal gas mixture calculations were performed to evaluate how much gas was needed to fill the Ringmaster and Fluokit switch disconnectors with various  $\text{CF}_3\text{I-CO}_2$  gas mixtures. These gas mixture calculations took into account the volumes of each gas chamber, the required filling pressure and how much gas was needed if the gas mixtures were recycled for each piece of switchgear.

A test rig was developed to prove the insulation capabilities of  $\text{CF}_3\text{I-CO}_2$  gas mixtures in the switch disconnectors connected to a Heafley lightning impulse generator. In this chapter, insulation tests are described, referring to BS EN 60060-1 [62] and BS EN 62271-1 [1], to identify experiments that can verify the capabilities of  $\text{CF}_3\text{I-CO}_2$  as an alternative insulation medium. The experiments identified are the basic lightning impulse  $U_{50}$  gas insulation test and the basic lightning impulse withstand test. Further preliminary tests showed that the best place to test the insulation strength of  $\text{CF}_3\text{I-CO}_2$  gas mixtures was between the open contacts of the load switch and not across phases. The preliminary tests conducted show that, across phases, the  $\text{CF}_3\text{I-CO}_2$  gas mixture can insulate the switchgear as well as  $\text{SF}_6$ , at the voltage levels tested.

## CHAPTER 5

# COMPARATIVE LIGHTNING IMPULSE WITHSTAND PERFORMANCE OF SF<sub>6</sub> AND CF<sub>3</sub>I-CO<sub>2</sub> GAS FILLED SWITCH DISCONNECTORS

---

### 5.1 Introduction

This chapter examines the positive standard lightning impulse tests that were conducted on the Ringmaster and Fluokit switch disconnectors in order to examine the insulation strength of the gas mixtures that were placed within their gas chambers. The test results obtained for various gas mixtures (10:90%, 20:80% and 30:70% CF<sub>3</sub>I-CO<sub>2</sub>) are compared with those obtained with equivalent switch disconnectors filled with pure SF<sub>6</sub>.

These tests were undertaken utilizing four different switch disconnectors, two of which remained constantly filled with SF<sub>6</sub> (R1 and F1) and two of which were filled with different gas mixtures (R2 and F2). Two different switch disconnectors were used throughout testing, namely the Ringmaster SE6 and the Fluokit M24+ unit, more details of this can be found in Chapter 4, section 4.2.

To test the insulation strength of gas mixtures of  $\text{CF}_3\text{I}-\text{CO}_2$ , a mixture ratio of 30:70% was initially trialled (due to the promising insulation strength shown in Chapter 2) and compared against 100% pure  $\text{SF}_6$ . From the promising results obtained from the mixture ratio of 30:70%  $\text{CF}_3\text{I}-\text{CO}_2$  (shown in this chapter), it was decided to trial the further applications of 20:80% and 10:90%  $\text{CF}_3\text{I}-\text{CO}_2$ . These  $\text{CF}_3\text{I}-\text{CO}_2$  gas mixtures were compared against 100%  $\text{CO}_2$ , to show the insulation strength  $\text{CF}_3\text{I}$  added to pure  $\text{CO}_2$ , and 100% Air as further proof of  $\text{CF}_3\text{I}$ 's insulation strength.

## 5.2 Open switch phase-earth gas insulation ( $U_{50}$ ) comparison results

The open switch phase – earth gas insulation comparison test, in the switch disconnectors, examines the insulation strength of the gas when the load switch is in the open position. The lightning impulse is applied to a single phase on the switch busbar contact and, therefore, to one side of the load break switch. The bottom main switch cable bushing contacts are earthed. The top main switch busbar contacts of the two phases to which an impulse is not applied are also earthed, as shown in Figure 5.1. The current transformer (CT) is used to help identify whether a lightning impulse breakdown occurs across the gas gap of the open switch.

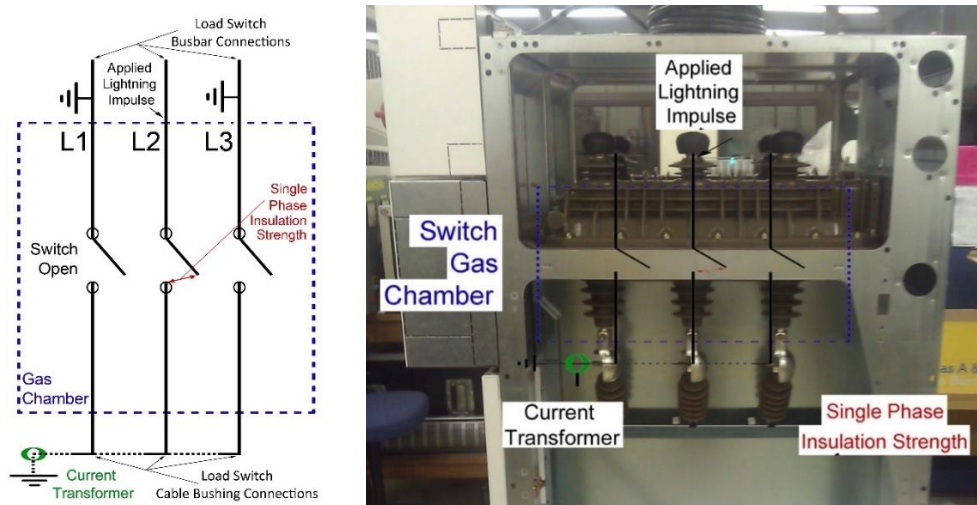


Figure 5.1: Single Phase open switch Phase-Earth LI insulation strength test connections.

The following results use the ‘up-and-down’ method [62] to determine the  $U_{50}$  breakdown strength of the insulation gas medium.

### 5.2.1 Breakdown voltage ( $U_{50}$ ) on the open switch phase-earth gas insulation of the Fluokit M24+

The results for the phase-earth insulation tests, in the Fluokit switch disconnecter unit when filled with various gas mixtures up to the rated pressure (0.45 bar G), are shown in Table 5.1.

Table 5.1: Fluokit M24+ switch disconnecter lightning impulse ( $U_{50}$ ) open switch Phase-Earth gas insulation results at the rated filling pressure of 0.45 bar G.

<b>Fluokit M24+ switch disconnecter lightning impulse (LI) gas insulation strength tests – <math>U_{50}</math> breakdown level (<math>\pm 3\%</math>)</b>					
	<b>Phase 1</b>	<b>Phase 2</b>	<b>Phase 3</b>	<b>Disconnecter Switch Average</b>	<b>Breakdown Description</b>
<b>100% SF<sub>6</sub> (0.45 bar G)</b>	146	158	151	<b>151</b>	Air Breakdown across busbar contacts
<b>30-70% CF<sub>3</sub>I-CO<sub>2</sub> (0.45 bar G)</b>	$\approx 152$	$\approx 152$	$\approx 152$	$\approx 152$	Air Breakdown or epoxy resin failure
<b>20-80% CF<sub>3</sub>I-CO<sub>2</sub> (0.45 bar G)</b>	$\approx 152$	$\approx 152$	$\approx 152$	$\approx 152$	Air Breakdown or epoxy resin failure
<b>10-90% CF<sub>3</sub>I-CO<sub>2</sub> (0.45 bar G)</b>	145	153	138	<b>145</b>	Air Breakdown or epoxy resin or gas failure
<b>100% CO<sub>2</sub> (0.45 bar G)</b>	107	<b>140</b>	118	<b>122</b>	Phase 1 & 3 Epoxy Failure, Phase 2 Gas Failure
<b>100% Air (0.45 bar G)</b>	142	157	137	<b>145</b>	Air Breakdown or epoxy resin failure

The results for the phase-earth gas gap insulation comparison in the Fluokit switch disconnecter unit when filled with various gas mixtures at a pressure of 0 bar G are shown in Table 5.2.

Table 5.2: Fluokit M24+ switch disconnecter lightning impulse ( $U_{50}$ ) open switch Phase-Earth gas insulation results at the minimum operating pressure of 0 bar G.

<b>Fluokit M24+ switch disconnecter lightning impulse (LI) gas insulation strength tests – <math>U_{50}</math> breakdown level (<math>\pm 3\%</math>)</b>					
	<b>Phase 1</b>	<b>Phase 2</b>	<b>Phase 3</b>	<b>Disconnecter Switch Average</b>	<b>Breakdown Description</b>
<b>30-70% <math>CF_3I</math>-<math>CO_2</math> (0 bar G)</b>	143	134	132	<b>137</b>	Air Breakdown or epoxy resin failure, Phase 2 had 1 Gas Failure
<b>20-80% <math>CF_3I</math>-<math>CO_2</math> (0 bar G)</b>	137	140	144	<b>140</b>	Air Breakdown (15 impulses each phase)
<b>10-90% <math>CF_3I</math>-<math>CO_2</math> (0 bar G)</b>	122	154	129	<b>135</b>	Phase 1 & 3 Majority Epoxy Failure, Phase 2 Gas & Air Failure
<b>100% <math>CO_2</math> (0 bar G)</b>	124	<b>121</b>	103	<b>116</b>	Phase 1 & 3 Majority Epoxy Failure, Phase 2 Gas & Air Failure
<b>100% Air (0 bar G)</b>	136	<b>130</b>	119	<b>128</b>	Phase 1 & 3 Majority Epoxy Failure, Phase 2 Gas & Air Failure

From the results in Tables 5.1 and 5.2, it is important to note that, at the rated pressure (0.45 bar G), all of the  $CF_3I$ - $CO_2$  gas mixtures have a  $U_{50}$  breakdown level above the rated 125 kV, as does pure  $SF_6$ . For the majority of cases, all of the  $CF_3I$ - $CO_2$  gas mixtures withstand the standard lightning impulse until the air around the equipment breaks down. When the gas pressure is lowered to 0 bar G, all gas mixtures'  $U_{50}$  breakdown strengths are lowered. Pure  $CO_2$  has the worst insulation performance of all gases and gas mixtures tested and is the only gas to achieve a  $U_{50}$  breakdown strength of less than the rated withstand voltage (125 kV) of the Fluokit switch disconnecter. Figure 5.2 shows the average breakdown strength and how the results can differ between phases. These differences can be accounted for by slight changes in contact geometry, differences in

contact separation distance between phases and the inherent nature of gaseous insulation strength. Table 5.3 and Figure 5.3 show the number of gas failures (GF) and equipment failures (EF) recorded during the tests carried out at 0.45 bar G. Table 5.4 and Figure 5.4 show the number of gas and equipment failures during the tests carried out at 0 bar G.

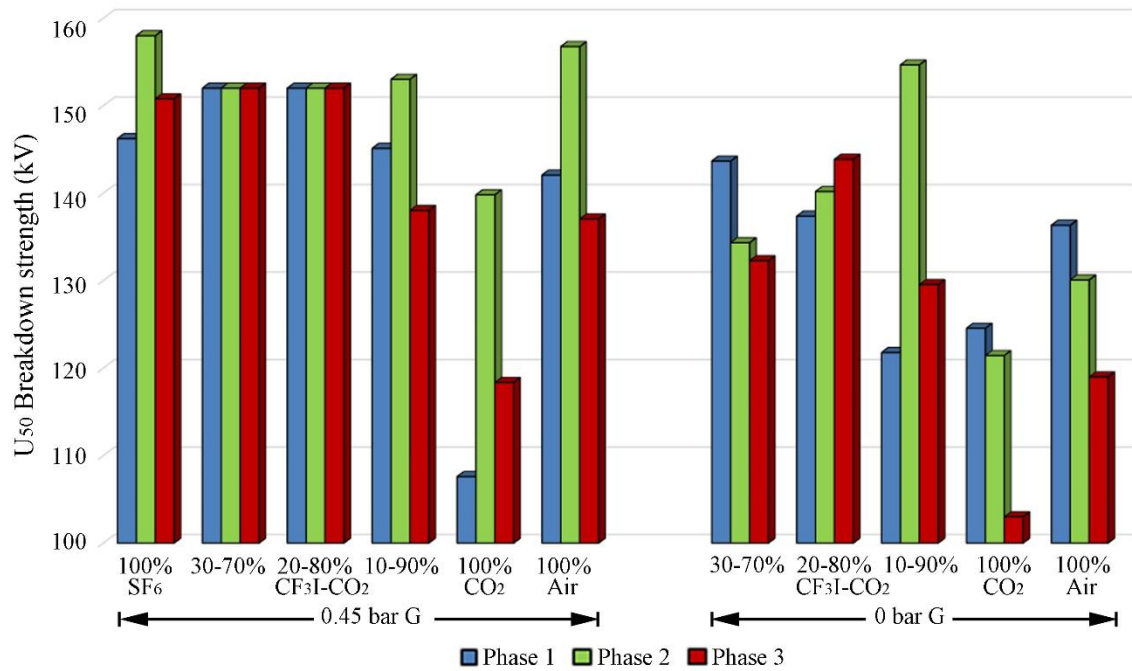


Figure 5.2: Fluokit M24+ switch disconnecter lightning impulse ( $U_{50}$ ) open switch Phase-Earth gas insulation results at 0.45 bar G and 0 bar G for all phases.

Table 5.3: Fluokit M24+ switch disconnecter number of gas failures during lightning impulse open switch Phase-Earth gas insulation tests at 0.45 bar G.

Number of gas failures during lightning impulse breakdown tests – Fluokit 0.45 bar G						
Gas Mixture	Phase 1 (L1)		Phase 2 (L2)		Phase 3 (L3)	
	GF	EF	GF	EF	GF	EF
100% SF <sub>6</sub> (+) Fluokit (F1) 0.45 bar G	0/20	9/20	0/25	9/25	0/20	10/20
10:90% CF <sub>3</sub> I:CO <sub>2</sub> (+) Fluokit (F2) 0.45 bar G	0/15	9/15	0/15	6/15	2/50	24/50
100% CO <sub>2</sub> (+) Fluokit (F2) 0.45 bar G	0/15	4/15	23/50	1/50	0/15	7/15
100% Air (+) Fluokit (F2) 0.45 bar G	0/15	7/15	0/5	0/5	0/15	7/15

Table 5.4: Fluokit M24+ switch disconnector number of gas failures during lightning impulse open switch Phase-Earth gas insulation tests at 0 bar G.

Number of gas failures during lightning impulse breakdown tests – Fluokit 0 bar G						
Gas Mixture	Phase 1 (L1)		Phase 2 (L2)		Phase 3 (L3)	
	GF	EF	GF	EF	GF	EF
30:70% CF <sub>3</sub> I:CO <sub>2</sub> (+) Fluokit (F2) 0 bar G	0/15	7/15	1/15	6/15	0/20	11/20
20:80% CF <sub>3</sub> I:CO <sub>2</sub> (+) Fluokit (F2) 0 bar G	0/15	8/15	1/15	6/15	0/15	6/15
10:90% CF <sub>3</sub> I:CO <sub>2</sub> (+) Fluokit (F2) 0 bar G	0/20	13/20	5/20	4/20	0/15	9/15
100% CO <sub>2</sub> (+) Fluokit (F2) 0 bar G	1/15	6/15	21/50	2/50	0/15	7/15
100% Air (+) Fluokit (F2) 0 bar G	0/20	11/20	15/50	12/50	0/15	9/15

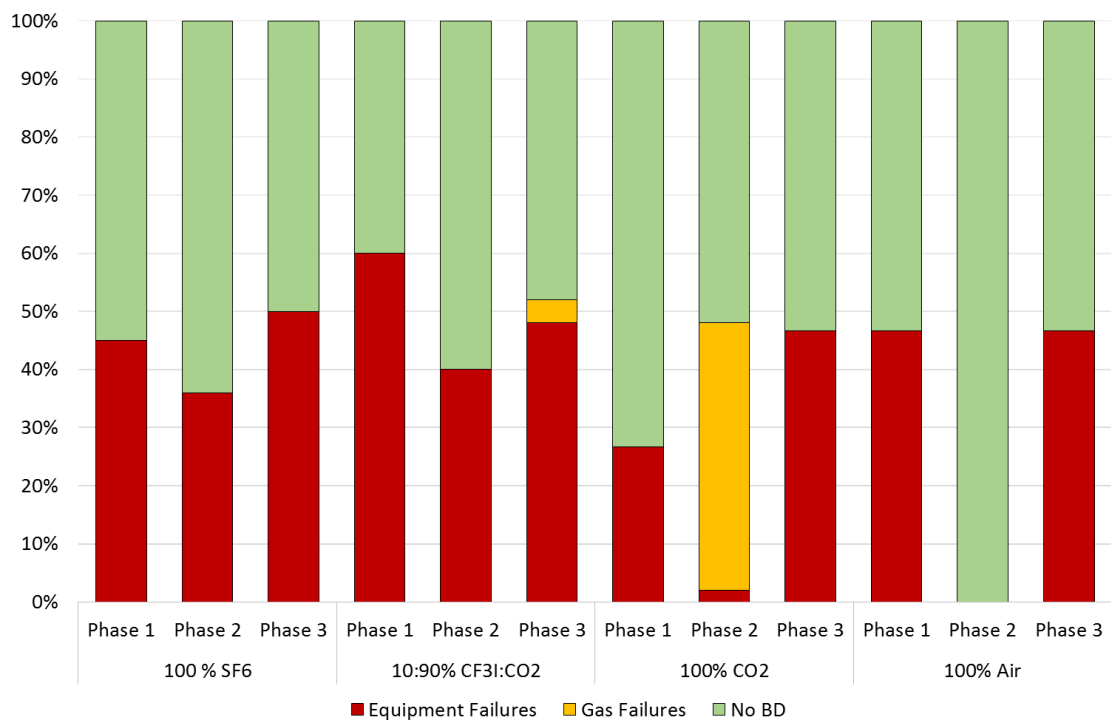


Figure 5.3: Percentage of gas and equipment breakdowns during Fluokit lightning impulse (U<sub>50</sub>) open switch Phase-Earth gas insulation tests at 0.45 bar G.

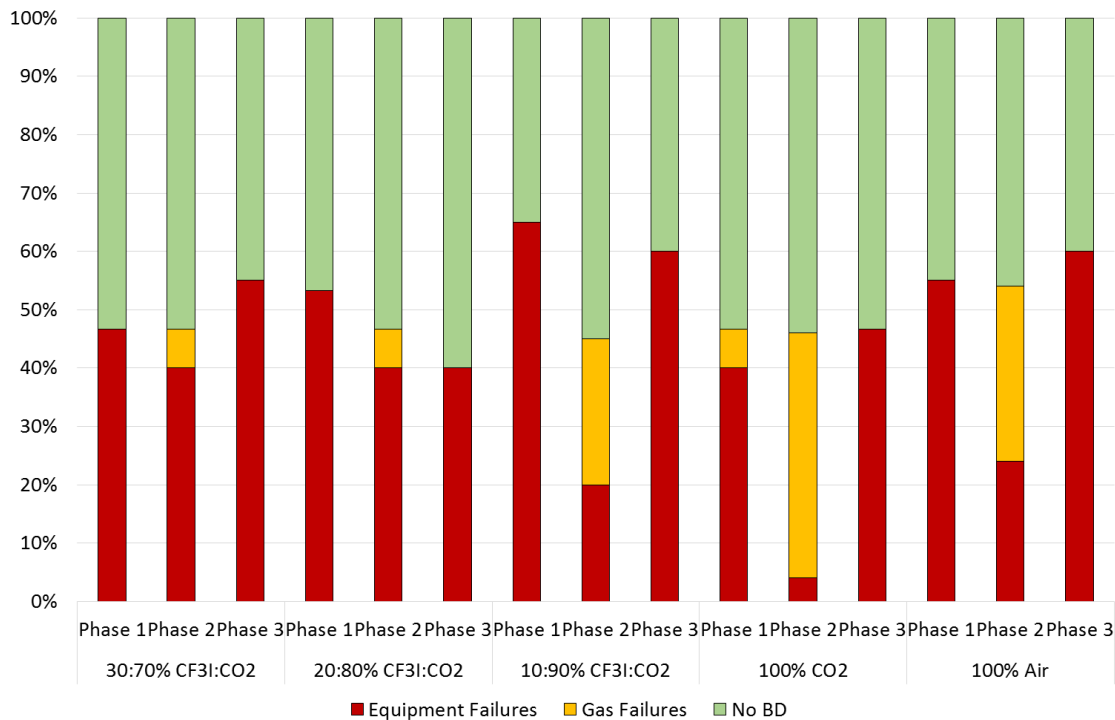


Figure 5.4: Percentage of gas and equipment breakdowns during Fluokit lightning impulse ( $U_{50}$ ) open switch Phase-Earth gas insulation tests at 0 bar G.

From the recorded number of gas failures (GF) and equipment failures (EF) (air breakdowns and epoxy resin failures) in Table 5.3 and Figure 5.3, it is clear that, at 0.45 bar G, all the gas mixtures insulation strengths are higher than the equipment's tolerance and only pure CO<sub>2</sub> has breakdowns occurring across the contacts in the gas chamber. When the gas pressure is lowered to 0 bar G, as shown in Table 5.4 and Figure 5.4, it appears that the insulation strength of 10:90% CF<sub>3</sub>I-CO<sub>2</sub>, pure CO<sub>2</sub> and air is low enough for breakdown to occur across the contacts in the gas chamber. At 0 bar G, gas mixtures of 30:70% and 20:80% CF<sub>3</sub>I:CO<sub>2</sub> are capable of insulating the contacts with only a few gas gap failures detected. It is also interesting to note that the most gas gap failures were recorded in phase 2 of the Fluokit equipment. This indicates that either phase 2 has a sharp point on its contacts in the gas chamber or that the contacts do not separate as far as they do in the other phases.

The rated lightning impulse withstand voltage ( $U_p$ ) for the Fluokit switch disconnecter is 125 kV. However, the results show a 50% probability of a breakdown occurring on the unit at an average peak impulse of up to 152 kV. From the results (Figure 5.3 and 5.4), it is apparent that some of these failures are not all breakdowns across the gas insulation and that the actual breakdown strength of the gas between the contacts of the load break switch is higher than recorded. After capturing these occurrences with a high speed camera, to be able to track the point where the lightning impulse is breaking down, it is apparent that some of the breakdowns are occurring in air outside the gas chamber. The breakdown occurs either across phases in air on the top main switch busbar contact to the next phase or to the earthed metal casing of the switch disconnecter. These occurrences are recorded as equipment failures - air breakdowns (Tables 5.1 and 5.2). From the high speed video recordings, it is also clear that sometimes the breakdown actually occurs across the inside surface of the epoxy resin of the pressurised gas chamber, referred to as epoxy resin failure. The effects seen on the Fluokit with a  $CF_3I$ - $CO_2$  gas mixture, i.e. the epoxy resin orange heat trace around the inside of the gas chamber (Figure 5.8), is likely to have occurred due to a build-up of positive charge around the inside of the epoxy resin gas chamber. It is speculated that this charge is a result of the number of lightning impulses being supplied to the unit in one polarity [50]. This charge is very difficult to neutralise. Sometimes applying several impulses in the opposite polarity can clear this effect but often it cannot be cleared so easily. It is worth noting that this is the result of the number of impulses being applied to the unit in one direction (positive), and this occurrence is highly unlikely upon the distribution network.

In phases 1, 2 and 3, when the switch disconnecter is filled with  $SF_6$  and all other gas mixtures, flashovers can occur between the top main switch busbar contact and the earthed metal casing above the phase connection through the air that surrounds the unit

(Figure 5.5 a, b and c). The flashover can also occur between the phase to which the impulse is applied and the nearest phase where the top main switch busbar contact is earthed (Figure 5.5 d and e), at around 150 kV.

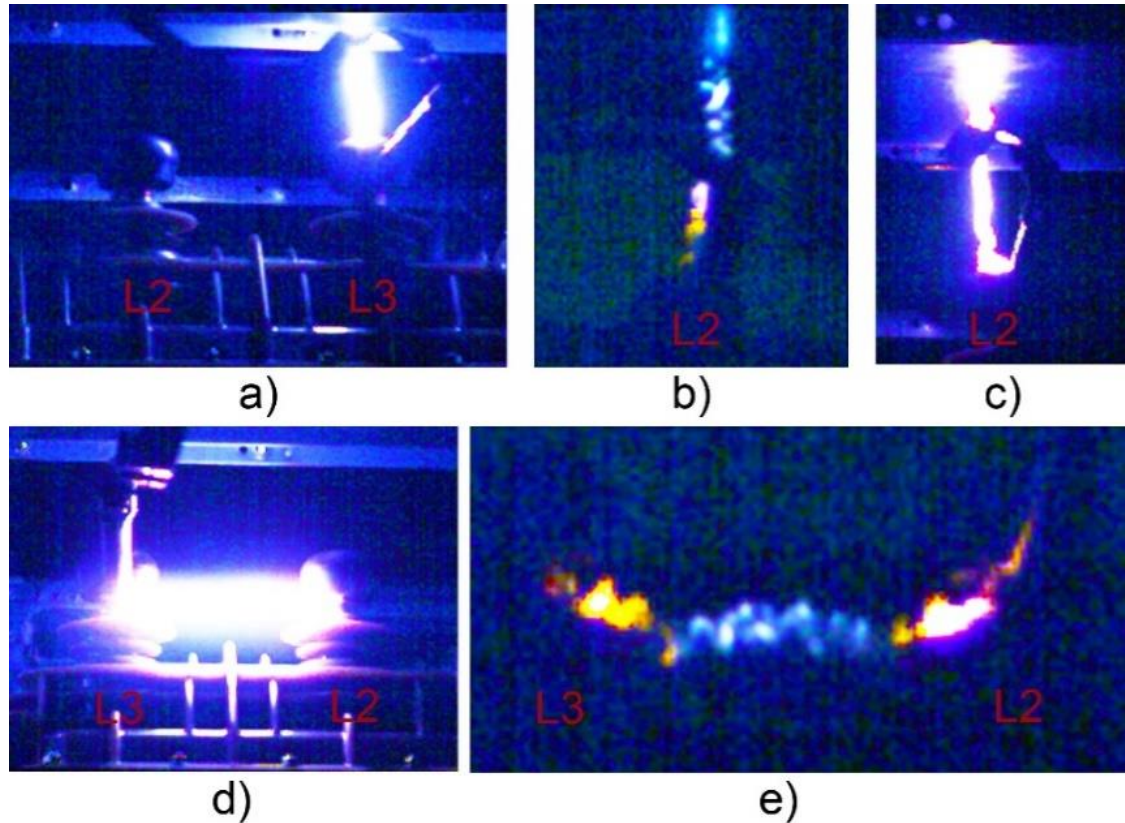


Figure 5.5: Fluokit Air breakdown between the top main switch busbar contact and the earthed metal casing above the phase connection or the closest earthed phase.

From the highlighted separation distances shown in Figure 5.6 of the Fluokit M24+ switch disconnecter, it can be seen that the distance between phases of the busbar contact on top of the main switch is 16 cm. This 16cm gap between phases has an average breakdown of 158 kV for SF<sub>6</sub> and occurs most often in phase 2. The distance from the busbar contact to the earthed metal casing above is 14 cm and has an average breakdown of 151 kV from the 100% SF<sub>6</sub> results. These results are similar for other CF<sub>3</sub>I-CO<sub>2</sub> gas mixtures for the Fluokit M24+ that withstand up until this level and then breakdown through the air instead of the gas between the contacts in the gas chamber.

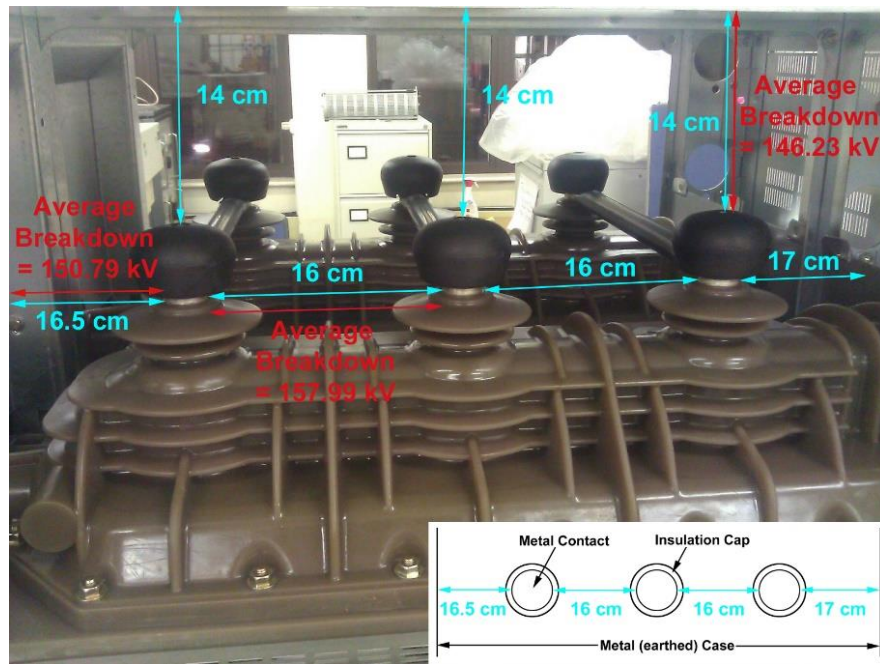


Figure 5.6: Fluokit Air gap length between the phase top main switch busbar contacts and the earthed metal casing or the nearest phase connection.

When the switch disconnecter (F2) is filled with a  $\text{CF}_3\text{I}-\text{CO}_2$  gas mixture, flashovers occur at 152 kV through air, the same impulse level as  $\text{SF}_6$ . However, for tests on phase 1, the impulse appears to travel around the inside of the epoxy resin gas chamber mould. This is attributed to residual charge on the inside of the epoxy resin gas chamber, until it reaches the point where it meets the metal gas filling point (Figure 5.7). The impulse then travels down this connection to flashover across the air between the metal filling point on the outside of the gas chamber and the earthed metal casing (right side of the switch) as shown in Figure 5.7. These flashovers are likely to have been caused by the introduction of an adapter (Appendix B, Figure B2 - k) to the gas valve which is very close to touching the earthed metal casing of the unit. For any of the gas mixtures used, the impulse was observed to travel around the open switch along the inside of the epoxy resin mould that makes up the gas chamber (Figure 5.8). The breakdown occurs to any metal earthed point, as previously being described as caused by residual charge on the inside of the epoxy resin gas chamber, as shown in Figure 5.8.

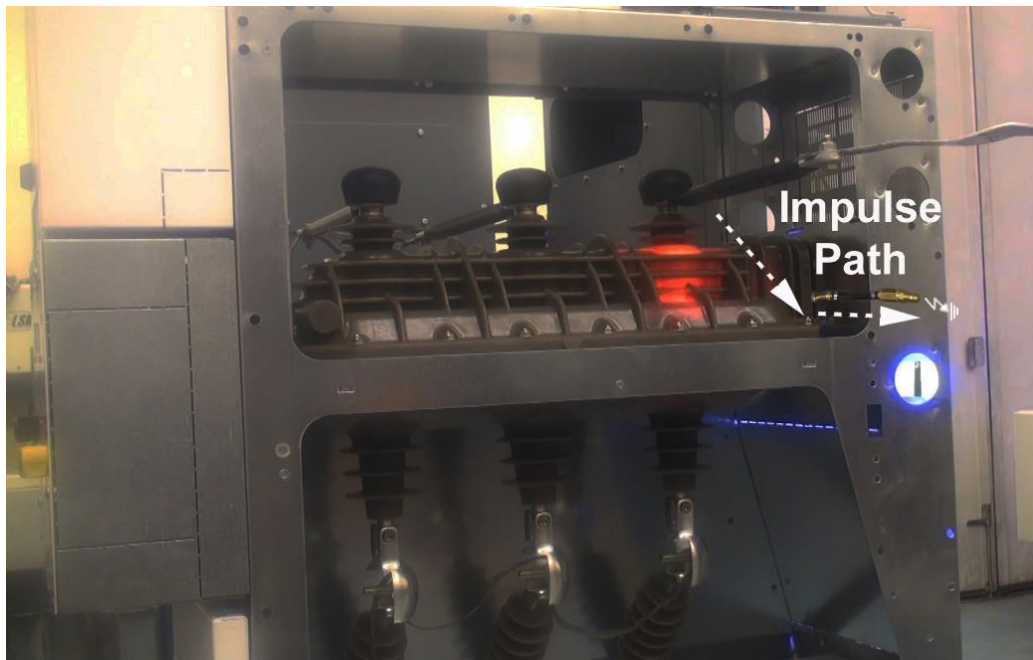


Figure 5.7: Fluokit Phase 1 epoxy resin breakdown / metal gas filling point adapter to earthed metal casing breakdown.

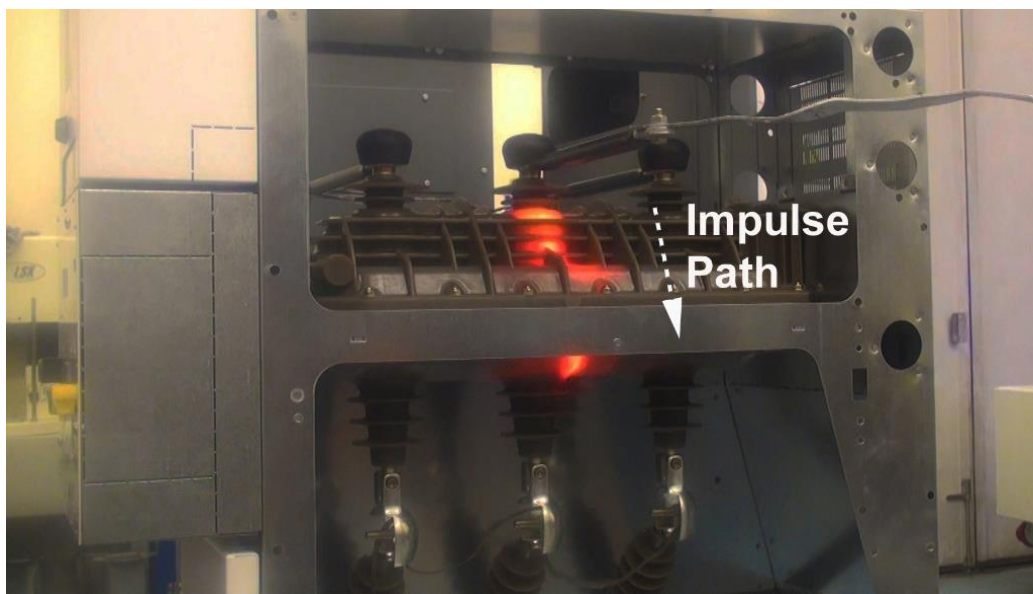


Figure 5.8: Fluokit Phase 2 epoxy resin failure possible caused by residual charge on the inside of the epoxy resin gas chamber.

### 5.2.2 Open switch phase-earth gas insulation ( $U_{50}$ ) Ringmaster SE6 results

The results for the phase-earth gas insulation tests, in the Ringmaster switch disconnecter, when filled with various gas mixtures up to the rated pressure (0.35 bar G) are shown in Table 5.5.

Table 5.5: Ringmaster SE6 switch disconnecter lightning impulse ( $U_{50}$ ) open switch  
Phase-Earth gas insulation results at 0.35 bar G.

<b>Ringmaster SE6 disconnecter switch lightning impulse gas insulation strength tests – <math>U_{50}</math> breakdown level (<math>\pm 3\%</math>)</b>					
	<b>Phase 1</b>	<b>Phase 2</b>	<b>Phase 3</b>	<b>Disconnecter Switch Average</b>	
<b>100% SF<sub>6</sub> (0.35 bar G)</b>	120	126	122	<b>123</b>	Equipment Failure
<b>30-70% CF<sub>3</sub>I-CO<sub>2</sub> (0.35 bar G)</b>	112	106	107	<b>108</b>	Equipment Failure
<b>20-80% CF<sub>3</sub>I-CO<sub>2</sub> (0.35 bar G)</b>	<b>104</b>	<b>112</b>	109	<b>108</b>	Phase 1 & 2 Predominantly Gas failure, Phase 3 Equipment Failure
<b>10-90% CF<sub>3</sub>I-CO<sub>2</sub> (0.35 bar G)</b>	<b>116</b>	<b>113</b>	112	<b>114</b>	Phase 1 & 2 Predominantly Gas failure, Phase 3 Equipment Failure
<b>100% CO<sub>2</sub> (0.35 bar G)</b>	<b>101</b>	<b>109</b>	<b>101</b>	<b>104</b>	Predominantly Gas failure
<b>100% Air (0.35 bar G)</b>	<b>91</b>	<b>102</b>	90	<b>94</b>	Predominantly Gas failure

The results for the phase-earth gas gap insulation comparison tests in the Ringmaster switch disconnecter unit, when filled with various gas mixtures at a minimum operating pressure of 0 bar G, are shown in Table 5.6.

Figure 5.9 shows the average breakdown strength of the different phases.

Table 5.6: Ringmaster SE6 switch disconnector lightning impulse ( $U_{50}$ ) open switch  
Phase-Earth gas insulation results at 0 bar G.

<b>Ringmaster SE6 disconnector switch lightning impulse gas insulation strength tests – <math>U_{50}</math> breakdown level (<math>\pm 3\%</math>)</b>					
	<b>Phase 1</b>	<b>Phase 2</b>	<b>Phase 3</b>	<b>Disconnector Switch Average</b>	
<b>30-70% <math>CF_3I</math>-<math>CO_2</math> (0 bar G)</b>	<b>104</b>	<b>105</b>	<b>97</b>	<b>102</b>	Predominantly Gas failure
<b>20-80% <math>CF_3I</math>-<math>CO_2</math> (0 bar G)</b>	<b>104</b>	<b>100</b>	<b>100</b>	<b>101</b>	Predominantly Gas failure
<b>10-90% <math>CF_3I</math>-<math>CO_2</math> (0 bar G)</b>	<b>109</b>	<b>88</b>	<b>103</b>	<b>100</b>	Predominantly Gas failure
<b>100% <math>CO_2</math> (0 bar G)</b>	<b>88</b>	<b>103</b>	<b>81</b>	<b>91</b>	Predominantly Gas failure
<b>100% Air (0 bar G)</b>	<b>79</b>	<b>90</b>	<b>84</b>	<b>85</b>	Predominantly Gas failure

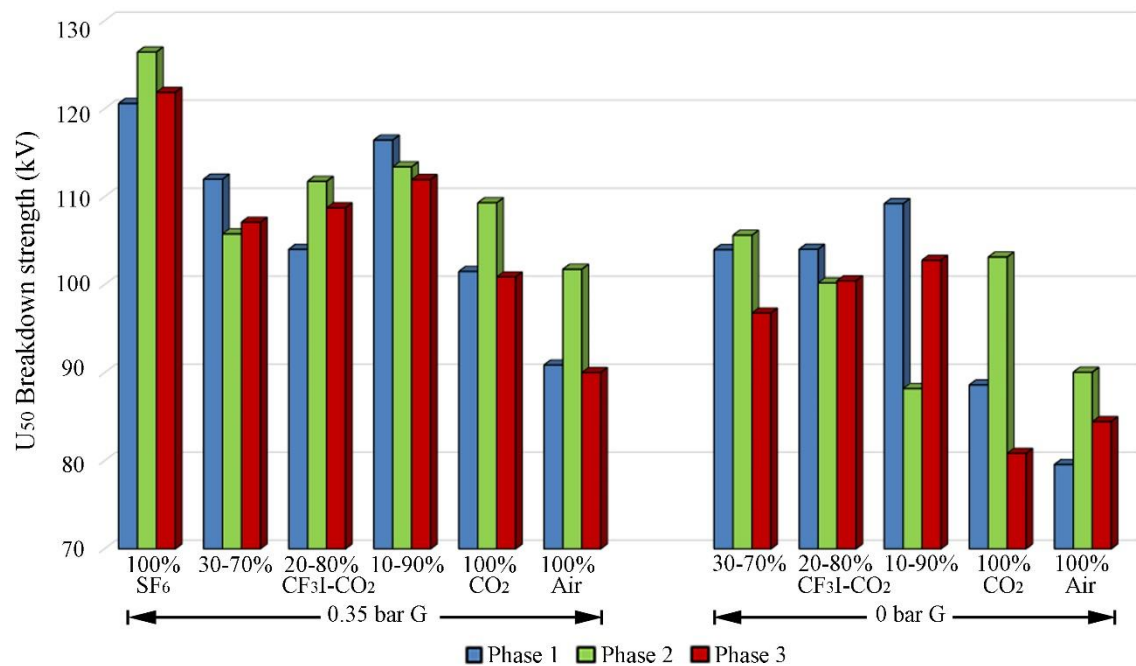


Figure 5.9: Ringmaster SE6 switch disconnector lightning impulse ( $U_{50}$ )

open switch Phase-Earth gas insulation results at 0.35 bar G and 0 bar G for all phases.

Table 5.7 and Figure 5.10 show the number of gas failures (GF) and equipment failures (EF) recorded during the tests carried out at 0.35 bar G. Table 5.8 and Figure 5.11 show the number of gas and equipment failures during the tests carried out a 0 bar G.

Table 5.7: Ringmaster SE6 switch disconnecter number of gas failures during lightning impulse open switch Phase-Earth gas insulation tests at 0.35 bar G.

Number of gas failures during lightning impulse breakdown tests – Ringmaster 0.35 bar G						
Gas Mixture	Phase 1 (L1)		Phase 2 (L2)		Phase 3 (L3)	
	GF	EF	GF	EF	GF	EF
100% SF <sub>6</sub> (+) Ringmaster (R1) 0.35 bar G	0/15	8/15	0/21	12/21	0/21	10/21
30:70% CF <sub>3</sub> I:CO <sub>2</sub> (+) Ringmaster (R2) 0.35 bar G	0/53	19/53	0/55	25/55	0/52	22/52
20:80% CF <sub>3</sub> I:CO <sub>2</sub> (+) Ringmaster (R2) 0.35 bar G	29/50	0/50	19/50	2/50	0/50	23/50
10:90% CF <sub>3</sub> I:CO <sub>2</sub> (+) Ringmaster (R2) 0.35 bar G	21/50	2/50	26/54	7/54	3/50	21/50
100% CO <sub>2</sub> (+) Ringmaster (R2) 0.35 bar G	24/50	0/50	22/50	1/50	18/50	7/50
100% Air (+) Ringmaster (R2) 0.35 bar G	25/50	1/50	24/50	0/50	9/50	18/50

Table 5.8: Ringmaster SE6 switch disconnecter number of gas failures during lightning impulse open switch Phase-Earth gas insulation tests at 0 bar G.

Number of gas failures during lightning impulse breakdown tests – Ringmaster 0 bar G						
Gas Mixture	Phase 1 (L1)		Phase 2 (L2)		Phase 3 (L3)	
	GF	EF	GF	EF	GF	EF
30:70% CF <sub>3</sub> I:CO <sub>2</sub> (+) Ringmaster (R2) 0 bar G	23/50	0/50	24/50	0/50	15/50	9/50
20:80% CF <sub>3</sub> I:CO <sub>2</sub> (+) Ringmaster (R2) 0 bar G	24/50	0/50	24/50	0/50	1/50	15/50
10:90% CF <sub>3</sub> I:CO <sub>2</sub> (+) Ringmaster (R2) 0 bar G	23/50	0/50	22/50	0/50	15/50	6/50
100% CO <sub>2</sub> (+) Ringmaster (R2) 0 bar G	27/50	0/50	23/50	0/50	24/50	0/50
100% Air (+) Ringmaster (R2) 0 bar G	25/50	0/50	24/50	0/50	26/50	0/50

Epoxy resin failures and a build-up of charge may be occurring on the inside of the gas chamber of the Ringmaster unit as in the Fluokit. However, epoxy resin failures cannot be photographed, as with the Fluokit, because the gas chamber is completely enclosed within the metal casing of the Ringmaster unit. It was also noted that the Ringmaster has an earthed coating on the outside of the gas chamber, so this is a potential earthing point for the applied lightning impulse.

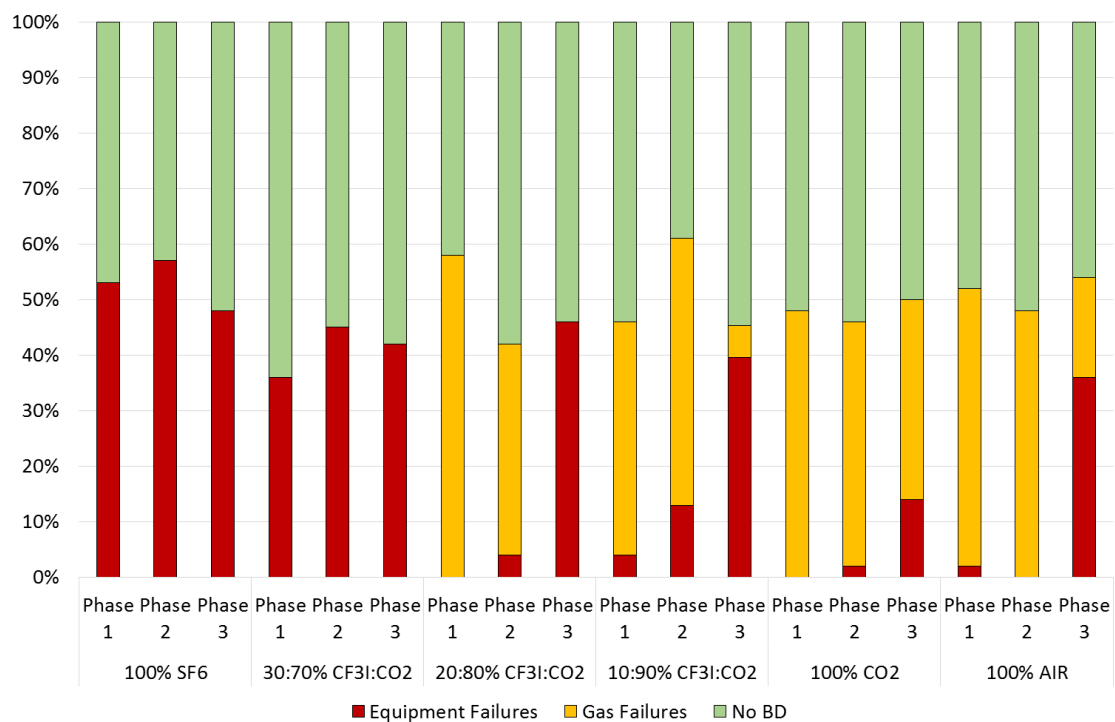


Figure 5.10: Percentage of gas and equipment breakdowns during Ringmaster lightning impulse open switch Phase-Earth gas insulation tests at 0.35 bar G.

From the results of the Ringmaster unit, it is clear that, at the rated pressure of the unit (0.35 bar G), all gas mixtures, except for air, have a  $U_{50}$  breakdown voltage above the equipment withstand voltage of 95 kV (Table 5.5). When the gas pressure is lowered to 0 bar G, all  $CF_3I$ - $CO_2$  gas mixtures have a  $U_{50}$  breakdown voltage above the units lightning impulse withstand voltage. However, air and  $CO_2$  do not (Table 5.6). It is also apparent that at atmospheric pressure (0 bar G), the 50% probability of a breakdown voltage being achieved is only slightly increased when 10% or 20%  $CF_3I$  is added to the

CF<sub>3</sub>I-CO<sub>2</sub> gas mixture. This means that the results of 30%:70%, 20%:80% and 10%:90% CF<sub>3</sub>I-CO<sub>2</sub> gas mixture tests are only slightly different, at 0 bar G (Table 5.6).

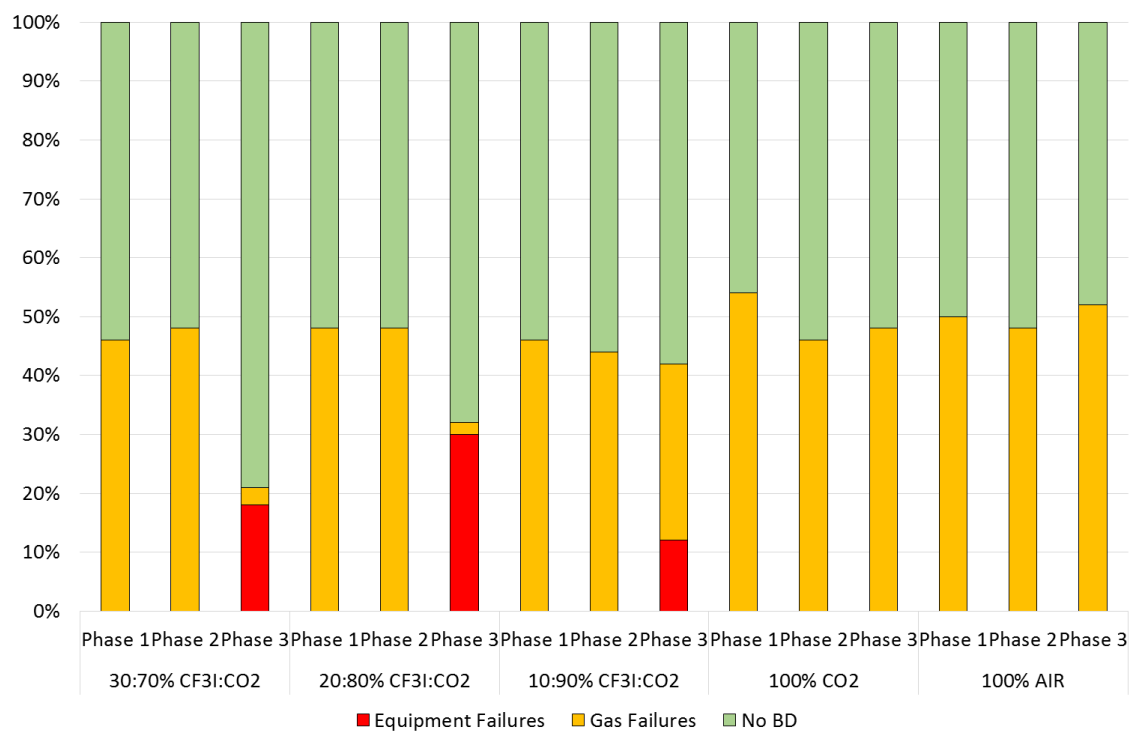


Figure 5.11: Percentage of gas and equipment breakdowns during Ringmaster lightning impulse open switch Phase-Earth gas insulation tests at 0 bar G.

From the number of gas failures recorded, for this test in the Ringmaster, it is possible to show that only pure SF<sub>6</sub> and 30%:70% CF<sub>3</sub>I:CO<sub>2</sub> gas mixtures, at 0.35 bar G, insulate the equipment without breakdown occurring across the contacts in the gas chamber (Table 5.7 and Figure 5.10). All other gas mixtures tested have recorded a significant number of gas failures across the contacts in the Ringmasters gas chamber (Tables 5.7 and 5.8) (Figures 5.10 and 5.11). With this considered, it means that the results are a fair representation of the gas mixtures insulation strength instead of a representation of air breakdown outside the equipment.

### 5.3 Open switch phase-earth gas withstand test results

The withstand test is a series of impulses applied one after the other to the open switch disconnector at its rated withstand level, 125 kV for the Fluokit and 95 kV for the

Ringmaster. A description of the procedure for the withstand test is given in Appendix C. The test circuit for this test is the same as used in open switch phase-earth gas insulation comparison tests (Figure 5.1). A minimum of 15 impulses is applied to each phase for each gas mixture with most phases having 50 impulses (2 full 25 impulse series) applied to test the withstand strength unless significant failure occurs.

### 5.3.1 Open switch phase-earth gas withstand Fluokit M24+ test results

The withstand test results for the Fluokit switch disconnecter are shown in Table 5.9. The withstand test results show the same as the gas insulation test results in that all the gas mixtures in the Fluokit unit pass the test except for pure CO<sub>2</sub>.

Table 5.9: Fluokit M24+ rated lightning impulse withstand test results.

<b>Fluokit rated lightning impulse withstand voltage (Up)</b>		
	<b>125 kV</b>	<b>Percentage of Gas Failures</b>
<b>100% SF<sub>6</sub> (0.45 bar G)</b>	<b>PASS</b>	<b>0%</b>
<b>30-70% CF<sub>3</sub>I-CO<sub>2</sub> (0 bar G)</b>	<b>PASS</b>	<b>0%</b>
<b>30-70% CF<sub>3</sub>I-CO<sub>2</sub> (0.45 bar G)</b>	<b>PASS</b>	<b>0%</b>
<b>20-80% CF<sub>3</sub>I-CO<sub>2</sub> (0 bar G)</b>	<b>PASS</b>	<b>0%</b>
<b>20-80% CF<sub>3</sub>I-CO<sub>2</sub> (0.45 bar G)</b>	<b>PASS</b>	<b>2.00%</b>
<b>10-90% CF<sub>3</sub>I-CO<sub>2</sub> (0 bar G)</b>	<b>PASS</b>	<b>0%</b>
<b>10-90% CF<sub>3</sub>I-CO<sub>2</sub> (0.45 bar G)</b>	<b>PASS</b>	<b>0.67%</b>
<b>100% CO<sub>2</sub> (0 bar G)</b>	<b>FAIL</b>	<b>24.45%</b>
<b>100% CO<sub>2</sub> (0.45 bar G)</b>	<b>PASS</b>	<b>0%</b>
<b>100% Air (0 bar G)</b>	<b>PASS</b>	<b>0.67%</b>
<b>100% Air (0.45 bar G)</b>	<b>PASS</b>	<b>0%</b>

### 5.3.2 Open switch phase-earth gas withstand Ringmaster SE6 test results

In the Ringmaster, the withstand tests show that SF<sub>6</sub> and all the CF<sub>3</sub>I-CO<sub>2</sub> gas mixtures pass the test at 0.35 bar G (Table 5.10 and Figure 5.12). At 0 bar G, all other gas mixtures fail the test except for 30%:70% CF<sub>3</sub>I-CO<sub>2</sub> and 20%:80% CF<sub>3</sub>I-CO<sub>2</sub> which have marginal results (Figure 5.13). A marginal pass / fail test result indicates at least one phase has failed the test.

Table 5.10: Ringmaster SE6 rated lightning impulse withstand test results.

<b>Ringmaster rated lightning impulse withstand voltage (Up)</b>		
	<b>95 kV</b>	<b>Percentage of Gas Failures</b>
<b>100% SF<sub>6</sub> (0.35 bar G)</b>	<b>PASS</b>	<b>0 %</b>
<b>30-70% CF<sub>3</sub>I-CO<sub>2</sub> (0 bar G)</b>	<b>MARGINAL PASS / FAIL</b>	<b>11.33 %</b>
<b>30-70% CF<sub>3</sub>I-CO<sub>2</sub> (0.35 bar G)</b>	<b>PASS</b>	<b>0 %</b>
<b>20-80% CF<sub>3</sub>I-CO<sub>2</sub> (0 bar G)</b>	<b>MARGINAL PASS / FAIL</b>	<b>4.67 %</b>
<b>20-80% CF<sub>3</sub>I-CO<sub>2</sub> (0.35 bar G)</b>	<b>PASS</b>	<b>0 %</b>
<b>10-90% CF<sub>3</sub>I-CO<sub>2</sub> (0 bar G)</b>	<b>FAIL</b>	<b>42.00 %</b>
<b>10-90% CF<sub>3</sub>I-CO<sub>2</sub> (0.35 bar G)</b>	<b>PASS</b>	<b>0.67 %</b>
<b>100% CO<sub>2</sub> (0 bar G)</b>	<b>FAIL</b>	<b>37.70 %</b>
<b>100% CO<sub>2</sub> (0.35 bar G)</b>	<b>MARGINAL PASS / FAIL</b>	<b>8.67 %</b>
<b>100% Air (0 bar G)</b>	<b>FAIL</b>	<b>88.33%</b>
<b>100% Air (0.35 bar G)</b>	<b>FAIL</b>	<b>38.00%</b>

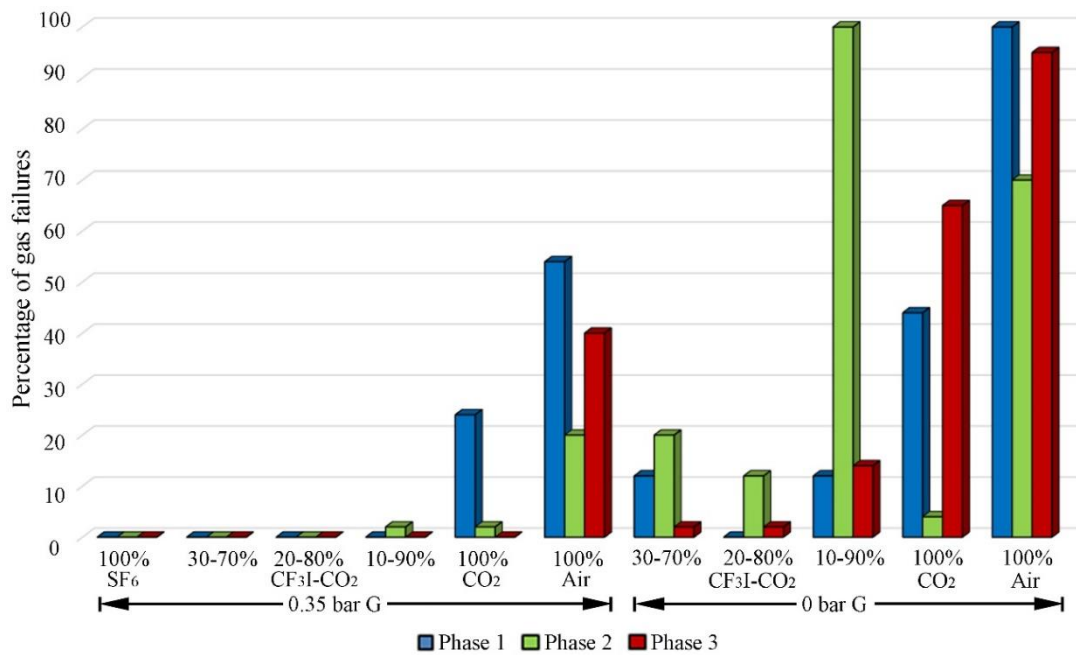


Figure 5.12: Percentage gas failure per phase during a 95 kV lightning impulse withstand test in the Ringmaster SE6 switch disconnector.

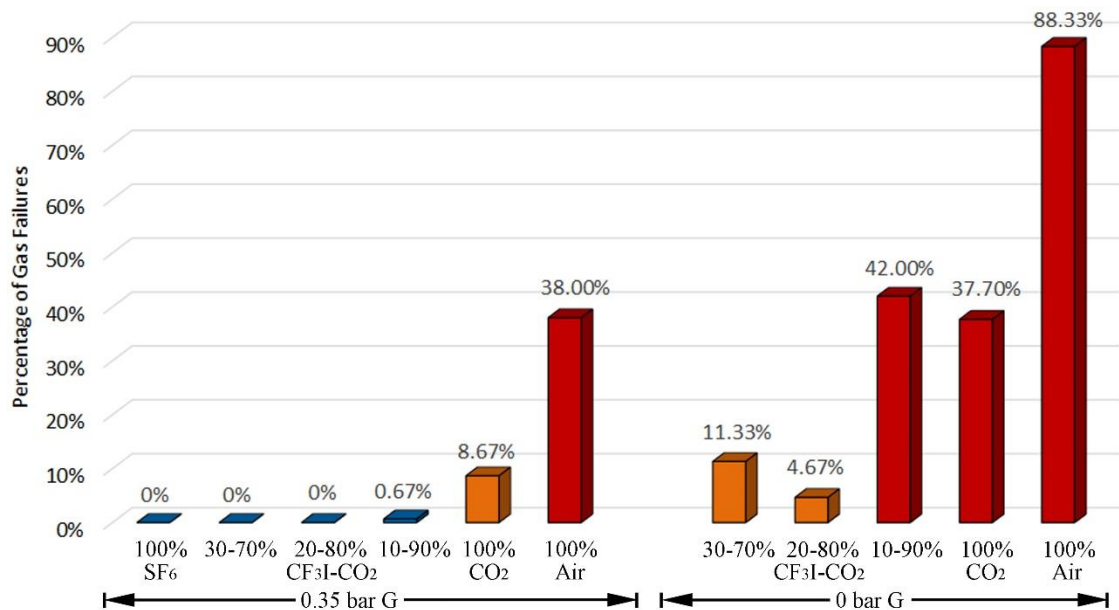


Figure 5.13: Average percentage gas failure per phase during a 95 kV lightning impulse withstand test in the Ringmaster SE6 switch disconnector.

#### 5.4 Fluokit and Ringmaster insulation and withstand tests

The results for the phase-earth gas gap ( $U_{50}$ ) insulation tests in the Fluokit switch disconnector unit, when filled with various gas mixtures at a pressure of 0 bar G and 0.45 bar G, as an average of all 3 phases is shown in Figure 5.14. The colour of the bars shown in the graph (Figure 5.14) also indicate the results of the withstand test.

It can be shown from Table 5.3 and Figure 5.3 that at a pressure of 0.45 bar G all gas mixtures can withstand 125 kV and CO<sub>2</sub> is the only gas that actually suffers gas gap breakdowns across the switch for the U<sub>50</sub> insulation strengths tests. At 0.45 bar G all other U<sub>50</sub> insulation strength test results refer to the level at which the unit suffers air breakdown around the unit and epoxy resin failures.

At 0 bar G the withstand tests carried out indicate that CO<sub>2</sub> is the only gas to fail. Table 5.4 and Figure 5.4 indicate that at 0 bar G all gas mixtures tested have breakdown occur across the gas gap in the switch disconnecter but most breakdowns occur in 10:90% CF<sub>3</sub>I-CO<sub>2</sub>, CO<sub>2</sub> and air. This indicates that of all the CF<sub>3</sub>I-CO<sub>2</sub> gas mixtures tested, 10:90% CF<sub>3</sub>I-CO<sub>2</sub> preforms the worst.

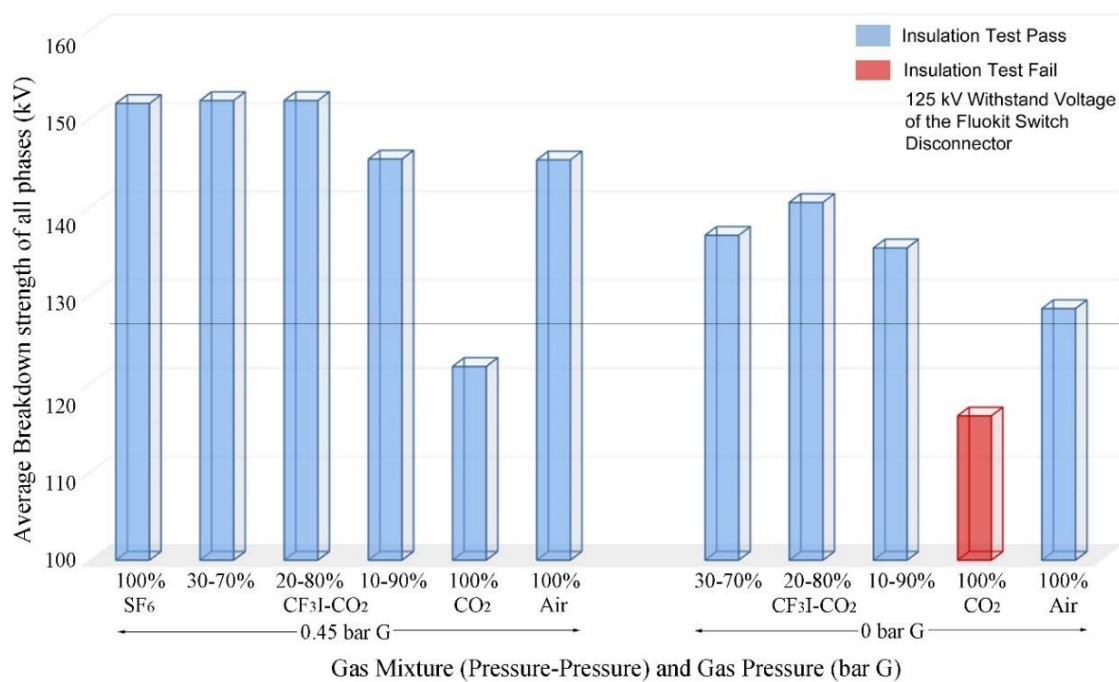


Figure 5.14: Fluokit M24+ switch disconnecter LI open switch Phase-Earth gas insulation results, at 0.45 bar G and 0 bar G, as an average for all phases.

The results for the phase-earth gas gap insulation comparison in the Ringmaster switch disconnecter unit when filled with various gas mixtures at a pressure of 0 bar G and 0.35 bar G, as an average of all 3 phases, is shown in Figure 5.15 along with the withstand test results.

In Table 5.7 and Figure 5.10 it is shown that, at a pressure of 0.35 bar G, all CF<sub>3</sub>I-CO<sub>2</sub> gas mixtures can withstand 95 kV. It can also be shown that all gas mixtures apart from pure SF<sub>6</sub> and 30:70% CF<sub>3</sub>I-CO<sub>2</sub> suffer gas gap breakdowns across the switch for the U<sub>50</sub> insulation strengths tests. Therefore, at 0.35 bar G, the U<sub>50</sub> insulation strength test results for pure SF<sub>6</sub> and 30:70% CF<sub>3</sub>I-CO<sub>2</sub> actually refer to the level at which the Ringmaster suffers air breakdown and epoxy resin failures.

At 0 bar G the withstand tests carried out indicate that all gas mixtures are likely to fail, although 30:70% CF<sub>3</sub>I-CO<sub>2</sub> and 20:80% CF<sub>3</sub>I-CO<sub>2</sub> preform the best out of all gas mixtures tested. Table 5.8 and Figure 5.11 indicate that, at 0 bar G, all gas mixtures tested breakdown across the gas gap in the switch disconnecter. At 0 bar G, these tests are a more accurate representation of all the CF<sub>3</sub>I-CO<sub>2</sub> gas mixtures insulation strengths as there are a lot less air breakdowns and epoxy resin failures recorded within the results.

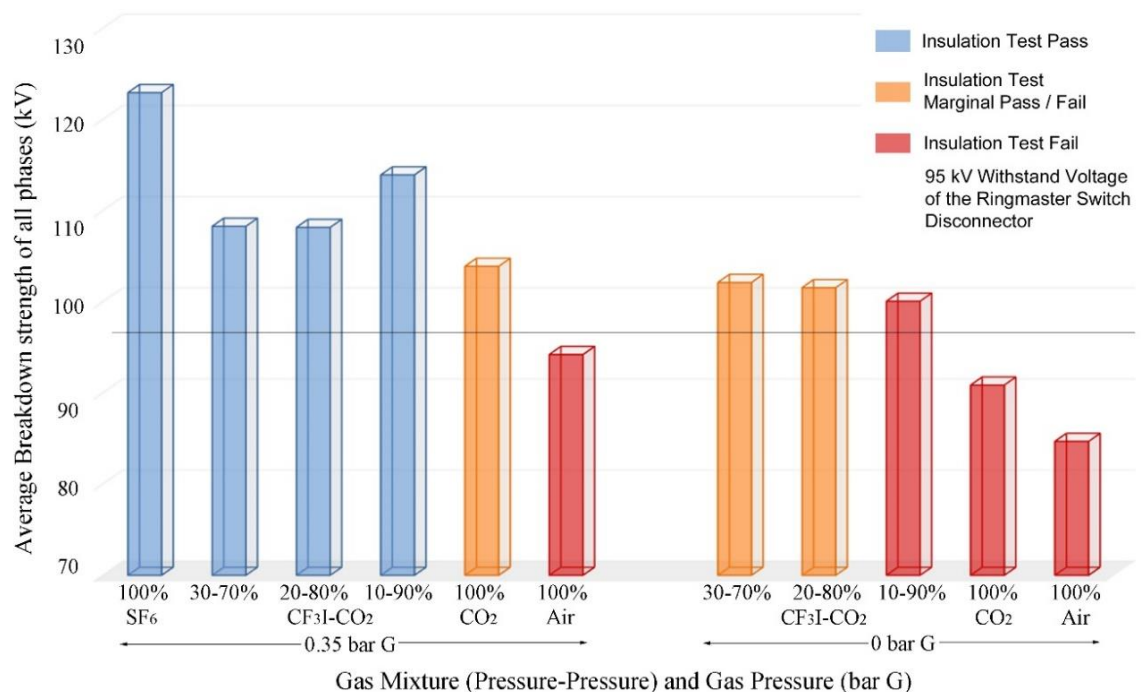


Figure 5.15: Ringmaster SE6 switch disconnecter LI open switch Phase-Earth gas insulation results, at 0.45 bar G and 0 bar G, as an average for all phases.

## 5.5 Conclusion

The results reported in this chapter indicate that, for the Fluokit M24+, all gas mixtures tested, except for CO<sub>2</sub>, could be used to insulate the contacts within the gas chamber of the load break switch when it is in the open position.

Furthermore, the results in this chapter indicate that for the Ringmaster SE6 all CF<sub>3</sub>I-CO<sub>2</sub> gas mixtures tested could be used to insulate the contacts within the gas chamber of the load break switch when it is in the open position at 0.35 bar G. At 0 bar G, 30%:70% CF<sub>3</sub>I-CO<sub>2</sub> and 20%:80% CF<sub>3</sub>I-CO<sub>2</sub> gas mixtures are marginal passes. Therefore, it is recommended that the pressure is kept above 0 bar G to insulate the equipment successfully. The results also indicate that both air and pure CO<sub>2</sub> could not be used to sufficiently insulate the contacts in the Ringmaster load switch.

At the rated operating pressure, the results indicate that when the Fluokit is filled with the CF<sub>3</sub>I-CO<sub>2</sub> gas mixtures it performs as well as SF<sub>6</sub>. However, in the Ringmaster the CF<sub>3</sub>I-CO<sub>2</sub> gas mixtures do not perform as well as SF<sub>6</sub>, this indicates that the field produced between the Fluokit contacts is more uniform than in the Ringmaster.

## CHAPTER 6

# RINGMASTER SWITCH DISCONNECTOR ELECTRIC FIELD SIMULATIONS AND EFFECTIVE IONIZATION COEFFICIENTS

---

### 6.1 Introduction

In this chapter Comsol software is used to build a finite element model of the Ringmaster SE6 switch disconnecter and investigate electric field distribution across an open contact gas gap. The simulation shows an evaluation of discharges occurring across the gas gap in the switchgear. These simulations utilise the effective ionization coefficients for  $\text{CF}_3\text{I}$  and  $\text{CF}_3\text{I-CO}_2$  gas mixtures, calculated in section 6.3, and compare their insulating performance with that of  $\text{SF}_6$ . This chapter also studies switchgear design and shows contact geometry simulations for suggestions on how to optimise the switches contacts for use with  $\text{CF}_3\text{I}$  and  $\text{CF}_3\text{I-CO}_2$  gas mixtures.

## 6.2 Ringmaster switch disconnecter electric field simulations

In order to carry out simulations, the schematics shown in Figure 6.1 were used to develop an accurate model of the Ringmaster switch disconnecter. The schematics are shown in Figure 6.2 overlaid on the Ringmaster to clarify the position the gas chamber takes within the unit.

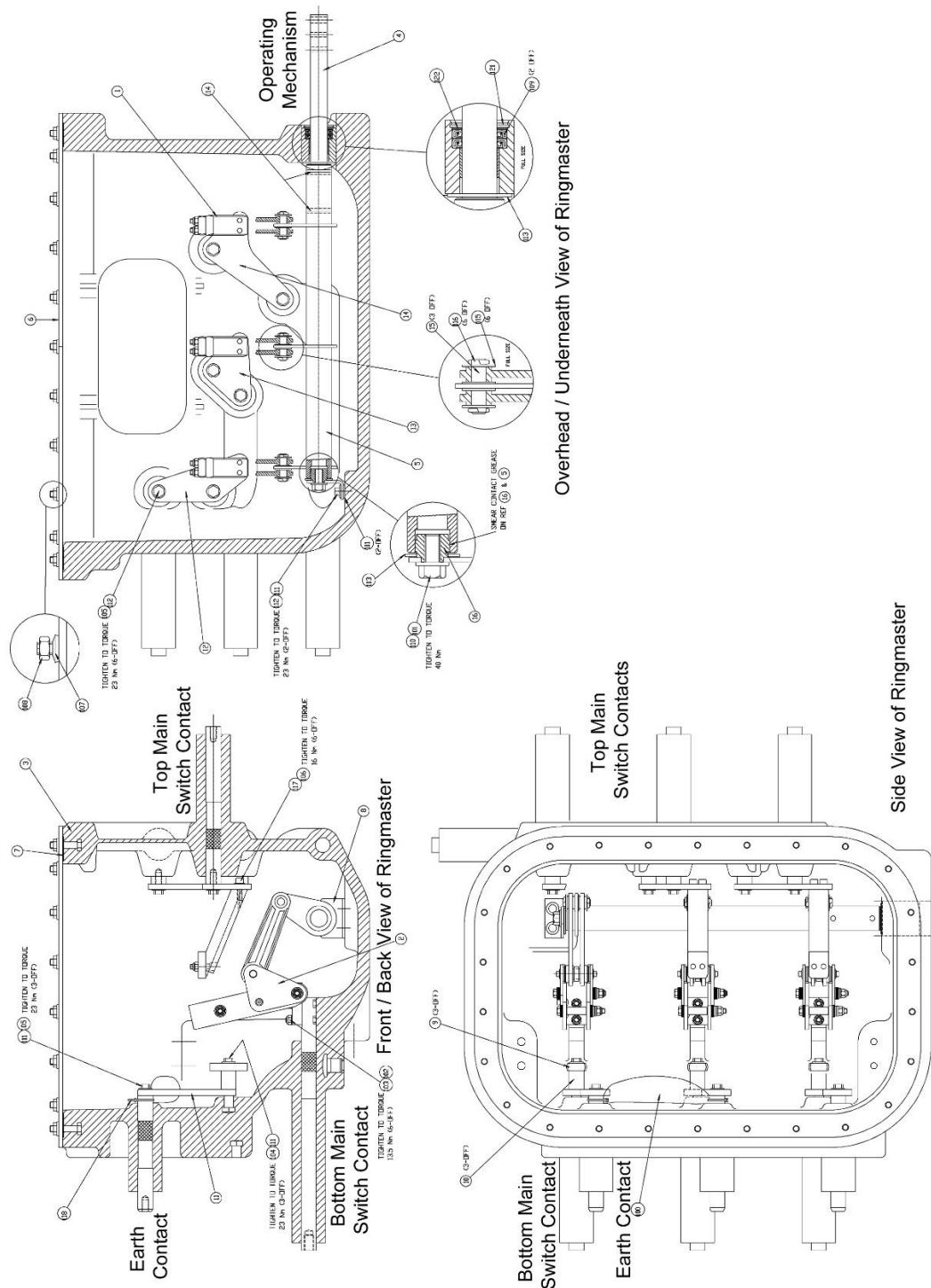


Figure 6.1: Schneider Electric Ringmaster SE6 switch disconnecter schematics [82].

To simulate the Ringmaster the model also utilises the materials shown in Figure 6.3. The relative permittivity for each material is shown in Table 6.1.

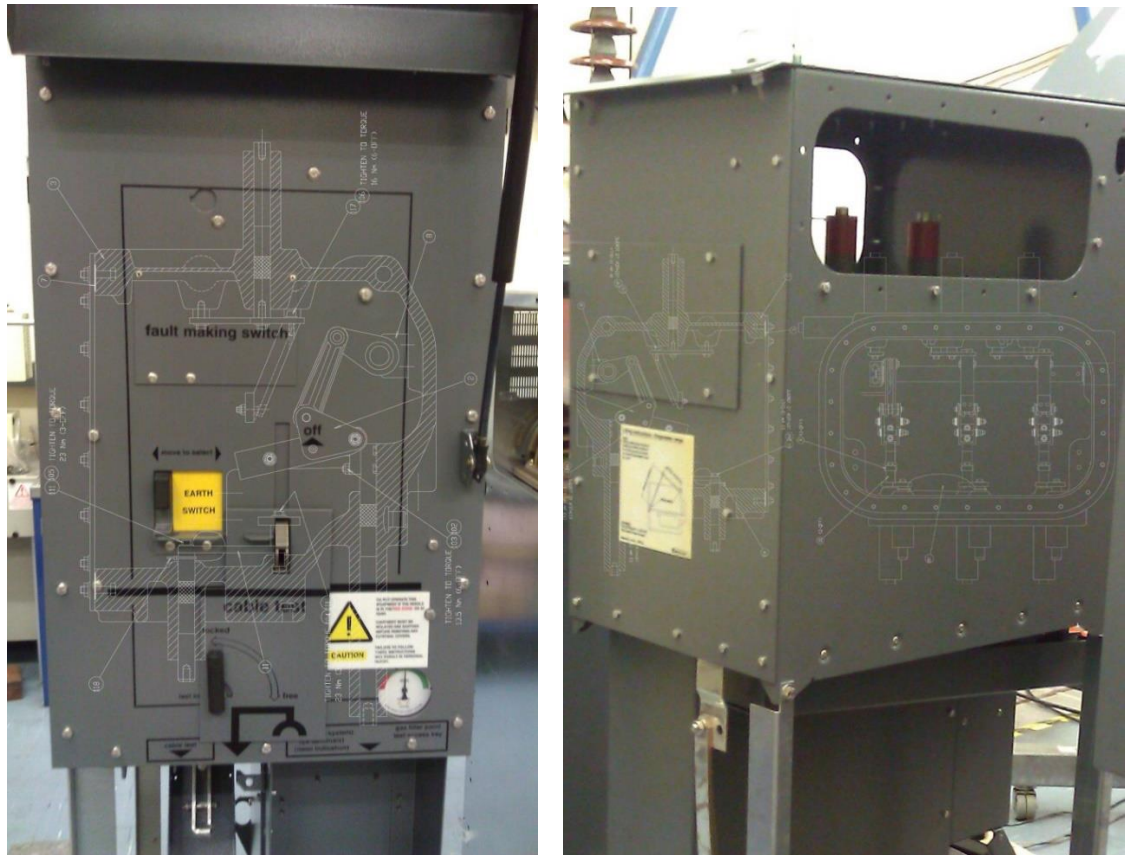


Figure 6.2: Ringmaster SE6 switch disconnector schematics overlaid on the unit [82].

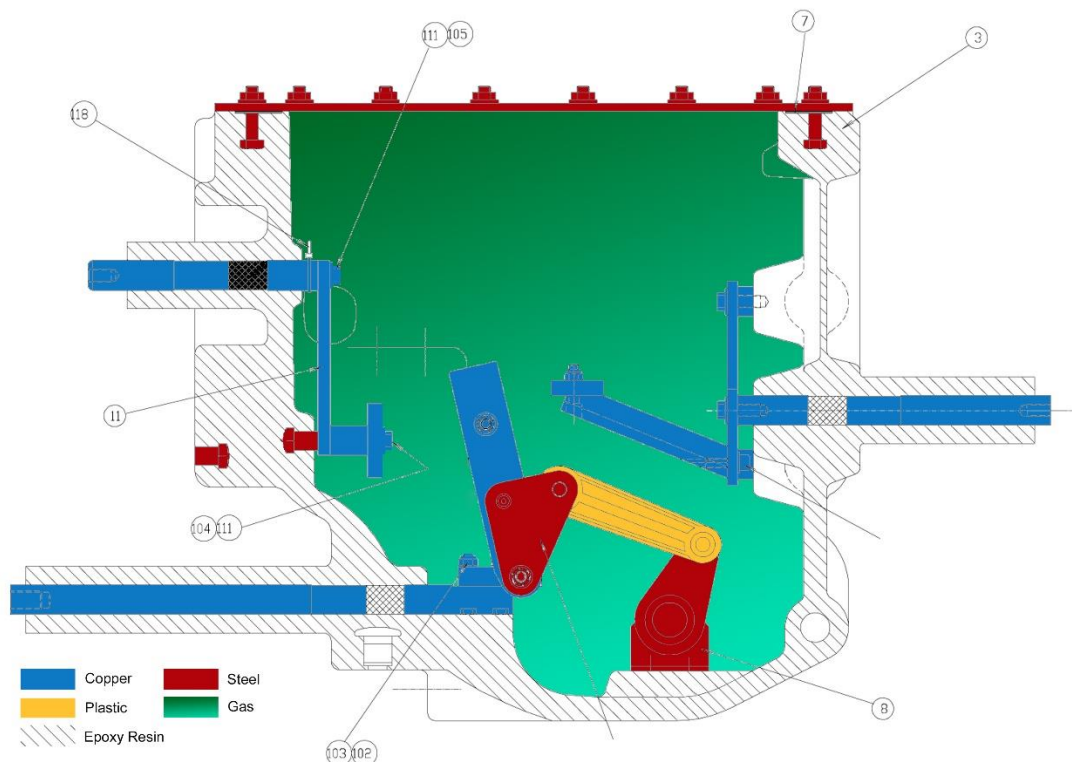


Figure 6.3: Materials used to manufacture the Ringmaster switch disconnector [82].

Table 6.1: Relative permittivity ( $\epsilon$ ) of each material modelled from COMSOL.

Material	Relative permittivity
Copper	1
Steel	1
Plastic (PTFE)	2.1
Epoxy Resin (cast)	3.6

From the schematics in Figure 6.1, a 3D Comsol multiphysics model shown in Figure 6.4 was developed including the 3 phase contacts for the load switch and epoxy resin gas chamber. The simulation process is further explained in Appendix D.

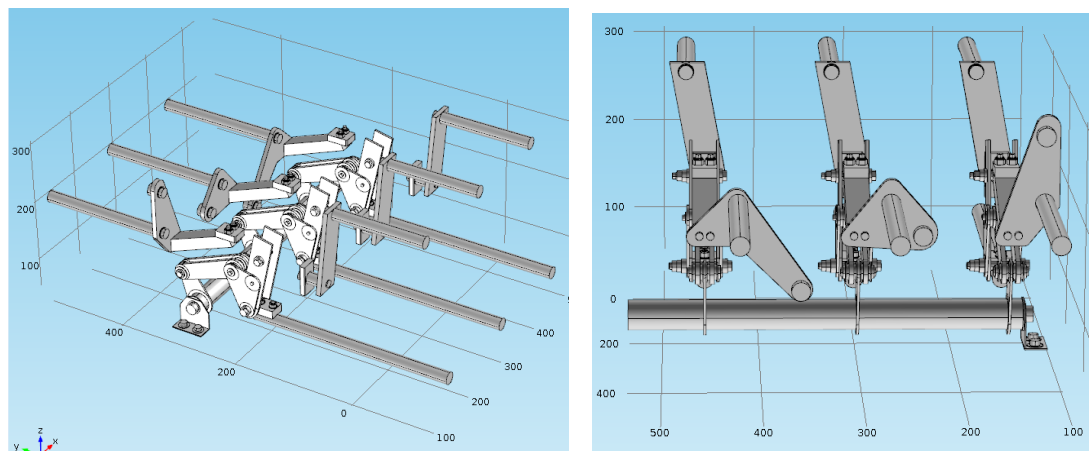


Figure 6.4: Ringmaster full contact simulation model.

The COMSOL model included using the Electrostatics module to simulate the applied voltages and charges on the contacts as shown in Figure 6.5. In Figure 6.5 (b), the floating potential shown is connected directly to the grounded point shown in Figure 6.5 (c). This means that, because the contact is modelled using copper, the whole contact is effectively earthed.

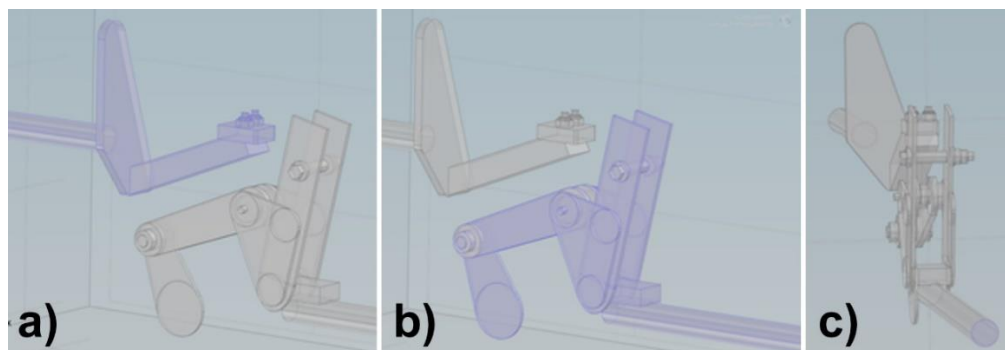


Figure 6.5: Electrostatic model elements – a) 95 kV applied terminal, b) floating potential and c) grounding point.

Figure 6.6 shows the mesh adopted for the model. The free triangular mesh was specified as a fine size and had a larger amount of elements at the corners and edges of the contacts so as to be able to calculate more accurate results at these points.

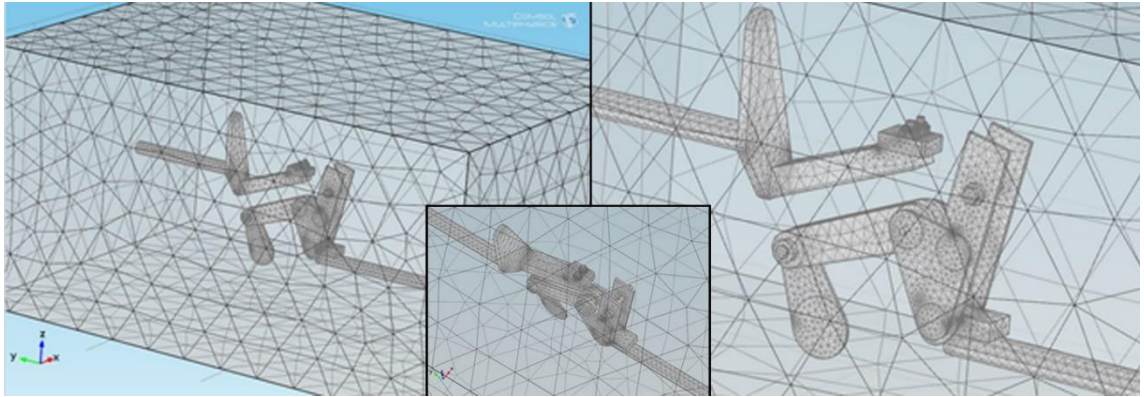


Figure 6.6: Ringmaster Comsol model mesh.

Figure 6.7 shows the computed equipotentials when a voltage of 95 kV was applied to one contact. From this distribution, the areas that are subjected to the highest electric field are seen to be closer to the contacts metal edges where the equipotentials changes fastest.

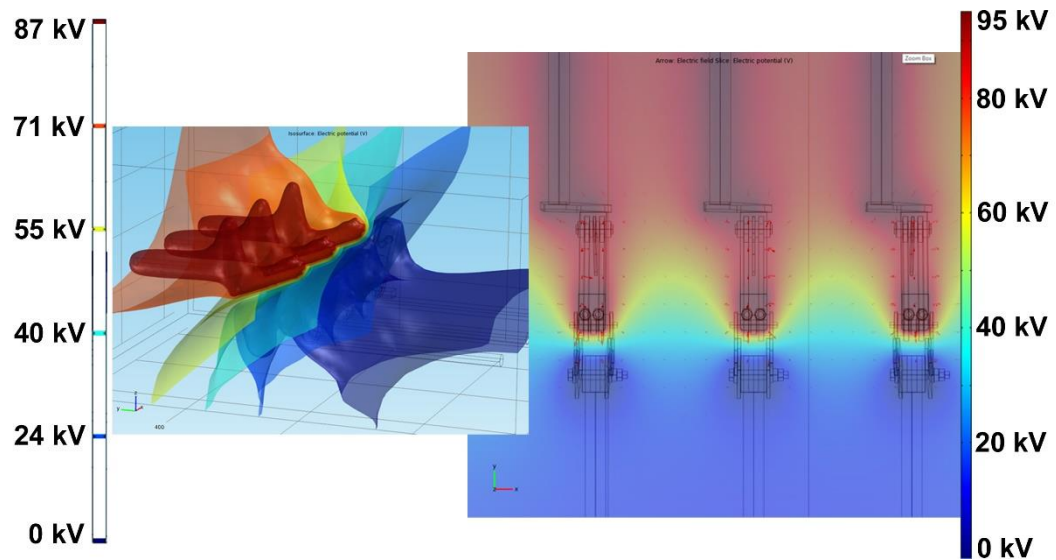


Figure 6.7: Computed equipotentials for the Ringmaster.

The same schematic diagrams (Figure 6.1) used for the 3D representation of the Ringmaster switch disconnecter were also used for the 2D model. This 2d model uses xy geometry so that only the gas box surrounding the contacts is simulated. The contacts themselves are removed from the gas box and its space left as a void so that only the gas

insulation is simulated around the edges of the contacts geometry. The 2d slice shown in Figure 6.8 (a) represents the weakest point of the Ringmaster design i.e. the outside of the 95 kV terminal and the inside of one of the grounded contacts. In Figure 6.8 (b), the applied voltage is 95 kV on the left contact and, in Figure 6.8 (c), a grounded terminal is used on the right side. The mesh is modelled so that its free triangular design is finer between the contacts (Figure 6.9).

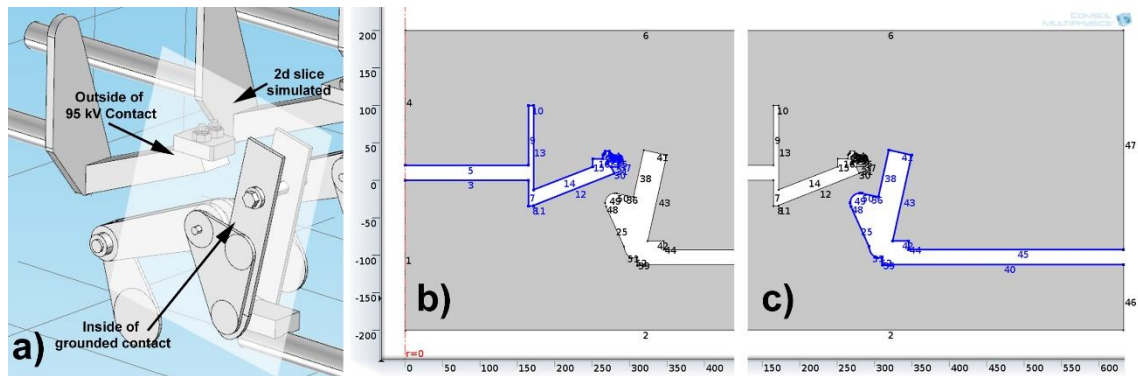


Figure 6.8: a) 2d Ringmaster slice model, b) applied electrostatic conditions – 95 kV electric potential and c) grounded terminal.

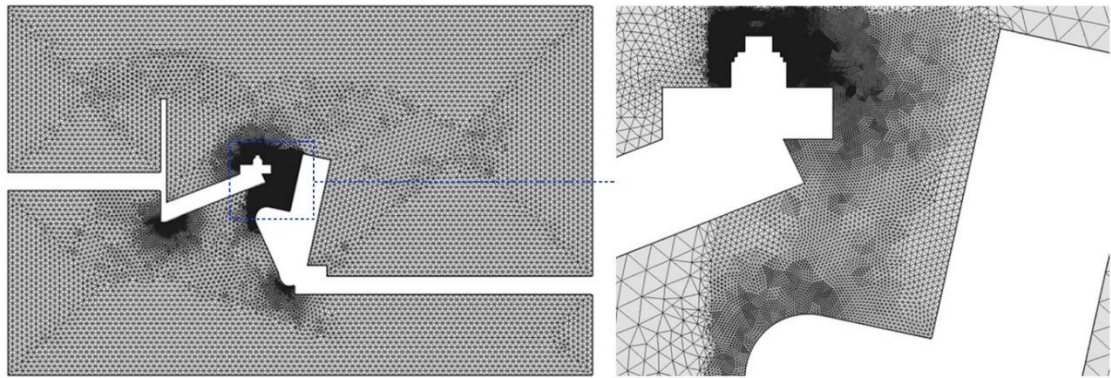


Figure 6.9: 2d Ringmaster Comsol model mesh size.

Figure 6.10 shows the computer equipotentials and the electric field lines for the model. The electric field magnitudes obtained from this computation were used in Section 6.4 to evaluate risk of flashover across these contacts.

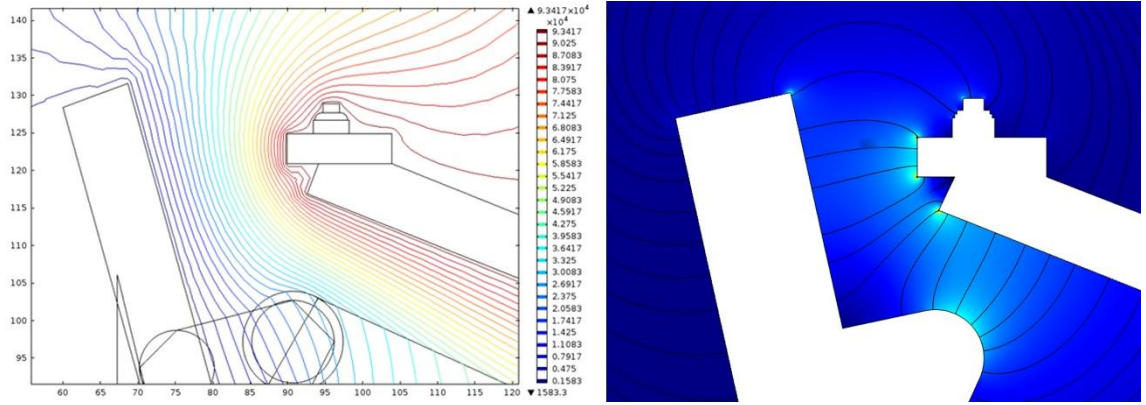


Figure 6.10: Computed 2d Ringmaster equipotentials and electric field lines.

As can be seen, the highest areas of electric stress are located around the sharp points of the HV electrode as shown in Figure 6.11 by the red areas.

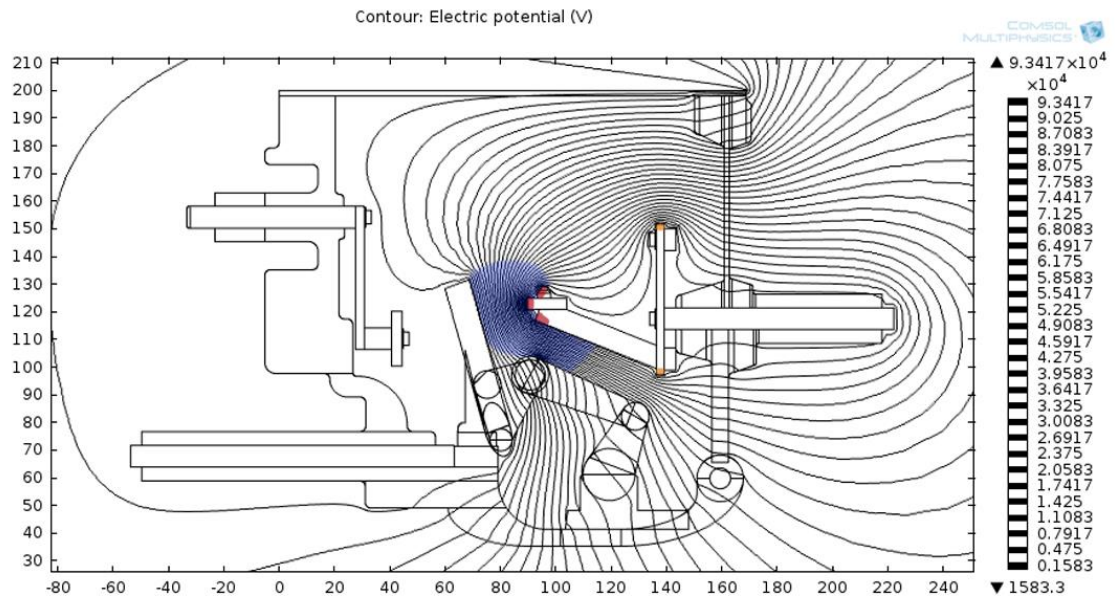


Figure 6.11: Ringmaster SE6 switch disconnector high electrical stress points.

### 6.3 Effective ionisation coefficients

Ideally, the next step would be to translate the electric field calculations into a clear answer as to whether a discharge or flashover will occur across the gas gap in the switchgear. However, this is not a straightforward process. The effective ionization ( $\alpha_{\text{eff}}$ ) plays an important role in the development of discharges as it quantifies the rate of net production of free electrons in the gas [83].

$$\text{Effective Ionization } (\alpha_{eff}) = \text{Ionization rate} - (\text{Recombination and Attachment rates}) \quad (6.1)$$

The following section develops and explores the effective ionisation coefficients previously discussed in Section 2.4.2. The net (pressure-reduced) ionisation coefficient  $(\alpha - \eta) / p$  as a function of  $E / p$  for air and SF<sub>6</sub> is shown in Figure 6.12. The critical reduced field strength at which  $(\alpha - \eta) = 0$  is about 89 kV/cm bar in SF<sub>6</sub> [11], compared with only about 27 kV/cm bar in air [11]. This explains the high dielectric strength of SF<sub>6</sub> relative to air which is roughly three times stronger. No build-up of ionisation can occur until the reduced field exceeds the critical value  $(E/p)_{crit}$  [11].

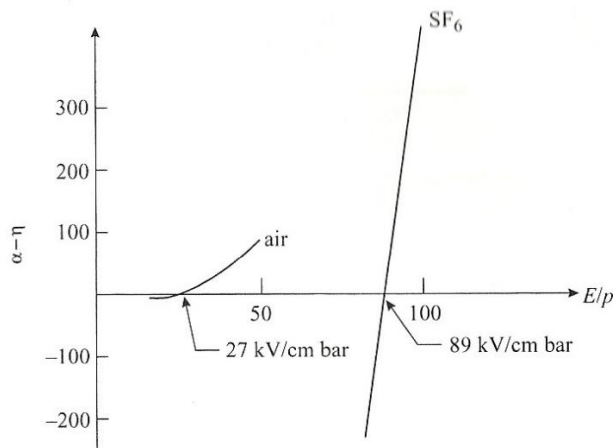


Figure 6.12: Effective ionisation coefficients in air and SF<sub>6</sub> [11].

It is worth noting the steep slope of the effective ionisation coefficient in SF<sub>6</sub>. “This means that SF<sub>6</sub> is a relatively brittle gas in that, once  $(E/p)_{crit}$  is exceeded, the growth of ionisation is very strong.” [11]

In situations where stress-raising defects have an effect on the electric field, in gas-insulated equipment, intense ionisation activity will occur in the regions where  $E/p > (E/p)_{crit}$ . This may initiate complete breakdown of the insulation [11].

It is, therefore, very useful to know the critical reduced field strength at which  $(\alpha - \eta) = 0$  as this will give an indication of areas where ionisation and the initiation of complete breakdown in gas insulated equipment may occur. It is apparent from the comparison drawn between air and  $\text{SF}_6$  that the critical reduced field strength of various  $\text{CF}_3\text{I}-\text{CO}_2$  gas mixtures will give an indication of which gas mixtures to use for insulating purposes in switchgear [11].

From the electron collisions cross section data of the  $\text{CF}_3\text{I}$  molecule [37] and  $\text{CO}_2$  molecule [84], the following effective ionisation coefficients were calculated. The calculations and analysis of the electron collisions cross section data was carried out using two-term approximation Boltzmann equation analysis [85] using the software BOLSIG+ [86].

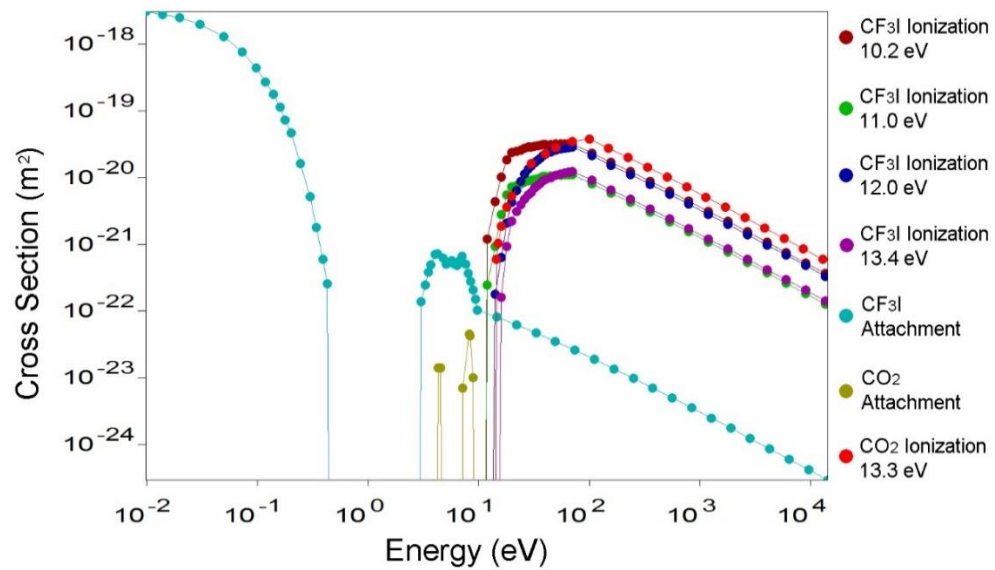


Figure 6.13: Electron collision cross section data used for BOLSIG+ calculations.

Using the electron collision cross section data in Figure 6.13, for  $\text{CF}_3\text{I}$  and  $\text{CO}_2$ , BOLSIG+ was used to calculate the transport coefficients, an example of which is shown in Table 6.2 and 6.3. The transport coefficients were calculated from the following equations and sources:

$$N = (N_A \times P) / R / T \text{ [31] [30]}, \quad (6.2)$$

Where: Gas constant (R) = 8.314472 [31], Pressure (P) = 101325 Pa = 1 atm,

T = temperature (Kelvin), N = number of moles of a gas,  $N_A$  = Avogadro Constant.

$N_A = 1 \times \text{Mol of atoms (of any element)} = 6.0221413 \times 10^{23} \text{ mol}^{-1}$  [30].

R# indicates the run number.

$$N = 6.0221413 \times 101325 / 8.314472 / (300) \times 10^{23} \text{ [m}^{-3}\text{]}.$$

Table 6.2: Transport coefficients.

m_e [kg]	9.11E-31 electron mass
1[eV] =	1.60E-19 [J]
N [m <sup>-3</sup> ]	2.45E+25: at 1bar, 300[K]

Table 6.3: An example of Townsend coefficients / N (m<sup>2</sup>) calculated using BOLSIG+ for the gas mixture 30% CF<sub>3</sub>I – 70% CO<sub>2</sub>.

R #	E/N (Td)	Energy (eV)	CF <sub>3</sub> I Ionization 10.20 eV	CF <sub>3</sub> I Ionization 11.00 eV	CF <sub>3</sub> I Ionization 12.00 eV	CF <sub>3</sub> I Ionization 13.40 eV	CF <sub>3</sub> I Attach ment	CO <sub>2</sub> Ionization 13.30 eV	CO <sub>2</sub> Attach ment
1	219.6	5.115	2.72E-21	6.56E-22	1.85E-22	6.20E-23	4.79E-21	3.21E-22	3.82E-23
2	226.4	5.189	2.94E-21	7.15E-22	2.07E-22	7.07E-23	4.65E-21	3.57E-22	3.78E-23
3	233.3	5.264	3.18E-21	7.78E-22	2.32E-22	8.04E-23	4.52E-21	3.96E-22	3.75E-23
4	240.5	5.34	3.42E-21	8.45E-22	2.58E-22	9.12E-23	4.39E-21	4.38E-22	3.71E-23
5	247.9	5.417	3.68E-21	9.16E-22	2.87E-22	1.03E-22	4.26E-21	4.84E-22	3.67E-23

The full data set of 30%:70% CF<sub>3</sub>I-CO<sub>2</sub> was plotted from the BOLSIG+ calculated Townsend coefficients / N (m<sup>2</sup>) as shown in Figure 6.14.

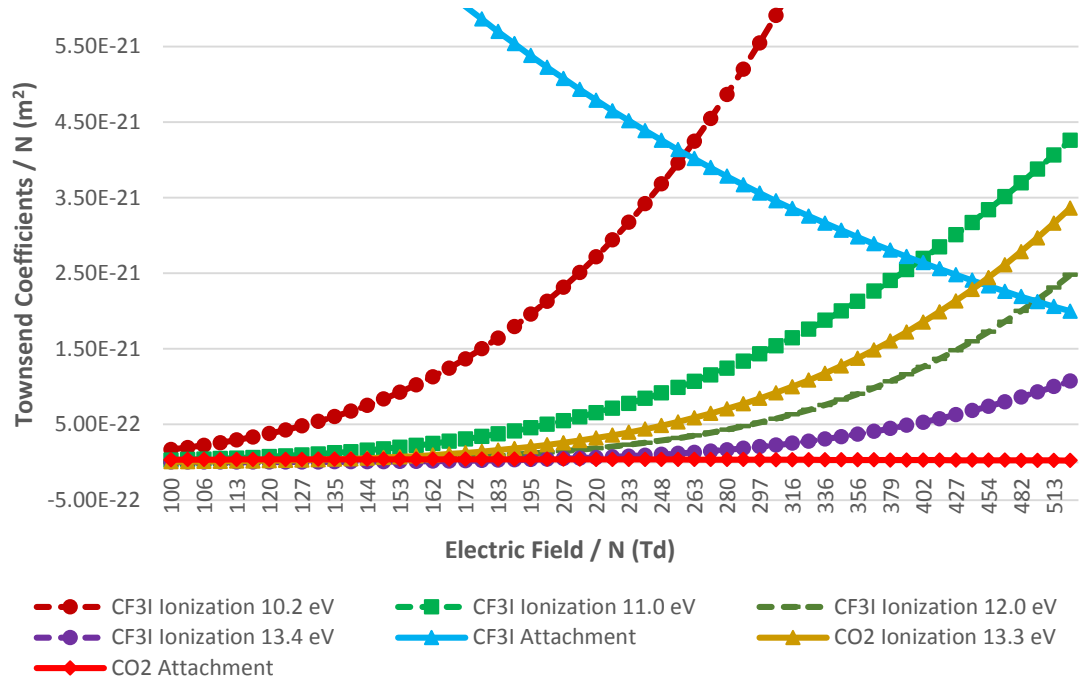


Figure 6.14: 30%:70% CF<sub>3</sub>I-CO<sub>2</sub> Townsend coefficients.

From the Townsend coefficients / N (m<sup>2</sup>), calculated using BOLSIG+ software, the electric field (kV/cm), the ionization rate ( $\alpha$  alpha), the attachment rate ( $\eta$  eta) and from these the effective ionization ( $\alpha_{eff}$  alpha effective) can be calculated as follows:

$$\begin{aligned} \text{Effective Ionization } (\alpha_{eff} \text{ Alpha Effective}) &= \text{Ionization rate } (\alpha \text{ alpha}) - \\ &\quad \text{Attachment rates } (\eta \text{ eta}) \text{ [11]} \\ \text{Alpha Effective [cm]} &= ((\text{Alpha}/N \text{ [m}^2] - \text{Eta}/N \text{ [m}^2]) \times 2.45\text{E}+25 \text{ (N) [m}^{-3}]) / 100 \quad (6.3) \end{aligned}$$

$$\begin{aligned} \text{Ionization rate } (\alpha \text{ alpha}) &= \text{Sum Total of all Ionization } (\alpha \text{ alpha}) \\ &= (0.7 \times \text{Total CO}_2 \text{ Ionization}) + (0.3 \times \text{Total CF}_3\text{I Ionization}) \\ \text{Alpha}/N \text{ [m}^2] &= (0.7 \times \text{CO}_2 \text{ Ionization 13.3 eV}) \\ &\quad + (0.3 \times (\text{CF}_3\text{I Ionization 10.2 eV} + 11 \text{ eV} + 12 \text{ eV} + 13.4 \text{ eV})) \text{ (for each run)} \quad (6.4) \end{aligned}$$

$$\begin{aligned} \text{Attachment rate } (\eta \text{ eta}) &= \text{Sum Total of all Attachment } (\eta \text{ eta}) \\ &= (0.7 \times \text{Total CO}_2 \text{ Attachment}) + (0.3 \times \text{Total CF}_3\text{I Attachment}) \\ \text{Eta}/N \text{ [m}^2] &= (0.7 \times \text{CO}_2 \text{ Attachment}) + (0.3 \times \text{CF}_3\text{I Attachment}) \text{ (for each run)} \quad (6.5) \end{aligned}$$

$$E/N \text{ [Vm}^2] = E/N \text{ [Td]} \times 1\text{E}-21 \quad (6.6)$$

$$E \text{ [V/m]} = E/N \text{ [Td]} \times 1\text{E}-21 \times 2.45\text{E}+25 \text{ (N m}^{-3}) \quad (6.7)$$

$$E \text{ [kV/cm bar]} = (E/N \text{ [Td]} \times 1\text{E}-21 \times 2.45\text{E}+25) / 1\text{E}+5 \quad (6.8)$$

From the calculated electric field, ionization rate, attachment rate and effective ionization, the full results for the example shown in Table 6.4 and 6.5 (30:70% CF<sub>3</sub>I-CO<sub>2</sub>) is shown in Figure 6.15. Note that the effective ionization is the ionization rate – attachment rate. Therefore, when these are equal i.e.  $(\alpha - \eta) = 0$ , this indicates the critical reduced field strength.

Using the same method as shown for 30%:70% CF<sub>3</sub>I-CO<sub>2</sub>, the effective ionisation for each gas mixture can be calculated as shown (Figure 6.16). The effective ionisation coefficient is determined from the linear relationship [11]:

$$\frac{\alpha - \eta}{p} = A \left( \frac{E}{p} \right) - B \quad (6.9)$$

Table 6.4: Calculated electric field (V/m), ionization rate / N (m<sup>2</sup>), attachment rate / N (m<sup>2</sup>) and effective ionization (/m).

R#	E/N [Td]	E/N [Vm <sup>2</sup> ]	E [V/m]	alpha/N [m <sup>2</sup> ]	eta/N [m <sup>2</sup> ]	Alpha effective [/m]
1	219.6	2.196E-19	5.37E+06	1.31139E-21	1.46E-21	-3.73E+03
2	226.4	2.264E-19	5.54E+06	1.42983E-21	1.42E-21	1.90E+02
3	233.3	2.333E-19	5.71E+06	1.55648E-21	1.38E-21	4.27E+03
4	240.5	2.405E-19	5.88E+06	1.69148E-21	1.34E-21	8.53E+03
5	247.9	2.479E-19	6.06E+06	1.83556E-21	1.30E-21	1.30E+04

Table 6.5: Calculated electric field (kV/cm) and effective ionization (/cm).

R#	E [kV/cm]	Alpha effective [/cm]
1	53.72098409	-3.73E+01
2	55.3844754	1.90E+00
3	57.07242982	4.27E+01
4	58.83377356	8.53E+01
5	60.64404351	1.30E+02

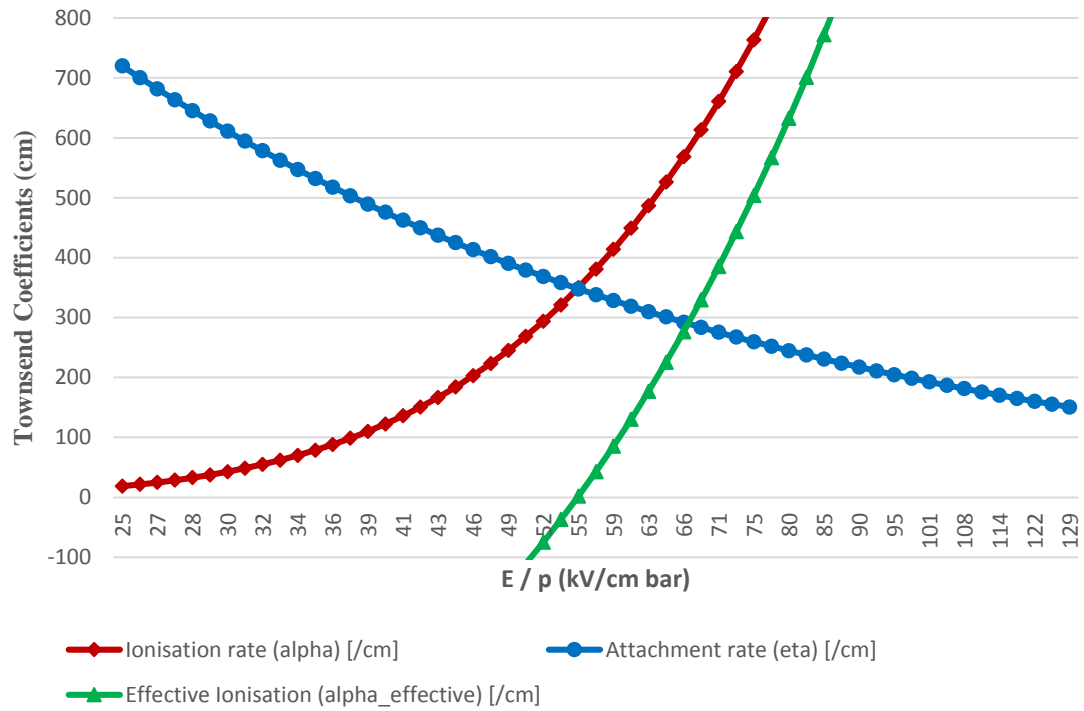


Figure 6.15: 30%:70% CF<sub>3</sub>I-CO<sub>2</sub> ionization rate, attachment rate and effective ionisation.

For SF<sub>6</sub>, A = 27.7 kV<sup>-1</sup> and B = 2460 bar<sup>-1</sup> cm<sup>-1</sup> [11], and the critical reduced field strength is estimated using [11]:

$$\left(\frac{E}{p}\right)_{crit} = \frac{Bp}{A} = 88.8 \text{ kV/cm bar} \quad (6.10)$$

This simple relationship is used to estimate critical field strengths in SF<sub>6</sub> as well as in the other gas mixtures. Calculated effective ionisation coefficients have been plotted and appropriate linear relationships shown for each gas mixture. The effective ionisation coefficients for air [83] and CO<sub>2</sub> are represented slightly differently because they are not as brittle gases as SF<sub>6</sub>. It is important to note that pure CF<sub>3</sub>I is just as brittle as SF<sub>6</sub> and the critical reduced field strength for each gas mixture increases as more CF<sub>3</sub>I is added. The calculations suggest that pure CF<sub>3</sub>I has a critical reduced field strength of 109 kV/cm bar, this is consistent with other results [45] which suggest that pure CF<sub>3</sub>I has a dielectric strength approximately 1.2 times that of SF<sub>6</sub>.

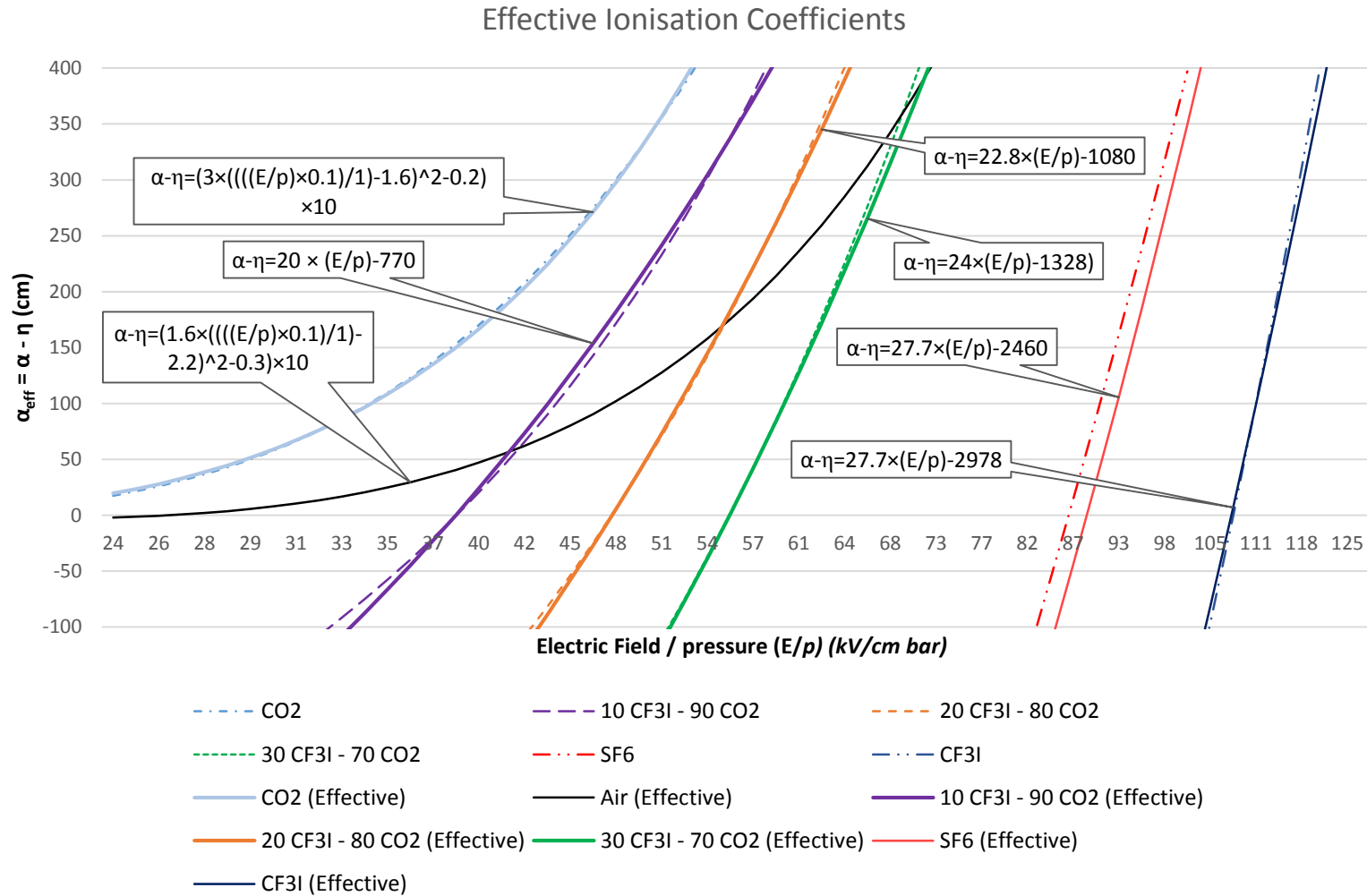


Figure 6.16: Effective ionisation for Air, CO<sub>2</sub>, CF<sub>3</sub>I, SF<sub>6</sub>, 10%:90% CF<sub>3</sub>I-CO<sub>2</sub>, 20%:80% CF<sub>3</sub>I-CO<sub>2</sub> and 30%:70% CF<sub>3</sub>I-CO<sub>2</sub>.

#### 6.4 Evaluation of flashover occurrences

The ionization rate and, therefore, the effective ionization are dependent on the electric field (E) which varies depending on the insulating gas used between the contacts.

For a discharge to occur, there must be free electrons in the gas to enable this process. Therefore,  $\alpha_{\text{eff}} > 0$  [11]. For a detectable discharge to occur, an electron avalanche must be formed i.e. “primary electrons accelerated in the electric field cause further ionization at an increasing rate” [83].

“A self-sustained discharge, independent of charge injection from the electrodes, will form provided the total number of electrons becomes larger than some critical number” [83] [11]. If an avalanche is extended along an electric field line, then the condition for a self-sustained avalanche is [83]:

$$S = \int \alpha_{\text{eff}}(E) dl > C_{\text{crit}} \quad (6.11)$$

Where the integral is performed along the field line under consideration and only where  $\alpha_{\text{eff}} > 0$ . Equation (6.11) is known as the streamer inception criterion [87] [88]. “The critical number,  $C_{\text{crit}}$ , for air is usually taken to be in the range 15 – 20” [83]. For the following simulations, 18.4 is used as the critical number for air, this is  $\approx 70\%$  of the critical reduced electric field strength. If the streamer inception criterion is met, it guarantees the formation of a stationary streamer (or corona) discharge extending from the electrode, usually from a sharp point where  $\alpha_{\text{eff}}(E)$  has a maximum, out to a surface where  $\alpha_{\text{eff}}(E) = 0$  (the electrode opposite).

If “ $\alpha_{\text{eff}}(E) > 0$  along the entire field line, from the high voltage to the grounded electrode, the fulfilment of the streamer inception criterion will lead to an immediate breakdown across the gap” [83]. If “ $\alpha_{\text{eff}}(E) < 0$  along part of the field line, there is still a chance for a complete flashover” [83].

A complete flashover may occur if the electric field just in front of the streamer head is so high that “the associated field ionization effectively moves the streamer head forward” [83]. This process is called streamer propagation. Streamer propagation can take place provided the average field,  $E$ , along the field line satisfies [83]:

$$E = \frac{U}{L} > \frac{U_0}{L} + E_0 \quad (6.12)$$

$U$  is the voltage difference between the electrodes

$L = \int dl$  is the length of the field line

$U_0 \approx 10\text{-}30$  kV as an empirical constant

$E_0 \approx 0.5$  kV/mm for a discharge starting from the positive electrode

$E_0 \approx 1.2$  kV/mm for a discharge starting from the negative electrode [83]

The effective ionization function is calculated depending on the insulation gas which has been previously evaluated for  $\text{SF}_6$  and air, and were calculated using Bolsig+ for  $\text{CF}_3\text{I}$  and  $\text{CF}_3\text{I-CO}_2$  gas mixtures.

The effective ionization function of air can be represented by the quadratic equation [83]:

$$\alpha_{\text{eff}}(E) = p \left[ 1.6 \left( \frac{E \times 0.1}{p} - 2.2 \right)^2 - 0.3 \right] \times 10 \quad (6.13)$$

Where:  $p$  = the pressure given in bar

This gives  $\alpha_{\text{eff}}(E) > 0$  for  $E > 2.6$  kV/mm. Therefore, the critical field strength of air is 26 kV/cm which is needed for a net production of charge carriers to occur [11].

The effective ionization function of  $\text{CO}_2$  can be represented as:

$$\alpha_{\text{eff}}(E) = \left[ 3 \left( \frac{E \times 0.1}{p} - 1.6 \right)^2 - 0.2 \right] \times 10 \quad (6.14)$$

The general formula for the effective ionization function of  $\text{SF}_6$ ,  $\text{CF}_3\text{I}$  or  $\text{CF}_3\text{I-CO}_2$  gas mixtures can be represented as [11]:

$$\alpha_{\text{eff}}(E) = p \left[ A \left( \frac{E}{p} \right) - B \right] \quad (6.15)$$

The critical reduced electric field strength can be approximated using [11]:

$$\left( \frac{E}{p} \right)_{\text{crit}} \approx \frac{B p}{A} \quad (6.16)$$

Table 6.6: Effective ionization functions and critical field strengths for SF<sub>6</sub>, CF<sub>3</sub>I and CF<sub>3</sub>I-CO<sub>2</sub> gas mixtures.

Gas mixture	A	B	$\left( \frac{E}{p} \right)_{\text{crit}}$
100% CF <sub>3</sub> I	27.7	2978	109 kV/cm bar
100% SF <sub>6</sub>	27.7 [11]	2460 [11]	88.8 kV/cm bar [11]
30:70 CF <sub>3</sub> I-CO <sub>2</sub>	24	1328	55.3 kV/cm bar
20:80 CF <sub>3</sub> I-CO <sub>2</sub>	22.8	1080	47.4 kV/cm bar
10:90 CF <sub>3</sub> I-CO <sub>2</sub>	20	770	38.5 kV/cm bar

Table 6.7: Critical reduced electric field strength and critical number of all gas mixtures [11].

Gas simulated	Critical reduced electric field strength $\left( \frac{E}{p} \right)_{\text{crit}}$	Critical number $C_{\text{crit}}$
CF <sub>3</sub> I	109 kV/cm	77.14
SF <sub>6</sub>	88.8 kV/cm	62.84
30:70% CF <sub>3</sub> I-CO <sub>2</sub>	55.3 kV/cm	39.14
20:80% CF <sub>3</sub> I-CO <sub>2</sub>	47.4 kV/cm	33.55
10:90% CF <sub>3</sub> I-CO <sub>2</sub>	38.5 kV/cm	27.25
Air	26 kV/cm	18.4

The simulations carried out in Comsol use the results of the electric field plots, calculated previously, and input them into the charged particle tracing module. In the charged particle tracing module, it is possible to use electric field lines as the trajectories of massless charged particles. Using Equation (6.15) and the effective ionisation coefficients (Table 6.6), the amount of free electrons along the electric field lines were calculated between the switchgear's contacts and define the likelihood of a flashover occurring across the contacts [83].

For the following simulations, the same model used as a 2d representation of the Ringmaster switch disconnecter is manipulated. However, the charged particle tracing module is added as a separate time-dependent study to run after the electrostatics module has finished calculating the electric field plots. In a charged particle tracing simulation, it is important to define the inlet from which the particles originate (the positive 95 kV electrode) and the wall at which the particles are to remain until the simulation concludes (all other boundaries) as shown in Figure 6.17.

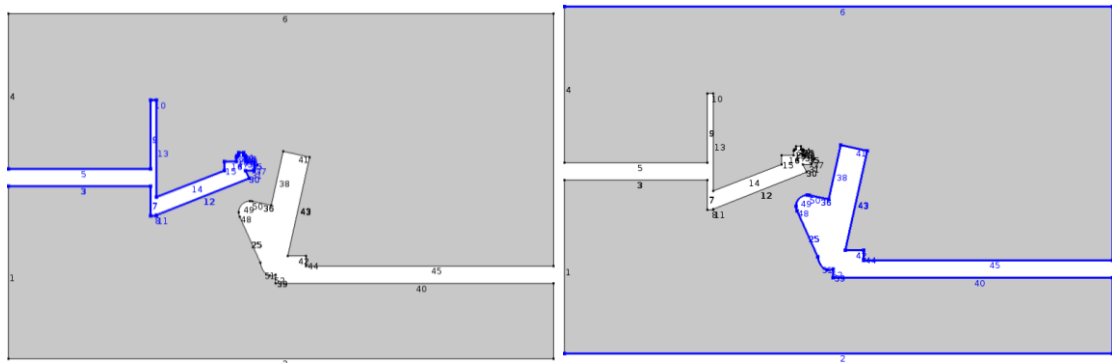


Figure 6.17: Ringmaster charged particle tracing simulation inlet (left) and wall (right) boundary conditions.

In the following sections (6.4.1, 6.4.2, 6.4.3 and 6.4.4), this 2d model (Figure 6.17) is used to predict the probability of a flashover occurring across the gas gap in the Ringmaster switch disconnecter.

#### 6.4.1 Ringmaster Comsol simulation - air – 0 bar (g)

For the following simulations, the Ringmaster 2d Comsol model (Figure 6.17) has been used to model the outcome of filling the switch disconnecter with air at atmospheric pressure or 0 bar (g).

The electric field simulations suggest that the regions around the sharp points of the high voltage electrode are the weakest points of the design (Figure 6.18 and 6.19). For one of the simulations, 95 kV is applied to the electrode (shown on the left) (Figure 6.18) whereas in the other simulation, 75 kV is applied (Figure 6.19). As would be expected,

the simulation with a 95 kV applied voltage has a higher predicted peak electric field than the simulation with 75 kV applied. Figures 6.18 and 6.19 also show the region in which the electric field is greater than 26 kV/cm bar, at atmospheric pressure this is the region in which there is a positive net production of free electrons for air.

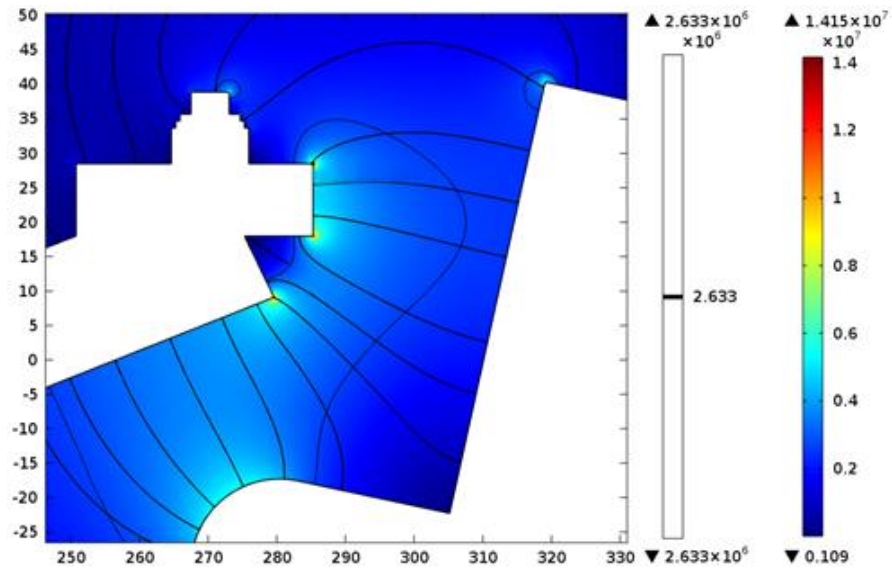


Figure 6.18: Electric field lines between high voltage contact (95 kV) and grounded contact and bounded region where the electric field is  $> 26$  kV/cm bar for air.

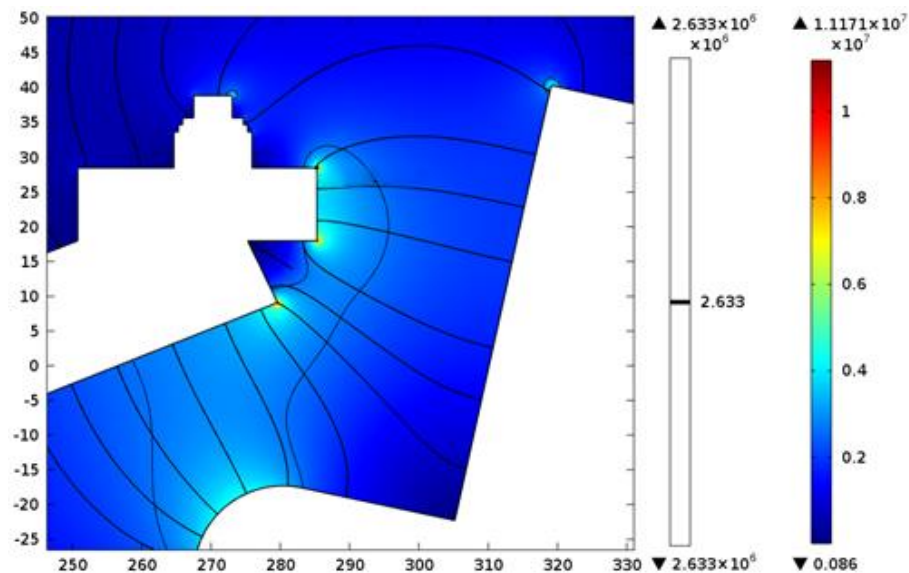


Figure 6.19: Electric field lines between high voltage contact (75 kV) and grounded contact and bounded region where the electric field is  $> 26$  kV/cm bar for air.

In the next set of figures (Figures 6.20 and 6.21), the bounded region shown indicates the area where the electric field is greater than the critical reduced electric field strength for air at atmospheric pressure i.e.  $> 26$  kV/cm bar. This region, which has a positive net

electron production, indicates the area where self-sustained discharges may occur. If this region expands far enough into the gas region to touch the grounded electrode, there is a high probability that flashovers will occur (Figure 6.20). For air, when 95 kV is applied (Figure 6.21), the simulation predicts a high probability of flashover between the contacts. When 75 kV is applied (Figure 6.21), the simulation shows the likelihood of a flashover is nowhere near as high. This is because the positive net electron production region does not touch the grounded electrode in the 75 kV simulation as it does with the 95kV simulation.

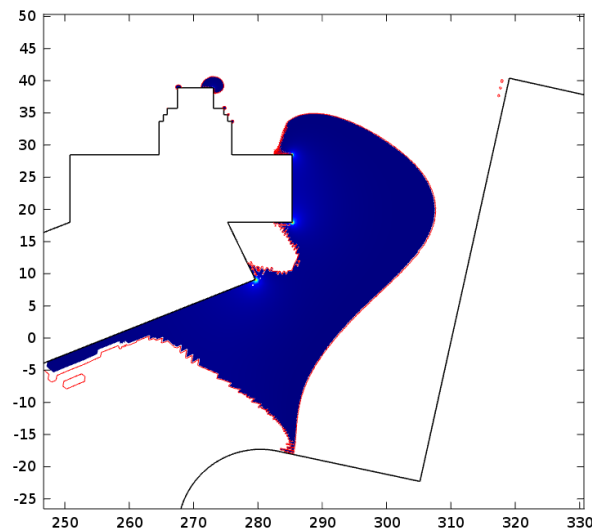


Figure 6.20: Region which has a positive net electron production (ionisation coefficient  $> 0$ ) close to the positive contact (95 kV) for air at atmospheric pressure.

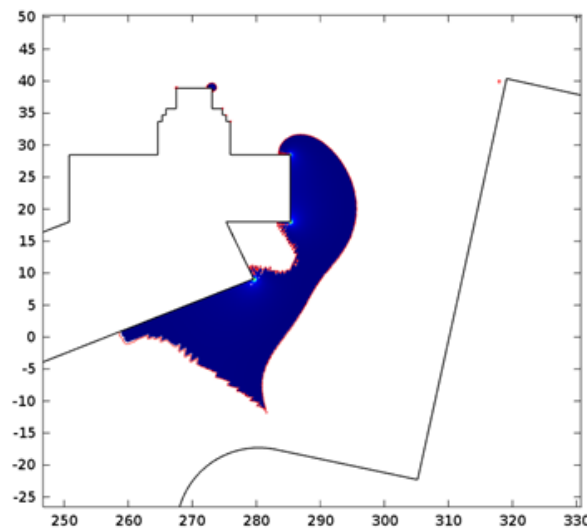


Figure 6.21: Region which has a positive net electron production (ionisation coefficient  $> 0$ ) close to the positive contact (75 kV) for air at atmospheric pressure.

The final stage of the simulation process predicts areas where streamer propagation may occur outside the region of positive net electron production and plots the probability of a discharge occurring along the previously generated electric field lines (Figure 6.18 and 6.19). The simulations indicate that when 95 kV is applied to the contact, the probability of a flashover occurring from the sharp points is high (Figure 6.22). It is also interesting to note that the probability of a flashover occurring between plane-plane contacts is always lower than with a point-plane contact geometry. With 75 kV the probability of a flashover occurring, in air at 0 bar (g), is nowhere near as high (Figure 6.23) as when 95 kV is applied. This probability of a flashover occurring is indicated by the colour scale to the immediate right of the plots; the higher the number is the higher the probability of a flashover occurring will be. The probability of a flashover occurring between the two contacts is more than double for 95 kV compared to 75 kV.

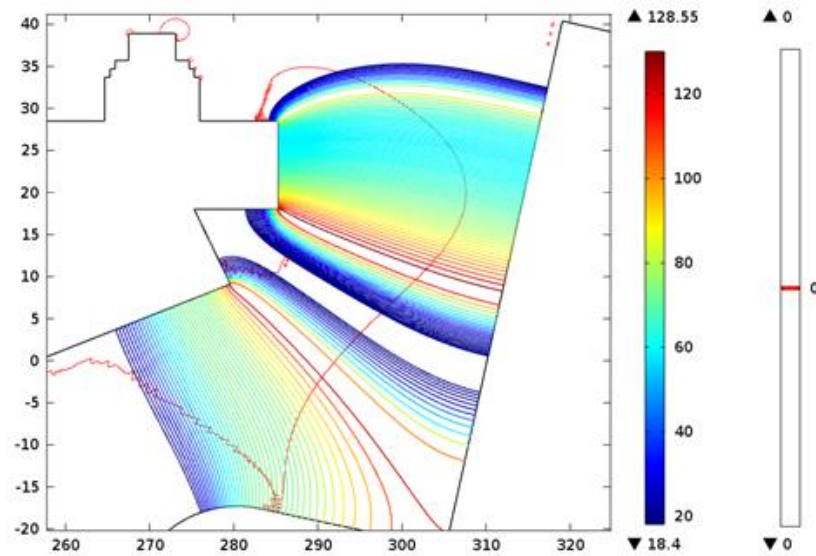


Figure 6.22: Field lines for discharges starting from the positive contact (95 kV) Air 0 bar (g).

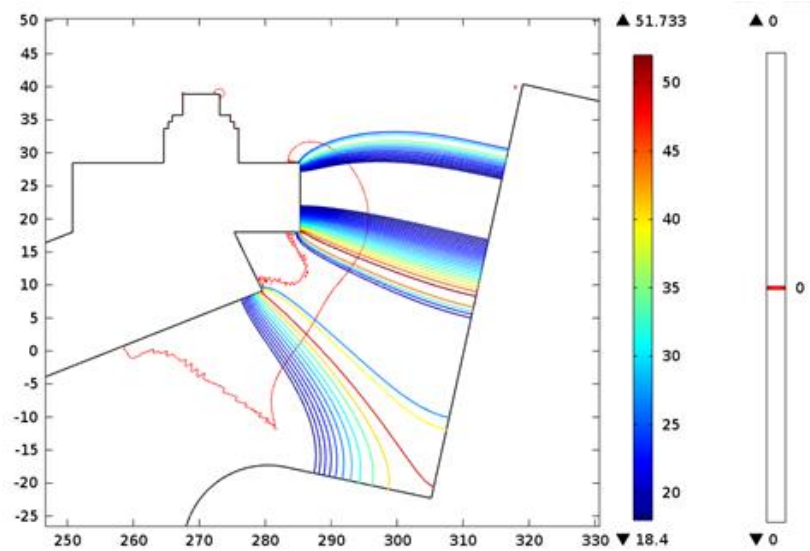


Figure 6.23: Field lines for discharges starting from the positive contact (75 kV) Air 0 bar (g).

The lightning impulse breakdown tests, reported in Chapter 5, indicate that air at 0 bar (g) has a 50% probability of flashover occurring at 85 kV and will not pass the withstand test at 95 kV. The simulation in Figure 6.22 supports this conclusion because it is predicted that when 95 kV is applied to the contact, air at atmospheric pressure, has a high chance of flashover occurring between the contacts and, therefore, it is likely to fail the withstand tests undertaken in Chapter 5. The simulation results in Figure 6.23 indicate that there is a low probability of a flashover occurring between the contacts when 75 kV is applied to the switch and, therefore, it is likely to pass the withstand tests undertaken in Chapter 5. Therefore, it can be predicted from the simulations results, shown in Figure 6.22 and 6.23, that the 50% probability of a flashover occurring will be between 75 kV and 95kV, this was shown to be 85 kV in the practical testing undertaken in Chapter 5.

#### 6.4.2 Ringmaster Comsol simulation - SF<sub>6</sub> - 0 bar (g)

To compare the results of various gases with SF<sub>6</sub>, the same 2d model is used to indicate flashovers occurring when the switch disconnecter is filled with SF<sub>6</sub> at a pressure of 0 bar (g). The simulations indicate that the electric field is the same as with air at 0 bar (g) when

95 kV is applied to one contact. However, the region which has a positive net electron production is very small (Figure 6.24). This region is primarily focused around the sharp points of the design. The simulation also predicts the probability of flashover occurring to be insignificantly small, compared to air at the same pressure. Therefore, it is expected that SF<sub>6</sub> will be capable of insulating this equipment at its rated minimum filling pressure. This also indicates that SF<sub>6</sub> should definitely be able to insulate the equipment when it is filled to its higher recommended filling pressure of 0.35 bar (g).

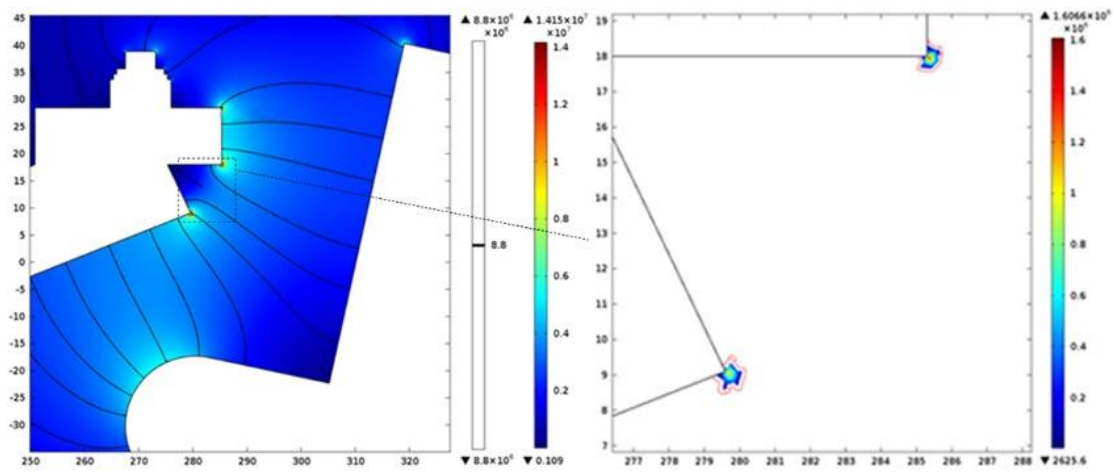


Figure 6.24: Electric field lines between high voltage contact (95 kV) and grounded contact and bounded region where the electric field is  $> 88$  kV/cm bar for SF<sub>6</sub>.

#### 6.4.3 Ringmaster net electron production region simulations

As with previous simulations (Figure 6.20 and 6.21), the method shown in section 6.4.1 was utilised to examine the results of replacing the SF<sub>6</sub> gas insulation in the switch disconnector with pure CF<sub>3</sub>I or mixtures of CF<sub>3</sub>I-CO<sub>2</sub>. The simulations show a bounded region where the electric field is greater than the critical reduced electric field strength, individual to each gas and gas mixture shown in Table 6.7. The simulations were carried out for all gas mixtures at pressures of both 0 bar (g) (the minimum operating pressure) shown in Figure 6.25 and 0.35 bar (g) (rated filling pressure) shown in Figure 6.26. A constant 95 kV was applied to one terminal. The results indicate that, for each gas

mixture, the net electron production region intensifies as the pressure is reduced (Figure 6.25 and 6.26).

The simulations (Figure 6.25 and 6.26) also show that the region where discharges are very likely to occur expand, depending on the gas. For pure  $\text{CF}_3\text{I}$  and  $\text{SF}_6$ , the region in which positive net electron production can occur is very small. As the content of  $\text{CF}_3\text{I}$  is reduced in a gas mixture of  $\text{CF}_3\text{I}-\text{CO}_2$ , the net electron production region increases as shown in Figure 6.27.

#### 6.4.4 Ringmaster discharge probability simulations

Using the electric field simulation (Figure 6.18) and the net electron production region simulations (Figure 6.25 and 6.26), the discharge probability for various gas mixtures can be simulated. The simulation results show that at 0 bar (g) all gas mixtures of  $\text{CF}_3\text{I}-\text{CO}_2$  could suffer flashover between the contacts in the switch disconnecter when 95 kV is applied (Figure 6.28 c, d and e). Reducing the amount of  $\text{CF}_3\text{I}$  in the  $\text{CF}_3\text{I}-\text{CO}_2$  gas mixture increases the probability of a flashover (Figure 6.28 b, c, d and e). At 0 bar (g), the simulations show that no flashovers will occur whilst the switch disconnecter is insulated with pure  $\text{SF}_6$  or  $\text{CF}_3\text{I}$  (Figure 6.28 a and b). When the pressure in the switch disconnecter is increased to 0.35 bar (g), the probability of a flashover occurring between the contacts is very low whilst the switch is filled with any of the  $\text{CF}_3\text{I}-\text{CO}_2$  gas mixtures (Figure 6.29 d, e and f). However, there is considerable partial discharge occurring around the contacts in the region where there is net positive electron production (Figure 6.29 d, e and f). At 0.35 bar (g), air is the only gas simulated that has any reasonable probability of a flashover occurring between the contacts (Figure 6.29 c). All of these simulated results are comparable with the practical withstand results of the Ringmaster switch disconnecter at 95 kV as previously examined in Chapter 5 (Figure 5.15).

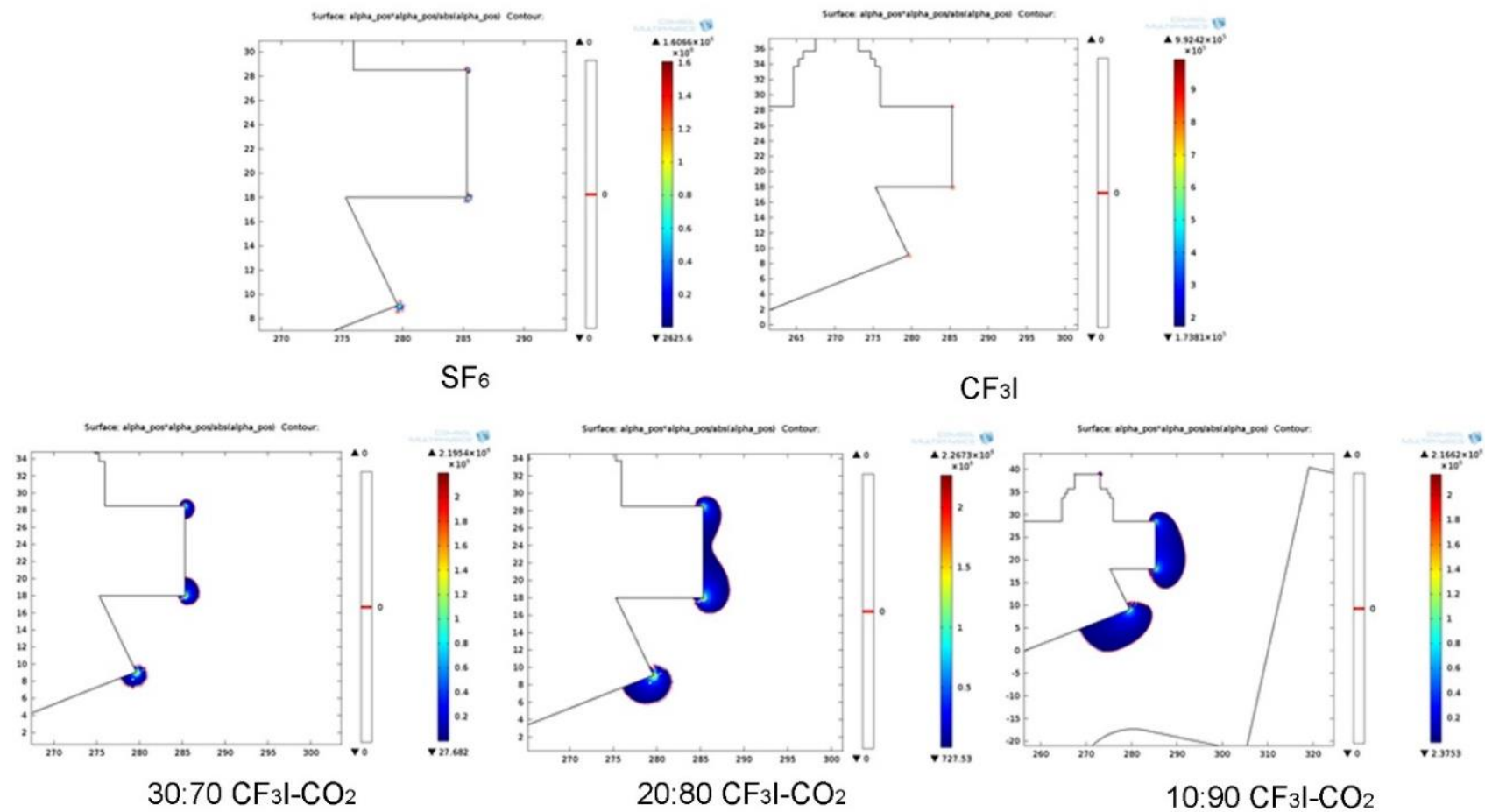


Figure 6.25: Region which has a positive net electron production (electric field > critical reduced electric field strength) close to the positive contact with an applied voltage of 95 kV at 0 bar (g).

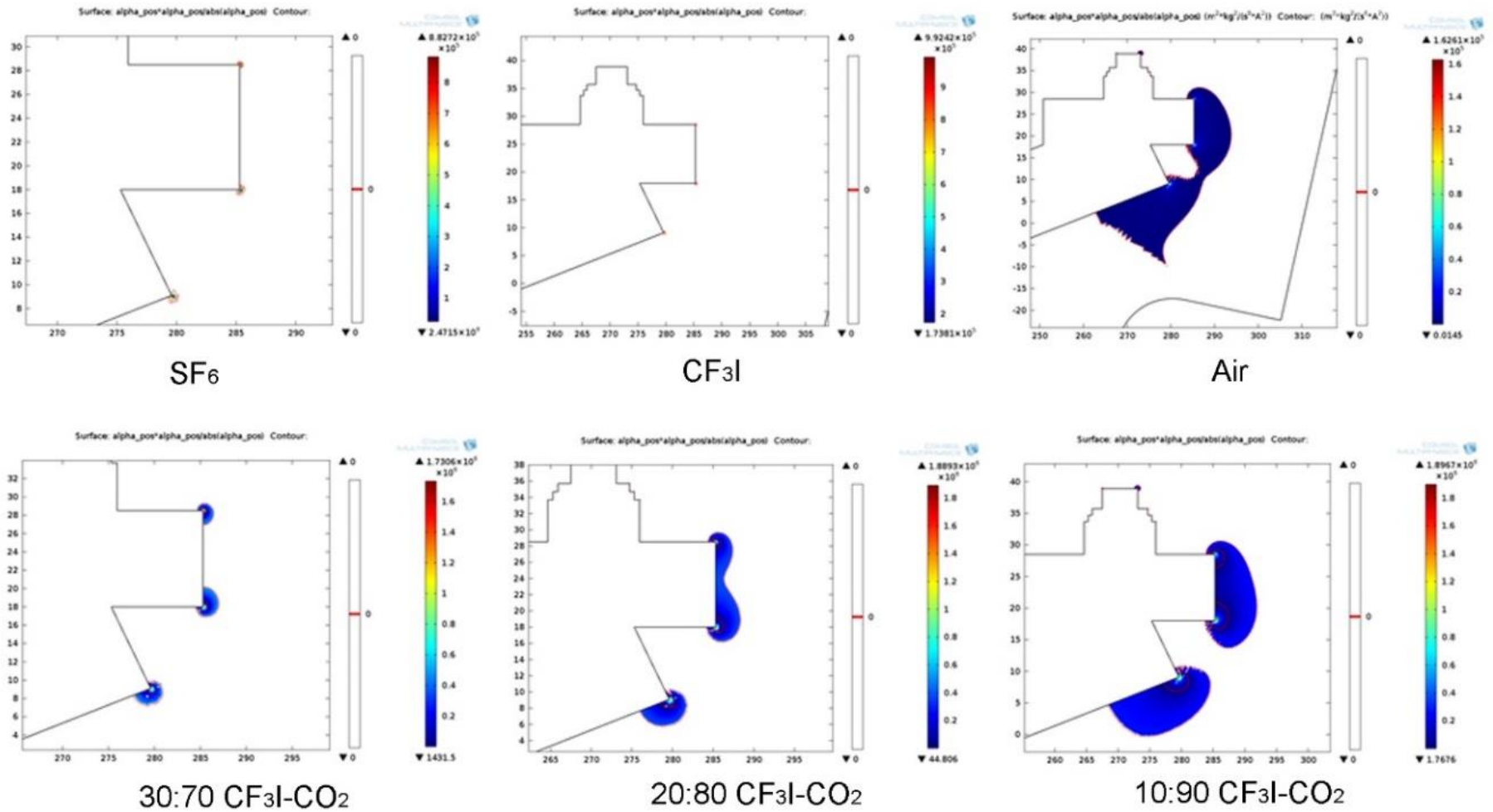


Figure 6.26: Region which has a positive net electron production (electric field > critical reduced electric field strength) close to the positive contact with an applied voltage of 95 kV at 0.35 bar (g).

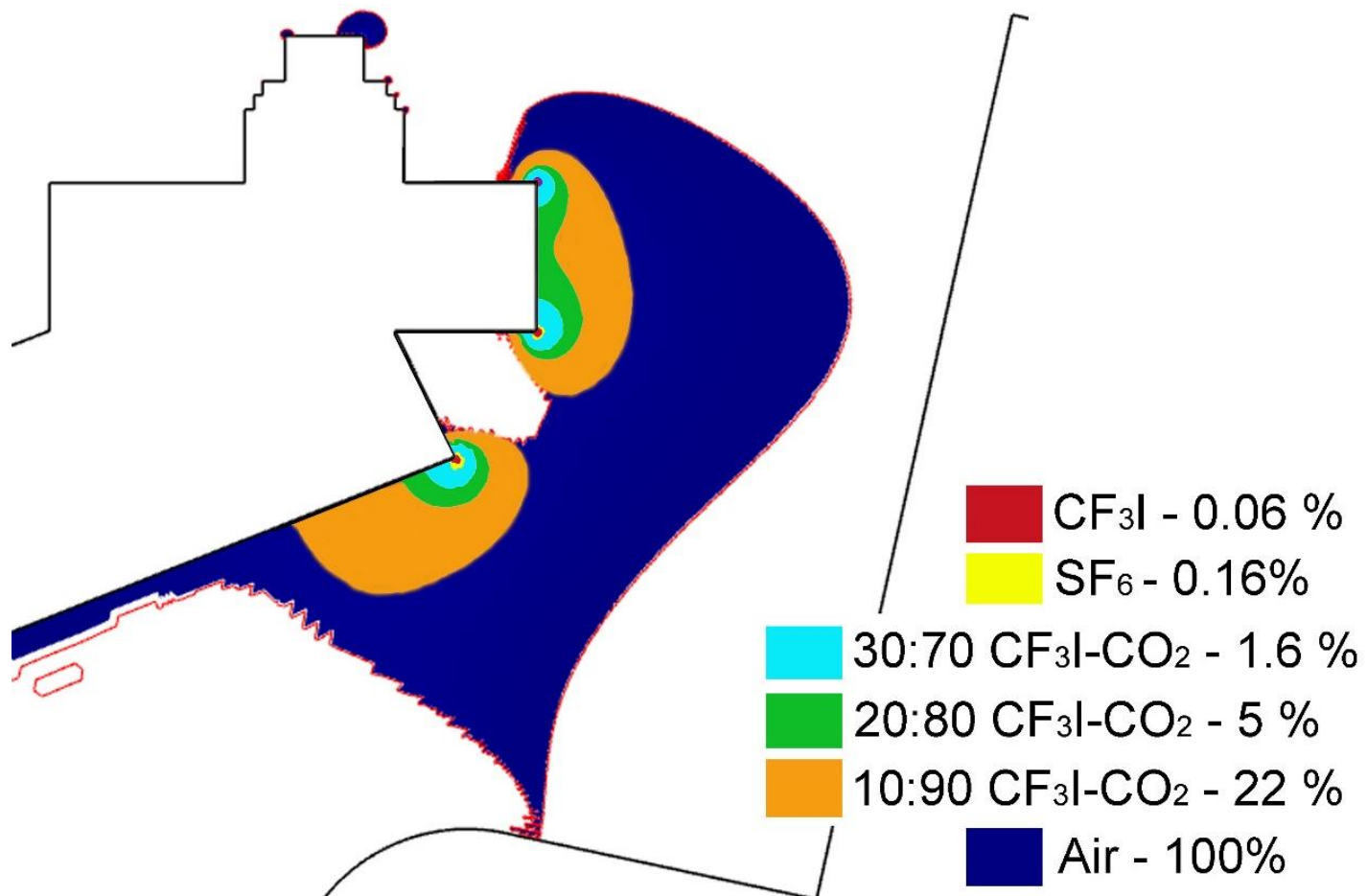


Figure 6.27: Expansion rate of the region which has a positive net electron production for Air, SF<sub>6</sub>, CF<sub>3</sub>I, 30:70% CF<sub>3</sub>I-CO<sub>2</sub>, 20:80% CF<sub>3</sub>I-CO<sub>2</sub> and 10:90% CF<sub>3</sub>I-CO<sub>2</sub> at 0 bar (g).

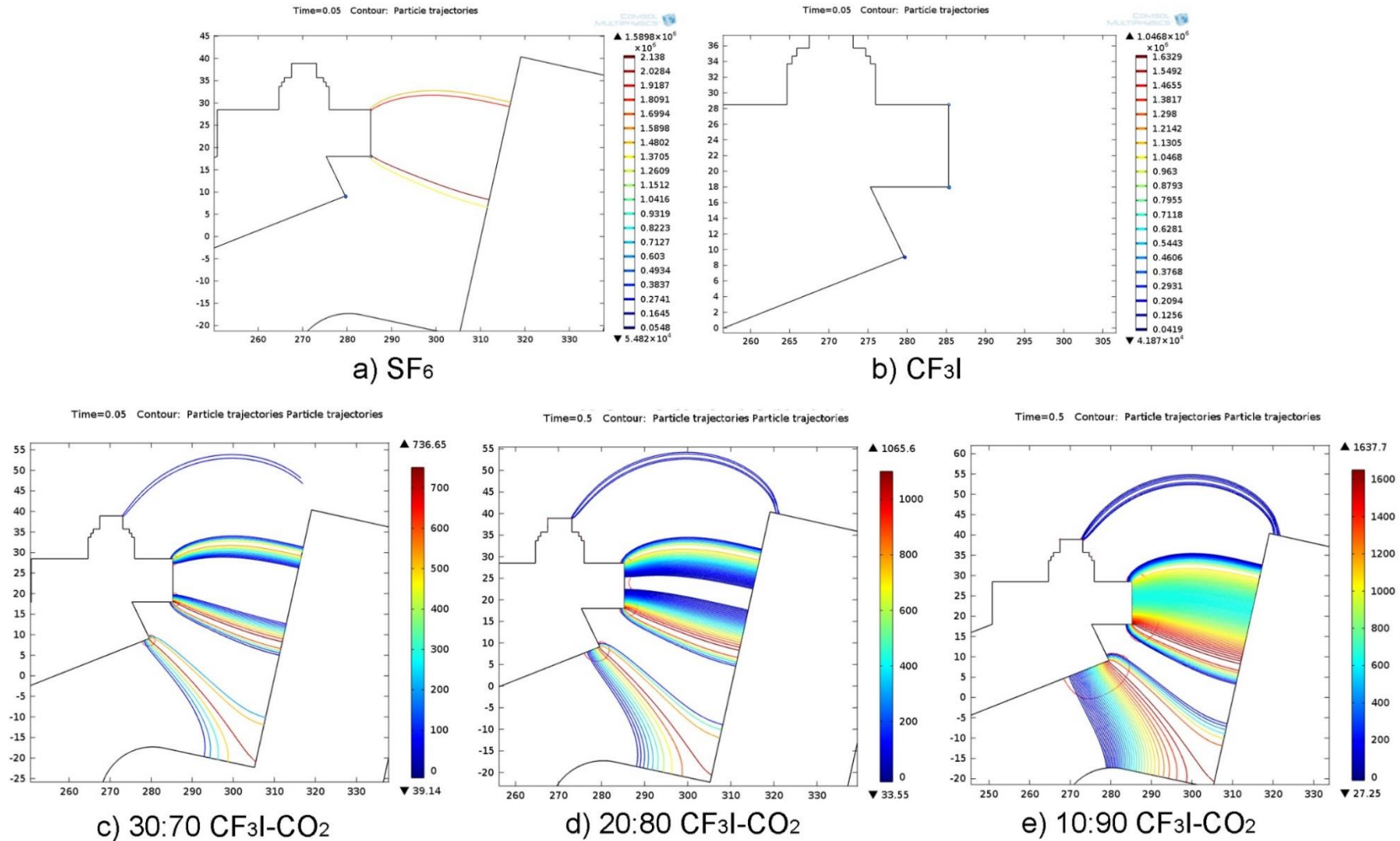


Figure 6.28: Field lines for discharges starting from the positive contact with an applied voltage of 95 kV at 0 bar (g).

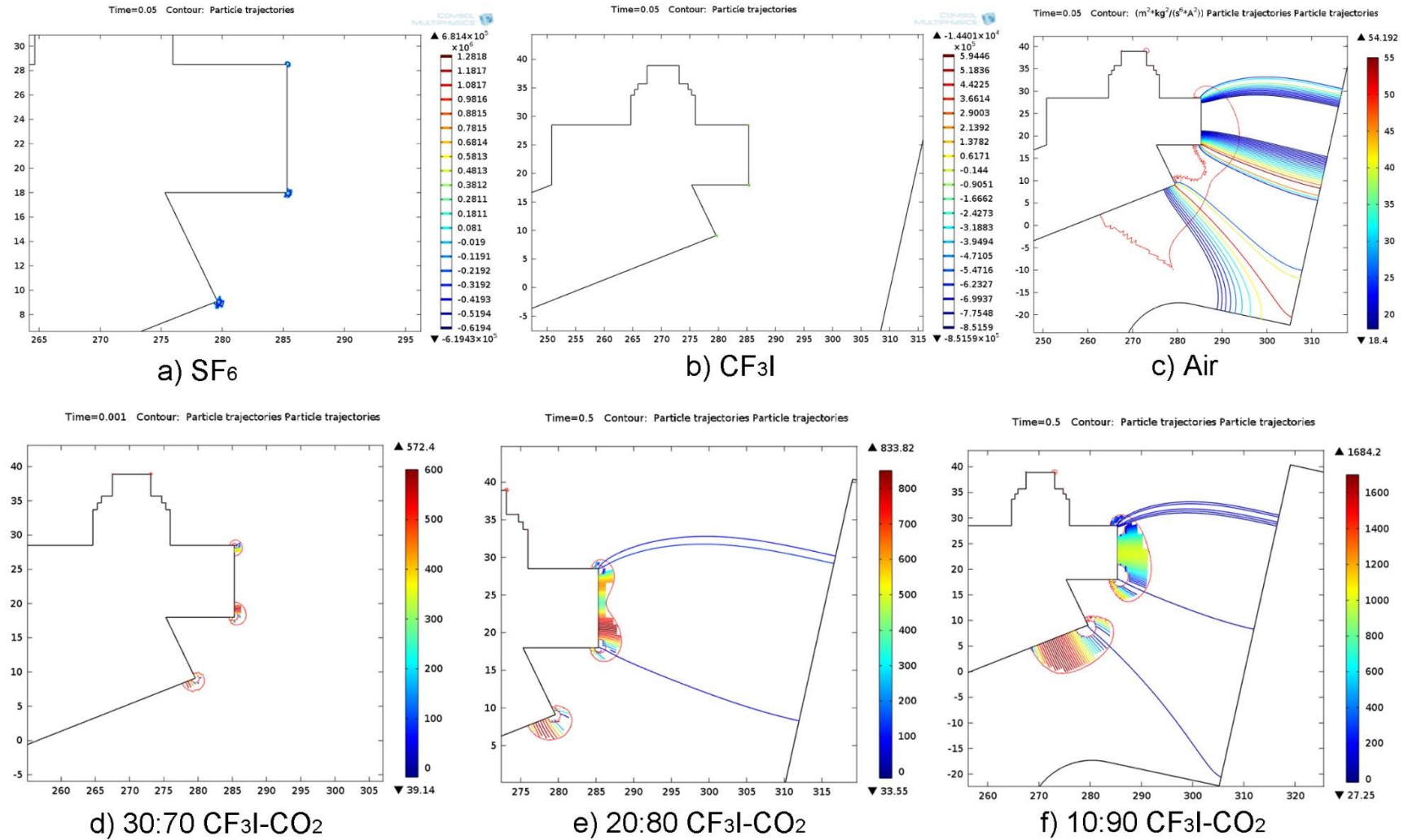


Figure 6.29: Field lines for discharges starting from the positive contact with an applied voltage of 95 kV at 0.35 bar (g).

## 6.5 Proposed options for Ringmaster contact design optimisation for CF<sub>3</sub>I-CO<sub>2</sub> gas mixtures

When designing switchgear, the contact design will be built depending on:

1. the contact materials
2. the number of contact fingers
3. the number of guaranteed points of contact per contact finger end
4. the contact dimensions, that is, parallel length and spacing
5. the ‘blow-off’ or repulsive force at the contact interface [13]

It is important to remember that the Ringmaster switch disconnecter has been manufactured with SF<sub>6</sub> as the insulation medium in the design. In order to optimise the equipment for use with CF<sub>3</sub>I or CF<sub>3</sub>I-CO<sub>2</sub> gas mixtures, it is useful to examine alterations that could be made. Previous research has shown that CF<sub>3</sub>I is a much better insulation medium when used in conjunction with a uniform electric field rather than non-uniform field [21]. The Ringmaster contact has been designed with sharp points on three corners of one contact (Figure 6.30). If these corners were rounded off (Figure 6.31), then the electric field around these regions becomes more uniform therefore increasing the insulation strength of CF<sub>3</sub>I gas mixtures.

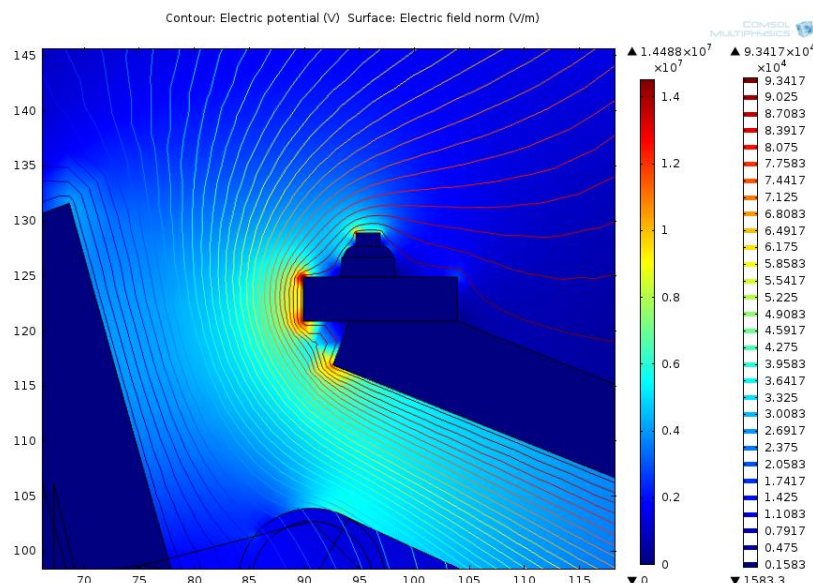


Figure 6.30: Electric field plot of Ringmaster contacts with sharp points.

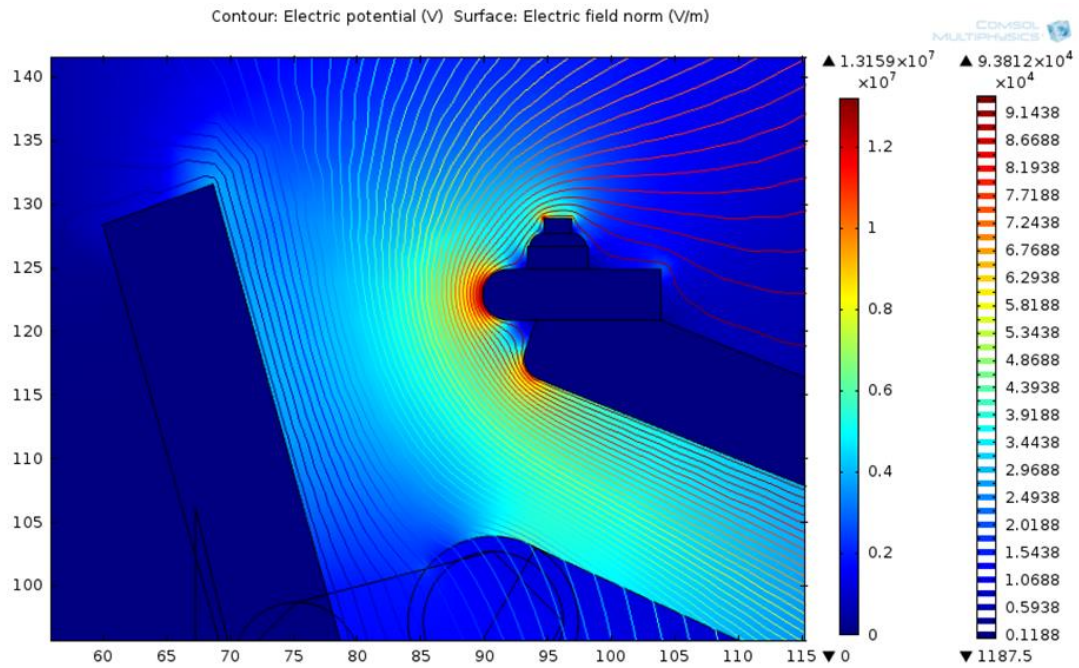


Figure 6.31: Electric field plot of Ringmaster contacts with rounded edges.

Although the rounding of these edges may be useful to achieve a more uniform electric field to help the insulation strength of  $\text{CF}_3\text{I-CO}_2$  gas mixtures, there are more factors that need to be considered. If both a fixed and moving contacts in switchgear have rounded corners, the danger is that any lateral displacement will result in a “variation in the contact entry forces” [13]. This contact entry force could result in very different alignments in the contacts each time the switch is closed and have a detrimental effect on the angle of contact between the two electrodes. It is also important to note that chamfering increases the cost of manufacturing switchgear and that often the minimal clearance between open contacts can be increased rather than alterations made to contact edges [13].

“When contacts are moving towards each other, a point will be reached where the dielectric strength of the remaining contact gap is unable to withstand the voltage stress that is being imposed upon it, and electrical current will start to flow. This will result in a measure of arc erosion of the contacts taking place. It is, therefore, important that the speed of contact closure is as fast as possible, and that contact loading is established as early as possible. However, a compromise needs to be made between minimising pre-

arcing by reducing the time to close and providing full contact loading” [13] i.e. ensuring the maximum amount of surface area of each contact is touching. It is also important to recognise that the lifetime, size and cost of the switchgear play an important role in the design decisions of contacts i.e. larger contacts have a higher cost implication but if it means a longer lifetime this cost may be acceptable. “It must be recognised that pre-arcing cannot be eliminated and, therefore, contact closure will always lead to a measure of contact erosion” [13]. When a piece of switchgear such as a switch is operated, the metal contacts physically make contact with each other. This means that sharp points may form at the edges of the contacts as they connect with each other, despite all the effort made at the manufacturing stage to smooth the surface. Therefore, it is important that the gas insulation, including a  $\text{CF}_3\text{I}$  gas mixture alternative, can withstand an electric field created by sharp points. Sharp points, such as the ones included in the original Ringmaster design (Figure 6.30), help to determine whether a  $\text{CF}_3\text{I}-\text{CO}_2$  gas mixture will be able to cope with other sharp points should the situation arise throughout the switch disconnectors lifetime [13].

## 6.6 Conclusion

In this chapter, electric field models, both 3d and 2d, have been examined to determine the weak areas of the switch disconnectors design. The electrostatic field plots have identified the sharp points of the contacts design where flashovers are likely to originate (Figure 6.30).

This chapter uses BOLSIG+ to calculate effective ionisation coefficients for 10%:90%, 20%:80% and 30%:70%  $\text{CF}_3\text{I}-\text{CO}_2$  gas mixtures and pure  $\text{CF}_3\text{I}$ . The effective ionisation coefficients are further explored to simulate the insulating capabilities of the respective gas mixtures in switchgear.

The positive net electron production region simulations and the discharge probability simulations have allowed the evaluation of flashover occurrences in the switch disconnecter when 95 kV is applied to one contact. The simulations show that at 0 bar (g) flashovers could occur between the contacts in the Ringmaster switch disconnecter when insulated with 30:70%, 20:80% and 10:90%  $\text{CF}_3\text{I}-\text{CO}_2$  (Figure 6.28 c, d and e). Reducing the amount of  $\text{CF}_3\text{I}$  in the  $\text{CF}_3\text{I}-\text{CO}_2$  gas mixture increases the probability of a flashover (Figure 6.28 b, c, d and e). If the pressure of any of the  $\text{CF}_3\text{I}-\text{CO}_2$  gas mixtures is increased to 0.35 bar (g), the probability of a flashover occurring between the contacts is very low (Figure 6.29 d, e and f). At 0.35 bar (g), air is the only gas simulated that has a strong probability of a flashover occurring between the contacts (Figure 6.29 c).

The discharge probability simulation results for  $\text{SF}_6$ , air and  $\text{CF}_3\text{I}-\text{CO}_2$  gas mixtures, in this chapter, support the results obtained through practical experimentation at the same pressures in Chapter 5, Section 5.4.

## CHAPTER 7

# A PROPOSAL FOR CF<sub>3</sub>I INSULATED VACUUM SWITCHGEAR

---

### 7.1 Introduction

From previous literature (Chapter 2), it has been reported that CF<sub>3</sub>I gas is not capable of high current interruption. This low current interruption is due to the by-products of CF<sub>3</sub>I. The attachment of iodine on the contacts in the switchgear that disassociates itself from pure CF<sub>3</sub>I during arcing, leads to reduced insulation performance [9]. Therefore, the use of 30%-70% CF<sub>3</sub>I-CO<sub>2</sub> has been suggested to negate this problem, by reducing the amount of pure CF<sub>3</sub>I used. However, an absorbent still needs to be found to remove this effect entirely. It also remains unclear how much gaseous by-products are produced by CF<sub>3</sub>I during current interruption, how much could be built up during a piece of switchgear lifetime and the reduced insulation performance this would create.

This chapter sets out a proposal for the use of a  $\text{CF}_3\text{I}-\text{CO}_2$  gas mixture replacement in switchgear and identifies a use for the mixture where it does not interrupt current and only insulates the equipment. In some equipment found on the network today there are several designs which utilise vacuum bottles / interrupters for interruption whilst utilising a gas to insulate the equipment [51].

In the switchgear proposed in this chapter, a Ring Main Unit (RMU) with vacuum interrupters has been insulated with a  $\text{CF}_3\text{I}-\text{CO}_2$  gas mixture and then tested to show the insulation qualities of the gas mixture.

## **7.2 Ring main unit chosen for testing**

To test the theory of using vacuum current interrupters in conjunction with gas insulation, in switchgear, a Lucy SCRMU (M) Ring Main Unit (RMU) has been utilised as shown in Figure 7.1. SCRMU (M) stands for single circuit ring main unit with interlocked cable test facility. This unit was provided by Western Power Distribution (WPD) after serving a 12 year lifetime on the network, insulated by  $\text{SF}_6$ . All  $\text{SF}_6$  was removed from the RMU prior to its arrival at Cardiff University for testing.

The RMU is made up of two low current ring switches and a tee-off vacuum circuit breaker contained within a common gas insulated chamber. The internal arrangement of the SCRMU(M) is similar to that of the Sabre VRN6a RMU, also manufactured by Lucy Switchgear as shown in Figure 7.2 [89].



Figure 7.1: A Lucy SCRMU(M) ring main unit.

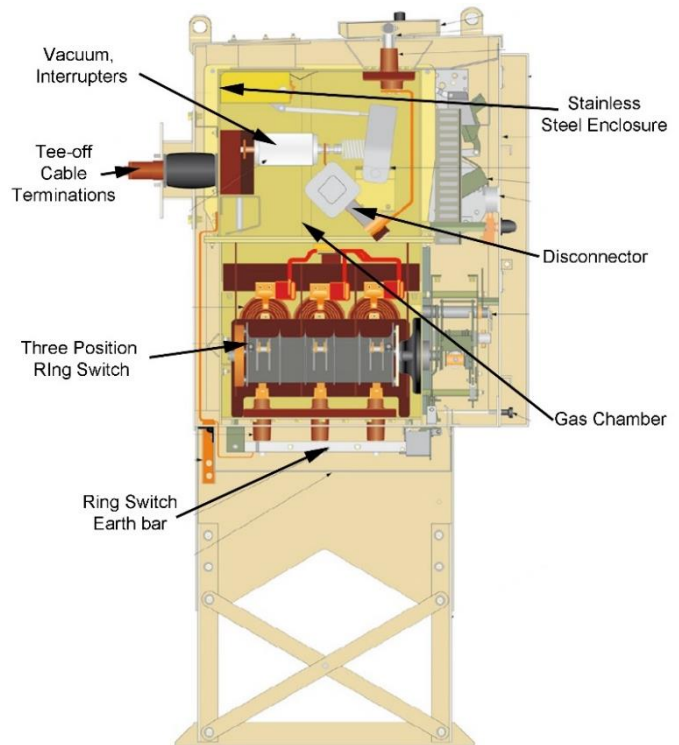


Figure 7.2: An internal view of a Lucy switchgear sabre VRN6a RMU [90].

From the manufacturers' specification of the SCRMU(M), as shown in Table 7.1, it is important to note that the 11 kV unit is expected to withstand a standard lightning impulse of 75 kV at a normal operating pressure of 0.4 bar G [89]. The insulation gas within the unit is expected to insulate two ring switches and a circuit breaker for each of the three phases. The SCRMU(M) gas chamber is quite large in comparison to the previously used pieces of switchgear (Ringmaster and Fluokit) and, therefore, needs more gas to fill it to operating pressure. For SF<sub>6</sub> to fill this unit to the recommended operating pressure, 1.3 kg of gas is needed.

Table 7.1: Manufacturers specifications of the SCRMU(M) RMU [89] [91].

Unit reference	SCRMUN (M)
Year of manufacture	2000
Weight (kg)	510
Rated voltage (kV)	11
Frequency (Hz)	50
Impulse withstand voltage (kV)	75
Minimum gas pressure (Bar G at 20°C)	0.05
Filling pressure (Bar G at 20°C)	0.4
Weight of gas at filling pressure (kg)	1.3
Minimum operating temperature	-25°C

	Ring switches	Circuit breaker
Normal current (A)	630	200
Short circuit peak making current (kA)	40	40
Short circuit breaking current (kA)	-	20
3 second short time current (kA)	16	16
Earth switch peak making current (kA)	40	40
Testing standards	IEC 265-1	IEC 265-1 IEC 420 IEC 56

### 7.3 SCRMU(M) gas connections

Taking into consideration the large volume of the SCRMU(M) gas chamber, the following tests were conducted when the unit was filled with 30% CF<sub>3</sub>I : 70% CO<sub>2</sub> to trial the applications of CF<sub>3</sub>I-CO<sub>2</sub> gas mixtures in switchgear. 30:70% CF<sub>3</sub>I-CO<sub>2</sub> was chosen to insulate the equipment because it was one of the best performing insulation gases tested in Chapter 5. The SCRMU was filled to the rated filling pressure of 0.4 bar G. The contacts inside the switchgear remained the same throughout testing and were left as the equipment was manufactured. It is also worth noting that this unit has been used on the UK network and was in operation for approximately 12 years of service and, therefore, it is expected that the contacts in the switches and circuit breaker may have degraded since they were manufactured.

To fill the SCRMU(M), the unit was first evacuated of all remaining air from the gas chamber, using the procedure explained in Appendix B, section B2. The RMU was then filled with new  $\text{CF}_3\text{I}$  and  $\text{CO}_2$  straight from their storage cylinders, as shown in Figure 7.3, to create a positive pressure inside the gas chamber of 0.4 bar G.

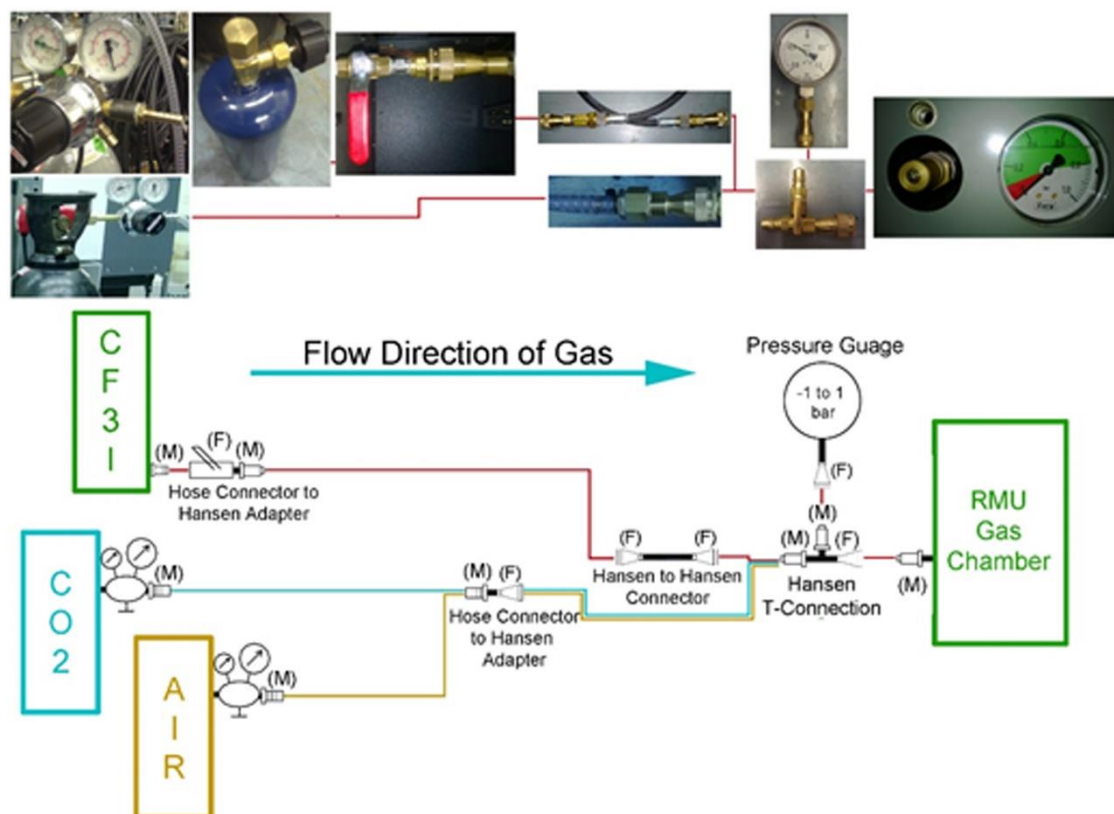


Figure 7.3: Filling of the SCRMU(M) gas chamber.

#### 7.4 SCRMU(M) gas mixture calculations

The total amount of  $\text{CF}_3\text{I}$  and  $\text{CO}_2$  needed to fill the SCRMU(M) with 30%:70%  $\text{CF}_3\text{I}$ : $\text{CO}_2$  to 0.4 bar G can be calculated as follows.

For the Lucy SCRMU(M) Unit:

The mass of  $\text{SF}_6$  needed to fill the gas chamber = 1300 g

The operating pressure of the unit = 0.4 bar G at  $20^\circ\text{C}$  = 1.4 bar

The filling temperature =  $20^\circ\text{C}$  = 293.15 K

$R = 0.0821$ , MW of  $\text{SF}_6$  = 146.0554192 g mol<sup>-1</sup>,

MW of  $\text{CF}_3\text{I}$  = 195.9104 g mol<sup>-1</sup>, MW of  $\text{CO}_2$  = 44.01 g mol<sup>-1</sup>.

When the Lucy SCRMU(M) Ring Main Unit is filled with pure SF<sub>6</sub>, the gas chamber volume is [30]:

$$V = \frac{mRT}{MW \times P} = \frac{1300 \times 0.0821 \times 293.15}{146.0554192 \times 1.4} = 153.01 \text{ L} \quad (7.1)$$

To fill the SCRMU with 30% pressure of CF<sub>3</sub>I, the mass of CF<sub>3</sub>I needed is [30]:

$$m = \frac{MW \times PV}{RT} = \frac{195.9104 \times 0.42 \times 153.01}{0.0821 \times 293.15} \quad (7.2)$$

$$m = 523.11 \text{ g}$$

To fill the SCRMU with 70% pressure of CO<sub>2</sub>, the mass of CO<sub>2</sub> needed is [30]:

$$m = \frac{MW \times PV}{RT} = \frac{44.01 \times 0.98 \times 153.01}{0.0821 \times 293.15} \quad (7.3)$$

$$m = 274.20 \text{ g}$$

The total amount of gas required to fill the Lucy SCRMU with 30% CF<sub>3</sub>I : 70% CO<sub>2</sub> is:

$$523.11 \text{ g CF}_3\text{I} : 274.20 \text{ g CO}_2$$

Giving a gas mixture ratio, for 30%:70% CF<sub>3</sub>I-CO<sub>2</sub>, of:

$$1.908 \text{ g} : 1 \text{ g} \quad \text{CF}_3\text{I} : \text{CO}_2$$

## 7.5 Lucy SCRMU(M) standard lightning impulse withstand tests and connections

The SCRMU(M) was connected to the lightning impulse generator, grounding points and operated using the components shown in Figure 7.4.

The RMU has a rated impulse withstand voltage of 75 kV. The RMU was subjected to the withstand voltage test outlined in procedure B in BS60060-1 [62], which has been adapted for switchgear and controlgear as set out in BS62271-1 [1] for impulse testing.

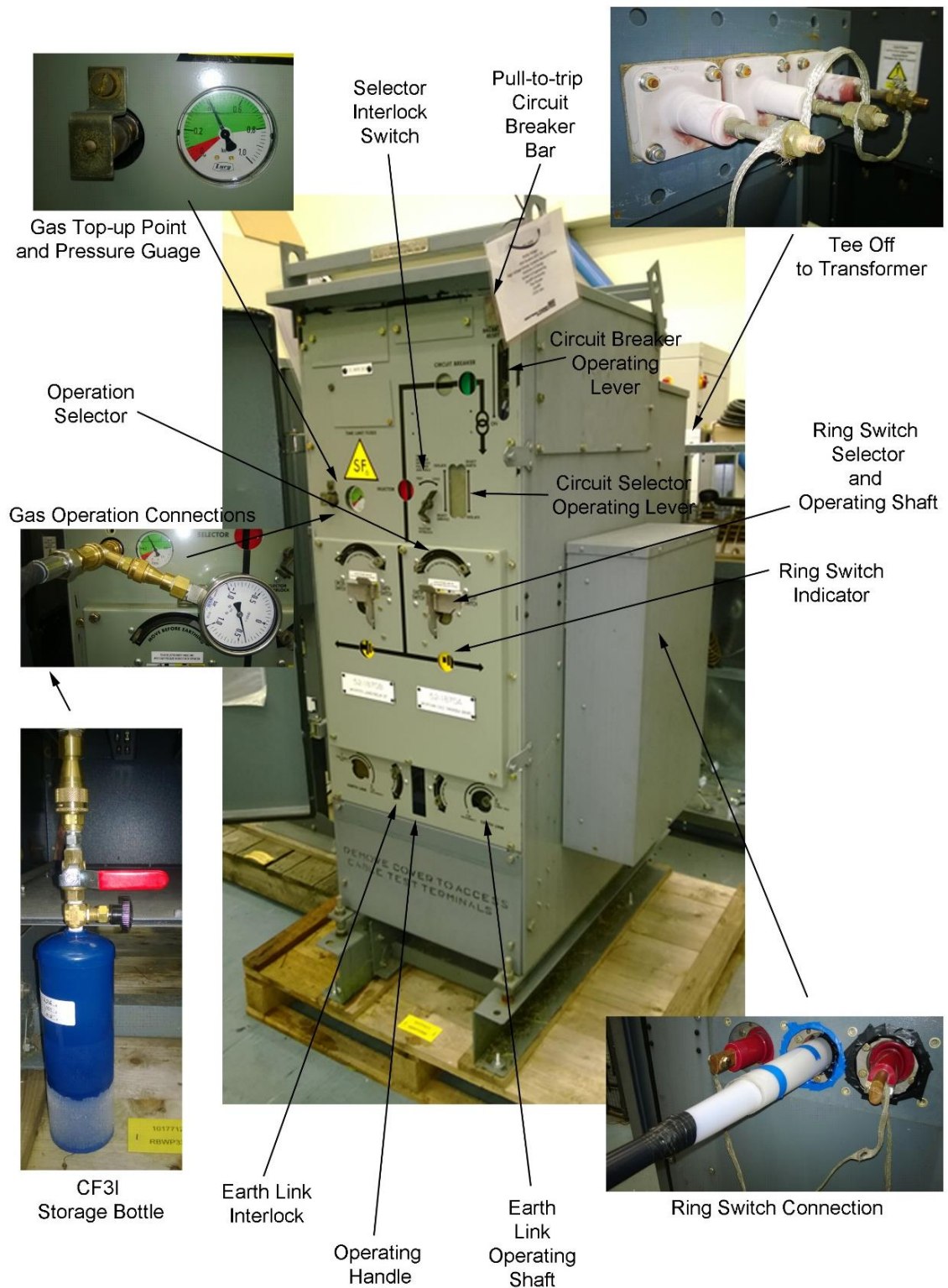


Figure 7.4: Connections and operational components of the SCRMU(M).

For the tests conducted, positive lightning impulses were applied to each phase in turn, one after the other, at a constant 75 kV. For the ring switches one maximum 25 impulse series was applied to each phase to test the insulating withstand strength of the  $\text{CF}_3\text{I-CO}_2$  gas mixture. For the vacuum circuit breakers, insulated by  $\text{CF}_3\text{I-CO}_2$  gas, two maximum

25 impulse series were applied to each phase of the RMU (a total of 50 impulses) to test the insulating withstand strength of the gas mixture. To test the insulation strength of the open ring switches and the gas surrounding the vacuum circuit breakers, the RMU was placed into the positions shown in Figure 7.5 and 7.6. A current transformer was used to identify a gas breakdown across the equipment.

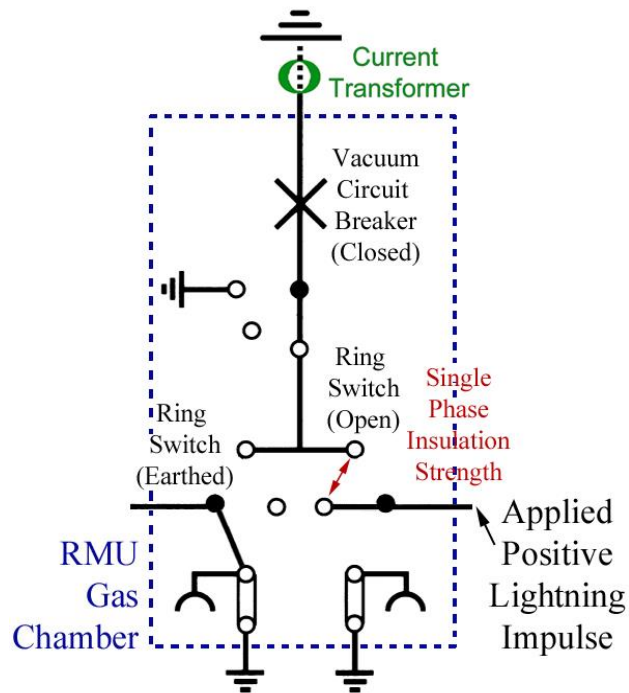


Figure 7.5: RMU positive lightning impulse gas insulation test position for ring switch.

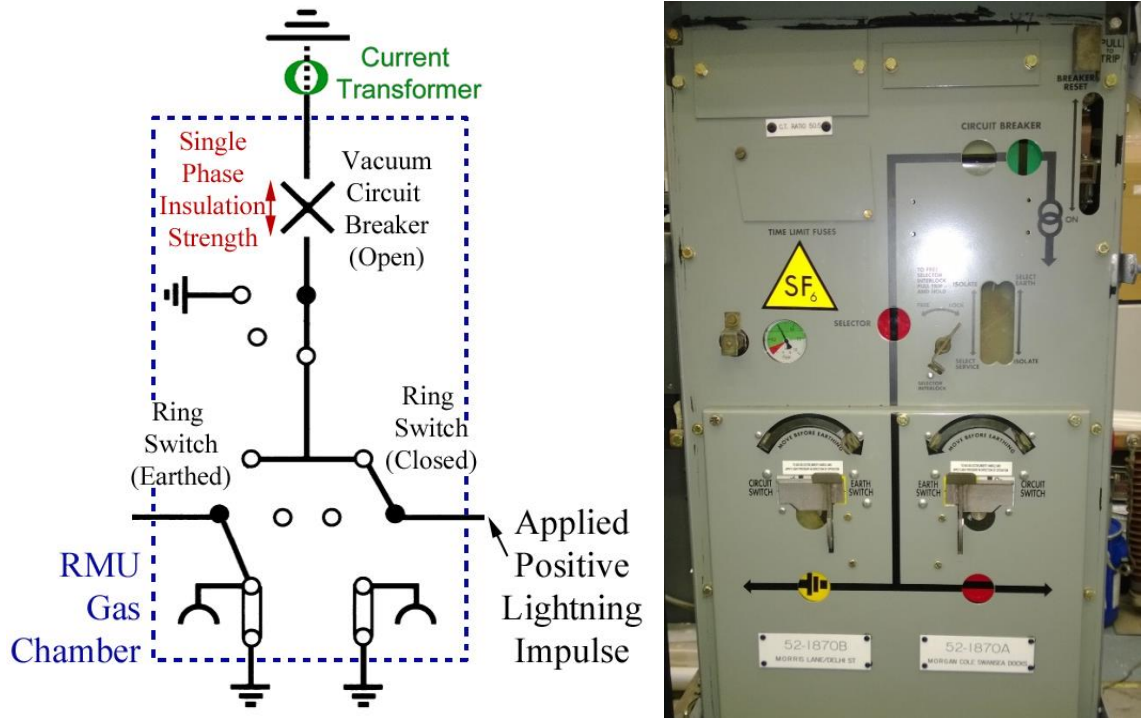


Figure 7.6: RMU positive lightning impulse gas insulation test position for circuit breaker.

## 7.6 Lucy SCRMU standard lightning impulse withstand test results

When the RMU is filled with SF<sub>6</sub>, it would be expected that no more than 2 breakdowns should occur across the insulating gas gap in a 25 impulse series [1]. When the RMU is filled with an insulating gas mixture of 30%:70% CF<sub>3</sub>I-CO<sub>2</sub>, no disruptive discharges were detected across the ring switch gas gap in a 25 impulse series and no disruptive discharges are detected across the vacuum circuit breaker in a 50 impulse series (Table 7.2 and 7.3).

Table 7.2: 30%:70% CF<sub>3</sub>I-CO<sub>2</sub> RMU 75 kV positive lightning impulse withstand voltage tests.

	Phase 1		Phase 2		Phase 3	
	Result	No. of gas breakdowns	Result	No. of gas breakdowns	Result	No. of gas breakdowns
<b>Ring switch</b>	PASS	0/25	PASS	0/25	PASS	0/25
<b>Circuit breaker</b>	PASS	0/50	PASS	0/50	PASS	0/50

Table 7.3: 30%:70% CF<sub>3</sub>I-CO<sub>2</sub> RMU average 75 kV positive lightning impulse withstand voltage tests.

<b>RMU average</b>		
	<b>Result</b>	<b>No. of gas breakdowns</b>
<b>Ring switch</b>	PASS	0/75
<b>Circuit breaker</b>	PASS	0/150

## 7.7 Conclusion

When considering the use of 30%-70% CF<sub>3</sub>I-CO<sub>2</sub> as an alternative to SF<sub>6</sub> it has been shown, in the ring switches in the RMU tested, that the insulation performance of the gas mixture is comparable to SF<sub>6</sub> in practical complex switchgear contact arrangements. However, the use of this gas mixture is for the interruption of low current only and so the practical applications in switchgear, such as the ring switches in the RMU discussed, are diminished because the gas between the contacts has to be able to break load current up to 630 A [89].

The proposed use of 30%-70% CF<sub>3</sub>I-CO<sub>2</sub> is to purely operate as an insulating medium around a vacuum circuit breaker, where the current is interrupted by a vacuum bottle and the gas mixture only insulates the equipment. The proposed insulation of CF<sub>3</sub>I-CO<sub>2</sub> is proven in the testing in this chapter and shows a practical application of CF<sub>3</sub>I-CO<sub>2</sub> gas mixtures for the future.

## CHAPTER 8.

# CONCLUSION

---

### 8.1 Conclusion

In this thesis, the research investigation that was undertaken to ascertain the usefulness of  $\text{CF}_3\text{I}$  as an alternative to  $\text{SF}_6$  has been explained. This has specifically focused on  $\text{CF}_3\text{I}$ - $\text{CO}_2$  gas mixtures as an insulation medium for distribution equipment. The review (Chapter 2) highlighted that  $\text{CF}_3\text{I}$  has a low global warming and ozone depleting potential, as well as an overall low environmental impact. Previous research also indicates that  $\text{CF}_3\text{I}$  has a better insulation strength than  $\text{SF}_6$  when used in a uniform electric field. However,  $\text{CF}_3\text{I}$  has a worse insulating performance than  $\text{SF}_6$  when used in conjunction with a non-uniform electric field.

The review recognised that  $\text{CF}_3\text{I}$  has a high boiling point, compared to  $\text{SF}_6$ , and in order for it to be used above MV and at high pressure, a mixture of  $\text{CF}_3\text{I}$  and another insulating gas would need to be formed. Gas mixtures would also help reduce the cost of

experimentation. Previous research determined that a mixture of  $\text{CF}_3\text{I}-\text{CO}_2$  does not critically reduce the insulation strength of pure  $\text{CF}_3\text{I}$ , although some decrease is noted.  $\text{CF}_3\text{I}-\text{CO}_2$  gas mixtures are also able to interrupt low currents ( $< 100 \text{ A}$ ) whilst a relatively small amount of  $\text{CF}_3\text{I}$  is used in the mixture. It was also noted that  $\text{CF}_3\text{I}$  generates iodine that can attach itself to contacts and reduce the dielectric strength and interruption capability of the gas when it is used as an insulation medium.

The potential problems of the increased and more frequent use of  $\text{SF}_6$ , in the power industry, have been highlighted in this project. The estimated leakage rates of  $\text{SF}_6$  equipment currently employed in UK Power Networks distribution network and worldwide was conducted and predicted (Chapter 3). The expected amount of  $\text{SF}_6$  released into the atmosphere over the equipment's lifetime has been compared to the equivalent  $\text{CO}_2$  emissions. These estimated results show that there will be a considerable amount of  $\text{SF}_6$  released into the atmosphere but that this is a relatively small amount compared to worldwide production of  $\text{CO}_2$ . It must be remembered that the current restrictions on leakage rates and protocols set out after the Kyoto agreement have not always been in place and that any  $\text{SF}_6$  previously released will be in the atmosphere for a long time with lasting effects. The predicted calculations do not include any extra leakage from gas handling operations and equipment containment failures, so the amount of  $\text{SF}_6$  released is likely to be higher than predicted.

During this research, MV switch disconnectors were identified and obtained for practical experimentation (Chapter 4 and 5) and simulation work was used to identify the potential insulation capability of  $\text{CF}_3\text{I}-\text{CO}_2$  (Chapter 6). Equipment for handling and moving  $\text{CF}_3\text{I}$  was also identified and a Dilo Mini Series was acquired to vacuum, fill the switchgear and remove gas once testing was complete. This gas system, along with the connectors, adapters and hoses, with the required specifications for moving  $\text{CF}_3\text{I}$ , especially focused

on the safe handling and storage of liquid gas, was commissioned to fill commercially available switchgear. Withstand and 50% probability of gas breakdown ( $U_{50}$ ) tests were also recognised as experimentation that would identify any problems in the insulation capabilities of  $CF_3I$ - $CO_2$  gas mixtures in a practical situation.

Practical standard lightning impulse experimentation identified that both the Ringmaster and the Fluokit MV switch disconnectors can be insulated from phase to phase breakdown, within the gas chamber, whilst  $CF_3I$ - $CO_2$  is used as an insulating medium.

In the Fluokit switch disconnector standard lightning impulse withstand tests, at the rated 125 kV, and  $U_{50}$  insulation strength tests identified that gas mixtures of 10:90%, 20:80% and 30:70%  $CF_3I$ - $CO_2$  can effectively insulate the equipment. These results hold true for the switch disconnector being filled at both its rated filling pressure (0.45 bar G) and its minimum operating pressure (0 bar G).

In the Ringmaster switch disconnector standard lightning impulse withstand tests, at the rated 95 kV, and  $U_{50}$  insulation strength tests indicated that gas mixtures of 10:90%, 20:80% and 30:70%  $CF_3I$ - $CO_2$  can insulate the equipment but only at the rated filling pressure (0.35 bar G). At the minimum operating pressure (0 bar G), 30:70% and 20:80%,  $CF_3I$ - $CO_2$  have a marginal pass / fail result for whether these mixtures would be able to insulate the equipment and 10:90%  $CF_3I$ - $CO_2$  cannot be used. It is, therefore, suggested that to insulate the Ringmaster successfully with  $CF_3I$ - $CO_2$  gas mixtures, the minimum operating pressure be raised closer to the operating pressure.

The results from the Ringmaster and Fluokit switch disconnectors practical experimentation indicates that:

- $CF_3I$ - $CO_2$  can be used to insulate this MV equipment and its complex contact geometry at the recommended filling pressure.

- Gas mixtures with 30% CF<sub>3</sub>I and below have an insulation strength below that of pure SF<sub>6</sub>.
- The insulation strength of CF<sub>3</sub>I-CO<sub>2</sub> gas mixtures is increased when the pressure of the gas is raised, even by 0.35 bar.
- 30:70% and 20:80% CF<sub>3</sub>I-CO<sub>2</sub> gas mixtures have the best insulation strength of all gas mixtures used, except for pure SF<sub>6</sub>.

In the Ringmaster and Fluokit switch disconnectors the manufacturer's specifications indicate that both units should be able to interrupt a current of 630A. From previous research, it seems unlikely that these CF<sub>3</sub>I-CO<sub>2</sub> gas mixtures will be able to successively interrupt this current without serious gas degradation.

Following on from the practical experimentation, a SCRMU(M) ring main unit was used to investigate the potential of a 30:70% CF<sub>3</sub>I-CO<sub>2</sub> gas mixture to insulate vacuum circuit breakers and ring switches (Chapter 7). The results indicated that 30:70% CF<sub>3</sub>I-CO<sub>2</sub> could be successfully used to insulate the equipment against the rated 75 kV lightning impulse. As with the switch disconnectors previously tested, the ring switches need to be able to break a high current which it seems unlikely that CF<sub>3</sub>I-CO<sub>2</sub> will be able to handle. However, the circuit breakers use vacuum bottles to interrupt the current and are only insulated by the gas mixture. Therefore, it is proposed that this type of hybrid design (as with the Lucy SCRMU(M)) using CF<sub>3</sub>I-CO<sub>2</sub> gas mixtures could be utilised in the future.

In order to simulate the insulation strength of various CF<sub>3</sub>I-CO<sub>2</sub> gas mixtures, the effective ionisation coefficients have been calculated using BOLSIG+ to estimate their linear representations and critical reduced electric field strengths (Chapter 6). These calculations suggest that pure CF<sub>3</sub>I has an insulation strength higher than SF<sub>6</sub>. The calculations also predict that 30:70%, 20:80% and 10:90% CF<sub>3</sub>I-CO<sub>2</sub> gas mixtures have

insulation strengths less than  $\text{SF}_6$  which decrease as the amount of  $\text{CF}_3\text{I}$  in the gas mixtures reduces.

COMSOL simulations using the effective ionisation coefficients and the geometry of the Ringmaster predicted the likelihood of a flashover occurring when 95 kV is applied to one side of the switch (Chapter 6). The simulation results suggest that, at 0 bar G, the 30:70%, 20:80% and 10:90%  $\text{CF}_3\text{I}$ - $\text{CO}_2$  gas mixtures are not likely to be able to insulate the equipment. As the content of  $\text{CF}_3\text{I}$  increases, so do the chances that it can withstand the 95 kV impulse. At 0.35 bar G, the simulations predict the same  $\text{CF}_3\text{I}$ - $\text{CO}_2$  gas mixtures will be able to withstand the 95 kV impulse. Partial discharge increases around the tip of the electrode as the content of  $\text{CF}_3\text{I}$  is reduced. It is also predicted that both pure  $\text{CF}_3\text{I}$  and  $\text{SF}_6$  will be able to insulate the contacts at both gas pressures. The simulated results of gas mixtures of  $\text{CF}_3\text{I}$ - $\text{CO}_2$  agree with the practical experimentation undertaken on the Ringmaster switch disconnecter.

COMSOL two dimensional and three dimensional simulations of the Ringmaster switch disconnecter were used to simulate the electrostatic field plots of the contacts and highlight areas where high electrical stress might occur. These areas indicated that the sharp points of the contact, to which 95 kV was applied, were the areas under the highest electrical stress, and the regions from which a flashover was most likely to originate.

In conclusion this research has shown that:

- $\text{CF}_3\text{I}$ - $\text{CO}_2$  gas mixtures can be used as a purely insulating medium in MV distribution equipment
- The insulation capability of the  $\text{CF}_3\text{I}$ - $\text{CO}_2$  gas mixture is dependent on pressure and contact geometry

- The higher the concentration of  $\text{CF}_3\text{I}$  in the  $\text{CF}_3\text{I-CO}_2$  gas mixture the higher the insulation capability
- As a potential alternative to  $\text{SF}_6$  previous research indicates that a low current interruption capability, iodine by-product and high boiling point will pose potential problems
- Most of these problems can be dismissed when a  $\text{CF}_3\text{I-CO}_2$  gas mixture is used to insulate vacuum interrupters
- Effective ionisation coefficients and electric field simulations can be used to identify the potential of a  $\text{CF}_3\text{I-CO}_2$  gas-mixtures ability to insulate MV distribution equipment

## 8.2 $\text{CF}_3\text{I}$ / $\text{CF}_3\text{I-CO}_2$ in power plant design

Based on the results in this thesis, it is clear that  $\text{CF}_3\text{I}$  and 30:70% / 20:80%  $\text{CF}_3\text{I-CO}_2$  gas mixtures have an insulation performance comparable with  $\text{SF}_6$ . However, there are many concerns about its current interruption performance, its boiling point and its inherent ability to produce iodine as a by-product.

From the results of medium voltage switchgear carried out in this investigation, and previous research, it is clear that there could be a place for  $\text{CF}_3\text{I}$  and  $\text{CF}_3\text{I}$  gas mixtures in conjunction with vacuum equipment in the future at MV. This is based solely on the insulation performance of  $\text{CF}_3\text{I-CO}_2$  gas mixtures. Research may also need to focus on the oxidation  $\text{CO}_2$  may cause to metal contacts or  $\text{CF}_3\text{I}$  gas mixtures with  $\text{N}_2$ .

If gas mixtures of  $\text{CF}_3\text{I}$  and another insulating gas have a boiling point that is high enough to increase the pressure, to a level where it would be able to withstand the maximum disruptive discharge voltage, then  $\text{CF}_3\text{I}$  could be used at HV and EHV for insulation purposes only, such as in GIL. At this stage of development, it is unlikely that  $\text{CF}_3\text{I}$  could

be used to interrupt current at anywhere near the level needed for HV and EHV equipment, such as in circuit breakers or switches, unless an absorbent for iodine was found.

### **8.3 Power industry adoption rate**

Given the adoption rate of SF<sub>6</sub>, it is not likely that a new insulation medium would be adopted very quickly into the power industry without first proving its safety and insulation capabilities through industry experience and track record. However, given the present day focus on reducing the emissions of global warming gases, the changeover may occur more rapidly. Given the fact that SF<sub>6</sub> is highly regulated and can only be used in the power industry, because no alternative exists, there is demand for a quick transition to a new gas insulation medium. The fact that a new gas (CF<sub>3</sub>I or otherwise) could be installed using the gas handling equipment currently available and fitted without further alterations made to the switchgear already in use could further increase the adoption rate of a new insulating medium. However, the long life-time and service operation of SF<sub>6</sub> equipment could prevent a full transition to a new insulating medium because equipment that has been newly commissioned and installed is not likely to be altered for some time. In the short term, a reduction in the amount of SF<sub>6</sub> used either by slimming equipment or by the use of an SF<sub>6</sub> gas mixture, with N<sub>2</sub> or similar, seems much more likely whilst a direct replacement for SF<sub>6</sub> is developed (especially in equipment where high current interruption is required).

### **8.4 Future work**

It is recommended that in the future, research based on CF<sub>3</sub>I and CF<sub>3</sub>I gas mixtures focus on the following key areas:

- *Investigation of more SF<sub>6</sub> / Vacuum insulated equipment:* Further SF<sub>6</sub> insulated / vacuum interruption equipment be examined to investigate whether CF<sub>3</sub>I gas mixtures could insulate a wide range of equipment. Focus should be undertaken to prove whether high current interruption is possible with vacuum interruption / CF<sub>3</sub>I gas insulation.
- *Investigation of other CF<sub>3</sub>I gas mixtures:* Further research be undertaken to improve the insulation strength of CF<sub>3</sub>I gas mixtures and its current handling capabilities, when used in conjunction with another insulation gas. This could include mixture ratios with a very low percentage content of CF<sub>3</sub>I or a mixture of three gases.
- *Investigation of CF<sub>3</sub>I gas mixtures boiling points:* An extension of the CF<sub>3</sub>I saturation vapour pressure curve at a range of pressures to include mixtures of CF<sub>3</sub>I-CO<sub>2</sub> and any other potential gas mixtures. This will include several different percentage ratios of each gas mixture.
- *Investigation of CF<sub>3</sub>I gas mixtures operational pressure range:* In addition to the saturation vapour pressure curve for various CF<sub>3</sub>I gas mixtures, it is important to note the operational pressures at which these mixtures can be used. Special consideration should be given to the minimum operating temperatures of indoor and outdoor switchgear and the pressures at which they would normally operate.
- *Investigation of absorbents of the iodine by-product from CF<sub>3</sub>I:* Further research should consider the build-up of iodine on contacts from successive discharges in CF<sub>3</sub>I. Absorbents should be considered that may reduce the effect iodine has on the insulation capabilities of the various gas mixtures under consideration.

## References

- [1] B. S. I. (BSI), "British Standard BS62271-1: High-voltage switchgear and controlgear - Part 1: Common specifications," 2008. [Online]. Available: [www.bsigroup.com/standards](http://www.bsigroup.com/standards). [Accessed 01 04 2014].
- [2] S. Théoleyre, "Cahier Technique no. 193: MV breaking techniques", Schneider Electric, 2000. [Online]. Available: <http://www.schneider-electric.com>. [Accessed 01 05 2013].
- [3] D. Koch, "SF<sub>6</sub> properties, and use in MV and HV switchgear," Schneider Electric, February 2003. [Online]. Available: <http://www.schneider-electric.com>. [Accessed 01 05 2013].
- [4] R. W. Blower, *Distribution Switchgear - Construction, performance, selection and Installation*. London: Collins Professional and Technical Books, 1986.
- [5] L. Hewitson, M. Brown and B. Ramesh, *Practical Power System Protection*, S. Mackay, Ed., Oxford: Newnes, Elsevier Ltd, IDC Technology, 2005.
- [6] P. Duquerroy, G. Sonzogni, G. Perrissin and B. J. Bouillon, "MV Switchgear breaking in SF<sub>6</sub>: The Situation after 20 Years in Service," in *Trends in Distribution Switchgear*, IEE Conference Publication No. 400, 1994.
- [7] L. T. Falkingham, M. Waldron and Vacuum Interrupters Ltd., "Vacuum for HV applications - Perhaps not so new? - Thirty Years Service Experience of 132kV Vacuum Circuit breaker," in *International Symposium on Discharges and Electrical Insulation in Vacuum*, ISDEIV '06 (Volume:1 ) , Matsue, 2006.
- [8] C. T. Dervos and P. Vassiliou, "Sulphur Hexafluoride (SF<sub>6</sub>): Global Environmental Effects and Toxic Byproduct Formation," in *Air & Waste Management Association*, vol. 50, no. ISSN 1047-3289, pp. 137-141, 2000.
- [9] H. Katagiri, H. Kasuya and S. Yanabu, "Measurement of Iodine Density Generated from CF<sub>3</sub>I-CO<sub>2</sub> Mixture after Current Interruption," Presented at *Japan-Korea Joint Symposium on Electrical Discharge and High Voltage Engineering*, Shibaura Institute of Technology, Tokyo, 2007.
- [10] H. Katagiri, H. Kasuya, H. Mizoguchi and S. Yanabu, "Investigation of the Performance of CF<sub>3</sub>I Gas as a Possible Substitute for SF<sub>6</sub>," in *IEEE Transactions on Dielectrics and Electrical Insulation*, Tokyo Denki Univ, vol. 15, Issue 5, pp. 1424 – 1429, 2008.
- [11] O. Farish, M. D. Judd, B. F. Hampton and J. S. Pearson, "SF<sub>6</sub> insulation systems and their monitoring," in *Advances in High Voltage Engineering*, vol. 40, A. Haddad and D. Warne, Eds., London, IEE Power & Energy Series 40, The Institute of Electric Engineers, p. 37-76, 2004.
- [12] Siemens Energy Sector, "Power Engineering Guide: Switchgear and Substations, 7th Edition," 02 08 2012. [Online]. Available: [http://www.energy.siemens.com/us/pool/hq/energy-topics/power%20engineering%20guide/PEG\\_70\\_KAP\\_03.pdf](http://www.energy.siemens.com/us/pool/hq/energy-topics/power%20engineering%20guide/PEG_70_KAP_03.pdf). [Accessed 01 03 2014].
- [13] S. Stewart, *Distribution Switchgear*, vol. IEE Power and Energy Series 46, A. T. Johns and D. F. Warne, Eds., London, UK: The Institution of Electrical Engineers (IEE), 2004.
- [14] Intergovernmental Panel on Climate Change (IPCC), *Working Group I Contribution to Fourth Assessment Report of the IPCC - Intergovernmental Panel on Climate Change*, Geneva, Switzerland: Addendum-Errata of Climate Change 2007 - The Physical Science Basis IPCC WG1 AR4 Report, 2008.
- [15] C.-H. Hwang, B.-T. Lee, C.-S. Huh, N.-R. Kim and Y.-M. Chang, "Breakdown Characteristics of SF<sub>6</sub>/CF<sub>4</sub> Mixtures in Test Chamber and 25.8kV GIS," in *International Conference on Electrical Machines and Systems (ICEMS)*, Engineering letter 15:1, Tokyo, 2009.
- [16] N. H. Malik and A. H. Qureshi, "Breakdown Gradients In SF<sub>6</sub>-N<sub>2</sub>, SF<sub>6</sub>-Air And SF<sub>6</sub>-CO<sub>2</sub> Mixtures," *IEEE Transactions on Electrical Insulation*, vol. EI-15, No. 5, pp. 413 - 418, 1980.

- [17] G. Schoeffner and R. Graf, "Suitability of N<sub>2</sub>-SF<sub>6</sub> Gas Mixtures for the Application at Gas Insulated Transmission Lines (GIL)," in *IEEE Power Tech Conference*, Bologna, Italy, Vol. 2, ISBN 0-7803-7967-5, 2003.
- [18] Siemens AG, "Siemens Energy Gas-Insulated Transmission Lines," Siemens AG, 2013. [Online]. Available: <http://www.energy.siemens.com/hq/en/power-transmission/gas-insulated-transmission-lines.htm#content=Description>. [Accessed 01 02 2014].
- [19] T. Takeda, S. Matsuoka, A. Kumada and K. Hidaka, "Sparkover and Surface Flashover Charactersitics of CF<sub>3</sub>I Gas under Application of Nanosecond Square Pulse Voltage," *Proceedings of the 16th International Symposium on High Voltage Engineering*, Paper C-55, pp. 1-6, 2009.
- [20] J. d. Urquijo, "Is CF<sub>3</sub>I a good gaseous dielectric? A comparative swarm study of CF<sub>3</sub>I and SF<sub>6</sub>," in *5th EU-Japan Joint Symposium on Plasma Processing*, Instituto de Ciencias Fisicas, Universidad Nacional Autonoma de Mexico, Journal of Physics: Conference series 86, Issue 1, pp. 012008, 2007.
- [21] H. Toyota, S. Nakauchi, S. Matsuoka and K. Hidaka, "Voltage-time Charactersitics in SF<sub>6</sub> and CF<sub>3</sub>I Gas within Non-uniform Electric Field," in *Proceedings of the XIVth International Symposium on High Voltage Engineering*, Beijing, China, Paper H-04, pp. 1-6, 2005.
- [22] United Nations Framework Convention on Climate Change (UNFCCC), "Kyoto Protocol," UNFCCC, 2008. [Online]. Available: [http://unfccc.int/kyoto\\_protocol/items/3145.php](http://unfccc.int/kyoto_protocol/items/3145.php). [Accessed 07 02 2014].
- [23] D. J. Jacob, "Introduction to Atmospheric Chemistry", Harvard: Princeton University Press, 1999. [Online]. Available: <http://www-as.harvard.edu/people/faculty/djj/book/.html>. [Accessed 01 02 2014].
- [24] J. L. Hernández-Ávila, A. M. Juárez, E. Basurto and J. d. Urquijo, "Electron interactions in CF<sub>3</sub>I and CF<sub>3</sub>I-N<sub>2</sub>," in *The 28th International Conference on Phenomena in Ionized Gases (ICPIG)*, Prague, Czech Republic, Topic No. 1, pp. 139-142, 2007.
- [25] H. Kasuya, H. Katagiri, Y. Kawamura, D. Saruhashi, Y. Nakamura, H. Mizoguchi and S. Yanabu, "Measurement of Decomposed Gas Density of CF<sub>3</sub>I-CO<sub>2</sub> Mixture," *Proceedings of the 16th International Symposium on High Voltage Engineering (ISH 2009)*, Cape Town - S. Africa, Paper C-41, pp. 1-4, 2009.
- [26] D. W. Fahey, "Twenty questions and aswers about the ozone layer: 2006 update," *Presented at Panel Review Meeting for the 2006 Ozone Assessment*, Les Diablerets, Switzerland, 2006.
- [27] J. A. Pyle, S. Soloman, D. Wuebbles and S. Zvenigorodsky, "Ozone depletion and chlorine loading potentials", Geneva: World Meteorological Organization: World Meteorological Organization Global Ozone Research and Monitoring Project - Report No. 25, Chapter 6 in Scientific assessment of ozone depletion, 1991. [Online]. Available: <http://ciesin.org/docs/011-551/011-551.html> [Accessed 20 06 2013].
- [28] N. M. Nguyen, A. Denat, N. Bonifaci, O. Lesaint and M. Hassanzadeh, "Impulse Partial Discharges and Breakdown of CF<sub>3</sub>I in Highly Non-Uniform Field," *Eighteenth International Conference on Gas Discharges and Their Applications*, Ernst-Moritz-Arndt-University, Greifswald, Germany, pp. 330-333, 2010.
- [29] United States Environmental Protection Agency (EPA), "EPA Overview of Greenhouse Gases," 09 09 2013. [Online]. Available:<http://epa.gov/climatechange/ghgemissions/gases/fgases.html>. [Accessed 01 02 2014].
- [30] R. H. Petrucci, W. S. Harwood and F. G. Herring, *General Chemistry Principles and Modern Applications (8th Edition)*, Eighth Edition, Upper Saddle River, New Jersey, New Jersey: Prentice-Hall Inc., ISBN 0-13-014329-4, 2002.
- [31] P. Atkins and L. Jones, *Chemistry Molecules, Matter, and Change*, Third Edition, New York: W. H. Freeman and Company, ISBN 0-7167-2832-X, 1997.

- [32] L. G. Christophorou, J. K. Olthoff and D. S. Green, "Gases for Electrical Insulation and Arc Interruption: Possible Present and Future Alternatives to Pure SF<sub>6</sub>," *NIST Technical Note 1425*, Gaithersburg, Maryland, 1997.
- [33] N. L. Allen, "Mechanisms of air breakdown," in *Advances in High Voltage Engineering*, vol. 40, A. Haddad and D. Warne, Eds., London, IEE Power & Energy Series 40, The Institution of Electric Engineers, pp. 1-35, 2004.
- [34] Deng Yun-Kun and Xiao Deng-Ming, "The effective ionization coefficients and electron drift velocities in gas mixtures of CF<sub>3</sub>I with N<sub>2</sub> and CO<sub>2</sub> obtained from Boltzmann equation analysis," *Chin. Phys. B*, vol. 22, no. 3, pp. 035101-1 - 035101-6, 2013.
- [35] J. d. Urquijo, A. M. Juárez, E. Basurto and J. L. Hernández-Ávila, "Electron impact ionization and attachment, drift velocities and longitudinal diffusion in CF<sub>3</sub>I and CF<sub>3</sub>I-N<sub>2</sub> mixtures," in *Journal of Physics D: Applied Physics*, Mexico, vol. 40, pp. 2205-2209, 2007.
- [36] H. Hasegawa, M. Shimosuma and H. Itoh, "Properties of electron swarms in CF<sub>3</sub>I," *Appl. Phys. Lett.* 95(10), vol. 101504, pp. 101504-1 - 101504-3, 2009.
- [37] M. Kimura and Y. Nakamura, "Electron swarm parameters in CF<sub>3</sub>I and a set of electron collision cross sections for the CF<sub>3</sub>I molecule," *J. Phys. D: Applied Physics* 43, vol. 43, no. 14, p. 145202, 2010.
- [38] S. Sangkasaad, "AC breakdown of point-plane gaps in compressed SF<sub>6</sub>," in *Proceedings of 2nd international symposium on HV technology*, Zurich, pp. 379-384, 1975.
- [39] M. kamarol, Y. Nakayama, T. Hara, S. Ohtsuka and M. Hikita, "Gas Decomposition Analysis of CF<sub>3</sub>I under AC Partial Discharge of Non-uniform Electric Field Configuration," *Japan-Korea Joint Symposium on Electrical Discharge and High Voltage Engineering*, Paper 17A-p8, pp. 161-164, 2007.
- [40] M. K. Donnelly, R. H. J. Harris and J. C. Yang, "CF<sub>3</sub>I Stability Under Storage," National Technical Information Service (NIST) Technical Note 1452, Technology Administration, U.S. Department of Commerce, Springfield, 2004.
- [41] T. A. Moore, S. R. Skaggs, M. R. Corbitt, R. E. Tapscott, D. S. Dierdorf and C. J. Kibert, "The Development of CF<sub>3</sub>I as a Halon Replacement", Albuquerque: The University of New Mexico, 1994. [Online]. Available: <http://oai.dtic.mil/oai/oai?verb=getRecord&metadataPrefix=html&identifier=ADA351312>. [Accessed 01 03 2014]
- [42] Y. Yokomizu, R. Ochiai and T. Matsumura, "Electrical and thermal conductivities of high tempertaure CO<sub>2</sub>-CF<sub>3</sub>I mixture and transient conductunce of residual arc during its extinction process," *Journal of Physics D: Applied Physics*, vol. 42, pp. 1-14, 2009.
- [43] M. S. Kamarudin, *Experimental investigation of CF<sub>3</sub>I-CO<sub>2</sub> gas mixture on the breakdown characteristics in uniform and non-uniform field configurations* (PhD Thesis), Cardiff, UK: Cardiff University, 2013.
- [44] M. K. M. Jamil, M. Ohtsuka, M. Hikita, H. Saitoh and M. Sakaki, "Gas by-products of CF<sub>3</sub>I under AC partial discharge," *Journal of Electrostatics* 69, vol. 69, pp. 611-617, 2011.
- [45] H. Toyota, S. Matsuoka and K. Hidaka, "Measurement of Sparkover Voltage and Time Lag Characteristics in CF<sub>3</sub>I-N<sub>2</sub> and CF<sub>3</sub>I-Air Gas Mixtures by using Steep-Front Square Voltage," in *Electrical Engineering in Japan, Translated from Denki Gakkai Ronbunshi*, Japan, Vol. 157, No.2, 2006.
- [46] Y. Y. Duan, M. S. Zhu and L. Z. Han, "Experimental vapor pressure data and a vapor pressure equation for Trifluoroiodomethane (CF<sub>3</sub>I)," in *Fluid Phase Equilibria*, Beijing, China, Vol. 121, pp. 227-234, 1996.
- [47] T. Takeda, S. Matsuoka, A. Kumada and K. Hidaka, "By-products of CF<sub>3</sub>I produced by spark discharge," *Presented at Japan-Korea Joint Symposium on Electrical Discharge and High Voltage Engineering*, Shibaura Institute of Technology, The University of Tokyo, Paper 17A-p7, pp. 157-160, 2007.

- [48] Y. Yokomizu, R. Ochiai and T. Matsumura, "Thermodynamic Properties at High Temperatures and Particles Present After Arc Extinction in CO<sub>2</sub>-CF<sub>3</sub>I Mixture," *The IEE Japan - Special Issue on IWHV 2008 (Sixth International WORKshop on High Voltage Engineering)*, Nagoya University, Japan, Paper 129-B, pp. 1187, 2009.
- [49] G. Dagan, G. Agam, V. Krakov and L. Kaplan, "Carbon Membrane Separator for Elimination of SF<sub>6</sub> Emissions from Gas-Insulated Electrical Utilities," United States Environmental Protection Agency (EPA), 08 01 2001. [Online]. Available: [http://www.epa.gov/electricpower-sf6/documents/conf00\\_dagan.pdf](http://www.epa.gov/electricpower-sf6/documents/conf00_dagan.pdf). [Accessed 01 01 2014].
- [50] H. M. Ryan, *High voltage engineering and testing (2nd Edition)*, Second Edition, vol. IEE Power and Energy Series 32, Stevenage: The Institution of Electrical Engineers, 2001.
- [51] H. M. Ryan, "Circuit breakers and Interruption," in *Advances in High Voltage Engineering*, vol. 40, A. Haddad and D. Warne, Eds., London, IEE Power & Energy Series 40, The Institute of Electric Engineers, p. 415-476, 2004.
- [52] L. Knudsen, "LKE Electric MV SF<sub>6</sub> switch," LKE Electric International, 2009. [Online]. Available: <http://lke-electric.com/mv-sf6.html>. [Accessed 01 01 2014].
- [53] UK Power Networks, *Estimated UK Power Networks Distribution Network Installed Switchgear (Special permission)*, London: UK Power Networks, 2013.
- [54] Schneider Electric, "Ringmaster range indoor/outdoor switchgear Installation, operation and maintenance instructions," Version 11, Leeds: Schneider Electric, 2007. [Online]. Available: <http://www.schneider-electric.com>. [Accessed 01 02 2013].
- [55] Schneider Electric, *Schneider Electric Ringmaster SE6 Faceplate*, Leeds: Schneider Electric, 2010.
- [56] C. Steed, "2012 Business Carbon Footprint (BCF) Report Commentary & Methodology," London: UK Power Networks (Operations) Limited, 2013. [Online]. Available: [http://www.ukpowernetworks.co.uk/internet/en/about-us/documents/UKPN-BCF-2013-for-External-Publishing-Final-for-sign-off\(Jul13\)](http://www.ukpowernetworks.co.uk/internet/en/about-us/documents/UKPN-BCF-2013-for-External-Publishing-Final-for-sign-off(Jul13)). [Accessed 01 03 2014].
- [57] Western Power Distribution, "Environmental facts and figures," Western Power Distribution, 01 04 2013. [Online]. Available: <http://www.westernpower.co.uk/Social-Responsibility/Environment/Facts-and-Figures.aspx>. [Accessed 01 03 2014].
- [58] Scottish and Southern Energy Power Distribution, "Environmental Impact Annual Report 2012/13," SSE Power Distribution, 2013. [Online]. Available: [http://www.ssepd.co.uk/uploadedFiles/Controls/Lists/Have\\_your\\_say/Environmental\\_impact/EnvironmentalImpactReport2012\\_2013.pdf](http://www.ssepd.co.uk/uploadedFiles/Controls/Lists/Have_your_say/Environmental_impact/EnvironmentalImpactReport2012_2013.pdf). [Accessed 01 03 2014].
- [59] European Commission Emission Database for Global Atmospheric Research (EDGAR), "CO<sub>2</sub> time series 1990-2012 per region/country," 08 09 2014. [Online]. Available: <http://edgar.jrc.ec.europa.eu/overview.php?v=CO2ts1990-2012>. [Accessed 05 09 2014].
- [60] Schneider Electric, "Discovering our offer at a glance: Products and equipment for Medium Voltage distribution networks up to 5 MVA," Schneider Electric Industries SAS, 2011. [Online]. Available: <http://www.schneider-electric.com>. [Accessed 01 06 2013].
- [61] Schneider Electric, "Electrical distribution: Medium voltage product panorama," Glasgow, Chippenham, Wilmslow: Schneider Electric Ltd., 2010. [Online]. Available: <http://www.schneider-electric.com>. [Accessed 01 06 2013].
- [62] British Standard Institution (BSI), "BS EN 60060-1: High-voltage test techniques Part 1: General definitions and test requirements," 2010. [Online]. Available: [www.bsigroup.com/standards](http://www.bsigroup.com/standards). [Accessed 01 04 2011].
- [63] Schneider Electric, "Medium Voltage Distribution Fluokit Air insulated switchgear up to 24 kV: Technical Characteristics Catalogue 2011," 2011. [Online]. Available: [www.schneider-electric.com](http://www.schneider-electric.com). [Accessed 01 05 2012].
- [64] Schneider Electric, *Fluokit M24+ Faceplate*, France: Schneider Electric, 2011.

- [65] Schneider Electric, "Ringmaster range indoor/outdoor switchgear: Installation, operation and maintenance instructions," Leeds: Schneider Electric, 2007. [Online]. Available: <http://www.schneider-electric.com>. [Accessed 01 02 2013].
- [66] Schneider Electric, "Secondary Distribution Switchgear Fluokit M24+ Air insulated switchgear: Instructions Installation - Commissioning - Operation - Maintenance," France: Schneider Electric, 2011. [Online]. Available: <http://www.schneider-electric.com>. [Accessed 01 02 2013].
- [67] Schneider Electric, "Medium Voltage Distribution Fluokit M24+ Replacement of an ISR switch Instructions," 2010. [Online]. Available: [www.schneider-electric.com](http://www.schneider-electric.com). [Accessed 01 05 2012].
- [68] Synquest Laboratories, Inc., "CF<sub>3</sub>I Material Safety Data Sheet," 2012. [Online]. Available: <http://synquestlabs.com/>. [Accessed 15 01 2014].
- [69] Synquest Laboratories, Inc., "C<sub>2</sub>F<sub>6</sub> Material Safety Data Sheet," 2012. [Online]. Available: <http://synquestlabs.com/>. [Accessed 15 01 2014].
- [70] SynQuest Laboratories, Inc., "CHF<sub>3</sub> Material Safety Data Sheet," 2011. [Online]. Available: <http://synquestlabs.com/>. [Accessed 15 01 2014].
- [71] SynQuest Laboratories, Inc., "C<sub>3</sub>F<sub>8</sub> Material Safety Data Sheet," 2013. [Online]. Available: <http://synquestlabs.com/>. [Accessed 15 01 2014].
- [72] SynQuest Laboratories, Inc., "C<sub>3</sub>F<sub>6</sub> Material Safety Data Sheet," 2013. [Online]. Available: <http://synquestlabs.com/>. [Accessed 15 01 2014].
- [73] SynQuest Laboratories, Inc., "C<sub>2</sub>F<sub>5</sub>I Material Safety Data Sheet," 2012. [Online]. Available: <http://synquestlabs.com/>. [Accessed 15 01 2014].
- [74] Apollo Scientific, *SF<sub>6</sub> and CF<sub>3</sub>I Goods and Transportation Quotation*, Manchester: Apollo Scientific, 2012.
- [75] Synquest Laboratories, *CF<sub>3</sub>I Goods and Transportation Quotation*, Synquest Laboratories, 2012.
- [76] Sigma-Aldrich, *SF<sub>6</sub> and CF<sub>3</sub>I Goods and Transportation Quotation*, Sigma-Aldrich, 2012.
- [77] Dilo, "Valves and connections for SF<sub>6</sub>" (Catalogue), Babenhausen: Dilo, 2012. [Online]. Available: <http://www.dilo-gmbh.com/index.php?id=697> [Accessed: 02 02 2012]
- [78] Dilo, "Dilo Mini Series Z579R02 Mini Components mounted on cylinder cart" (Brochure), Babenhausen: Dilo, 2012. [Online]. Available: <http://www.dilo-gmbh.com/index.php?id=697> [Accessed: 02 02 2012]
- [79] J. Wolf, *Manual Instruction of Impulse Voltage Generator Type SGS*, Switzerland: Haefely Test AG, 2002.
- [80] DRS Data & Imaging systems Inc., "DRS's Lightning RDT High-speed digital camera," 26 02 2004. [Online]. Available: <http://www.mctcameras.com/specsheets/Lightning%20RDT%20data%20sheet.pdf>. [Accessed 01 03 2014].
- [81] Schneider Electric, *ISR Load break switch Technical drawings*, France: Special permission from Schneider Electric, 2006.
- [82] Schneider Electric, *SA SE Gas Enclosure Technical Drawings*, Leeds, England.: Yorkshire Switchgear & Engineering Co Ltd., Special permission from Schneider Electric, 1992.
- [83] G. Eriksson and ABB AB, Corporate Research, "Easy Evaluation of Streamer Discharge Criteria," in *Proceedings of the 2012 COMSOL Conference*, Milan, 2012.
- [84] M. database, "LXCAT," [Online]. Available: <http://www.lxcat.laplace.univ-tlse.fr>. [Accessed 04 06 2013].
- [85] G. J. Hagelaar and L. C. Pitchford, "Solving the Boltzmann equation to obtain electron transport coefficients and rate coefficients for fluid models," *Plasma Sources Science and Technology*, vol. 14, no. 4, pp. 722-733, 2005.

- [86] G. J. Hagelaar, "BOLSIG+: Electron Boltzmann Equation Solver," Toulouse, France, 2010. [Online]. Available: <http://www.bolsig.laplace.univ-tlse.fr/download.php>. [Accessed 06 06 2013]
- [87] T. Christen, "Nonstandard High-Voltage Electric Insulation Models," *Excerpt from the Proceedings of the 2012 COMSOL Conference, ABB Corporate Research*, Milan, 2012.
- [88] T. Christen, "Streamer Inception and Propagation from Electric Field Simulations," in *Proceedings of the 2012 COMSOL Conference, ABB Corporate Research*, Milan, 2012.
- [89] Lucy Switchgear, *SCRMU Instruction & Operation Manual Medium Voltage 12 -24 kV*, Oxford: Lucy Switchgear, 1999.
- [90] Lucy Switchgear, "SABRE VRN6a SF6 RMU Automated distribution solutions - towards smarter electrical networks," Selangnor, Malaysia: Lucy Switchgear, LS00001 SABRE VRN6a (Asia) 06 2013 9776, 2013. [Online]. Available: [www.lucyswitchgear.com](http://www.lucyswitchgear.com) [Accessed 04 07 2013]
- [91] W. Lucy & Co. Ltd. Oxford., *Lucy Swithgear SCRMU(M) Faceplate*, Oxford: Lucy Switchgear, 2000.
- [92] J. C. Tobias, R. P. Leeuwerke, A. L. Brayford and A. J. Robinson, "The use of Sectionalising Circuit Breakers in Urban MV Distribution Networks," in *Fifth International Conference on Trends in Distribution Switchgear: 400V-145kV for Utilities and Private Networks, Conference Publication No. 459*, London, pp. 102-108, 1998.
- [93] Schneider Electric SA, "Medium Voltage Distribution: Rollarc R400-R400D contactor 1 to 12 kV," Nadar, France: Schneider Electric SA, REF AC0226/3E, 1998. [Online]. Available: <http://www.schneider-electric.com>. [Accessed 01 02 2013].
- [94] B. M. Weedy and B. J. Cory, *Electric Power Systems*, Fourth Edition, New York: John Wiley Sons, 1998.
- [95] H. M. Ryan and G. R. Jones, *SF<sub>6</sub> Switchgear*, IEE Power Engineering Series 10, London: Peter Peregrinus Ltd. on behalf of the Institute of Electrical Engineers (IEE), 1989.
- [96] ABB, "Product brochure: Gas-insulated Switchgear Type ELK-3 GIS for maximum performance, 420 kV," 2011. [Online]. Available: [http://www05.abb.com/global/scot/scot245.nsf/veritydisplay/9b34650a375c3666c1257b130057bd1b/\\$file/ELK-3\\_420\\_1HC0029799AGEn.pdf](http://www05.abb.com/global/scot/scot245.nsf/veritydisplay/9b34650a375c3666c1257b130057bd1b/$file/ELK-3_420_1HC0029799AGEn.pdf). [Accessed 15 02 2013].
- [97] Siemens AG, "Gas-insulated transmission lines (GIL) - High-power transmission technology," Germany: Siemens AG, 2012. [Online]. Available: <http://www.energy.siemens.com/hq/en/power-transmission/gas-insulated-transmission-lines.htm>. [Accessed 04 02 2014]
- [98] Dilo, "Dilo Evacuating and refilling devices," Babenhausen: Dilo, 2012. [Online]. Available: [http://www.dilo-gmbh.com/index.php?eID=tx\\_nawsecuredl&u=0&file=fileadmin/user\\_upload/Downloads/englisch/SF6-Gashandling/Gasnachfuell-\\_und\\_Evakuiergeraete/SF6\\_gas\\_refilling\\_device\\_3-393-R001\\_R002\\_GB.pdf&t=1399479434&hash=0cc0ef58ee9606d15b1d962ca2465ff8bcf20a50](http://www.dilo-gmbh.com/index.php?eID=tx_nawsecuredl&u=0&file=fileadmin/user_upload/Downloads/englisch/SF6-Gashandling/Gasnachfuell-_und_Evakuiergeraete/SF6_gas_refilling_device_3-393-R001_R002_GB.pdf&t=1399479434&hash=0cc0ef58ee9606d15b1d962ca2465ff8bcf20a50). [Accessed 02 02 2014].
- [99] Dilo Armaturen und Anlagen GmbH, *Dilo Operating Manual for Z579R03*, Babenhausen: Dilo, 2012.

# APPENDIX A

## A1. Primary substations

The double busbar arrangement is widely used for large important supplies (i.e. as bulk supply points), which in the UK typically operate at 132/33 kV [51]. For large industrial customers, higher security may be built into the substation design and, therefore, more switchgear is often implemented. Modern busbar protection is very reliable such that the same degree of availability can normally be achieved without the need to resort to a second busbar system [51].

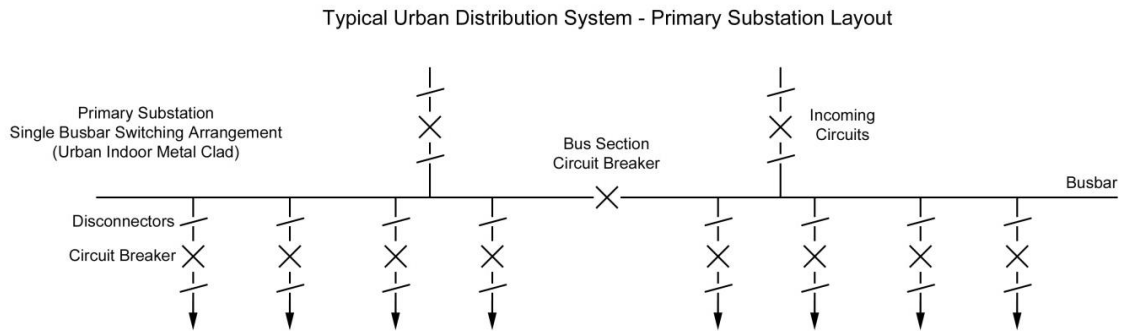


Figure A1: Typical distribution primary substation layout: single busbar switching arrangement [51].

A primary substation feeding urban networks commonly has indoor metal enclosed switchgear whereas a primary substation feeding a rural network is more commonly of the open terminal air-insulated design. A common switching arrangement for either substation design is single busbar. This single busbar is often split into two sections and interconnected via a bus section circuit breaker, as shown in Figure A1. There are usually two incoming circuits – one feeding each section of the busbar; there may be typically five outgoing circuits [51] feeding either multi-radial networks for overhead rural systems or ring circuits for urban connected networks. For maintenance purposes, disconnectors are fitted either side of the circuit breaker [51]. Facilities are also provided for earthing

outgoing or incoming circuits and for earthing each section of the busbar; current transformers (CTs) may be fitted on the outgoing circuit for either protection or for tariff metering purposes (e.g. for large single customers) [51].

## **A2. Urban distribution system switching arrangements and secondary substations**

This system is fed from a primary distribution switchboard, each outgoing feeder on one section of the busbar feeds via an 11 kV cable network to typically 10 to 12 secondary distribution substations which are electrically connected within the ring circuit. This ring circuit is connected back to a feeder on the adjacent section of busbar at the same substation [50]. Typical distribution voltages used outside the UK may range from 10 kV to 20 kV. 6.6 kV systems were common at one time within the UK, but have now been largely phased out. This ring circuit usually has a normally open point, the purpose of which is to minimise the number of customers affected by a faulted section of the ring circuit [51].

Ring main units (RMU) can be manually operated; hence fault location and customer re-energisation is time consuming; a modern tendency is for the RMUs to be fitted with remotely operable mechanisms. This ensures that the switching times can be reduced by allowing remote substation switching or, with modern intelligence systems, to allow automatic deenergisation of a section around the point fault. The tee-off point of the ring circuit feeds via an 11 kV/415 V, three-phase transformer to an LV fuse board, typically having up to five outgoing circuits which feed directly to large customers or groups of customers; in most of these LV circuits, it is possible to achieve an LV backfeed from an adjacent ring main unit, thus maximising the number of customers on supply while fault repairs are in progress [51].

Open ring configuration is the most commonly used topology for MV distribution networks. Open rings are simple to operate and can be implemented using low cost MV switchgear. The ring provides at least two alternative paths to each secondary MV/LV substation fed from it, the maximum number of substations connected to a single ring being typically 20. The MV/LV substations are connected to the ring by load break switches, all of which are closed except one, which is referred to as the Normal Open Point (NOP). Each section of the ring can be treated as a simple radial feeder, with the only protection being time graded IDMT overcurrent protection at the primary substation. An MV cable fault causes the feeder breaker to trip, disconnecting all the MV/LV substations fed from it. Supply can then be restored to the healthy part of the system by opening switches at each end of the faulted cable to isolate the fault, closing the primary feeder breaker and switch at the NOP. Traditionally, restoration has been achieved manually, a process that takes several hours. Telecontrol systems enable the restoration of supplies to a large number of customers within minutes by monitoring and controlling a few strategically positioned MV switches. This improves availability by reducing the time taken to identify and isolate the faulty network section [92].

### **A3. MV distribution equipment design**

For MV contactors such as the Rollarc R400 – 400D design, manufactured by Schneider Electric, the arc rotation method is employed to break the arc between contacts using SF<sub>6</sub> gas. In the rotating arc technique, the arc is set in motion between two circular arcing contacts as shown in Figure A2 [93]. When this occurs, SF<sub>6</sub> is utilised to extinguish the arc which rotates through it between the open contacts. After the arc is extinguished, the gap between the contacts recovers its initial dielectric strength because of the inherent qualities of SF<sub>6</sub> and its fast recovery time [4] [13].

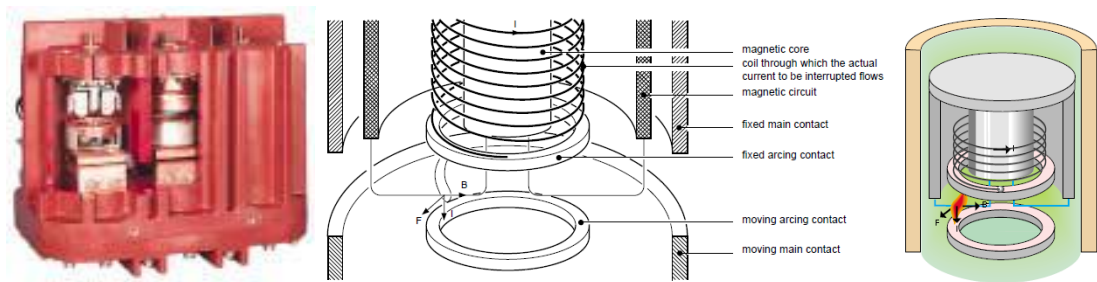


Figure A2: Rollarc R400 – 400D arc rotation contactor [93].

For switchgear such as SF<sub>6</sub> gas circuit breakers, the self-blast (puffer) contact design is commonly employed to break various circuits on the network. One such design is shown in Figure A3 where the SF<sub>6</sub> gas is trapped in a compartment whilst the circuit breaker is in its fully closed position. When the moving cylinder to which the contacts are attached is retracted, the SF<sub>6</sub> gas is compressed and then released through a nozzle at the point where the arc between contacts takes place. During the arc extinction process, the SF<sub>6</sub> is ‘puffed’ over the arc and continues for a period of time until the arc is extinguished and the contact space filled with a reasonable amount of gas [50] [4] [94] [95]. A circuit breaker of self-blast puffer design is shown in Figure A3.

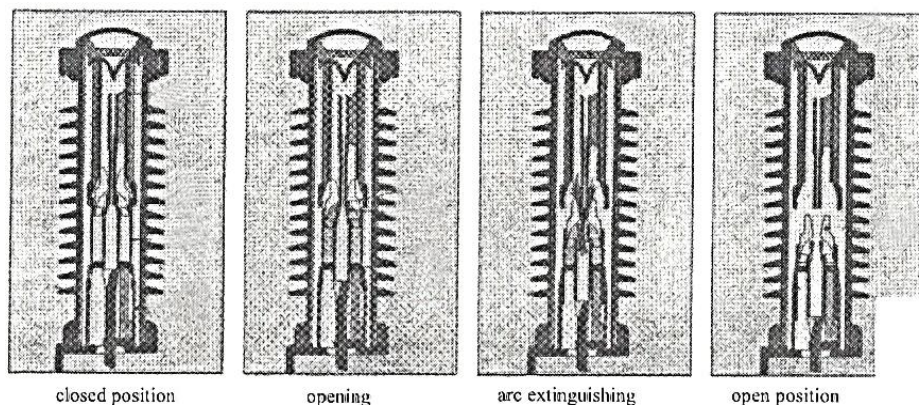


Figure A3: Self blast puffer circuit breaker [50].

#### A4. HV gas insulated switchgear (GIS)

The most common equipment used in HV distribution is gas insulated switchgear (GIS) and refers to all types of equipment commonly incorporated into a modular design so that various tasks can be achieved without a re-design of each piece of equipment [95]. Some

of the equipment incorporated into GIS includes circuit breakers, disconnectors, earthing switches, voltage and current transformers and several different line connections between these parts, all being insulated by SF<sub>6</sub> gas [94]. An example of a bay of SF<sub>6</sub> GIS is shown in Figure A4, manufactured by ABB with a rated voltage of 550 kV.

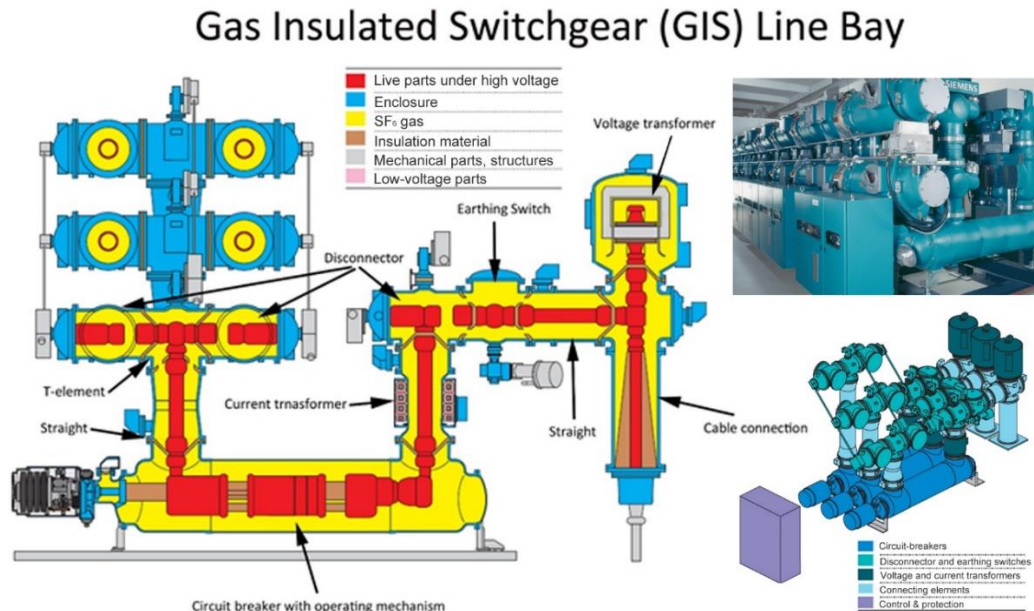


Figure A4: ABB SF<sub>6</sub> gas insulated switchgear (GIS) line bay ELK-3 model for 550 kV [96] and Siemens SF<sub>6</sub> GIS line bays, 8DN9 model [12].

SF<sub>6</sub> GIS is generally found in areas where substation space is at a premium, and to keep the cost low, the substation must be kept within certain site limits, such as in the urban environment. Therefore, HV SF<sub>6</sub> GIS has been specifically designed to minimize the space needed and typically operates at a pressure of 0.5 MPa (abs) or 5 bar G [10].

### A5. Gas insulated lines (GIL)

Gas insulated lines (GIL) are an alternative to overhead lines when the project demands a line capable of transmitting extra high voltage (EHV) and / or extra high currents (EHC) within a restricted space or underground. An example of a GIL is shown in Figure A5.

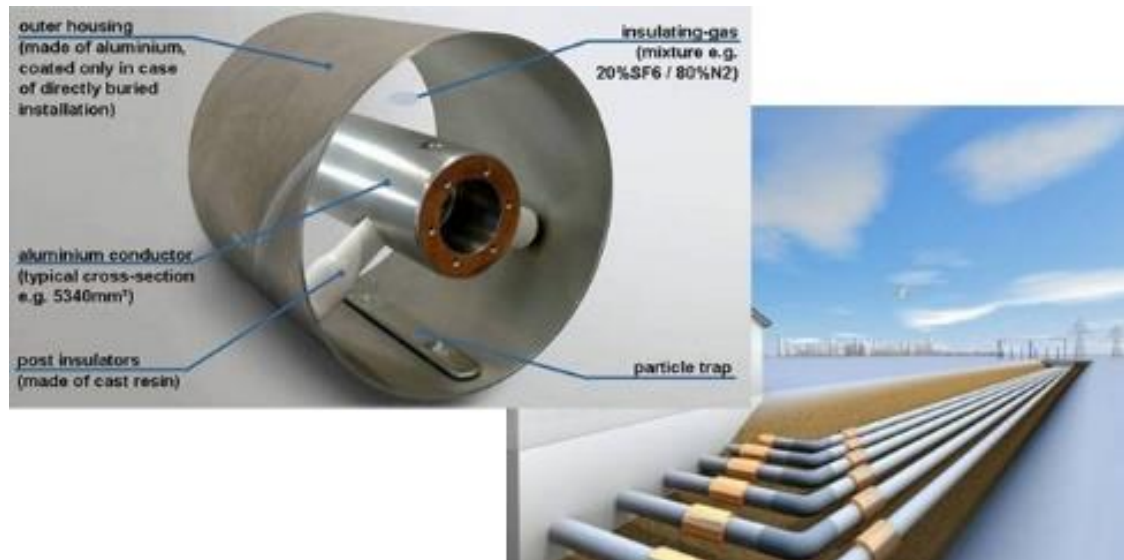


Figure A5: Siemens gas insulated lines [18] [97].

Typical GIL installations can have a length of 100 m up to 100 km and have an operating voltage between 220 kV and 550 kV for transmission purposes. The operational current of GIL can be between 2000 A and 5000 A. GIL is commonly filled with a mixture of  $\text{SF}_6$  and nitrogen ( $\text{N}_2$ ), as lines filled with pure  $\text{SF}_6$  would be very expensive and potentially pose a very high environmental risk. The gas mixture used to fill GIL is commonly 20%  $\text{SF}_6$  and 80%  $\text{N}_2$  so as to minimise the use and cost of  $\text{SF}_6$  whilst retaining a relatively high insulation strength of the gas mixture. Such a mixture operates up to a pressure of 0.7 MPa (abs) or 7 bar G. The GIL that are used are then sealed for their lifetime which can be greater than 50 years long [97]. The use of GIL is similar to applications of power cables but in situations where a higher voltage and higher transmission power are needed. GIL can be a very attractive option for specific projects with a proven operational safety and a 35 year service record [18].

## APPENDIX B

This section describes and outlines the vacuuming, gassing and de-gassing operations which were achieved with the Dilo Mini Series. The various gas connections for each operation are shown specific to the piece of switchgear utilised for testing. The Dilo equipment uses a connection known as a DN8 connector. The Ringmaster uses a quick release Hansen connector and the Fluokit uses a Raccord valve. For testing the Raccord valve had a permanent adapter to a Hansen connector attached to it.

### B1. Gas connections and adapters

Figures B1 and B2 show the equipment used throughout testing. To clarify the gas connections used throughout testing the labels shown in these figures are repeated throughout this appendix.

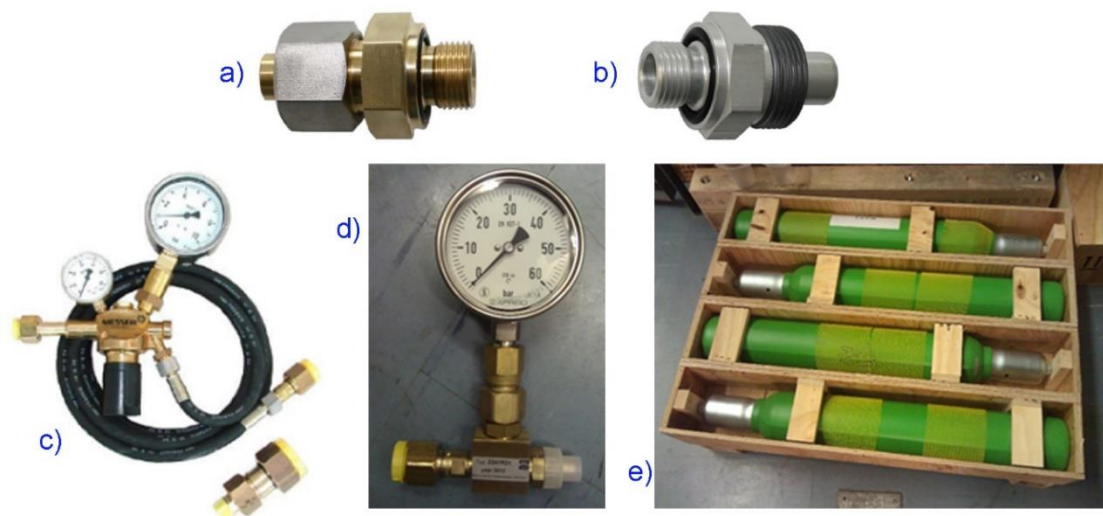


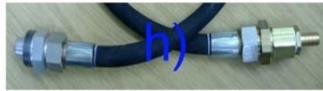
Figure B1: a) Dilo soldering union with O-ring PN64 b) VK/A-02/8 T coupling groove part DN8 with O-ring c) 3-393-R001 gas refilling device d) Z247R21 Tee piece 0-60 bar pressure gauge e) 4 x 10 L steel gas storage cylinder [77] [98].



Pressure gauge (-1 to 1 bar) with 1/2" (M) BSP fitting attached to 1/2" (F) to 1/4" (M) BSP decreasing joint to Hansen (F) coupling used for gas filling and recovery of all switchgear



CF3I Bottle 1/4" (F-F) NPT Ball valve connected to 1/4" (M) NPT to 1/4" (M) BSP screw thread adapter to Hansen (M) adapter used to connect CF3I bottle for filling of CF3I-CO2 storage cylinder and straight filling of switch disconnectors



Dilo DN8 (M) connector attached to Dilo 1/2" (F-F) Hose attached to Dilo 1/2" (M) to 3/8" (M) BSP Adapter attached to 3/8" BSP (F-F) joint connected to 3/8" (M-M) BSP Hose Tail used for filling of CF3I-CO2 storage cylinder without gas mixture vessel



Dilo DN8 (M) connector attached to Dilo 1/2" (F-F) Hose attached to 1/2" (M) to 1/4" (M) decreasing joint attached to 1/4" (F) BSP Hansen adapter used for gas filling and recovery of all switchgear



Raccord thumb lock valve (F) to Dilo 1/2" (F-F) Hose attached to Dilo DN8 (M) Adapter used to adapt Fluokit M24+ gas point for all operations – this piece was not used as the screw lock adapter (below) was found to fit the connection more securely



Raccord valve (F) connected to Hansen (M) Adapter used to permanently adapt the Fluokit M24+ switch disconnector gas point for all operations



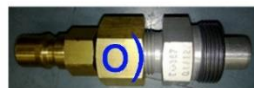
Hansen (F) to Hansen (M) extension used for the gas filling and recovery of the Ringmaster switch disconnector



Hansen T-connection, 2 x Hansen (M) and 1 x Hansen (F) used to connect pressure gauge for the gas filling and recovery of all switchgear



Dilo W 21.8 x 1.14 (F) Bottle Connection to Dilo DN8 (M) used to allow the vacuum pump to be connected to the empty Dilo storage cylinders to evacuate them of air before they were filled with CF3I-CO2

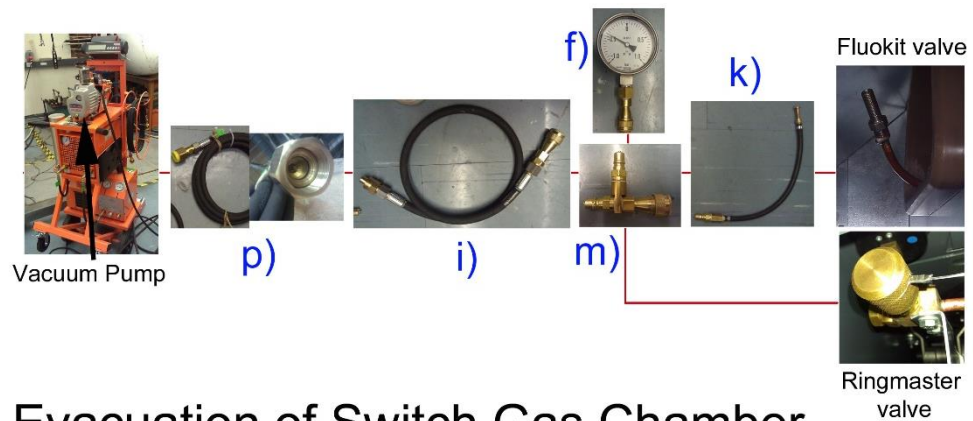


Dilo DN8 (M) connected to 1/2" (F) BSP to 1/4" (M) decreasing joint to Hansen (M) adapter used for the evacuation of any Hansen Connected part and hoses with the vacuum pump

Figure B2: Connections used for vacuuming, gassing and de-gassing the switch disconnectors.

## B2. Evacuation of the gas compartment with Dilo equipment

To vacuum the gas compartment, either the Ringmaster (l) or the Fluokit (k) from Schneider Electric, Figure B3 can be used to show how the Dilo vacuum pump can be connected to the gas compartment.



## Evacuation of Switch Gas Chamber

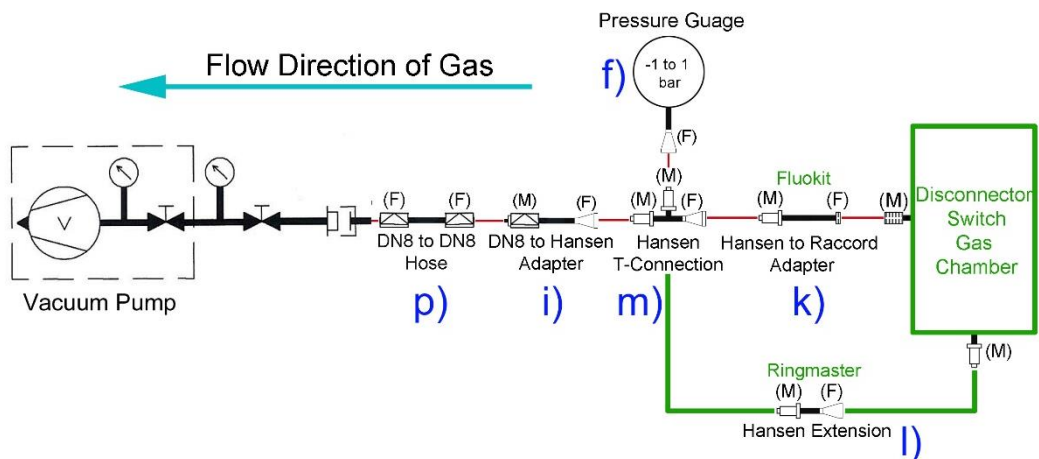


Figure B3: Evacuation of the switch disconnectors with Dilo equipment [99].

The following operational instructions can be used to vacuum the gas compartment [99]:

1. Connect the gas compartment to the vacuum pump unit.

If there is gas overpressure the gas must first be recovered (see recovery of gas later in this section). The Vacuum pump could be damaged by overpressure.

2. Switch on the vacuum pump.
3. Open the ball valve
4. Slowly open the stop valve

5. After evacuation of the connected gas compartment, confirmed by the connected vacuum gauge (approximately 30 mins for the Ringmaster and Fluokit for sufficient moisture content evaporation) close the ball valve and then the stop valve once again.
6. Switch off the vacuum pump [99].

### B3. Filling the gas compartment with gas with overpressure with Dilo equipment

To fill the Ringmaster (l) or the Fluokit (k) with gas overpressure using the Dilo equipment, Figure B4 can be used to show how to connect the Dilo equipment.

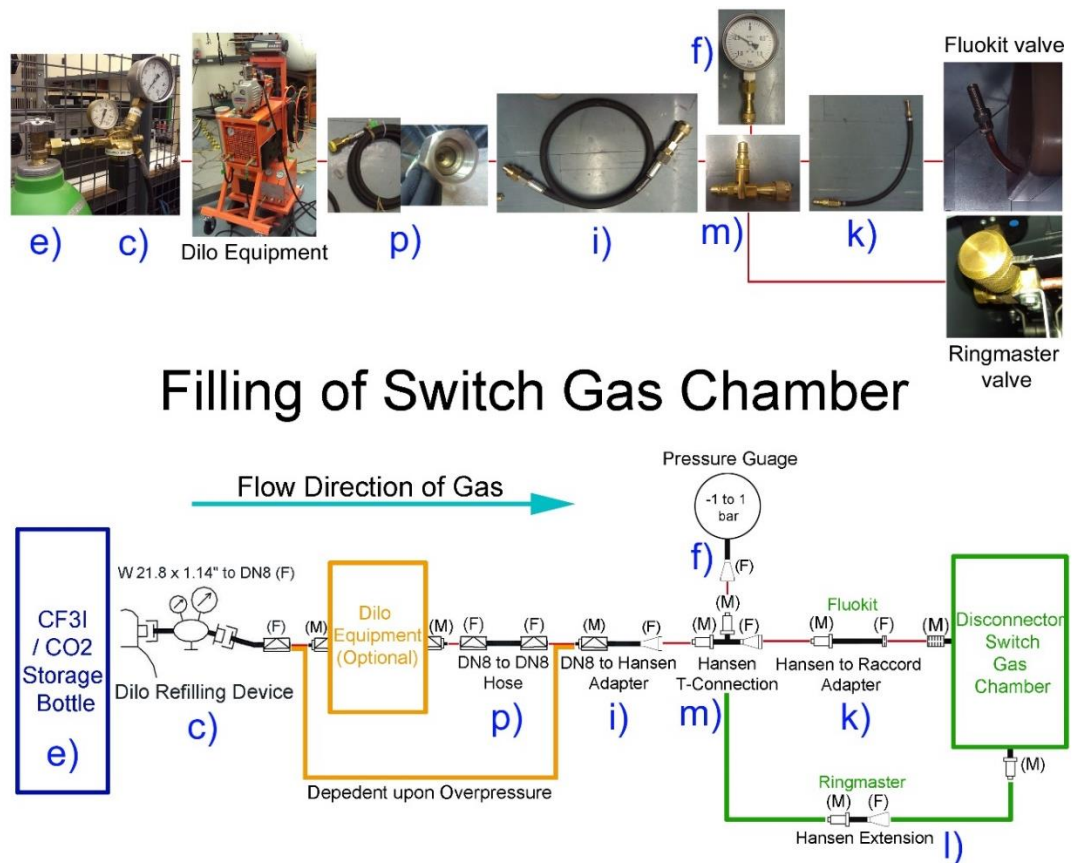


Figure B4: Filling the switch disconnectors with gas with overpressure with Dilo equipment [99].

The following operational instructions can be used to fill the gas compartment when the pressure in the storage bottle is higher than that required in the gas compartment (i.e. the dependent on overpressure line) [99]:

1. Connect the gas refilling device (c) to the storage bottle (e)

The connecting hoses (c, p, i, m, f, k and l) must be evacuated or filled with CF<sub>3</sub>I-CO<sub>2</sub>.

2. Set the pressure reducer (c) to the required filling pressure (0.35 bar G or 0.45 bar G), do not connect the switch disconnecter gas chamber.
3. Close the bottle valve (e) and connect the gas refilling device (c) directly to the switch disconnecter gas compartment.
4. Open the bottle valve (e) once again and fill the gas compartment to the required pressure.
5. After filling close the bottle valve (e) once again and disconnect the gas refilling device (c) [99].

#### **B4. Recovery and storage of the gas compartment with Dilo equipment**

To recover and store the gas in either the Ringmaster (l) or the Fluokit (k) from Schneider Electric, Figure B5 can be used to show how to connect the Dilo equipment. The following operational instructions can be used to recover and store the gas in the gas compartment [99]:

1. Connect the switchgear and the storage bottle (e) to the Dilo mini series as shown in Figure A5.

The connecting hoses (p, i, m, f, k and l) must be evacuated or filled with CF<sub>3</sub>I-CO<sub>2</sub> gas.

The input pressure must not exceed  $p_e$  10 bar (1100 kPa absolute).

2. Turn the ball valve to the illustrated position and open the storage bottle valve (e).
3. Start the compressor.
4. The input and output pressure can be read on the gauges.

5. After having reached the required suction pressure stop the compressor [99].

Do not overfill the storage bottles. Do not exceed the filling ratio of 1 kg SF<sub>6</sub>-gas per litre storage volume. In the Dilo mini series the compressor recovers gas from the switchgear down to 0 bar (g) or atmospheric pressure and the vacuum compressor recovers gas close to vacuum or -1 bar (g).

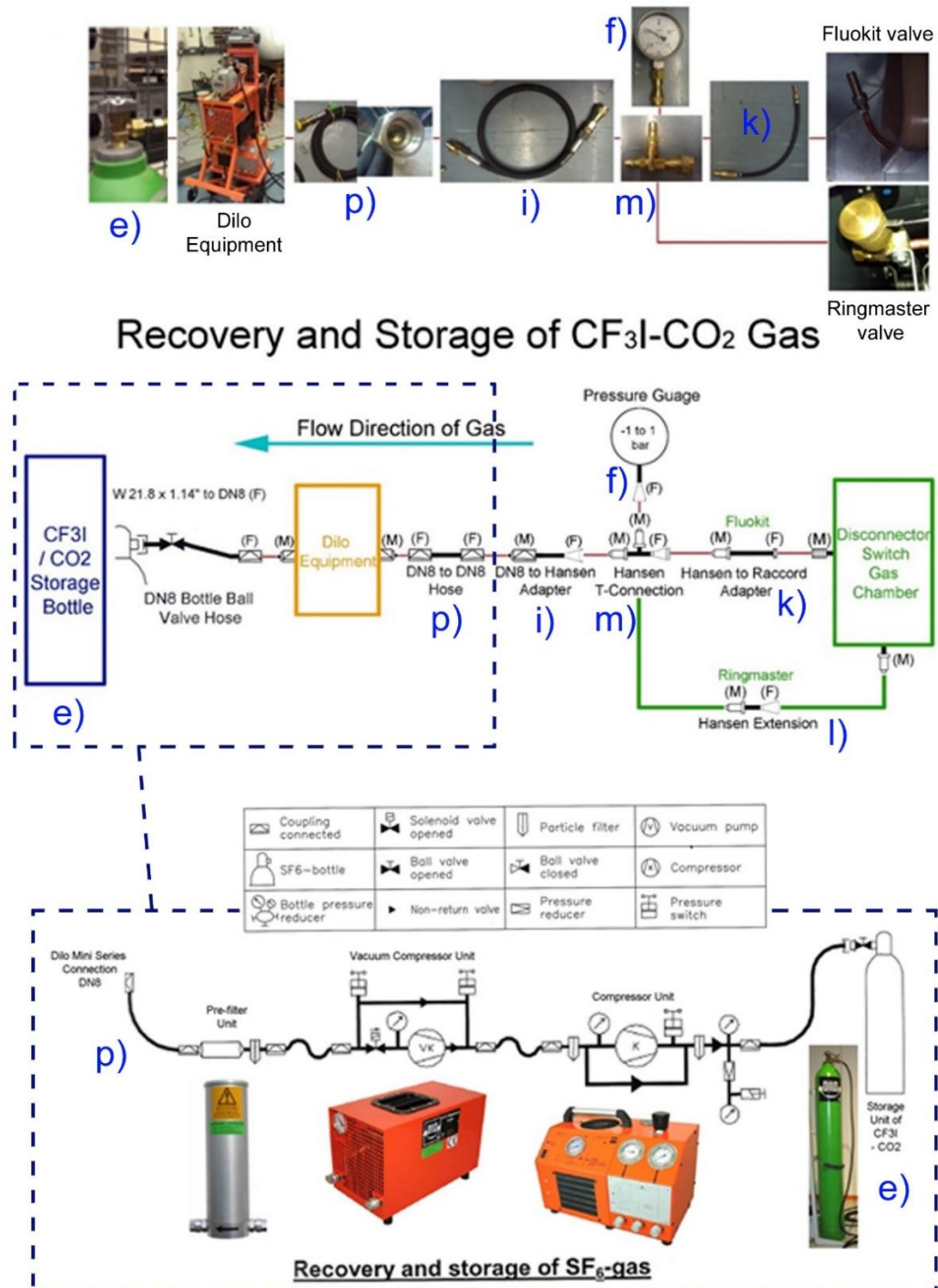


Figure B5: Recovery and storage of the gas compartment with Dilo equipment [99].

## B5. Main connection diagram for gas filling and recovery

Figure B6 shows the majority of gas connections that were utilised throughout testing.

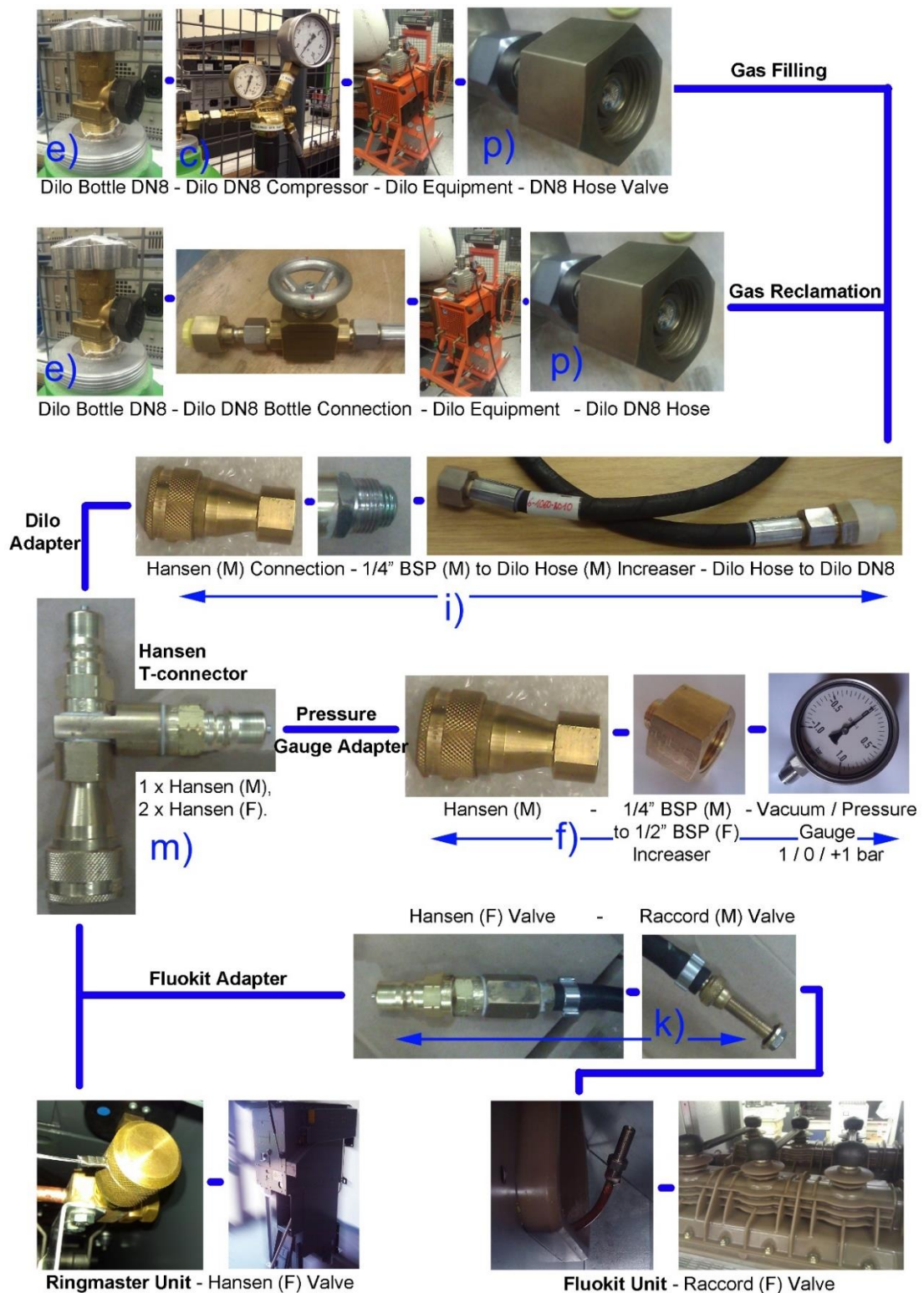
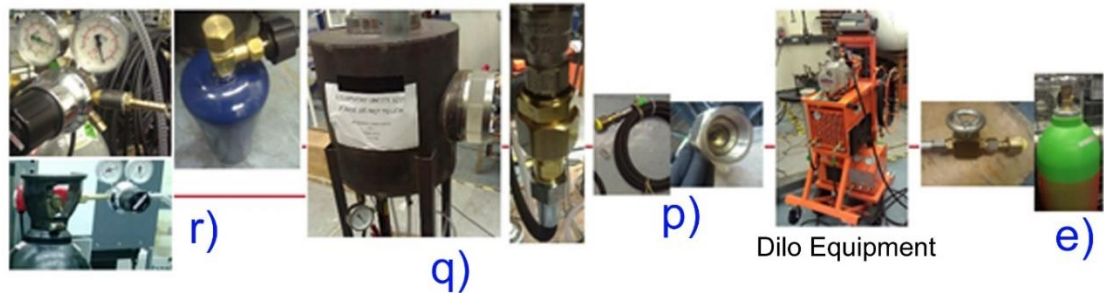


Figure B6: Dilo equipment connections to Fluokit and Ringmaster.

## B6. Gas connection for filling CF<sub>3</sub>I-CO<sub>2</sub> pressure-pressure mixture storage cylinders

Figure B7 shows the gas connections that were made in order to fill storage cylinders with CF<sub>3</sub>I-CO<sub>2</sub> gas mixtures. An extra gas chamber (q) was used to mix gases before the mixture was stored in a storage cylinder (e).



### Filling of CF<sub>3</sub>I / CO<sub>2</sub> Storage Cylinders via Gas Mixture Chamber

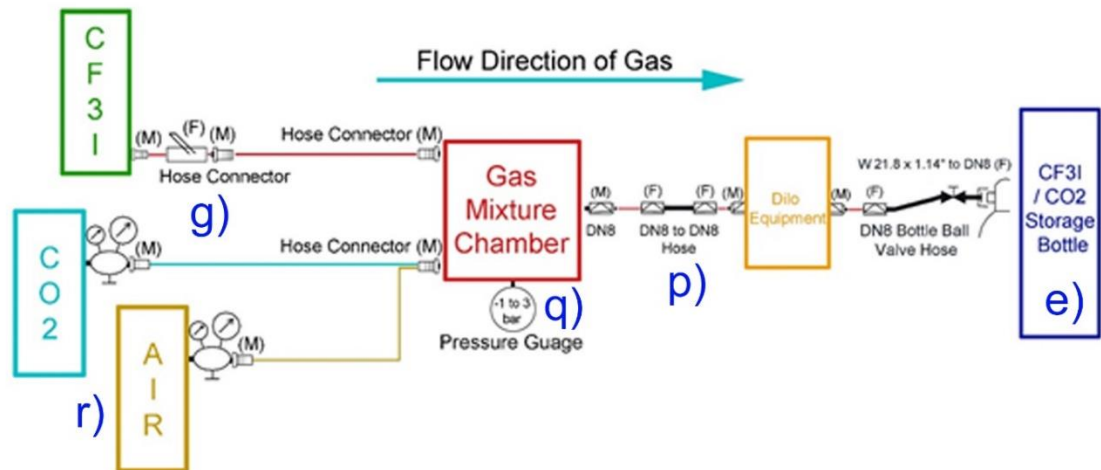


Figure B7: Filling of CF<sub>3</sub>I-CO<sub>2</sub> storage cylinders via gas mixture chamber.



Figure B8: Complete gas connections for the Ringmaster and Fluokit switch disconnectors.

# APPENDIX C

---

This section shows how the results of each gas mixture were recorded and an example resulting graph.

The following test procedure B of BS EN 60060-1, adapted for switchgear and controlgear that have self-restoring and non-self-restoring insulation, is the test procedure used for withstand testing. The switchgear has passed the impulse tests if the following conditions are fulfilled:

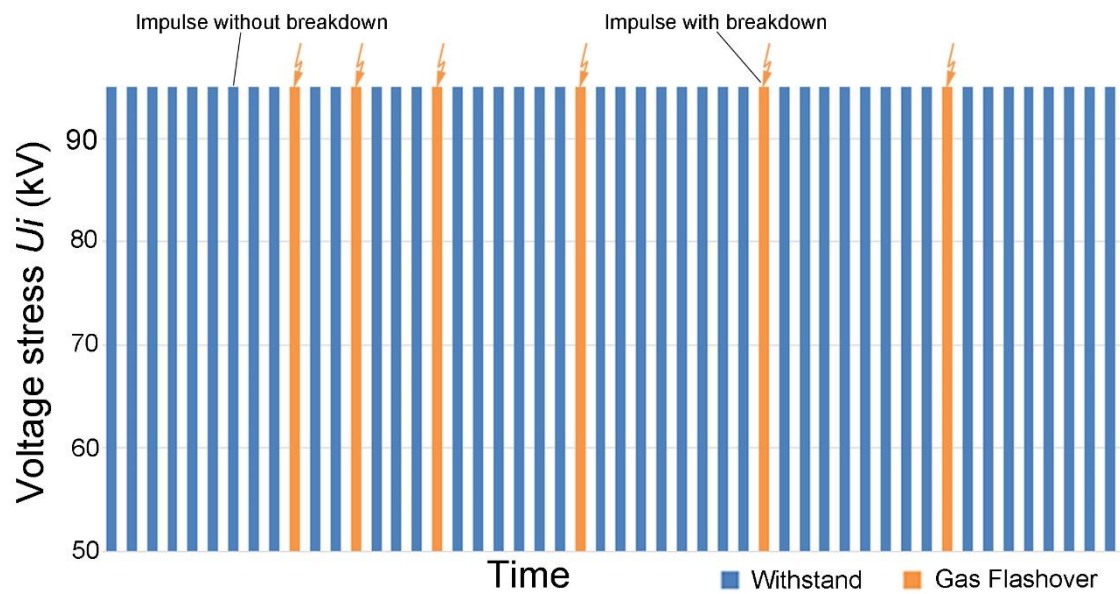
- each series has at least 15 tests
- the number of disruptive discharges shall not exceed two for each complete series
- no disruptive discharge on non-self restoring insulation shall occur. This is confirmed by 5 consecutive impulse withstands following the last disruptive discharge.

This procedure leads to a maximum possible number of 25 impulses per series [62] [1].

Figure C1 shows the resulting graph from a 95 kV withstand test where 50 lightning impulses are applied to Phase 1 of the Ringmaster switch disconnecter (R2). The results shown are for a gas mixture of 30:70%  $\text{CF}_3\text{I}-\text{CO}_2$  at 0 bar (g), each impulse that results in a breakdown is shown in orange with a flashover symbol above, other impulses that result without a breakdown are withstood and are shown in blue (Figure C1).

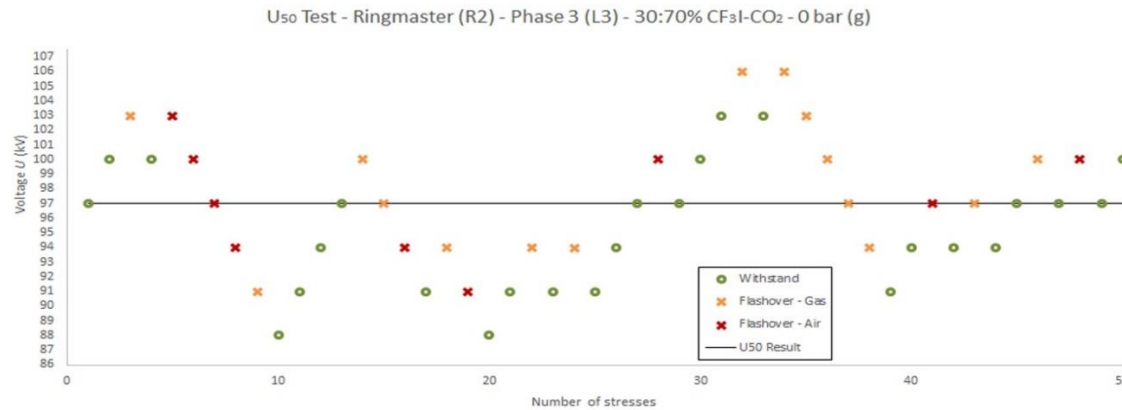
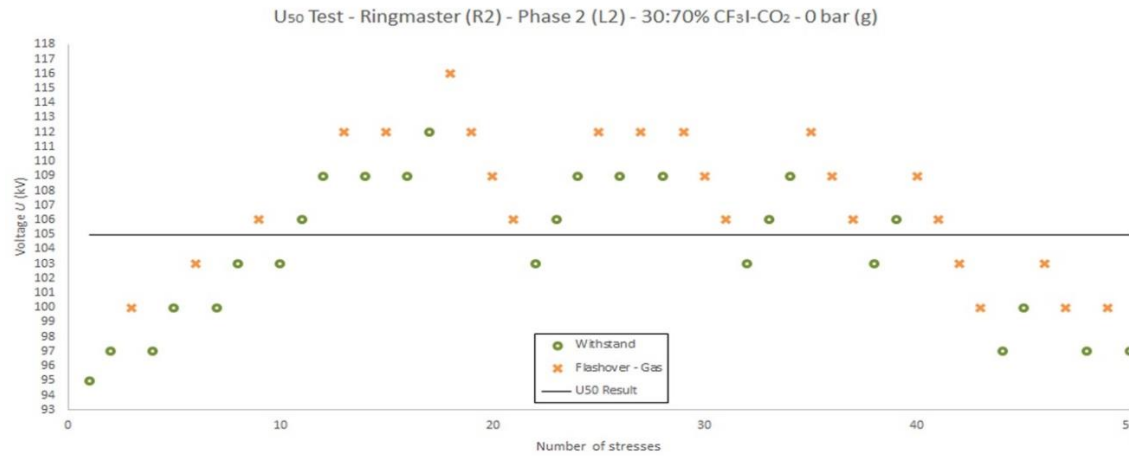
An example of a  $U_{50}$  lightning impulse test is shown in Figure C2 for the Ringmaster (R2) when filled with 30:70%  $\text{CF}_3\text{I}-\text{CO}_2$  at 0 bar (g).

95 kV Withstand test - Ringmaster (R2) - Phase 1 (L1) - 30:70% CF<sub>3</sub>I-CO<sub>2</sub> - 0 bar(g)



Number of voltage applications ( $n_i$ )	50
Number of disruptive discharges ( $k_i$ )	6
Disruptive-discharge frequency ( $f_i = k_i / n_i$ )	0.12

Figure C1: Example of a 95 kV withstand (Class 1) test – Ringmaster (R2) – Phase 1 (L1) – 30:70% CF<sub>3</sub>I-CO<sub>2</sub> – 0 bar (g).



1	8	1	116	50	116	$p = 50\%$	U <sub>50</sub> 105 kV
8	7	8	112		896		
11	6	11	109		1199		
9	5	9	106		954		
8	4	8	103		824		
7	3	7	100		700		
5	2	5	97		485		
1	1	1	95		95		
Number of $k_i$ groups at $u_i$	Number $i = 1, \dots, n$ of accepted voltages	Number $k_i$ of accepted groups	Voltages $u_i$ of accepted groups (kV)	Total number $m$ of accepted groups	Term $k_i \cdot u_i$	Disruptive voltage probability	Disruptive voltage $u_p$
2	7	2	106	50	212	$p = 50\%$	U <sub>50</sub> 97 kV
5	6	5	103		515		
10	5	10	100		1000		
12	4	12	97		1164		
11	3	11	94		1034		
8	2	8	91		728		
2	1	2	88		176		

Figure C2: Example of U<sub>50</sub> (Class 2) tests – Ringmaster (R2) – Phase 2 (L2) and Phase 3 (L3) – 30:70% CF<sub>3</sub>I-CO<sub>2</sub> – 0 bar (g).

## APPENDIX D

---

The 3D COMSOL model was made using one phase of contacts inside a gas filled box (Figure D1) and then duplicating this phase to create the other two phases. In creating these contacts it was important to replicate the schematics in as much detail as possible.

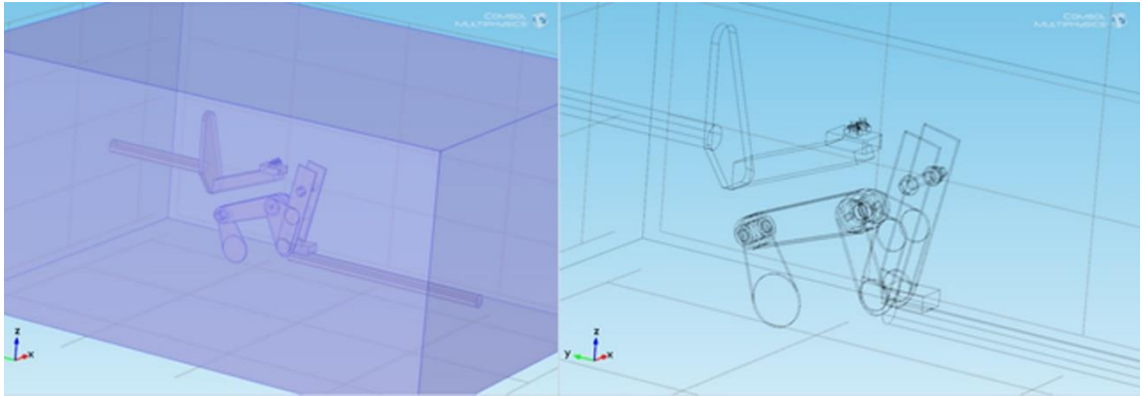


Figure D1: A gas chamber surrounding one phase of the Ringmaster Comsol model and its schematics.

Another element of the modelling process involved choosing the materials for each part of the design as shown in Figure D2.

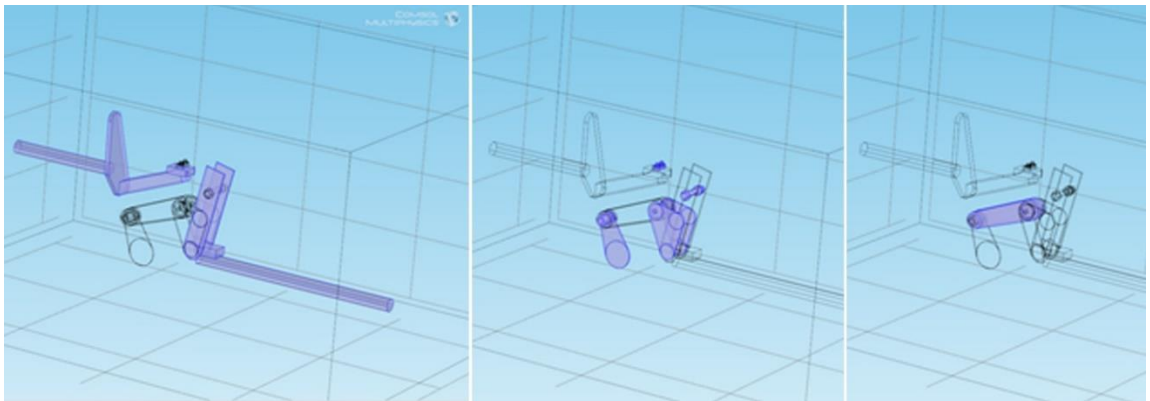


Figure D2: Materials used for the simulation model included: copper, steel and plastic (left to right).